THE UNIVERSITY OF HULL

'ULTRALOW INTERFACIAL TENSIONS AND MICROEMULSION FORMATION IN OIL-WATER-SURFACTANT SYSTEMS'

being a Thesis submitted for the Degree of

Doctor of Philosophy

in the University of Hull

by

Bernard Paul Binks, B.Sc.

August, 1986

SUMMARY Summary of Thesis submitted for Ph.D. degree

by Bernard Paul Binks

on

Ultralow interfacial tensions and microemulsion formation in oil-water-surfactant systems

The thesis is concerned with aspects of the surface and colloid chemistry of various oil + water systems containing pure surfactants. In alkane plus aqueous NaCl systems containing the surfactant diethylhexyl sodium sulphosuccinate (AOT), the alkane-aqueous solution interfacial tension becomes constant at the onset of surfactant aggregation, which can occur in either the aqueous or alkane phase. This constant tension, γ_c, can attain ultralow values ($< 10^{-3}$ mN m^{-1}) and can pass through a minimum value with respect to salt concentration, temperature and alkane chain length. Surfactant transfer between phases, and phase inversion of macroemulsions are shown to occur around the condition which produces minimum γ_c.

The origin of the low tensions is thought to be due to monolayer adsorption. Aggregates in equilibrium with the plane monolayer are shown to be spherical microemulsion droplets, whose sizes increase as a minimum in γ_c is approached.

The results are discussed in terms of the effective molecular geometry of the surfactant and how this is affected by the variables of interest. Minimum γ_c occurs for the condition such that the effective headgroup area is equal to the effective chain area at a plane interface.

A thermodynamic treatment has been used to describe the tension variations; minimum γ_c is shown to result when there is some kind of equivalence between the plane oil-water interface and the surface of the aggregates. For example, minimum tension with respect to salt concentration occurs (in the case of ionic surfactants) when the degree of dissociation of surfactant in the micelle and at the plane oil-water interface are equal.

For the single-chain surfactant sodium dodecyl sulphate, salt alone cannot yield a minimum in γ_c, nor is γ_c very low. Addition of octanol as cosurfactant however can produce very low values of γ_c and a minimum as cosurfactant concentration is varied. A geometrical description of these effects is given which is in accord with the findings relating to the composition of interfacial monolayers emerging from thermodynamics.

ACKNOWLEDGEMENTS

The author would like to express his very real gratitude to his supervisor, Dr. Robert Aveyard, for his complete support at all times and for his unfailing encouragement and guidance. Thanks also go to Dr. Jeremy Mead and Dr. Paul Fletcher for helpful discussions.

The author thanks British Petroleum Research, Sunbury-on-Thames for the award of a B.P. Research Studentship; the work contained in this thesis was in conjunction with their Enhanced Oil Recovery programme.

Finally, the author wishes to thank Mrs. Sandie McCollin for the superb typing of this thesis.

B.P.B.

TO MY PARENTS

'Science is built of facts the way a house is built of bricks; but an accumulation of facts is no more science than a pile of bricks is a house.'

Henri Poincaré, La Science et l'hypothese (1902)

'Scientific discovery consists in the interpretation for our own convenience of a system of existence which has been made with no eye to our convenience at all.'

Norbett Wiener, The Human Use of Human Beings (1954)

ABSTRACT

The thesis is concerned with aspects of the surface and colloid chemistry of various oil + water systems containing pure surfactants. In alkane plus aqueous NaCl systems containing the surfactant diethylhexyl sodium sulphosuccinate (AOT), the alkane-aqueous solution interfacial tension becomes constant at the onset of surfactant aggregation, which can occur in either the aqueous or alkane phase, depending on conditions. This constant tension, γ_c, can attain ultralow values ($< 10^{-3}$ mN m^{-1}) and can pass through a minimum value with respect to salt concentration, temperature and alkane chain length. Surfactant transfer between phases, and phase inversion of macroemulsions are shown to occur around the condition which produces minimum γ_c.

The origin of the low tensions is thought to be due to monolayer adsorption. Aggregates in equilibrium with the plane monolayer are shown to be spherical microemulsion droplets, whose sizes increase as a minimum in γ_c is approached.

The results are discussed in terms of the effective molecular geometry of the surfactant and how this is affected by the variables of interest. Minimum γ_c occurs for the condition such that the effective headgroup area is equal to the effective chain area at a plane interface.

A thermodynamic treatment has been used to describe tension variations; minimum γ_c is shown to result when there is some kind of equivalence between the plane oil-water interface and

the surface of the aggregates. For example, minimum tension with respect to salt concentration occurs (in the case of ionic surfactants) when the degree of dissociation of surfactant in the micelle and at the plane oil-water interface are equal. A thermodynamic treatment of the effect of the addition of cosurfactant (e.g. n-alkanol) demonstrates that minimum tension results when the ratio of surfactant to cosurfactant is equal at the plane oil-water interface and in the mixed aggregates.

For the single-chain surfactant sodium dodecyl sulphate, salt alone cannot yield a minimum in γ_c, nor is γ_c very low. Addition of octanol as cosurfactant however can produce very low values of γ_c and a minimum as cosurfactant concentration is varied. A geometrical description of these effects is given which is in accord with the findings relating to the composition of interfacial monolayers emerging from thermodynamics.

GLOSSARY

Some abbreviations and terms used throughout this thesis are given below. Other symbols are defined locally within the text.

A	area per surfactant molecule
A_s	area per surfactant molecule in saturated film
A_s^{ℓ}	limiting value of A_s for high salt concentration
A_D	area per surfactant molecule at droplet surface
a_h	effective cross-sectional area of a surfactant headgroup
a_c	effective cross-sectional area of surfactant chain region
A'	absorbance in a 1 cm pathlength cell
AOT	Aerosol OT sodium bis-(2-ethylhexyl)sulphosuccinate
aq.	as subscript, denotes aqueous phase
a_i	activity of component i
α	fraction of monomers
α_m	micellar degree of dissociation
α_p	degree of dissociation of surfactant at plane monolayer
B or B'	integration constants
$C_{12}E_5$	dodecyl pentaoxyethylene glycol monoether
c.m.c.	surfactant concentration in aqueous phase for onset of aggregation in either aqueous or oil phase
d	differential
∂	partial differential
$\Delta\rho$	difference in solution density
D	collective diffusion coefficient

DHBS	dihexylbenzene sodium sulphonate
ε	molar extinction coefficient ($dm^3\ mol^{-1}\ cm^{-1}$)
f_i	bulk activity coefficient of component i
$f_\pm$	mean ionic activity coefficient
Γ_i	surface excess ≡ surface concentration for strong adsorption
Γ_D	Γ of surfactant in saturated monolayer
i	as subscript, general index for component i
j	auxillary index for all components other than the i'th
K	distribution ratio or scattering vector
k	Boltzmann's constant
ℓ	correlation length
ℓ	effective length of hydrocarbon chain
ln	natural logarithm
m	concentration in aqueous phase
microemulsion	thermodynamically stable, optically clear dispersion of one fluid phase in another
N	n-alkane chain length
N_i	average number of molecules per micelle
n_i	number of moles of i
oil	as superscript, denotes oil phase
P	geometric packing parameter
ϕ_D	volume fraction of dispersed phase
r_c	radius of water core
r_H	hydrodynamic radius
R	mole ratio of water to surfactant in droplet

R	gas constant per mole
*	indicates condition for minimum γ_c
subscripts	D, S and A denote surfactant, salt (NaCl) and cosurfactant respectively
Σ	symbol for summation
SDS	sodium dodecyl sulphate
S_u^s	entropy of unit area of surface
ΔS_m	molar entropy of micelle formation
T	temperature
t	effective thickness of surfactant film in droplet
μ_i	chemical potential of component i
$\mu_i^{\ominus}$	standard chemical potential
v	volume of surfactant chain region
w	Simha factor
x_i	mole fraction of i
γ	tension of plane alkane (or air) - aqueous solution interface for $m_D < c.m.c.$
γ_c	tension of plane alkane-aqueous solution interface for $m_D \geq c.m.c.$

CONTENTS

Chapter One

CHAPTER 1

INTRODUCTION

1.1 General surfactant phenomenology

Surface active agents (or *surfactants*) are amphipathic molecules consisting of a nonpolar hydrophobic part, usually a straight or branched hydrocarbon chain or chains, attached to a polar hydrophilic headgroup. Sodium dodecyl sulphate (SDS) and sodium bis-(2-ethylhexyl)sulphosuccinate (AOT), in which the hydrophilic moiety bears a negative charge, are termed *anionic* surfactants. Examples of *cationic* surfactants are compounds derived from substituted ammonium compounds such as cetyl trimethylammonium bromide (CTAB). A number of *nonionic* surfactants have the formula $C_nH_{2n+1}(OCH_2CH_2)_mOH$ e.g. dodecyl hexaoxyethylene glycol monoether $C_{12}H_{25}(OCH_2CH_2)_6OH$, abbreviated to $C_{12}E_6$.

Most surfactants are soluble in water to some extent. The hydrocarbon chain interacts relatively weakly with the water molecules in an aqueous environment. The polar headgroup however interacts strongly with the water via dipole-dipole or ion-dipole interactions and is solvated. It is essentially the balance between the solubility of the hydrophobic and hydrophilic parts of the molecule which gives the special properties associated with surfactants.

The unique property of these materials is their ability to adsorb strongly at various interfaces and hence lower the *interfacial tension*, γ. At low concentration in water, the

surfactant behaves like a normal electrolyte. At higher concentrations, contact between the water and the hydrocarbon chains is minimised by association to form larger units called *micelles*.[1] The concentration corresponding to the onset of association is known as the *critical micelle concentration* (c.m.c.) and is marked by a sharp change in, for example, the colligative properties of the solution.

In 'normal' micelles (i.e. those formed in aqueous solution), the hydrophilic groups are oriented outwards towards the water and the hydrophobic groups mix in the centre of the micelle which is devoid of water. The reverse situation occurs in hydrocarbon media (containing a certain amount of water) where 'reverse' micelles form.[2] The interior of a normal micelle has the properties of a liquid hydrocarbon. When an oil or an oil-soluble substance is added to an aqueous micellar solution, it can be solubilised into the micelle, forming a 'swollen' micelle.

Hoar and Schulman[3] have described transparent systems which form spontaneously when oil and water are mixed with relatively large amounts of an ionic surfactant combined with a cosurfactant e.g. a short chain alcohol. These systems are called *microemulsions* and consist of dispersions of very small drops (radius of the order of 10 nm, larger than micelles) of water in oil (w/o) or of oil in water (o/w). Microemulsions differ from macroemulsions not only in their lack of turbidity but, more essentially, in being thermodynamically i.e. indefinitely, stable. In recent years, microemulsions have attracted a great deal of attention, and several reviews[4-7] concerned with the

stability, structural aspects and applications of microemulsions have appeared.

The origin of the thermodynamic stability of microemulsions has been discussed for example by Ruckenstein,[8] who defines a reference state in which water and oil are not dispersed and the surfactant is distributed at equilibrium between the two. This state is the stable one when microemulsions do not form. A dispersion of one phase in the other in the form of droplets then leads to two effects: (i) an increase in the entropy of the system and (ii) adsorption of surfactant on the large oil-water interface generated. The accumulation of surfactant reduces the interfacial tension from a value of about 50 mN m^{-1} (which exists at an oil-water interface devoid of surfactant) to some ultralow value ($< 10^{-2}$ mN m^{-1}). In addition, the decrease in the concentration of surfactant in the dispersed and continuous media reduces their chemical potentials below those of the reference state, thereby generating a negative free energy change. Thermodynamically stable microemulsions form when the negative free energy changes resulting from both the entropy of dispersion of one phase in the other and the adsorption of surfactant overcomes the positive product of the low positive interfacial tension and the large interfacial area generated through spontaneous dispersion. There are conditions in which it is thermodynamically favourable for a microemulsion phase to exist in equilibrium with excess oil and/or water phase because the system thereby can achieve a lower free energy. This is the case for nearly all the systems described in this thesis.

1.2 Ultralow interfacial tensions and microemulsion formation

The occurrence of *ultralow interfacial tensions* (ULT) and associated phenomena in systems containing oil, water and surfactant are currently of considerable interest.[9-12] There have been a number of approaches towards an understanding of the origins of ULT e.g. references 13-16, but there is scope for much further insight, and a need for experimental data for systems containing pure surfactants.

Perhaps the best understood systems are those containing pure nonionic surfactants. In systems containing, for example, polyoxyethylene surfactants C_nE_m (m = 1-8), alkane and water, single phase microemulsions can be formed, or two or three phases may coexist.[17] Very low interfacial tensions may occur between the phases, the lowest tensions being observed in the three-phase régimes. The effect of temperature on the phase behaviour in a system of oil + water with a constant weight % of nonionic surfactant is shown schematically in Figure 1.1 after Shinoda and Kunieda.[18] Consider the mixture containing oil and water at 0.5 wt. fraction, represented by the dashed line. At low temperatures, below point A, the system will be two-phase and the surfactant will reside mainly in the aqueous phase. If a macroemulsion is formed by shaking, it will be of the oil-in-water (o/w) type. Above point B, a two-phase region again exists which, however, when shaken results in a water-in-oil (w/o) emulsion, the bulk of the surfactant now residing in the

Figure 1.1 Schematic phase diagram in water-oil-nonionic surfactant system versus temperature. Roman numerals represent number of coexisting phases.

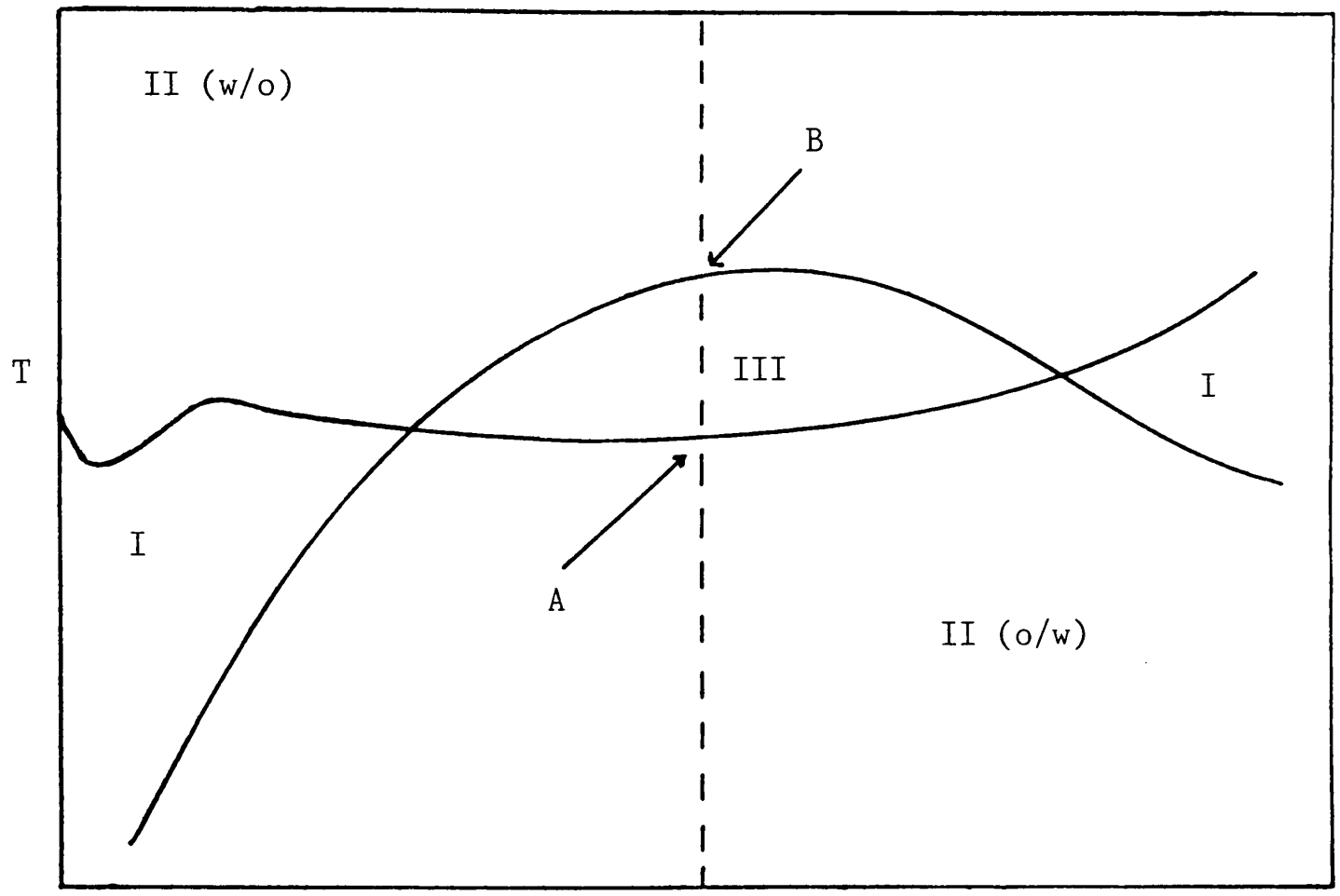

Figure 1.2 Interfacial tensions between the various phases versus temperature for a system of fixed composition.

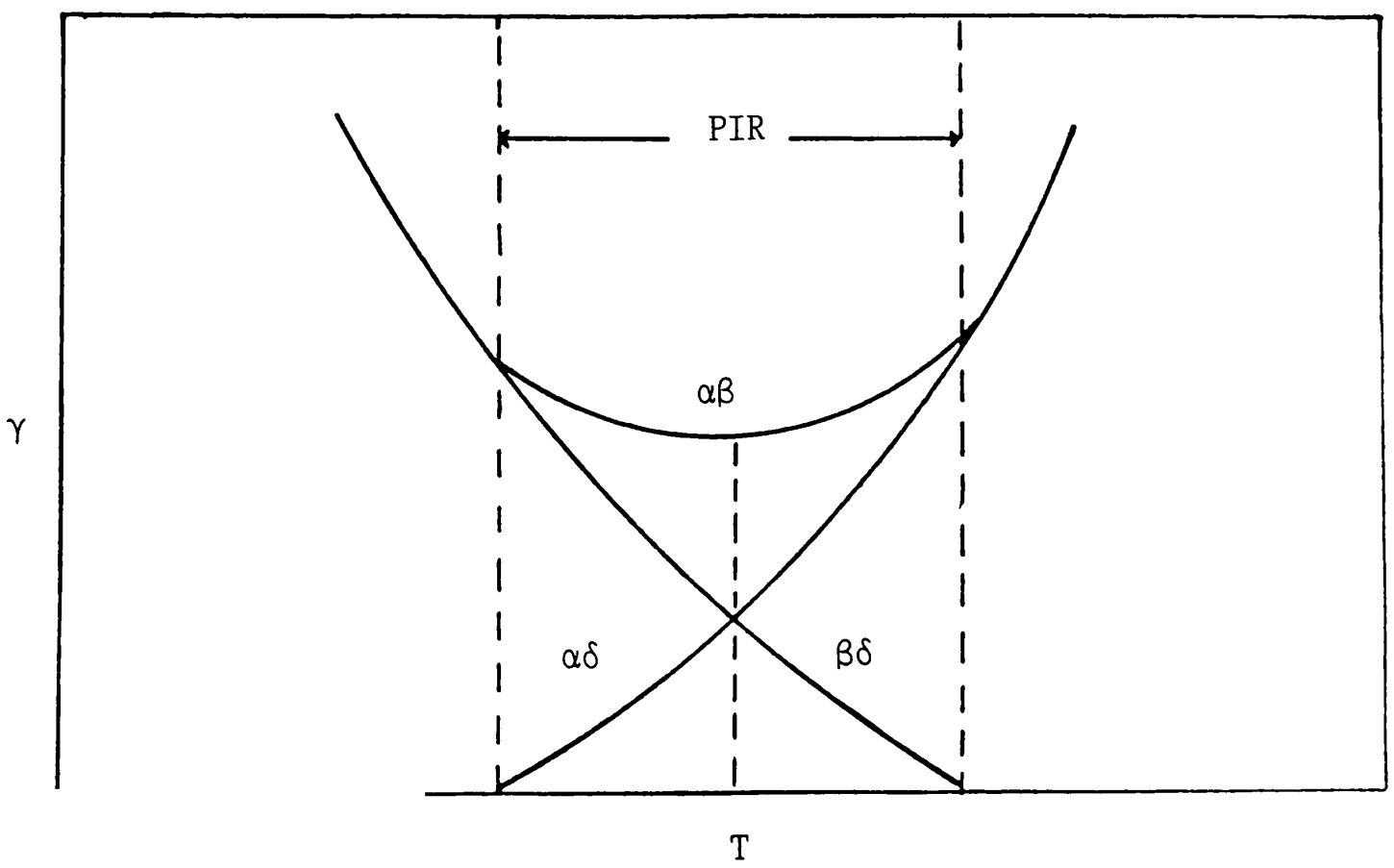

oil-phase. Between A and B, the *phase inversion region* (PIR), three phases coexist, the so-called middle phase being surfactant-rich. The aqueous phase (α) contains micellar surfactant with solubilised oil, the oil phase (β) is often a water-in-oil microemulsion (droplet diameters between 2 and 50 nm), and the middle phase (δ) is a phase of undetermined structure.

The interfacial tensions of the various interfaces vary as shown schematically in Figure 1.2.[19] Widom *et al.*[20,21] have shown that at equilibrium in any 3-phase system

$$\gamma_{\alpha\beta} \leqslant \gamma_{\alpha\delta} + \gamma_{\beta\delta}$$

where the equality is Antonoff's rule. The inequality holds for the results reported in reference 19. In the work of Pouchelon *et al.*[22] (for toluene-aqueous NaCl - SDS - butanol systems) it was found that $\gamma_{\alpha\beta}$ was always equal to the larger of $\gamma_{\alpha\delta}$ and $\gamma_{\beta\delta}$, so again the inequality holds. Where $\gamma_{\alpha\beta}$ is greater than the sum of $\gamma_{\alpha\delta}$ and $\gamma_{\beta\delta}$ it is inferred that true equilibrium is not established, as appears to be the case for the results of Ross and Patterson[23] discussed by Fleming and Vinatieri.[24]

The situation for systems containing pure ionic surfactants is less well established. However, results are presented here which show that for a micelle-forming anionic surfactant in the presence of sodium chloride, the behaviour is very similar to that described for the nonionics but with phase inversion and surfactant transfer with respect to temperature (but not salt concentration or alkane chain length) occurring in the opposite sense.

The general features of the variation of low tensions brought about by variations in salt concentration, temperature and changes in alkane chain length in systems containing a wide range of pure alkylbenzene sulphonates have been extensively reported in a series of papers by Wade and Schechter and coworkers e.g. reference 25. These investigators have concentrated on producing optimal conditions for low tensions to occur rather than on gaining an insight into the reasons for the existence of the low values.

Broadly, there are three views concerning the processes involved in the attainment of ultralow tensions. It is clear from Figures 1.1 and 1.2 that the low interfacial tensions are associated with the critical end points (e.g. A and B in Figure 1.1) where the δ phase disappears. Attention has been given to the role of critical phenomena in systems containing surfactants;[13,26] the surfactant plays a dual role, the one associated with its solvent character, the other with its surface activity. It has been shown that the interfacial tension approaching the critical point T_c at the critical composition can be expressed by the scaling law[27]

$$\gamma = \gamma_o \left\{ \frac{T_c - T}{T_c} \right\}^W \qquad (1.1)$$

where W is a universal critical exponent and γ_o is the tension scale factor which depends on the fluid properties. The quantity γ_o in part reflects the surface activity of the surfactant and is much smaller in systems containing surfactants than in those

without surfactants.[26] It is treated as a fitting constant in equation 1.1 and at present its value appears to be useful only in an empirical way. Nonetheless, the above approach to understanding the evolution of ultralow tensions is clearly of fundamental importance; it has not, however, been pursued further in the present study.

Hall,[28] using data obtained with a commercial surfactant mixture, argues that ultralow tensions in aqueous surfactant/hydrocarbon systems arise from the formation of a liquid crystal surfactant mesophase at the oil-water interface. Franses *et al.*[14,29] have studied systems containing pure p-(1-heptylnonyl)benzene sulphonate (often referred to as Texas 1). Their work is in accord with and extends the conclusions of Hall. At room temperatures Texas 1 has a very low solubility in water and forms dispersions of liquid crystallites in solution; attainment of ULT is discussed in terms of these. In determining tensions (via the spinning-drop technique), it is suggested that the crystallites take up alkane at the oil drop surface, forming a third phase which exhibits, under optimal conditions, ULT with both oil and water phases. When ULT are observed, the third phase is always present on the surface of the drop. Since the third phase is viscous, the tensions recorded are not reproducible, and they vary with time. Nonetheless, it is claimed that,[29] as the surfactant concentration in solution is increased, the interfacial tension attains a low, plateau value. Micelles are said not to be involved in the production of ULT i.e. micelles are surface inactive since micelle formation is an alternative

to adsorption. In surfactant mixtures (e.g. Texas 1 with added SDS) minima are observed and it is proposed that liquid crystallites of the optimum composition (with respect to Texas 1 and SDS) are required for ULT, and as this composition is departed from the tension rises. Similar conclusions have been arrived at using pure AOT as surfactant,[30] alone and in mixtures with SDS (see later). It is interesting in this context to note that Billoudet and Dupeyrat[31] have claimed that micelles are absolutely essential for ULT in systems containing alkylbenzene sulphonates together with alcohol cosurfactants.

Possibly the most uncomplicated approach to the problem is that put forward by Overbeek *et al.*[16,32] to the effect that monolayer adsorption causes a reduction in tension and in favourable cases ULT results, which give rise to a third phase, either liquid crystalline or microemulsion. Chan and Shah[33] have proposed a simple 'classical' picture of the occurrence of ULT in systems containing commercial anionic surfactant mixtures. It is believed that ULT are attained at the c.m.c. of the surfactant in the aqueous phase, and is produced by monolayer adsorption. No mention is made of the production and role of a third phase. Minima in tensions observed as the surfactant concentration is increased are attributed to the formation of mixed micelles and the ensuing reduction of monomer concentration. Interesting work has been done on the system SDS + aqueous NaCl + toluene + butanol.[34] In two-phase régimes Cazabat *et al.*[34] believe that ULT are associated with a 'very thin' adsorbed surfactant layer; although reflectivity data indicate that the

thickness of the surfactant layer is smaller than 10 nm,[35] it is expected that, as in micellar systems, the surfactant layer is monomolecular.

What might be called 'geometrical' approaches have been made in attempts to reveal the origins of the enhanced surface activity of surfactants producing ultralow tensions, and leading to the formation of microemulsion and liquid crystalline phases.[15,36] Thus Mitchell and Ninham[15] define a packing factor P for surfactant molecules which is essentially the ratio of the cross-sectional areas of the chain and head, and when it has a value of unity it is argued that the tension of an oil-water interface containing the surfactant will be minimum, and the system will be at a phase inversion point. In the work of Mukherjee *et al.*,[36] the specific role of the oil in producing low tensions is explored.

In commenting on the views outlined above, we incline to the opinion that several of the differences are matters of semantics. It is unfortunate that some of the most extensive investigations into the origins of ULT have involved a system containing a surfactant (Texas 1) which gives liquid crystallites at low concentration in aqueous solution. We believe that statements to the effect that liquid crystallites are responsible for ULT can be misleading. It would be more acceptable to say that when ULT are achieved a third surfactant-rich phase (liquid crystalline or microemulsion) may spontaneously form.

1.3 Introduction to thermodynamics involving surfactants

The surface of a liquid is the boundary between two bulk phases, frequently between the liquid and air containing vapour of the liquid. Similarly, an interface is formed between two 'immiscible' liquids. Stability of the interface requires that the free energy should increase if the area of the interface increases. This requirement leads to a convenient definition of the surface tension γ at a liquid surface or interface, as the differential of the Helmholtz energy A (at constant temperature, T, and composition) with respect to the interfacial area Ω:

$$\gamma = \left\{ \frac{\partial A}{\partial \Omega} \right\}_{T,V,n_i}$$

where n_i = number of moles of each component i and V is the volume of the system. In real systems, there is a finite distance normal to an interface in which the properties of one bulk phase change into those of the other. One way of treating a surface is to consider it as a phase which is separate from the adjacent bulk phases, and which has a finite thickness and volume.[37] Figure 1.3 depicts such a model. The regions α and β are homogeneous bulk phases separated by the planar surface phase, s. Phase α is homogeneous up to the plane AA' and phase β up to the plane BB'. Thus all changes in properties from α to β take place in the region between AA' and BB'. Using this approach the extensive thermodynamic functions and numbers

of moles which appear in expressions relating to the surface phase are total quantities.

Figure 1.3

The surface phase

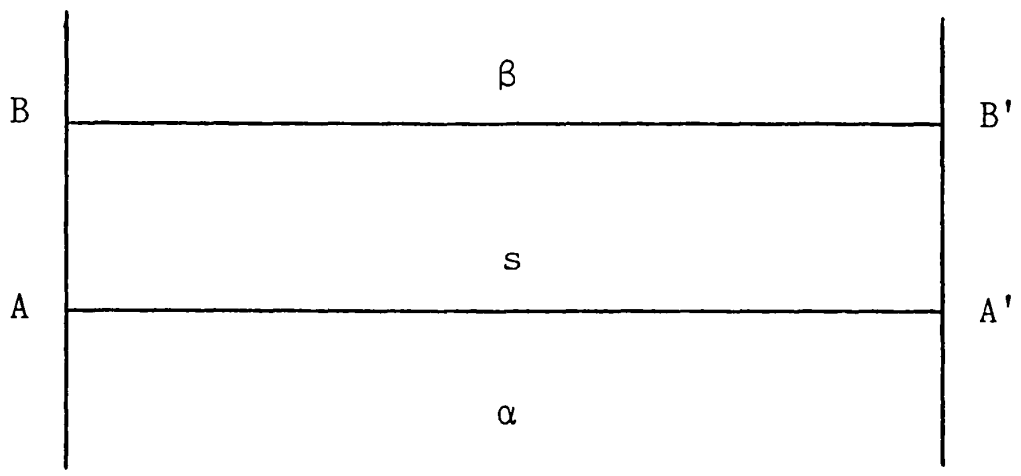

In the Gibbs treatment[38] the interface is regarded as a mathematical dividing plane, the Gibbs surface. This is illustrated in Figure 1.4. The dividing surface is designated SS' and is placed between and parallel to, AA' and BB' in some arbitrary position. The extent of adsorption of component i is measured by its surface excess, defined as the amount of i in unit area of the region between AA' and BB' less the amount that there would be if α and β extended unchanged to SS'.

Figure 1.4

The Gibbs dividing surface

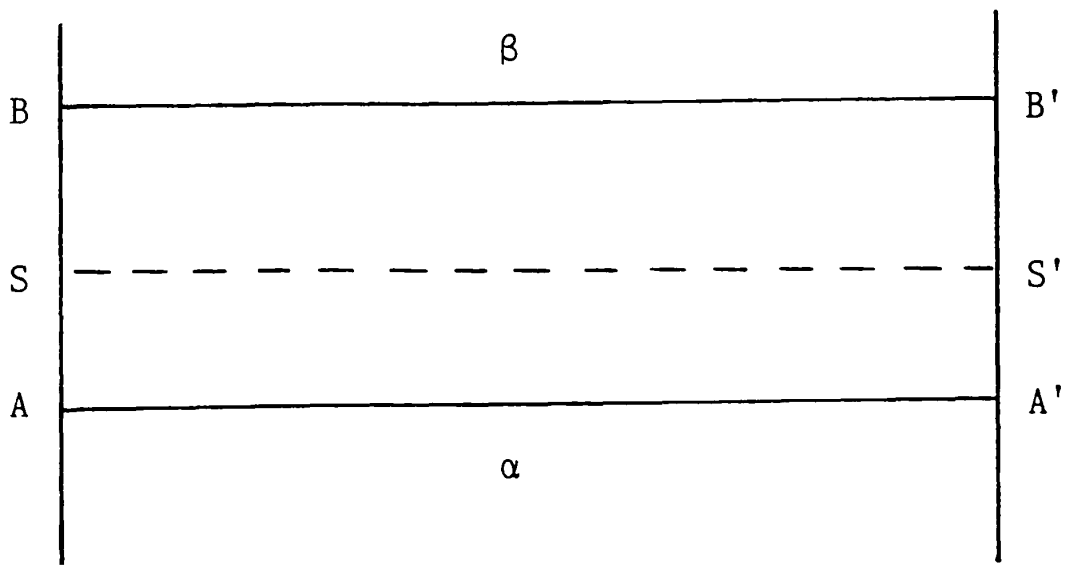

In other words, the surface excess is the extra amount of a component in between AA' and BB' which results from adsorption. In the systems of interest in the present study, where strongly adsorbing species are used, the distinction between the total and surface excess quantities essentially disappears.[38]

When adsorption takes place at an interface, the tension γ falls. A common objective in surface chemistry is to determine the amount of material adsorbed at an interface. The Gibbs adsorption equation is a thermodynamic expression which relates the surface concentration (or excess) of a species to both the tension and the bulk activity of the adsorbate. The general form may be written as[38]

$$-d\gamma = \sum_i \Gamma_i \, d\mu_i \quad \text{(constant temperature)} \qquad (1.2)$$

where Γ_i is the total or excess surface concentration of i, μ_i is the chemical potential of the i'th species and $\sum_i$ denotes the summation over all the species i. The equation finds wide application in the study of adsorption, and some relevant ways in which it can be used will now be outlined.

Consider first the adsorption of a strongly surface-active solute 2 from dilute solution in solvent 1 to the air-solution interface. Equation 1.2 for such a situation becomes

$$-d\gamma = \Gamma_1 \, d\mu_1 + \Gamma_2 \, d\mu_2 \qquad (1.3)$$

Introducing the Gibbs-Duhem equation for this system

$$d\mu_1 = -n_2 \, d\mu_2 / n_1 \qquad (1.4)$$

where the n are numbers of moles in the system, and substituting for $d\mu_1$ in equation 1.3 yields

$$-d\gamma = (\Gamma_2 - n_2 \Gamma_1/n_1)\, d\mu_2 \qquad (1.5)$$

In the case of dilute solutions, $n_2/n_1 \ll 1$ and equation 1.5 becomes to a good approximation

$$-d\gamma = \Gamma_2\, d\mu_2 \qquad (1.6)$$

It can similarly be shown for a system consisting of two immiscible solvents 1 and 3 (such as oil and water) and solute 2 distributed between them and dilute in each phase, that

$$-d\gamma = (\Gamma_2 - \Gamma_1 n_2/n_1 - \Gamma_3 n_2/n_3)\, d\mu_2 \qquad (1.7)$$

which, noting that $n_2/n_1 \ll 1$, $n_2/n_3 \ll 1$, again reduces to equation 1.6. Thus to a very good approximation, values of Γ_2 can be obtained from the variation of γ with μ_2.

The values of the Γ depend on the positions of the planes AA' and BB'. However, the quantities in brackets in equations 1.5 and 1.7 are clearly invariant with respect to these positions since $d\gamma/d\mu_2$ is an experimentally determined quantity. The reason that Γ_2 is obtained without reference to the thickness of the surface is that 2 is strongly adsorbed from dilute solution, and is located close to the physical surface. Thus, if the thickness of s is increased, relatively very little more of component 2 is included in this phase.

Changes in the activity, a_2, of 2 are related to $d\mu_2$ by

$$\mu_2 = \mu_2^{\ominus} + RT \ln a_2 \qquad (1.8)$$

where $\mu_2^{\ominus}$ is a standard chemical potential. From equation 1.8

$$d\mu_2 = RT\ d\ln a_2 \qquad (1.9)$$

and hence equation 1.6 may be written

$$-d\gamma = RT\Gamma_2\ d\ln a_2 \qquad (1.10)$$

For systems where the solute activity coefficients are effectively unity, equation 1.10 becomes

$$-d\gamma = RT\Gamma_2\ d\ln m_2 \qquad (1.11)$$

where m_2 is the molar concentration of 2 in the phase from which adsorption is taking place. As will be seen, equation 1.11 can be used for the study of adsorption of anionic surfactants in the presence of swamping electrolyte and nonionic surfactants without salt. Direct measurements (by a radiotracer technique) of Γ_2 have confirmed the validity of equation 1.11 for adsorption at both air-water[39] and oil-water[40] surfaces.

For anionic surfactants in the absence of salt, the Gibbs equation 1.2 becomes

$$-d\gamma = 2RT\Gamma_2\ d\ln m_2 \qquad (1.12)$$

where the factor of 2 indicates adsorption of both surfactant ion and counterion. The experimental verification of equation 1.12 has been reported by Tajima *et al.*[40,41] In salt concentrations other than 'swamping', Matijevic and Pethica[42] show that the Gibbs equation may be written

$$-d\gamma = x\ RT\Gamma_2\ d\ln m_2 \qquad (1.13)$$

in which

$$x = 1 + \left\{ \frac{m_2}{m_2 + m_S} \right\} \qquad (1.14)$$

where m_S = concentration of salt. Tajima[43] has verified the applicability of equation 1.13, which is used extensively throughout the present work.

1.4 Presentation of thesis

The present work is conveniently presented in two parts. Chapters 3 to 8 are concerned with the interfacial tension and associated colloid behaviour of oil + water systems containing (for the most part) the double-chain anionic surfactant AOT, with and without cosurfactant. In Chapter 9 data are presented for systems containing the single-chain surfactant, SDS, mainly in the presence of added cosurfactant.

Experimental data for the effects of salt concentration on the attainment of ultralow tensions and formation of microemulsions stabilised by AOT are presented in Chapter 3; a thermodynamic description of salt effects is given in Chapter 4. Effects of temperature on surfactant behaviour are discussed in Chapters 5 and 6, followed by the influence of changes in oil type in Chapter 7. Changes resulting from the addition of cosurfactants (n-alkanols) are the subject of Chapter 8. Chapter 2 is concerned with the experimental techniques and materials used in the present study. A summary of the work is given in Chapter 10.

Chapter Two

CHAPTER 2

EXPERIMENTAL

2.1 Measurement of surface and interfacial tension by ring and plate methods

2.1.1 Theory

There are broadly two types of method for the determination of surface and interfacial tension (γ) in fluid/fluid systems. In one type, the system containing the surface is at stable equilibrium, such as in the capillary rise, Wilhelmy plate, pendant and spinning-drop methods. Otherwise the method involves taking the liquid meniscus past a critical equilibrium as in the drop-volume technique.

The choice of method depends very much on the type of system being investigated e.g. pure liquid, dilute surfactant solution, liquid/vapour surface or liquid/liquid interface, the accuracy required, the quantity of liquid available etc. In the present work, attempts to measure tensions in systems containing surfactant using the drop-volume method failed since, however long a drop of solution had previously aged, at the point of detachment the surface stretches and the tension increases, giving rise to a high, erroneous value. A static method is therefore required i.e. one which does not depend on detachment.

The methods employed in the present work are the plate and ring methods. Wilhelmy[44] was the first to suggest that the

surface tension of a liquid may be derived from a measurement of the maximum force required to pull a glass plate from the surface of a liquid. The plate was cleaned carefully so that the angle of contact was small, probably zero, and by measuring the maximum pull, the need to apply buoyancy corrections was avoided. The function of the plate is to raise a meniscus of liquid above the general level of the flat surface. The form of such a meniscus in the case of the vertical plate is shown in Figure 2.1a as the shaded area. The weight of the meniscus increases to some maximum value as the plate is withdrawn from the surface. This maximum value is reached when the meniscus is fully formed, and then the force acting on it equals the surface tension times the perimeter provided that the contact angle $\theta = 0$ and that there are no buoyancy corrections. The latter are avoided by having the lower edge of the plate at the same level as the plane surface.

Figure 2.1a

The Wilhelmy plate

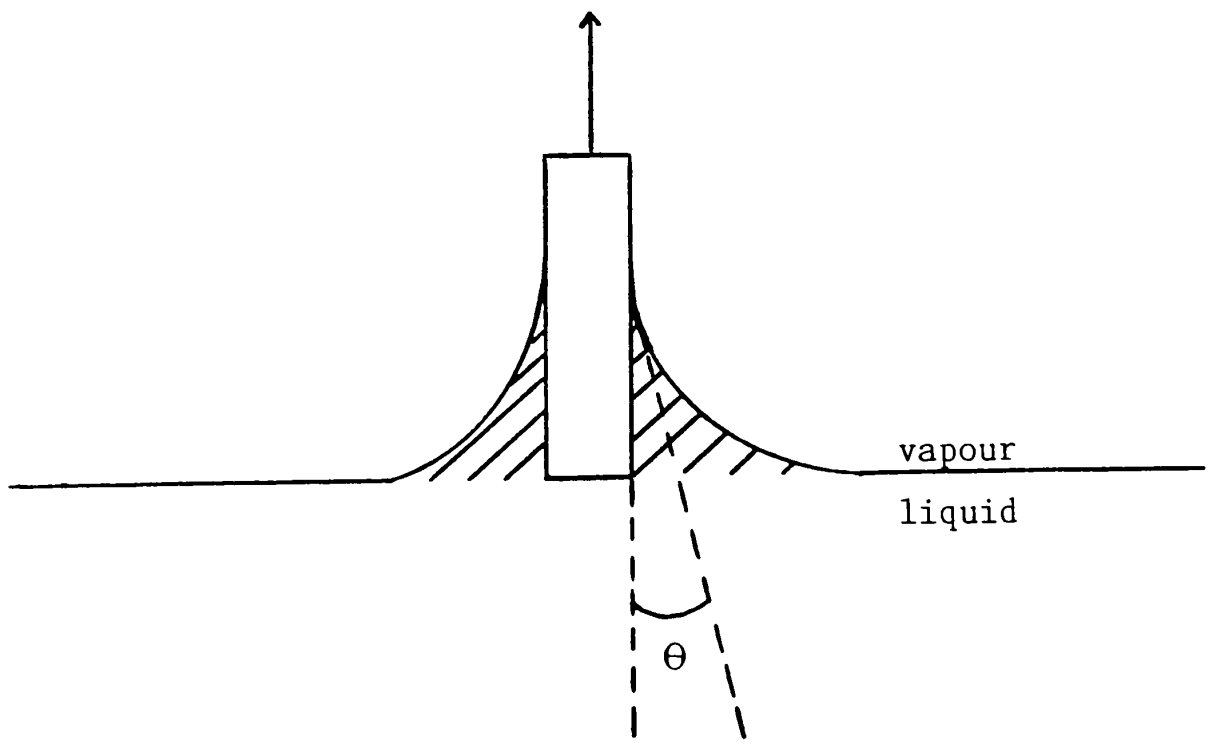

Dognon and Abribat[45] improved the Wilhelmy method by devising a means whereby the maximum force on the plate was measured without detaching it from the surface and this technique has been incorporated into modern tensiometers. The tension can be calculated from equation 2.1,

$$\gamma = \frac{K}{L\cos\theta} \qquad (2.1)$$

where K = measured force on the plate and L = wetted length of the plate. Assuming that the plate is perfectly wetted, i.e. $\theta = 0$, and of known perimeter, the tensiometer can be calibrated in order to give a direct reading of the tension γ.

The du Noüy ring method for the determination of surface and interfacial tension[46] is very widely used. It is convenient because the experimental procedure necessary to obtain a good degree of accuracy can be made very simple. The central features of the tensiometer are a ring, capable of being wetted, suspended horizontally in the surface of a liquid (or interface between liquids), and some device to measure the force necessary to separate ring and liquid. So that the applied force may be changed gradually, a torsion balance is often used. In much of the early work, the maximum pull on the ring was thought to equal the surface/interfacial tension according to $mg = 4\pi R\gamma$, where mg is the maximum upward force applied to a ring of inner radius R. The quantity m is the maximum weight of liquid raised above the free surface of the liquid. Harkins and Jordan[47] showed that this equation could be seriously in error because the meniscus formed by the ring was not of the same form as that formed by a

plate. They, and Freud and Freud[48] in a separate paper, derived a correction factor, F, that must be applied so that $mg = 4\pi R\gamma/F$. The factor F is found to be a function of R^3/V and of R/r, where V is the volume of liquid raised above the plane surface by the maximum pull of the ring, and r is the radius of the wire of which the ring is made. The physical significance of the correction factor is best understood by reference to Figure 2.1b which shows three successive stages of pulling a ring from the surface of a liquid. Provided that the wire is completely wetted, the meniscus begins to form as a force, f, is applied. When lifting the ring, the tension is acting along its wetted line. The resultant, due to the forces acting on the ring, reaches a maximum as soon as the tangent on the point of wetting is vertical to the surface. This maximum is measured and so it is not normally necessary, as is often done, to raise the ring until interruption. Besides the resultant of the tension, the hydrostatic weight of the liquid volume underneath the ring has to be measured. This additional force must be eliminated by the correction factor.

The correction factors are applied by measuring the radii of the ring R, and of the wire r, and the density difference between the liquids, $\Delta\rho$. If the maximum force, f_{max}, necessary to raise the ring can be determined, then the maximum total volume of the meniscus is given by

$$V = \frac{4\pi R f_{max}}{\Delta\rho g}$$

Figure 2.1b

Stages in measurement with the ring

Parallelogram of forces acting on a cross-section element with respect to lamella height

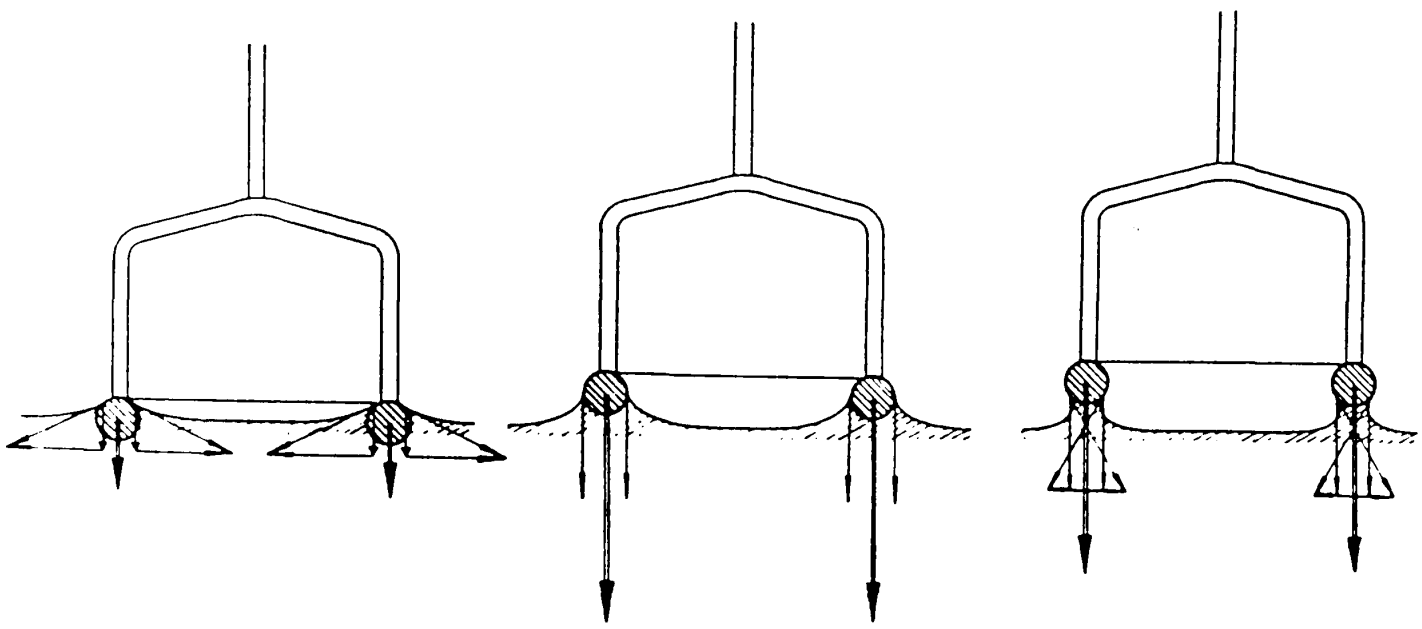

< maximum force	maximum force	lamella break

The forces acting on the ring reach a maximum when the tangent to the wetting point is completely vertical.

A value of R^3/V is calculated for each determination and the correction factor F obtained from tables[47] according to the value of the ring constant R/r. Surface tensions measured by the capillary rise method were used as standards to evaluate F in reference 47. The accuracy of these tables has been proved with a variation of 0.25% by theoretical investigation of meniscus shapes.[48] An alternative formulation of the correction factors

has been developed by Zuidema and Waters[49] who extended the data of Harkins and Jordan required for application to measurement of lower interfacial tensions (< 25 mN m^{-1}).

In general, any rigorous theory of the ring method would require the following criteria:

(i) that the wire of the ring lie in one plane

(ii) that the plane of the ring be horizontal

(iii) that the vessel containing the liquid (s) be large enough so that any curvature of the free surface of the liquid would not be great enough to affect the shape of the liquid raised by the ring

(iv) that there be no motion of the ring except a slow upward movement

(v) that the ring be circular.

The most important source of error arises from the ring not being horizontal. It was shown[47] that a departure of 1° from horizontal introduces an error of 0.5%, 2° an error of 1.5%.

2.1.2 Use of digital tensiometer

The tensiometer used for the determination of surface and relatively high interfacial tensions was a digital K10 supplied by Krüss (Plate 1) and had both Wilhelmy plate and du Noüy ring attachments. It consists of a water thermostatted vessel capable of being raised by automatic motors, and a torsion balance. The


KRÜSS
0.0
DIGITAL-TENSIOMETER K10
Plate
Ring
Off
Zero
Run
Zero - Adjustment
Sample Scale
Reversal
Stop Cal.
Geo. Corr.
Recorder
A. Krüss - Hamburg
Instr. - Nr.
Typ
Made in Germany

PLATE 1

ring, made of Pt Ir 20 had the following dimensions:

R = 9.545 mm, r = 0.185 mm, L (wetted length) = 119.95 mm.

These are dictated by a compromise between high precision measurement, convenience, mechanical stability and a minimum of sample material. The surfaces of the platinum plate had been roughened to aid wetting. The plate was of length 15.0 mm and thickness 0.10 mm. Ring and plate were rinsed in chromic acid, then pure water and briefly heated to glowing by holding above a burner. The glass measuring vessels were similarly cleaned and dried in an oven. They were filled with the appropriate liquid (or liquids) and allowed to attain the correct temperature before measurements were made. That the ring and plate were free of kinks and as horizontal as possible was frequently checked by observing their reflection in the surface of the liquid. A small kit was provided that enabled both probes to be carefully reshaped if out of alignment.

For the determination of the surface tensions of liquids and surfactant solutions, the balance is first zeroed with the appropriate probe suspended in air but close to the surface of the liquid. In the case of the plate, the sample is further raised by electric motors until the plate is wetted. In this moment the plate is drawn into the liquid and the motors stop automatically. As the measuring procedure commences the plate is drawn out of the liquid until its lower edge exactly reaches the level of the free liquid surface. The measured tension is now indicated digitally. If the surface tension of the sample

changes owing to enrichment of the surface with surfactant, the electronics will in every case provide a new balance. Hence changes in tension can be continuously monitored.

The procedure is slightly different for the ring. After zeroing, the vessel is raised enough to cause the ring to immerse in the liquid. The vessel is now lowered until the servomotors start and these stop when the maximum force is measured. The zero adjustment in the less dense phase is necessary to compensate the buoyancy and the surface tension which acts on the shafts of the ring. For low concentration surfactant solutions, the surface tension is often dependent on the age of the surface. However, a very useful facility available on the Krüss tensiometer is that after stopping at the precise point of measurement, the ring can be lowered very slightly and it is possible to reach the maximum again in a few seconds without forming any appreciable amount of new surface. The reversal button on the machine thus allows an exact determination of the variation in tension with time.

The tensiometer is calibrated, using trimming potentiometers, such that the surface tension of water at 25°C reads 71.9 mN m^{-1} (the value determined by various other methods) for the plate and uncorrected ring display. The Krüss tensiometer is said to be linear compensated and correction factors determined as stated previously should be multiplied by 1.07 before being applied to the measured value.

The measuring procedure for oil-water interfacial tensions is similar to that described for surface tensions, except that

the zero point of the instrument is set with either probe totally submerged in the less dense (oil) phase. The oil is carefully pipetted on top of the aqueous phase by allowing it to run down the sides of the vessel. Tensions were found to be independent of the relative volumes of the two phases. In most measurements, fresh phases were contacted together; it will be shown later that tensions between pre-equilibrated phases were in good agreement with those for surfactant concentrations both below and above the aqueous phase c.m.c.

For surface and interfacial tensions above $\simeq$15 mN m^{-1}, both the ring and plate methods gave results in good mutual agreement i.e. within 0.2 mN m^{-1}. Separate determinations by each method were typically reproducible to $\pm$ 0.1 mN m^{-1}. Below tensions of 15 mN m^{-1}, the plate method became unsatisfactory and only the ring method could be used, down to $\simeq$3 mN m^{-1}. Interfacial tensions below 10 mN m^{-1} were also measured using the spinning-drop technique (see later) and excellent agreement between the methods was attained.

2.2 Measurement of interfacial tension by spinning-drop technique

2.2.1 Theory

Several classical methods for measuring interfacial tensions are limited to values larger than 0.1 mN m^{-1} e.g. Wilhelmy plate and drop-volume techniques.[50] Convenient methods allowing the measurement of low interfacial tensions include the sessile-drop technique,[51] the surface laser light scattering method[52] and the so-called spinning-drop technique.[53]

The spinning-drop is a relatively simple method for obtaining interfacial tensions by the measurement of the shape of a liquid drop in a more dense liquid contained in a horizontal tube rotating about its long axis. When a closed vessel, containing a liquid and a drop of a lighter immiscible liquid, is rotated about a horizontal axis, the drop will take up an equilibrium position on the axis of rotation because of the pressure caused by the centrifugal force. As the rotation frequency is increased, the drop will elongate until finally it is in the form of a cylinder with rounded ends. For each speed of rotation the drop will come to an equilibrium shape dictated by rotation forces and opposing interfacial tension forces.

A mathematical solution for the shape of the drop is complex, but, if the effects of gravity are neglected and the drop shape can be approximated by a cylinder with hemispherical caps, the treatment is simplified. The expression relating the tension of the drop surface to the angular velocity, the dimensions of the drop and the densities of the two phases can be derived in several ways. Probably the simplest method is that developed by Vonnegut,[53] who sets up an expression for the energy of the drop and solves it for the equilibrium shape in which the total energy is a minimum. More recently, Couper *et al.*[54] have presented a simpler derivation of Vonnegut's equation by calculating the kinetic energy of rotation of the system from a consideration of its moment of inertia. The most thorough treatment of the problem is provided by Princen *et al.*[55] They compute drop shape factors for various extents of deformation, from slightly deformed spheres

to long cylindrical droplets. They find that if the drop length exceeds about four times its width, it has a central section which is a near-perfect circular cylinder. Slattery and Chen[56] have also presented a procedure by which the interfacial tension may be calculated for all drop shapes. In this case the determination requires the measurement of both the maximum radius and maximum length of the drop, and the tension is given by

$$\gamma = 0.5 \left\{ \frac{r_{max}}{r^*_{max}} \right\}^3 \Delta\rho\omega^2 \qquad (2.2)$$

where r^*_{max} is a function of the maximum radius r_{max}, and the maximum length ℓ_{max}, of the drop and ω is the angular velocity.

Determination of ℓ_{max} is in practice difficult and introduces a source of error in the calculation of γ. However, it can be shown that if the condition $\ell_{max} \geq 8\ r_{max}$ is satisfied, equation 2.2 reduces to

$$\gamma = 0.25\ r^3\ \Delta\rho\omega^2 \qquad (2.3)$$

where r is the radius of the cylindrical part of the drop.

2.2.2 Description of apparatus

The spinning-drop tensiometers used were supplied by Krüss (Models Site 02 and Site 04). Plate 2 depicts the layout of the apparatus with thermostat. As seen, the tensiometer consists of a high speed rotating capillary tube (internal diameter ≃ 2.5 mm) open at both ends. The tube in its housing is pivoted and sealed so that the open ends rotate inside the chambers filled with the denser aqueous phase, and its middle section is observable through the cylinder windows. This arrangement allows the injection of

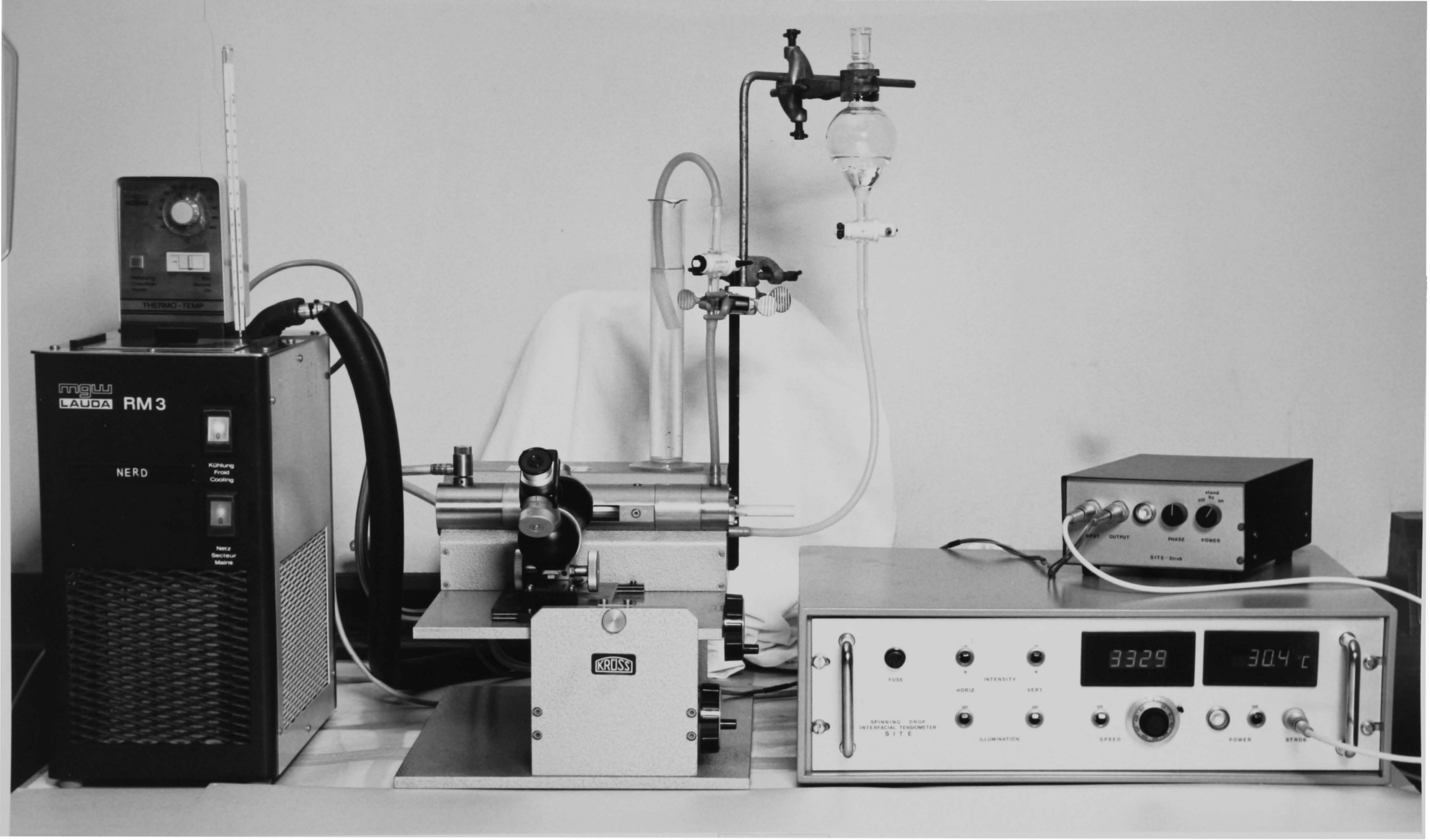
mgw
LAUDA RM3
NERD
Kühlung
Froid
Cooling
Netz
Secteur
Mains
THERMO-TEMP
KRÜSS
FUSE
INTENSITY
HORIZ
VERT
SPINNING DROP
INTERFACIAL TENSIOMETER
SITE
ILLUMINATION
SPEED
POWER
STROB
3329
30.4 °C
INPUT
OUTPUT
PHASE
POWER
stand
off by on
SITE-Strob

PLATE 2

a drop of the less dense oil phase into the filled and rotating system, so that the drop may be stabilised in the axis of rotation.

Illumination of the capillary can be with either a constant light source or a stroboscope 'in-phase' with the rotation of the capillary. The control box of the instrument displays the speed of rotation of the capillary, n, up to 10,000 r.p.m., which can be controlled to ± 5 r.p.m. There is also a digital read-out of the temperature. Thermostatting of the capillary is achieved by circulating a thin lubricating oil around it, from a Colora or Lauda thermostat. Temperature can be controlled to ± 0.2°C.

A precision-measuring microscope with two eyepieces of 2.5 and 3.5 times magnification is used to determine the drop diameter. Equation 2.3 shows that the accuracy of this method is strongly dependent on the accuracy by which the droplet diameter (2r) can be measured. Any error in r will result in a threefold percentage error in γ. After focussing on the drop, the ocular on the microscope is adjusted until the horizontal crosschair line is parallel to the upper edge of the drop. The zero on the scale is then brought to coincide with the upper edge of the drop whilst the crosschair line is made to coincide with the lower edge. The whole number of the scale reading can be seen in the ocular, the tenth and hundreth on the micrometer. Thus, optical reading of drop diameter can be made to an accuracy of three decimal places (on a vernier scale).

The measuring process is very straightforward. The capillary system is filled, through valves, with the heavy phase e.g. aqueous surfactant solution. With the tube in motion (≃ 2,000 r.p.m.), a small volume of the lighter oil phase is injected from a

microsyringe. The oil drop formed is brought into the field of view by inclination of the apparatus, and the rotation speed is adjusted to produce a cylindrical drop. The diameter is measured as a function of time in order that equilibrium be attained. In general, the tension quoted is from drops whose diameters remained constant for at least 1 h. The drop volume varies depending on the tension. Typically, for ultralow tensions (< 0.1 mN m^{-1}) 5 mm^3 are injected at low speeds ($\simeq 2{,}000$ r.p.m.), but volumes as high as 50 mm^3 and speeds > 5,000 r.p.m. are needed to measure tensions of the order of 20 mN m^{-1}.

After the measurement, the drop is rejected and the capillary is cleaned out with $\simeq$100 cm^3 of the new aqueous phase before a new measurement is made. For tensions measured at temperatures above $\simeq$40°C, it was necessary to degas the aqueous samples first, since air bubbles developed in the capillary. Degassing was achieved by attaching a water pump and causing the solution to foam.

For the common capillary tubes with an inner diameter of 2.5 mm, it is possible to measure tensions as low as 10^{-4} mN m^{-1} and as high as 50 mN m^{-1}, depending on the density difference between phases. The spinning-drop method is therefore a reasonable extension of the ring and plate methods for measurements of low interfacial tension. An outstanding advantage of the method is that an interface can be studied which is not in direct contact with any solid surface. Thus, the uncertainties caused by an unknown contact angle in the plate or capillary rise methods, or by deviations from cylindrical symmetry in pendant or sessile-drop methods, are avoided.

The most serious disadvantages of this method are, on the one hand, the formation of artifacts e.g. 'dumbell' or 'dogbone' drop shapes which can appear when the tension is low, and, on the other hand, the difficulty of specifying criteria characteristic of hydrodynamic equilibrium. Drop shapes other than cylindrical are avoided by increasing the speed of rotation. As will be seen later, a reasonable test of equilibrium is the agreement (or otherwise) between tensions from phases that have been contacted prior to measurement and those obtained from systems not originally at equilibrium.

2.2.3 Calibration of spinning-drop tensiometers

To transform equation 2.3 into one containing direct measurable quantities, it is necessary to define a magnification factor X, which depends on both the refractive index of the more dense liquid and thermostatting oil, and also on the temperature. Equation 2.3 can be redefined as

$$\gamma = X\, d^3\, n^2\, \Delta\rho \qquad (2.4)$$

where d is the apparent drop diameter in vernier units and n is the capillary rotation speed in r.p.m. Manning and Scriven[57] recommended calibration of the measurement of d using low density plastic rods or hollow cylinders which centre themselves at the axis of rotation of the tube. This was attempted using a steel wire of diameter 1.000 mm and a silvered glass capillary, both floating in an aqueous phase. Unfortunately, neither appeared to centre correctly and measurement of d was suspect.

An alternative calibration is to measure the product $d^3\, n^2$ for various pairs of liquids whose mutual interfacial tensions

are reliably available. From equation 2.4, a plot of $\gamma_{(lit)}/\Delta\rho$ against $d^3\ n^2$ should be linear of slope X. Obviously, this method depends crucially on the purity of materials. In this work, a series of n-alkanols were pre-equilibrated with water in order to mutually saturate both phases. Intermittent shaking in a water bath held at 25 ± 0.1°C was performed for a period of two days. Subsequently, the aqueous phase was transferred into the reservoir and capillary of the tensiometer, and the organic phase into a syringe for injection. Values of d were measured at varying n and Figure 2.2 shows sample calibration plots using interfacial tensions and density differences taken from reference 58.

The data in reference 58 was obtained using high grade materials which were further purified by fractional distillation. Tensions were measured by the pendant drop technique[59] and showed no ageing effects. Since there are no systematic variations in plots like those in Figure 2.2, the purity of our ('puriss' grade) materials is assumed to be very high.

Values of X for both tensiometers with high and low magnification eyepieces are given in Table 2.1. Calibration in this way was only performed at 25°C. In theory, corrections should be made for application at other temperatures due to changes in the refractive index of the aqueous phase, but since the refractive index of water decreases by only 0.5% between 10 and 70°C, it was thought that the magnitude of these differences would be small.

Figure 2.2 Calibration plots for Site 04 spinning-drop tensiometer

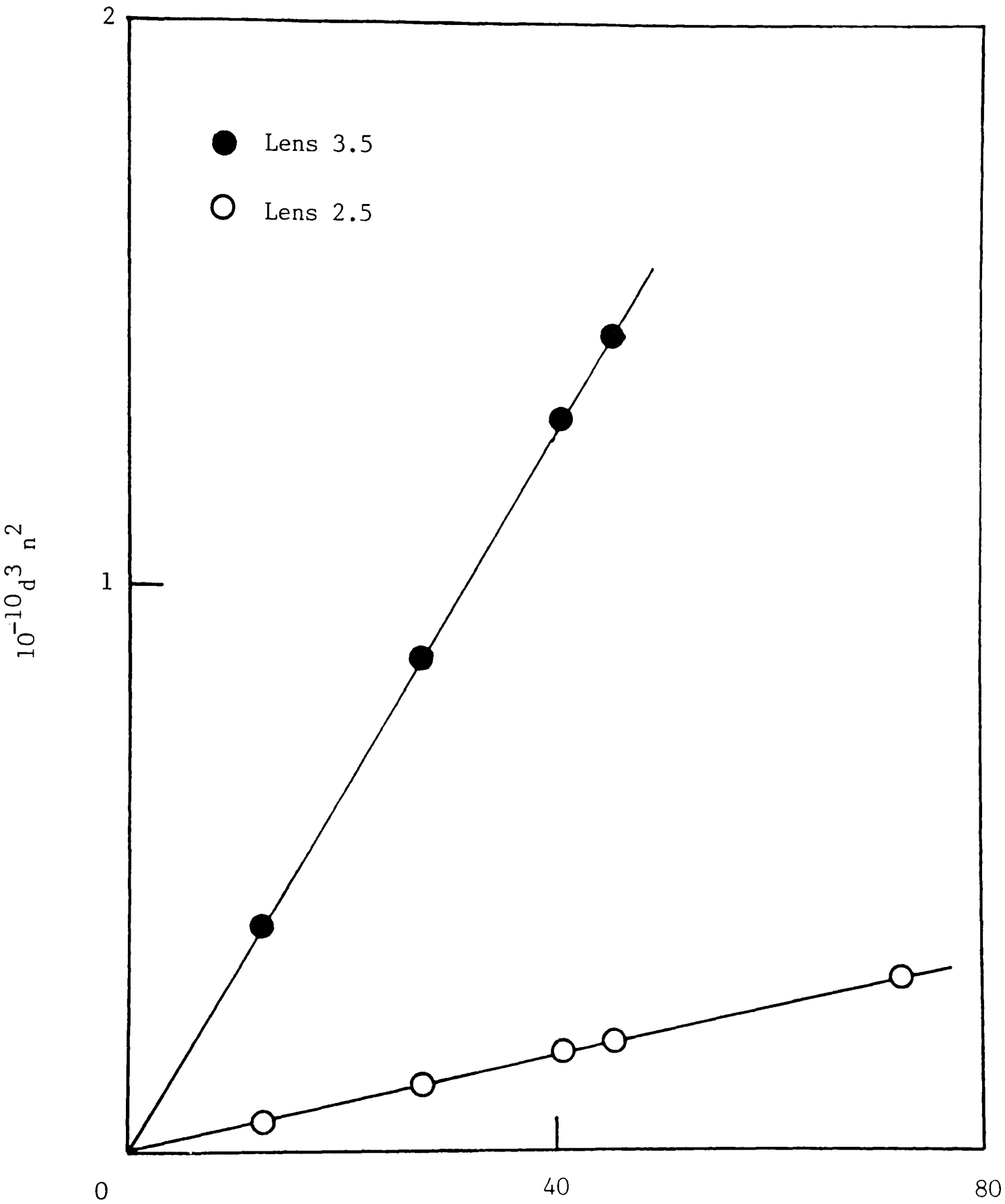

Figure 2.2 Calibration plots for Site 04 spinning-drop tensiometer

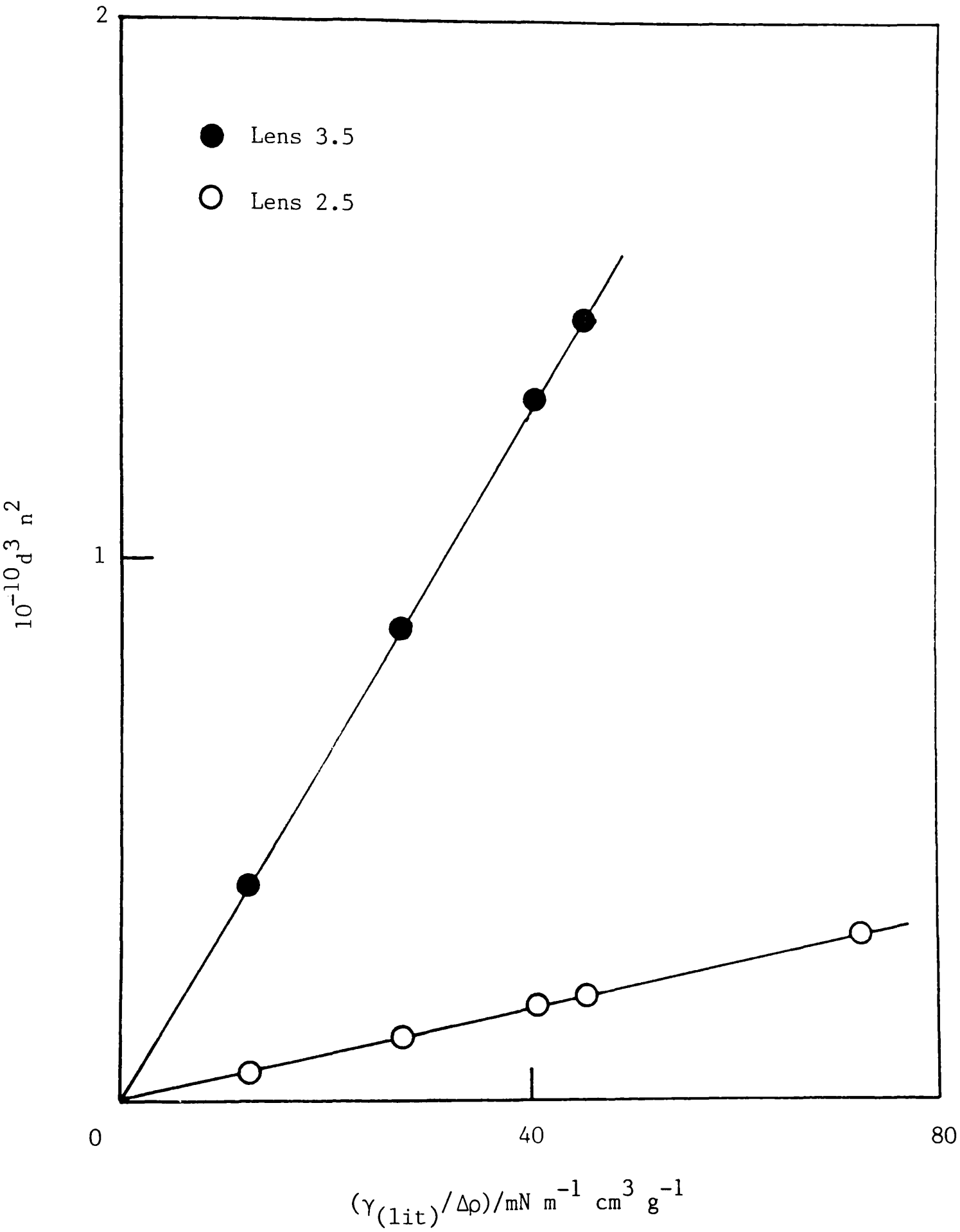

Table 2.1

Values of X determined in connection with equation 2.4

Tensiometer	Eyepiece magnification	
	x 2.5	x 3.5
Site 02	2.49×10^{-8}	1.68×10^{-9}
Site 04	2.29×10^{-8}	3.13×10^{-9}

For a fluid-like oil-water interface, the measured interfacial tension should be independent of the speed of rotation of the capillary. That this is the case can be seen in Figure 2.3 for a system containing Aerosol OT (see later). Puig *et al.*[29] have reported tensions in systems containing Texas 1 that were dependent on capillary speed and attribute this to a viscous coating of liquid-crystalline material around oil drops. No such effects were observed in tensions at equilibrium reported in this thesis. A fuller discussion concerning shapes and appearances of spinning drops will be given in Chapter 3.

2.3 Photon Correlation Spectroscopy

2.3.1 Introduction

One of various techniques used for the investigation of the dynamics of particle motion in solution is photon correlation

Figure 2.3 Plot of the recorded tension, γ, against the frequency of rotation n of the capillary for the system AOT + heptane + aq. 0.1 mol dm^{-3} NaCl at 25°C.

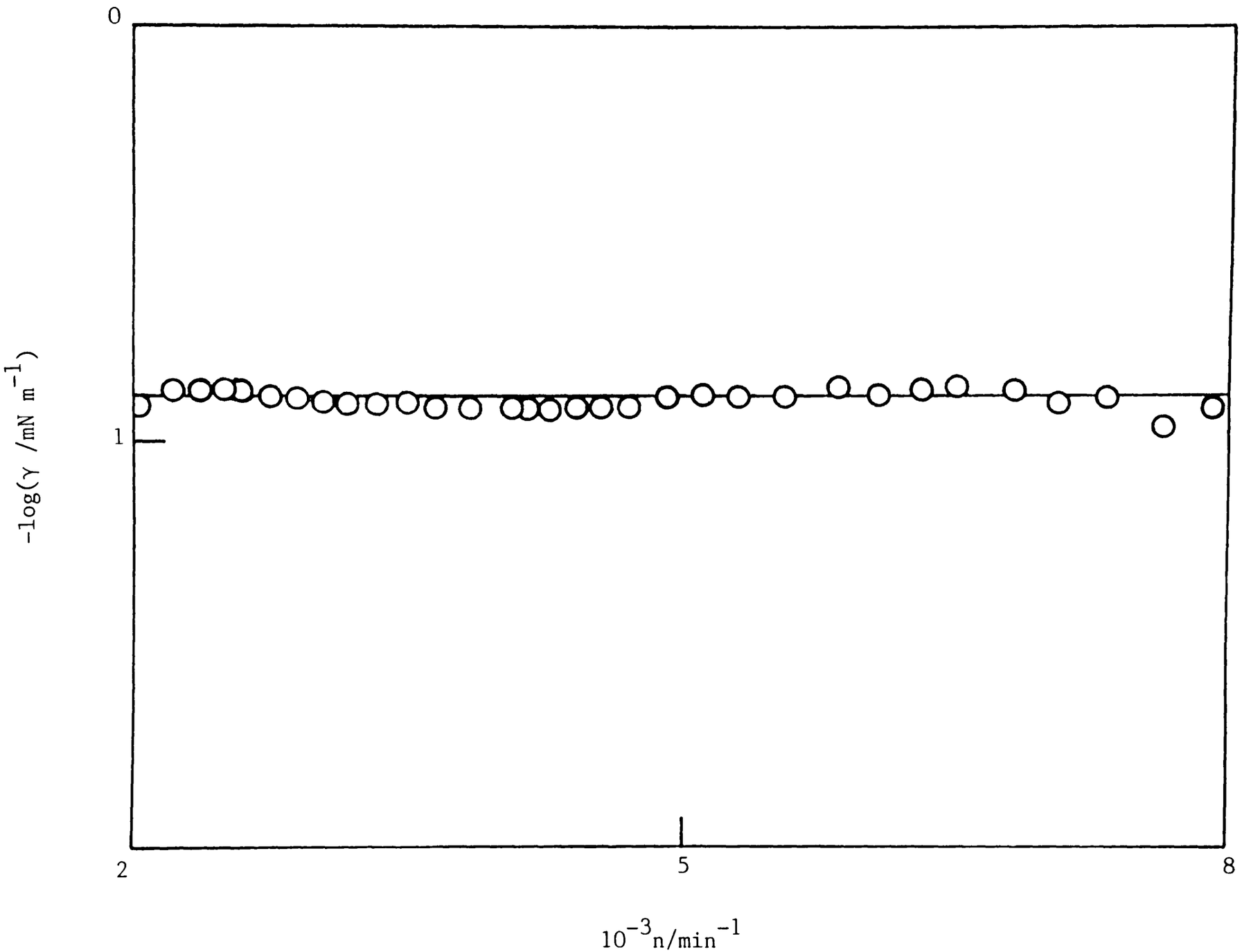

spectroscopy (P.C.S.).[60] The technique has rapidly developed since the advent of the laser and has found a wealth of applications in physics, chemistry and biology including work on latex particles.[61] It has also been used extensively to study micellar and microemulsion systems in aqueous solutions.[62] The first reports of studies of water/AOT/organic solvent systems were in 1978 by Day *et al.*,[63] and by Zulauf and Eicke.[64] Other water-in-oil microemulsion systems have been investigated e.g. in reference 65.

Photon correlation spectroscopy is concerned with the time dependent fluctuations in the intensity of light scattered from a sample. When plane-polarised light is directed at a system containing a dispersed phase e.g. liquid droplets in a dispersion medium, the intensity of light scattered at a particular angle depends on the number of droplets per unit volume, their size and their relative positions. As a result of Brownian motion, their relative positions will vary with time, and so the constructive and destructive interference between waves scattered from individual droplets will vary as the result of translational and rotational diffusion. This gives rise to fluctuations in the intensity of light scattered from the sample.

The rate of fluctuations will depend on the rate of movement of the droplets. It also depends on the angle θ at which the scattered light is observed with respect to the incident light. For microemulsions, the coherence time, t_c, which is the time taken for a maximum to replace a minimum, is in the millisecond region. It can be shown that

$$t_c = \frac{1}{2DK^2} \qquad (2.5)$$

where D is the diffusion coefficient and K is the scattering vector correcting the scattering angle with the refractive index p of the medium, and is given by

$$K = \frac{4\pi}{\lambda} \; p \sin\left\{\theta/_2\right\} \qquad (2.6)$$

In P.C.S., the fluctuations in intensity are analysed in time domains. Two experimental techniques are possible. In the heterodyne experiment, the scattered light is mixed with unscattered laser light which is then measured. The homodyne experiment is an analysis of the scattered light alone. The difference is that the homodyne technique displays a frequency twice that of the heterodyne. The spectrometer used in this work had been designed to give homodyne signals.

2.3.2 Apparatus

The layout of the photon correlation spectrometer is shown in Plate 3. A Spectra Physics 15 mW He-Ne laser (λ = 630 nm), powered by a Spectra Physics exciter supply, was directed at the centre of a cell compartment, centred at the axis of a goniometer (Malvern Instruments P.C.S. 100 SM). All this was mounted on a concrete support for maximum stability. A photomultiplier, mounted on the swinging arm of the goniometer, could be adjusted to scattering angles between 0 and 150° relative to the laser beam. Photons registered at the photomultiplier were counted by a Malvern dual function digital correlator (type K7027) and the correlation function calculated. The function generated was transferred to a Commodore 4023 printer for analysis.

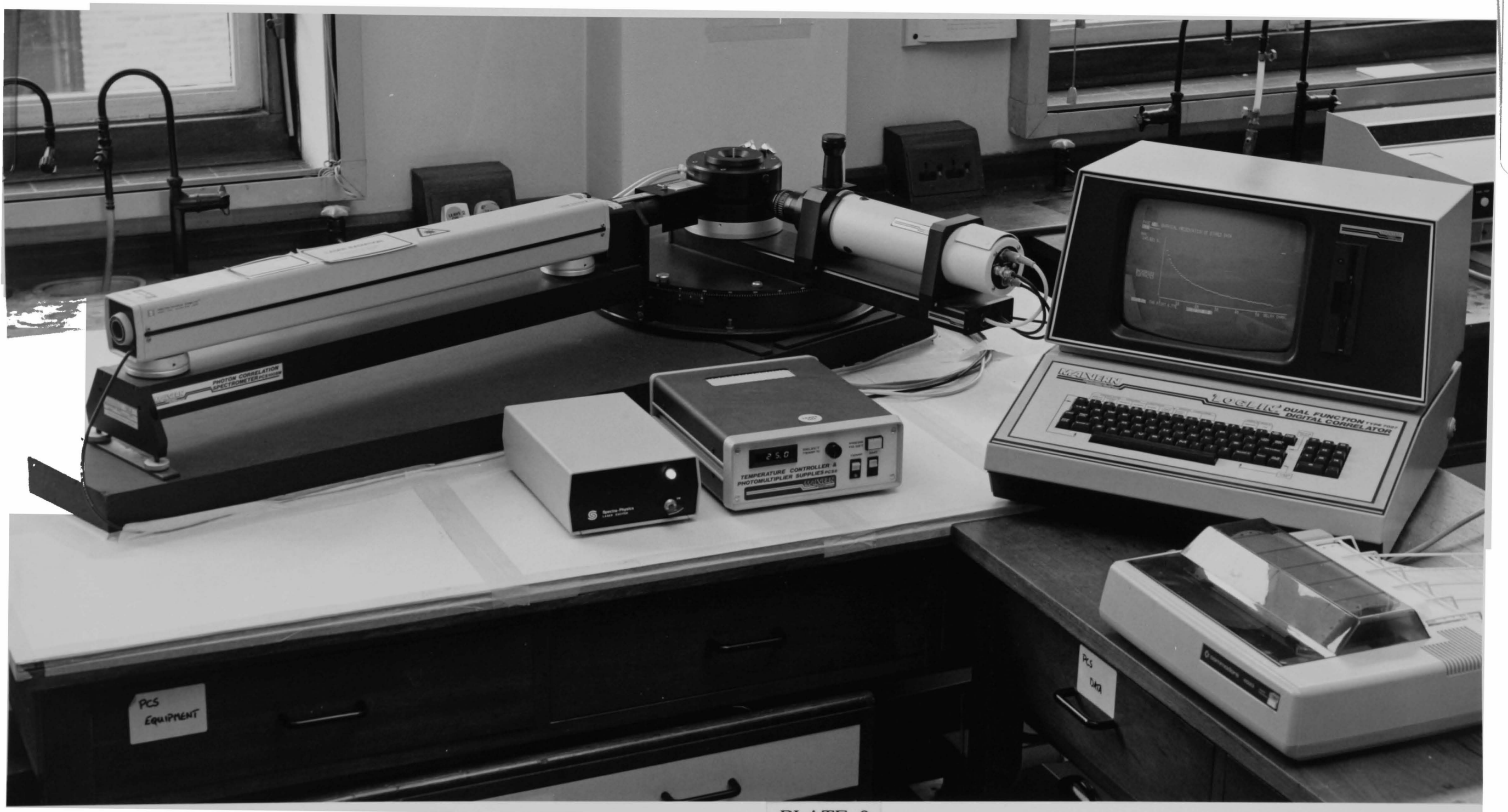
PHOTON CORRELATION SPECTROMETER
TEMPERATURE CONTROLLER & PHOTOMULTIPLIER SUPPLIES
LOGLIN DUAL FUNCTION DIGITAL CORRELATOR
PCS EQUIPMENT
PCS DATA

PLATE 3

The sample cells (1 x 1 cm fluorescence cuvettes) were mounted in a cylindrical glass dish containing water, the temperature of which was controlled using a Malvern temperature controller (P.C.S. 8). The scattered light intensity was converted into bursts of photons which were registered as pulses from the photomultiplier and its associated amplifier/discriminator. Peaks of intensity were observed as 'bunching' in the pulse train (see Figure 2.4). This type of signal was fed directly into the digital correlator.

Figure 2.4

Intensity fluctuation of scattered light with real time

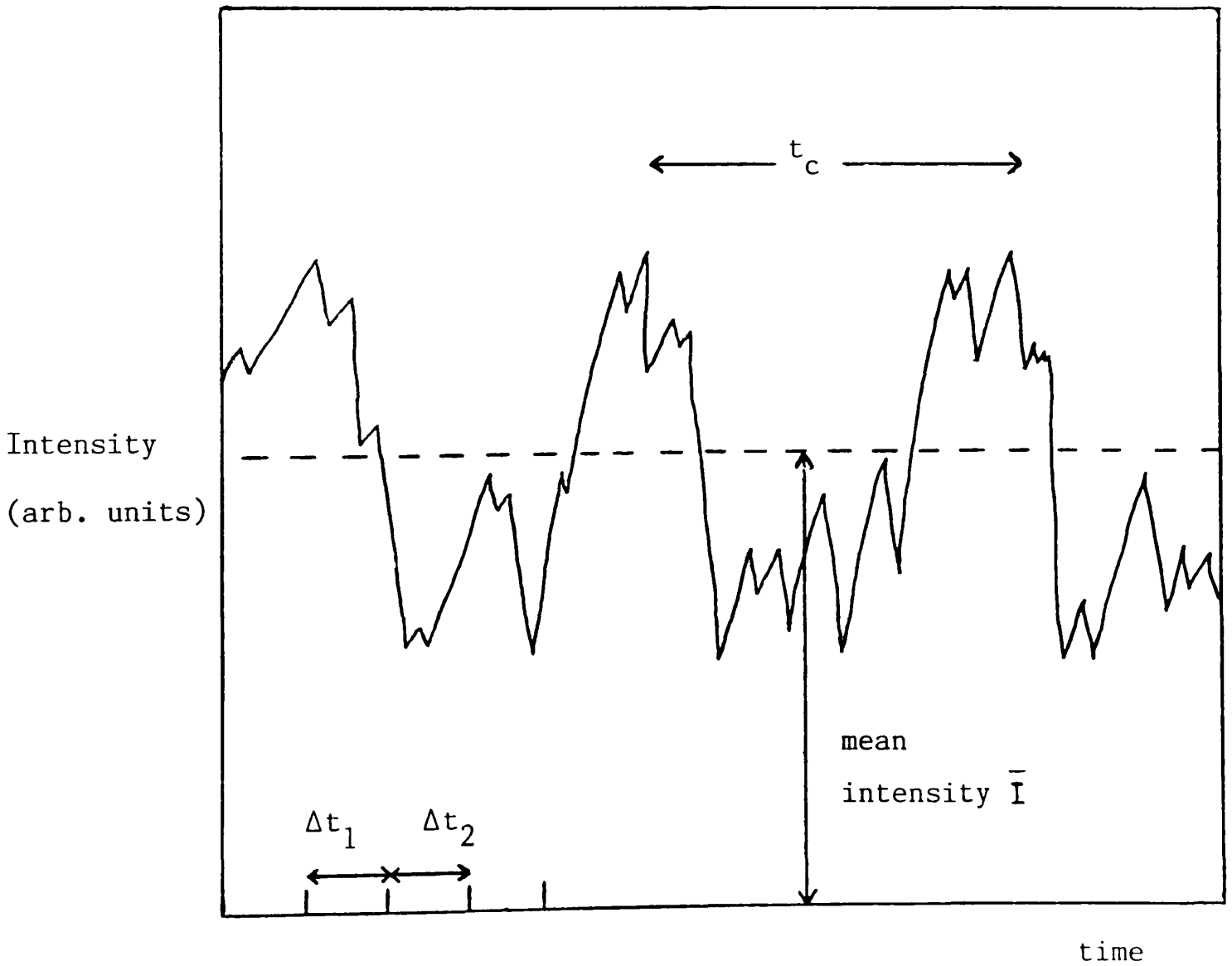

The correlation function of the intensity of scattered light measures the similarity between a fluctuation in intensity over one period of time and another. In a digital correlator, the correlation time T is divided into many short intervals, Δt, called sample times. The intensity of light at a given time can be expressed as the number of photons collected over a period of time, Δt. The correlation function is then formed by multiplying the number arriving in the current sample time with all previous samples, up to the maximum time T.

As a further simplification, the copy of the signal is 'clipped' i.e. if the number of photons arriving in the current sample time is greater than some preset value C, then the signal fed in is set to 1, otherwise 0. The correlation function G(t) can be expressed as[66]

$$G(t) = \sum_{i=1}^{N} n_i \, m_{i-k}$$

where: N is the total number of samples taken in an experiment

$k = 1,2 \cdots M$

M is the number of correlator channels (60) i.e. $M\Delta t = T$

n_i is the number of photons arriving in the i'th sample time

$m_i = 1$ if $n_i > C$

$= 0$ is $n_i \leqslant C$

In most cases one sets the sample times so that the correlation function forms in the early part of the store and has decayed significantly by the end of the store i.e. so that T is considerably larger than the duration of structure of interest

in the correlogram. The value to which the correlation function will decay as $T \rightarrow \infty$(where all signals must be uncorrelated) forms the baseline of the signal. This may be measured due to the inclusion of a post-computational delay in which the last four channels (delay channels) are pushed out to long sample times.

2.3.3 A typical measurement

Samples should be as free from dust as possible. Filtration of solutions through Millipore filters is necessary. The sample time is best set by observing the trace building up on the screen. Ideally, the intensity should fall to about 5% of the amplitude in the screen width. Before running an experiment the burst time should be set. The choice of this is very much dependent on the scattering power of the sample and the correlation amplitude, but is usually of the order of one second. Whilst the correlator is running the trace should be observed to ascertain if there are any irregular features in the growth of the profile. Occasional 'leaps' of the function followed by a downward tilting of the tail of the profile are commonly observed. This is caused by dust floating through the laser beam in the sample. If a 'clean' trace is observed, the correlator is run for the full period.

To analyse the decay, some measure of the baseline must be made. The far point (i.e. at time $\rightarrow \infty$) of the correlation function is in principle equal to the square of the total count. It can be measured from the 4 delay channels provided by the correlator. In addition, the monitor channels are used to calculate the theoretical baseline. A value of the baseline discrepancy (BD) of the correlation function is given after

normalisation of the traces. In practice it is usual to abort experiments with BD > 0.01.

The P.C.S. programme requires values for various constants related to the sample for use in the calculation of the size of the particles. These include the temperature, the scattering angle, the solution refractive index and the viscosity of the solvent.

2.3.4 *Data analysis*

For a solution of monodisperse, non-interacting spheres the normalised correlation function, G'(t) can be described by a single exponential i.e.

$$G'(t) = B \exp(-\tau t)$$

where B depends on the area of detector and the effect of clipping and is typically ≃ 0.6. The decay rate constant, $\tau\,(s^{-1})$, is related to the diffusion coefficient, D, by

$$\tau = 2DK^2 \qquad (2.7)$$

Polydisperse samples will have correlation functions which can be described by a sum of exponentials. One treatment of polydispersity has been developed by Koppel[67] which treats the function as a cumulant expansion. The analysis procedure evaluates τ and the normalised variance, which is a measure of the polydispersity of the distribution. This approach has been used in the present work. The relation between D and the particle size will be discussed in Chapter 3.

2.3.5 Testing of P.C.S.

The parameters derived from correlation functions collected at different angles provide a stringent test for the optical arrangement of the instrument. The angular dependence of correlation functions obtained for a water-in-heptane microemulsion containing 0.034 mol dm^{-3} AOT was investigated for this reason. Table 2.2 lists the values of τ as a function of θ, together with the calculated values of the scattering vestor K (from equation 2.6), and derived values of D (from equation 2.7). In Figure 2.5, τ is plotted against K^2; the data are seen to be linear with respect to K^2 with a zero intercept, in accordance with equation 2.7. Since in the present work no information concerning angular variations was sought, measurements were restricted to $\theta = 90°$.

2.4 Analytical determinations

2.4.1 Anionic surfactant

The two-phase Epton titration[68] for the determination of anionic surfactants is now the method universally accepted for the analysis of these materials. The method relies on the fact that an anionic surfactant will react with a cationic surfactant to form a salt which usually lacks surfactant properties; the end point is obtained using an indicator.

The mixed indicator used consists of the anionic dyestuff disulphine blue VN and the cationic dyestuff dimidium bromide. It is usually used as an acidic reagent. The cationic titrant preferred is a tetra-substituted ammonium salt called Hyamine 1622. Very good endpoints are obtained with this combination.

Table 2.2

Angular dependence of the decay rate for 0.034 mol dm^{-3} AOT, W/O microemulsion at 25°C.*

Scattering angle, θ	$10^{7}K/m^{-1}$	$10^{14}K^{2}/m^{-2}$	$10^{-4}\tau/s^{-1}$	$10^{11}D/m^{2}\ s^{-1}$
20	0.472	0.223	0.16	3.59
30	0.704	0.495	0.33	3.33
40	0.929	0.864	0.58	3.36
50	1.149	1.320	0.90	3.40
60	1.359	1.847	1.25	3.38
70	1.559	2.431	1.70	3.50
80	1.747	3.053	2.11	3.46
90	1.922	3.694	2.44	3.30
100	2.082	4.336	2.89	3.33
110	2.227	4.958	3.24	3.27
120	2.354	5.541	3.71	3.35
130	2.463	6.069	4.08	3.36
140	2.554	6.524	4.44	3.40
150	2.625	6.893	4.74	3.44

* The microemulsion used for the above work was of R value (defined as $[H_2O]/[AOT]$ in the heptane phase, see later) equal to 65.5.

Figure 2.5 Plot of τ against K^2 for AOT water-in-heptane microemulsion

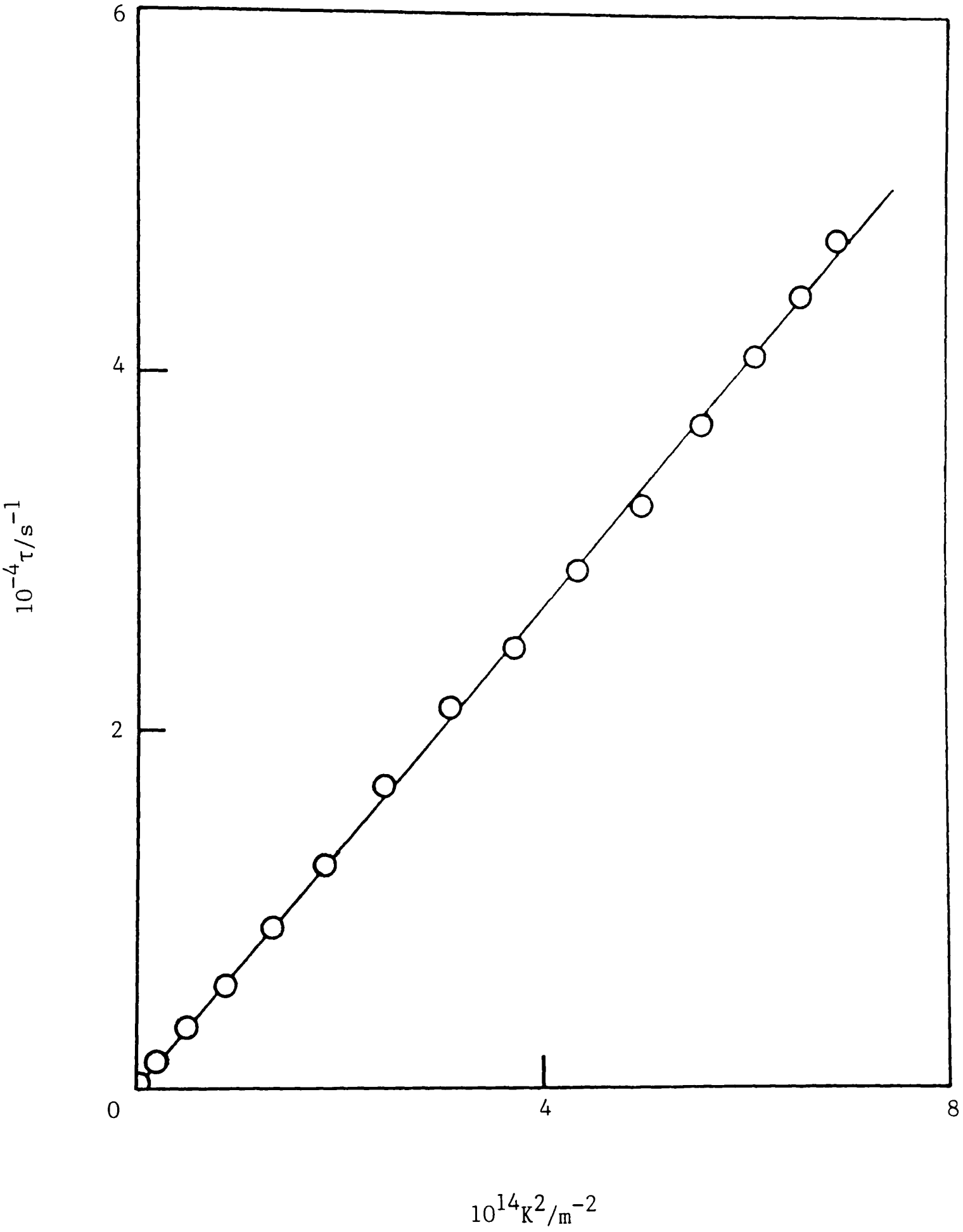

The titration proceeds in a two-phase system, following the observation by Jones[69] that the anionic salt of a cationic dye is soluble in chloroform, whereas the normal chloride salt is insoluble and remains in the aqueous phase. The following colour changes take place during the course of the titration:

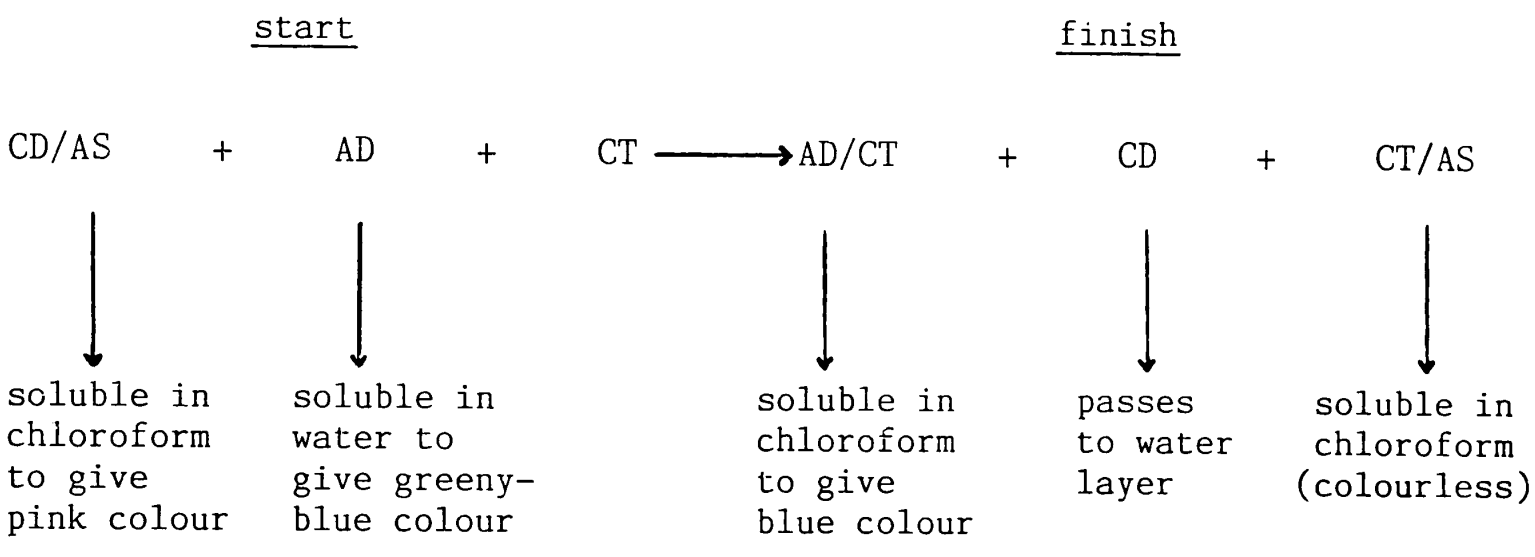

where AS = anionic sample CD = cationic dyestuff
CT = cationic titrant AD = anionic dyestuff

The colour change is observed in the chloroform layer, which is coloured pink in the presence of excess anionic sample and blue with excess cationic titrant. The endpoint is a grey-blue colour which probably coincides with the transfer of a small quantity of the anionic dye/cationic salt to the chloroform layer. The clarity of the mixed indicator is superior to that of any indicator for two-phase titrations which have been examined.

The data concerned with the stoichiometry of the reaction indicates that one mole of anionic-active material reacts with 0.96-0.97 moles of Hyamine. It appears desirable to employ a pure anionic-active material as reference standard, therefore, in order that this deviation from true stoichiometry does not affect the accuracy of the analysis. Analytical tests indicated that the specially purified grade of sodium dodecyl sulphate (SDS) obtainable from B.D.H. was of adequate purity for use as a reference standard.

The method described below may be applied to the analysis of alkyl sulphates, alkylbenzene sulphonates and dialkylsulphosuccinates amongst others. The accuracy of the method is of the order of ± 2% of the determined value. All reagents for the titration were purchased from Fluka. The anionic purity of SDS from B.D.H. was first assessed. A weighed amount was refluxed with exactly 25 cm^3 of 1.0 mol dm^{-3} sulphuric acid for 2 h. After cooling, phenolphthalein indicator was added and the solution titrated with standardised 1.0 mol dm^{-3} sodium hydroxide. The purity determined in this way was 99.1 ± 0.2%. The Hyamine was then standardised by taking 20.0 cm^3 of a 0.004 mol dm^{-3} SDS solution in water, adding 10 cm^3 of water, 15 cm^3 of AnalaR chloroform and 10 cm^3 of the acid indicator solution. This was titrated with 0.004 mol dm^{-3} Hyamine solution, with vigorous shaking between each addition.

A similar titration procedure was employed to determine unknown concentrations of surfactant in equilibrium aqueous phases. For oil phase analyses, it was first necessary to evaporate the solvent and then make up an aqueous solution with the surfactant

residue. At least two determinations were made per sample. Examination of the influence of adding various concentrations of alkanol to the aqueous phase during titration showed that no interference occurs. This was done in anticipation of work to be carried out using alkanol cosurfactants.

2.4.2 *Nonionic surfactant*

One of the most accepted methods for the determination of polyoxyethylene-type nonionic surfactants in low concentration is that developed by Greff *et al.*,[70] based on the formation of a blue complex between surfactant and ammonium cobaltothiocyanate reagent. This complex is extracted into benzene from a saturated salt solution and its absorbance compared to that of a standard. The reaction probably involves oxonium ion formation and subsequent precipitation. Wurzschmitt[71] postulated that ammonium ion is complexed by the ether oxygen of polyethoxylated compounds, forming a cationic oxonium ion. This in turn reacts with suitable anions:

$$R\text{-}CH_2\text{-}(O\text{-}CH_2\text{-}CH_2)_m\text{-}CH_2OH + M^+X^- \longrightarrow [R\text{-}CH_2\text{-}(\underset{\displaystyle M}{O}\text{-}CH_2\text{-}CH_2)_m\text{-}CH_2OH]^{m+}X^{m-}$$

With ammonium cobaltothiocyanate, the ammonium ion would react to form the oxonium ion, which would then be precipitated by the cobaltothiocyanate anion $[Co(SCN)_4]^{2-}$.

The reagent was prepared by dissolving 620 g of B.D.H. AnalaR ammonium thiocyanate and 280 g of B.D.H. AnalaR cobalt nitrate hexahydrate in one litre of water. For aqueous phase determinations, 20 cm^3 of sample were placed in a separating funnel. After

addition of 3 cm^3 of reagent and 10 g of sodium chloride, the mixture was shaken to dissolve the salt and left to stand. Exactly 5.0 cm^3 of benzene were added, shaken and the organic layer centrifuged for 10 minutes. The peak absorbance at 325 mm was measured using an LKB Spectrophotometer and 5 cm^3 matched quartz cells, against a reagent blank. For oil phase determinations, various quantities of oil (from 100 mm^3 to 0.5 cm^3) were mixed directly with the salt/reagent/benzene solution and reproducible readings were obtained. In one determination, the oil was removed completely and no difference in absorbance was detected. Calibration was achieved by measuring absorbance as a function of nonionic surfactant concentration in water.

2.4.3 Water

The analysis for water in oil phases was performed via the Karl Fischer technique[72] using a Baird and Tatlock AF3 automatic titrator. The method, as formulated by Fischer and modified by Smith *et al.*,[73] relies on the chemical reaction between iodine, sulphur dioxide and water in the presence of anhydrous methanol and pyridine. It may be represented as:

$$SO_2 + I_2 + H_2O + 3C_5H_5N \longrightarrow 2C_5H_5N.HI + C_5H_5N\begin{cases}\diagup \\ \diagdown\end{cases}\begin{matrix}SO_2 \\ | \\ O\end{matrix} \qquad \text{(a)}$$

$$C_5H_5N\begin{cases}\diagup \\ \diagdown\end{cases}\begin{matrix}SO_2 \\ | \\ O\end{matrix} + CH_3OH \longrightarrow C_5H_5N\begin{cases}\diagup \\ \diagdown\end{cases}\begin{matrix}SO_4CH_3 \\ \\ H\end{matrix} \qquad \text{(b)}$$

Since each mole of iodine is equivalent to one mole of water, the principle is that the sample is dissolved in a moisture free

solvent e.g. methanol, and titrated with standardised Karl Fischer reagent to an endpoint detected in this case electrometrically.

Initial calibration using pure water was necessary in order to determine the water equivalent of the Karl Fischer reagent (B.D.H. AnalaR). Because of instability of the reagent, this was carried out immediately prior to any measurements. Care was taken to ensure that the conditions of the determination conformed as closely as possible to those of standardisation. Weighed amounts of alkane phase were then admitted to the titration vessel as quickly as possible and a digital readout of mg H_2O was taken. At least three separate determinations were made for each solution. The accuracy was better than 1 mg/cm^3 and concentrations were always greater than 20 mg/cm^3.

2.5 General experimental techniques

2.5.1 Conductance measurement

The conductances of macroemulsions were measured using a digital conductivity meter with the added facility for the digital read-out of temperature (Jenway, model PCM3). Typically, the separate oil and water phases were mixed using a magnetic stirrer and temperature was controlled using a water bath on a hotplate. Measurements were made on well mixed systems after stabilisation of the reading had occurred.

2.5.2 Viscosity measurement

Ubbelohde viscometers were suspended vertically in a glass tank containing water. Thermostatting by this method was to ± 0.1°C. The viscometers were calibrated by measuring flow times of various

pure liquids of known viscosity.[74] Outflow times were reproducible to < 0.4 s and since these were always > 200 s, kinematic viscosities were accurate to ± 0.2%.

2.5.3 *Density measurement*

Densities of all the hydrocarbons used and of water-in-oil microemulsions stabilised by Aerosol OT were measured at 25.0°C using a Paar DMA 55 densimeter. Thermostatting was by means of a Haake F3-C water thermostat. Densities of alkanes and aqueous salt solutions at other temperatures were obtained from data in reference 74.

2.5.4 *Refractive index measurement*

A thermostatted Abbé refractometer and sodium lamp were used to measure the refractive indices of microemulsions stabilised by both Aerosol OT and dihexylbenzene sodium sulphonate (see later). Measurements could be made to ± 0.0001 and were corrected to $\lambda = 630$ nm (the laser wavelength).[75]

2.5.5 *Preparation of glassware*

All glassware was washed thoroughly in chromic acid, rinsed twice with hot water and then three times using ultrapure water. Drying was achieved using a surface-chemically clean oven.

2.5.6 *Distribution procedures*

In order to allow transfer of components between aqueous and oil phases, batches of up to a dozen 100 cm^3 stoppered flasks were shaken mechanically in a thermostat for several days. The

surfactant was either initially in salt solution and mixed with pure oil, or was dissolved in oil and mixed with an aqueous phase. A variety of phase volume ratios were employed depending on whether the variable was salt concentration, alkane chain length etc., and details of these will be given in the appropriate chapters. In addition to gentle mechanical shaking, the contents of the flasks were shaken more vigorously by hand at the start of the equilibration period.

In general, the phases were separated when the upper and lower phase appeared clear. In some cases, a third phase formed (between aqueous and oil phases) which was of low volume and milky in appearance. Phases were carefully pipetted into sample tubes for analysis and then recombined in the spinning-drop apparatus to determine equilibrium tensions. In the latter experiments, it was only possible to measure oil-water tensions; injection of the third phase resulted in it being dispersed into the aqueous phase, presumably because of the very low tension between them.

2.6 Materials

2.6.1 Water

All water was distilled once, passed through an Elgastat ion-exchange column and then through a Milli-Q reagent water system. Water treated in this way had a surface tension against air (determined by various methods) of 71.9 ± 0.1 mN m^{-1} at 25.0°C in excellent agreement with the best literature values.[76,77] Although this does not give a measure of the absolute purity of the sample, it shows that there are no significant quantities of

surface-active impurities present, which is of prime importance in the present work.

2.6.2 Hydrocarbons

The hydrocarbons were obtained from various commercial sources as either 'purum' or 'puriss' samples and the purities were generally greater than 99%. Further purification was achieved by percolating the sample twice through chromatographic alumina to remove traces of polar impurities. Table 2.3 lists the source and final purity, as estimated by gas-liquid chromatography, of each sample.

Oil-water interfacial tensions showed no ageing and were in good agreement with previously reported values.[78]

2.6.3 Inorganic salts and n-alkanols

Table 2.4 lists the sources and purities of the salts and alkanols used. In particular, the sodium chloride was used as received, after confirmation that aqueous solutions had surface tensions in agreement with those obtained using samples roasted for 12 h at 450°C.[79] The salts were dried and stored in a dessicator.

2.6.4 Surfactants

(i) Sodium bis-(2-ethylhexyl)sulphosuccinate (Aerosol OT, AOT) was obtained from the Sigma chemical company and used without

Table 2.3

The purities of various hydrocarbons

hydrocarbon	source	purity (%)
n-pentane	B.D.H.	99.8
n-hexane	B.D.H.	99.9
n-heptane	Fisons HPLC grade	99.9
n-octane	Fluka purum	99.9
n-nonane	Fluka purum	99.5
n-decane	Fluka purum	99.7
n-undecane	Koch-Light 'puriss'	99.9
n-dodecane	Aldrich Chem. Co. Ltd.	99.9
n-tridecane	Koch-Light 'puriss'	99.8
n-tetradecane	Koch-Light 'puriss'	99.7
n-pentadecane	Koch-Light 'puriss'	99.7
n-hexadecane	Aldrich Chem. Co. Ltd.	99.9
cyclohexane	Fisons Spectrograde	99.8
benzene	Koch-Light 'puriss'	99.6
toluene	Fluka purum	99.5

Table 2.4

The purities of various solutes

material	source	purity (%)
sodium chloride	B.D.H AnalaR	> 99.9
calcium chloride	Hopkin & Williams AnalaR	99.0
n-butanol	Koch-Light 'puriss'	99.6
n-pentanol	Fluka 'puriss'	99.5
n-hexanol	Aldrich > 98%	99.5
n-heptanol	Fluka 'puriss'	99.0
n-octanol	Fluka 'puriss'	99.4
n-nonanol	Fluka 'purum'	99.5
n-decanol	Koch-Light 'puriss'	99.0
n-undecanol	Fluka 'purum'	99.5
n-dodecanol	Fluka 'puriss'	99.6
n-tridecanol	Fluka 'puriss'	99.0
n-tetradecanol	Fluka 'purum'	99.0
n-hexadecanol	Koch-Light 'puriss'	99.5

purification. It has the structure shown below:

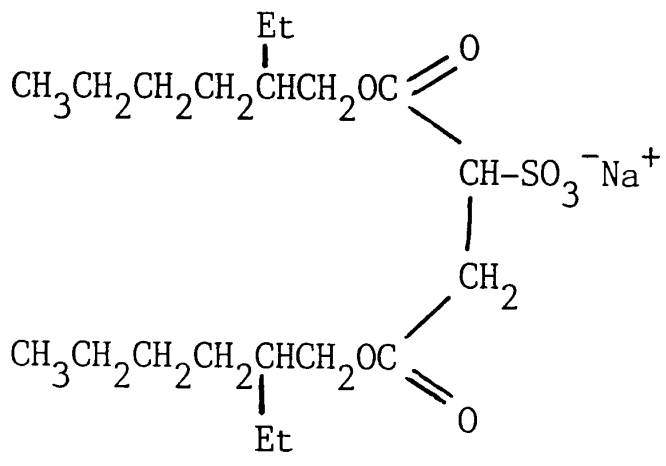

Two different samples were employed and gave complete mutual agreement in the distribution and interfacial tension experiments. The purity, as determined by the Hyamine titration method, was 99.5 ± 1.0%. Elemental analyses were consistent with the molecular formula of $C_{20}H_{37}O_7SNa$:

	expected	found
% C	53.98	53.41
% H	8.32	8.19
% S	7.20	7.08

No minima were observed in plots of surface or interfacial tension against surfactant concentration, indicating the absence of impurities more surface-active than the surfactant itself. Such plots were of the normal shape for a micelle-forming surfactant. Figure 2.6 shows such a plot for three samples of AOT; the agreement between a Fluka purified sample[80] and one from Sigma confirms the purity of the latter. The critical micelle concentration (c.m.c.) is found to be 2.25×10^{-3} mol dm^{-3} at 25°C, comparing well with a value of 2.3×10^{-3} mol dm^{-3} found by

Figure 2.6 Interfacial tensions between heptane and water at 25°C for different samples of AOT

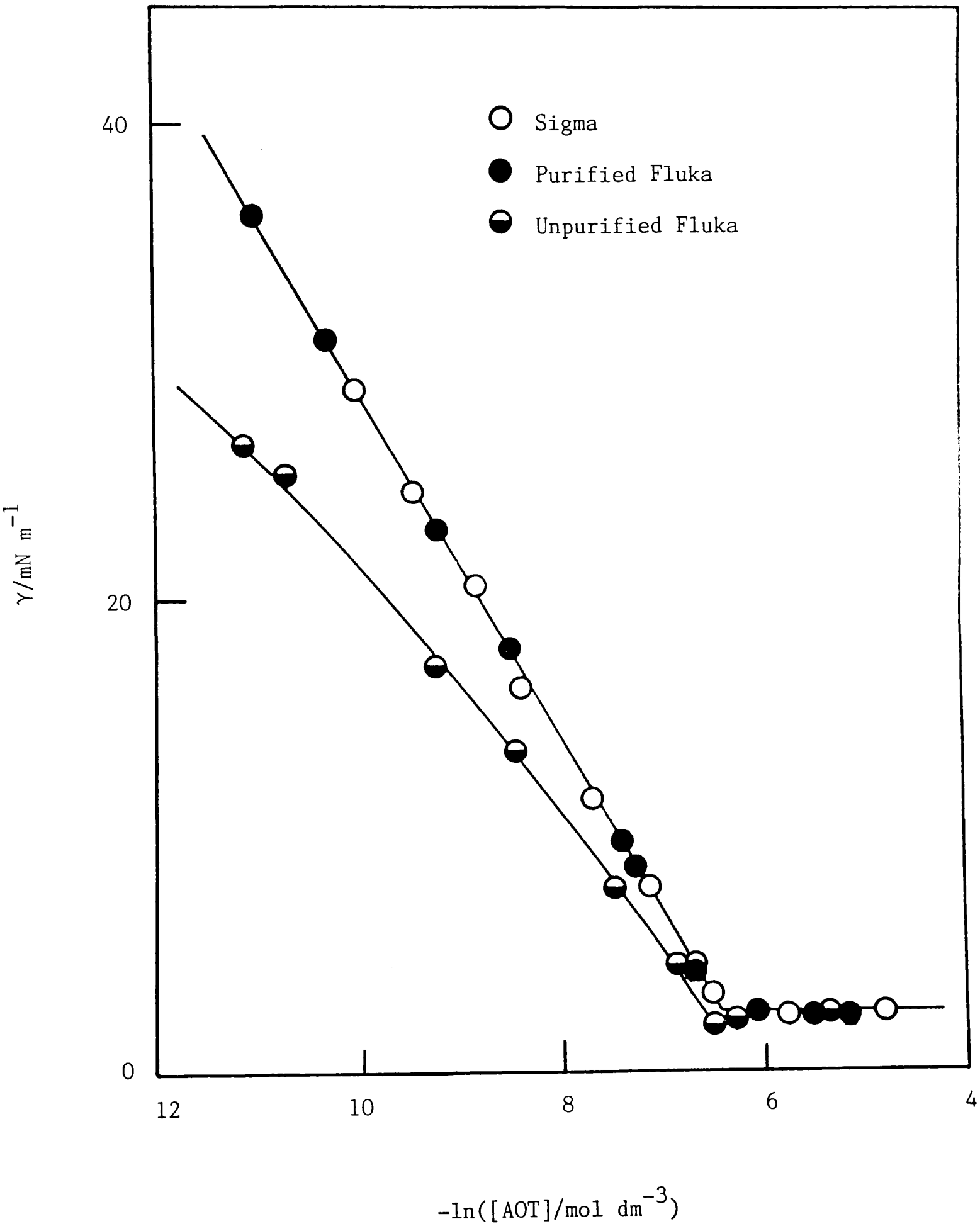

Corkill *et al.*,[81] and 2.52×10^{-3} mol dm^{-3} reported by Williams *et al.*[82]

In most of the experiments undertaken, the AOT was used in the presence of swamping excess of NaCl and one does not expect small amounts of uni-univalent electrolyte impurities to sensibly affect results. However, the presence of divalent metal ions could significantly affect the surfactant behaviour.[83] Using atomic absorption spectrometry, the AOT was found to contain 0.5 ± 0.2 mole % Ca^{2+} ions. In the worst case in the present experiments the molar ratio of Ca^{2+} : Na^{+} is 1 : 7000, and it has been ascertained that addition of Ca^{2+} at the levels as already present has no detectable effect on the low oil-water interfacial tensions of interest.

(ii) Dihexylbenzene sodium sulphonate (DHBS) was synthesised and purified by Dr. E. Tinley's group at B.P. Research, Sunbury and has the structure:

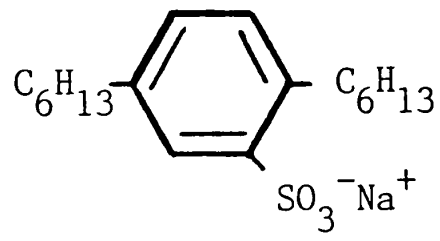

The hydrocarbon, 1,4-dihexylbenzene was sulphonated at low temperature using chlorosulphonic acid and neutralised by sodium carbonate. Purification was by preparative HPLC. The purified product was a colourless, powdery solid. Two samples were each > 99% pure by HPLC and TLC and the ^{1}H and ^{13}C n.m.r. spectra were consistent with the required structure. Tension-concentration plots showed no minima near the c.m.c. and low tensions in systems containing the two samples were in good agreement.

(iii) Sodium dodecyl sulphate (SDS) was a pure sample kindly donated by Fisons Scientific as a PrimaR 99.5% min. pure product. Many sources of this surfactant are known to contain quantities of surface-active impurities, whose presence dramatically affects the adsorption behaviour.[84] A sufficient test of purity was thought to be to compare interfacial tensions of the sample with those (in the literature) of a sample purified very carefully. Such a comparison with results of Cockbain[85] (obtained by the drop-volume technique) for SDS adsorbed at the decane-0.1 mol dm^{-3} NaCl aqueous interface is given in Figure 2.7. Agreement between the two sets of data is excellent, and the area per SDS molecule (0.44 nm^2), obtained from the slope of the graph below the c.m.c. using the appropriate form of the Gibbs equation (see § 1.3), is the same in both cases. The c.m.c. obtained is 1.3×10^{-3} mol dm^{-3}, similar to that (1.4×10^{-3} mol dm^{-3}) given by Vijayendran and Bursh[86] for a similar system but containing heptane. In this latter work however, the area per SDS molecule is quoted as 0.50 nm^2 even though tensions up to about 10 mN m^{-1} are very close to our own (Figure 2.7).

(iv) The nonionic surfactants used were n-dodecyl polyoxyethylene ethers, designated $C_{12}E_m$, of structure:

$$C_{12}H_{25}(OCH_2CH_2)_mOH$$

Pure homogeneous samples were supplied by Nikko Chemicals Co. (Japan) and used without further purification. Gas-liquid chromatographs were enclosed with each sample, a single peak being observed in all cases. The purities (> 99%) were confirmed in this laboratory.

Figure 2.7 Interfacial tensions as a function of SDS concentration at the decane-aq. 0.1 mol dm^{-3} NaCl interface at 20°C

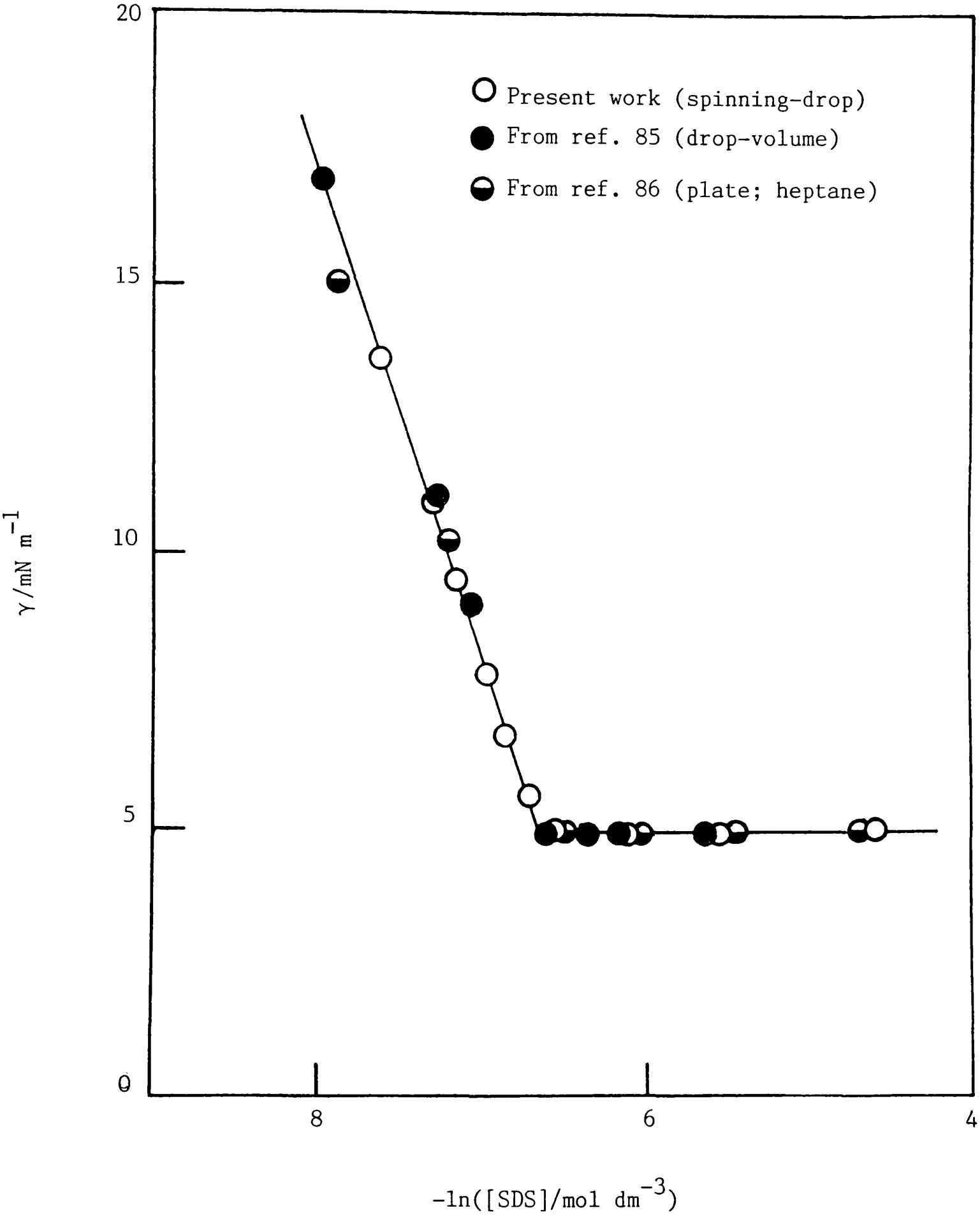

Chapter Three

CHAPTER 3

SALT EFFECTS IN OIL + WATER SYSTEMS CONTAINING THE DOUBLE-CHAIN ANIONIC SURFACTANT AEROSOL OT

3.1 Introduction

Unless otherwise stated the work reported in this chapter is concerned with the system AOT/aqueous NaCl/heptane at 25°C; all original data are listed in Appendix I. The anionic surfactant Aerosol OT has a small double-branched tail. There is evidence that AOT forms an isotropic micellar solution up to the solubility limit of 1.4 wt. % in water at 25°C.[87] Beyond this, various liquid crystalline phases are formed, the nature of which have been investigated by Franses and Hart.[88] In aqueous solutions containing NaCl the solubility limit is reduced.

The nature of surfactant-salt-water mixtures can be dependent on the mode of preparation, e.g. whether surfactant is added to a concentrated salt solution in water or the order of addition is reversed. For all aqueous solutions studied here, the surfactant was first dissolved in water at room temperature and a salt solution was then added to give the required final concentrations. This procedure resulted in relatively optically clear phases. If reagents were mixed in reverse order, turbid solutions formed presumably due to dispersed particles of a surfactant-rich phase, probably liquid crystallites.[30] Solutions

were used within two days of preparation as evidence exists for the hydrolysis of AOT in samples kept for longer intervals.[89]

3.2 Effect of AOT concentration on surface and interfacial tensions

The variation of the surface tension of aqueous AOT solutions with ln (surfactant concentration, m_D) is shown in Figure 3.1, for various concentrations of NaCl, m_s. The shapes of such plots are those expected for an ionic micelle-forming surfactant in the presence of added electrolyte. The agreement between tensions measured by the ring and plate is good. Below the break point, which corresponds to the aggregation point (c.m.c.), the plots are linear over a wide range of concentration. In this region, the surface excess of surfactant, Γ_D, obtained using the appropriate form of the Gibbs equation (see §1.3) is effectively constant and corresponds to the presence of a 'saturated' monolayer. The continuing decrease in tension with increasing bulk concentration after the onset of 'saturation' adsorption is presumably due to an (undetectable) increase in total surface concentration of surfactant. Because the 'saturated' monolayer is incompressible, slight increases in adsorption produce large decreases in the tension.[90]

In the presence of salt, the tension remains constant above the c.m.c. since the activity of the monomers, which adsorb, remains constant. Addition of salt lowers the c.m.c. as a result of the decrease in the repulsion between charged headgroups at the micelle surface caused by screening.[91] A discussion of how

Figure 3.1 Surface tensions as a function of AOT concentration at 25°C.

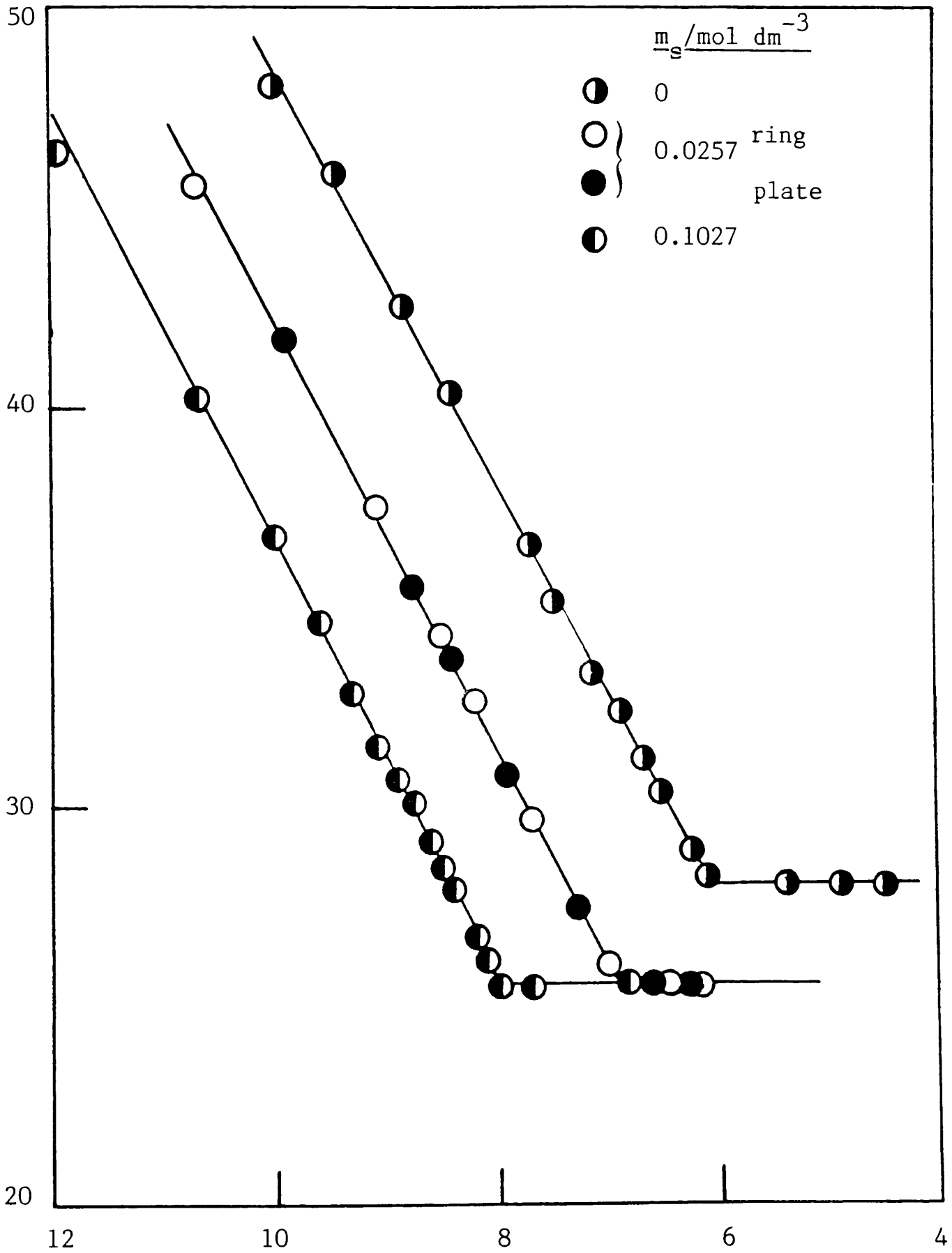

salt affects the area occupied per surfactant molecule at an air-water surface will follow later.

Oil-water interfacial tensions, γ, can be reduced by a much greater extent than air-water tensions, particularly in the presence of, for example, a salt or cosurfactant. Oil + water + surfactant systems are known to exhibit complex phase equilibria, where extremely low interfacial tensions are found between the various phases.[34] Depending on the relative amounts of the components, the mixture may form a single phase or separate into two or three phases. One of these phases is usually a microemulsion that contains most of the surfactant. The partitioning of the surfactant therefore determines whether the microemulsion forms in the lower (aqueous) phase, upper (oil) phase or middle ('surfactant-rich') phase and is in equilibrium with respectively 'excess' oil, 'excess' water, or both. Winsor referred to these respective equilibria as types I, II, and III.[92]

Shinoda and co-workers[93,94] reported that the solubilisation of oil (or water) in micellar (or reversed micellar) solutions is abruptly increased, and a three-phase region composed of water, oil, and surfactant phases appears, as the temperature is raised in nonionic surfactant + oil + water systems. Moreover, they found that low interfacial tensions are attained between the surfactant phase and the oil (or water) phase.[95]

In systems containing a wide range of pure alkylbenzene sulphonates, Wade and co-workers[25] have reported that ultralow tensions are attained in the three-phase region as the salt concentration or alkane chain length is varied. These

investigators in their very valuable and pioneering work have tended to concentrate on producing optimal conditions for low tensions to occur rather than on gaining a detailed insight into the reasons for the existence of the ultralow values.

In any case, it appears that there is a close relationship between phase equilibria involving microemulsions and the occurrence of ultralow interfacial tensions. At present, however, the nature of this relationship is not clearly established. Some of the most recent work on dilute pure anionic surfactant systems has involved the use of 8-phenylhexadecane sodium sulphonate (Texas 1) which forms, rather than micelles, dilute dispersions of liquid crystallites at room temperature.[29,96] In these systems occurrence of ultralow tensions has been attributed to the formation of three-component liquid crystalline phases at the oil-water interface. It is in the nature of the systems that tensions age considerably and cannot be determined reproducibly.

Interesting work has been done on the system sodium dodecyl sulphate + aqeuous NaCl + toluene with butanol added as cosurfactant. In a series of papers, Pouchelon *et al.*[22,34,97,98] argue that in two-phase régimes ultralow tension is associated with a 'very thin' adsorbed surfactant layer, presumably a monolayer. In the three-phase régime, however, tensions between the third ('middle' or 'surfactant-rich') phase and one of the outer (oil or aqueous) phases, which are lower than the minimum oil-water tension, are thought to have a quite different origin. Interfacial thicknesses are large and it is appropriate to view these tensions in terms of critical phenomena.

There clearly exists some controversy as to the origins of ultralow tensions in pure surfactant systems. The main aim in carrying out the work reported in this chapter was to obtain a corpus of reproducible experimental data concerning the tension and associated phase behaviour in oil + water systems containing AOT, and to attempt to explain the data in both empirical and thermodynamic terms.

3.3 Ultralow interfacial tensions

3.3.1 Attainment of ultralow tensions

Aerosol OT can form microemulsions in oil + water systems in the absence of cosurfactant; at equilibrium, two or three phases can form depending on conditions.[99] The adsorption of AOT at oil-water interfaces is affected, *inter alia*, by the salt concentration, m_s, in the aqueous phase. Figure 3.2 shows that as the concentration of AOT in the aqueous phase, m_D, is increased, the heptane-water interfacial tension falls. At a particular value of m_D, which depends on m_s, γ assumes a constant value, γ_c, at which point m_D = c.m.c. (see later).

As seen (Figure 3.2), the value of γ_c can become very low and the important point in the present context is that the γ vs $\ln m_D$ curves retain the same form even when γ_c is ultralow. There is no changeover between 'high' and 'low' tension régimes and the implication is that ultralow tensions are produced by simple monolayer adsorption.

It is possible from the (γ, $\ln m_D$) plots to obtain interfacial

Figure 3.2 Interfacial tensions between heptane and aqueous phases at 25°C versus AOT concentration (m_D) in the aqueous phase.

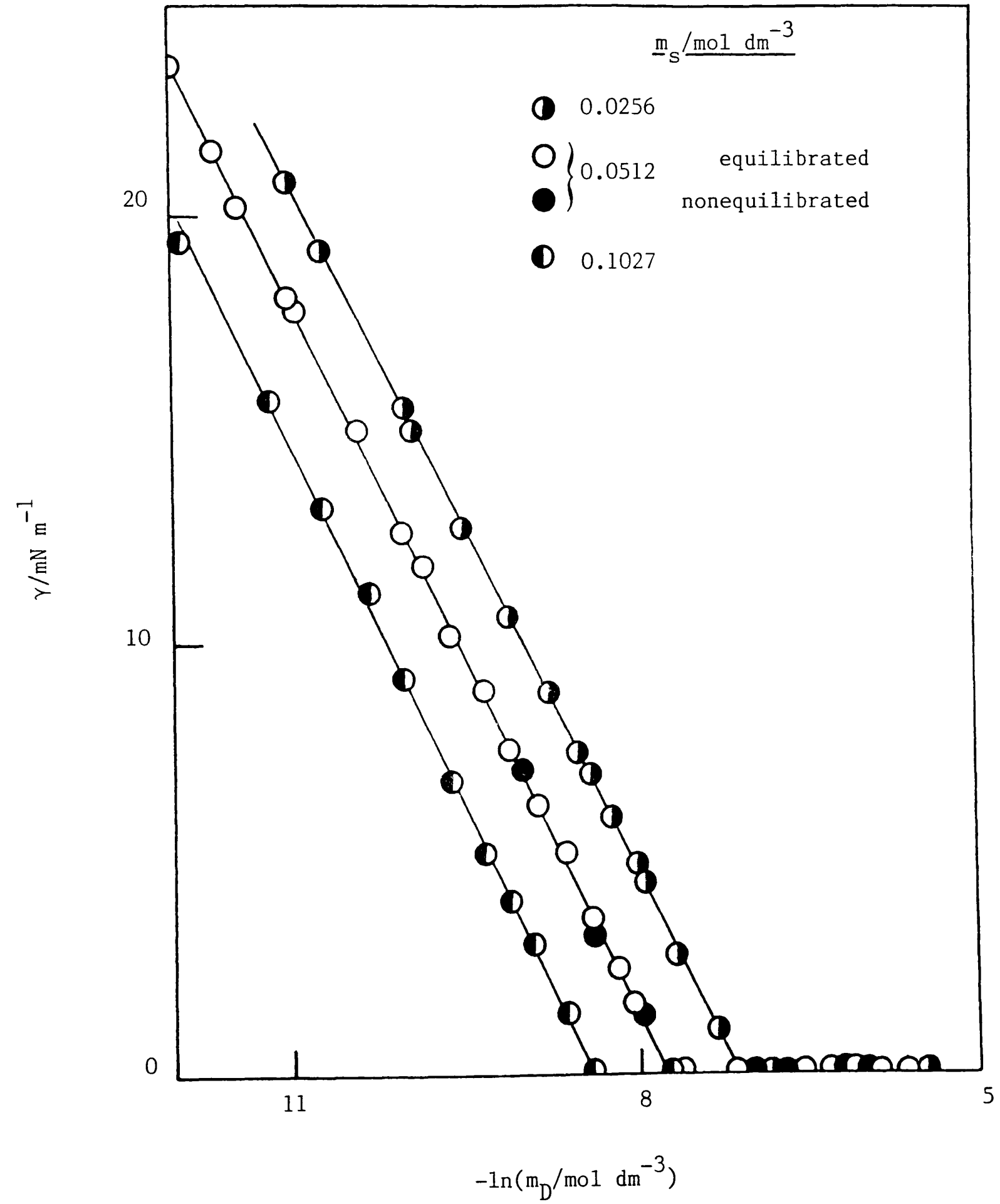

concentrations of surfactant, Γ_D, and hence the area per surfactant molecule, A, at the oil-water interface, using the form of the Gibbs equation[42]

$$A = -kT\left[1 + \left(\frac{cmc}{cmc + m_s}\right)\right]\left[\frac{d\ln m_D}{d\gamma}\right] \qquad (3.1)$$

In the region of m_D studied γ is, within experimental error, a linear function of $\ln m_D$ for all the systems i.e. A becomes effectively equal to the area per surfactant molecule in a saturated film, A_s, well below the c.m.c. Table 3.1 lists the values of A_s for various m_s for AOT adsorbed at the heptane-water interface. It can be seen that A_s is substantially reduced by addition of (swamping) electrolyte. The reduction results from the screening of the headgroup charge and possibly from changes in headgroup hydration.[39] Similar reductions in A_s have been reported for alkyl-benzene sulphonates.[100]

Table 3.1

Values of A_s as a function of m_s in AOT/heptane/aqueous NaCl/25°C

m_s/mol dm^{-3}	A_s/nm^2 molecule^{-1}
0	1.100 ± 0.03
0.0043	1.143 ± 0.02
0.0086	0.974 ± 0.04
0.0171	0.833 ± 0.01
0.0257	0.801 ± 0.02
0.0513	0.747 ± 0.01
0.0770	0.740 ± 0.01
0.1027	0.717 ± 0.02

3.3.2 Minimum in γ_c with respect to salt concentration

The dependence of γ_c on m_s for the system is shown in Figure 3.3; log γ_c passes through a sharp ultralow minimum ($< 10^{-3}$ mN m^{-1}). In experiments yielding the 'nonequilibrated' points in Figure 3.3, a drop of pure heptane was introduced into the capillary of the spinning-drop tensiometer which was filled with aqueous surfactant above the c.m.c. (so that $\gamma = \gamma_c$). Also included in Figure 3.3. are γ_c values from plots like those in Figure 3.2, as well as those for systems that had been pre-equilibrated. The remarkable correspondence of the tensions is reassuring and demonstrates that the systems in the spinning-drop tensiometer have reached quasi equilibrium.

3.4 Surfactant concentration effects

3.4.1 Effect of AOT concentration on distribution between phases

In order to understand the origins of the low tension minimum, the distribution of the surfactant between phases has been determined. Chan and Shah[33] conclude that minimum tension (in systems containing commercial petroleum sulphonates) occurs when the equilibrium aqueous phase is at its c.m.c. and simultaneously the distribution coefficient of surfactant between oil and water is unity (concentration units not specified); it is claimed that this condition also corresponds to maximum surface excess of surfactant in the monolayer at the oil-water interface.

In the present work the distribution of AOT between heptane and aqueous phases at 25°C has been measured as a function of

Figure 3.3 Variation of γ_c with salt concentration for AOT-heptane-aq.NaCl systems at 25°C.

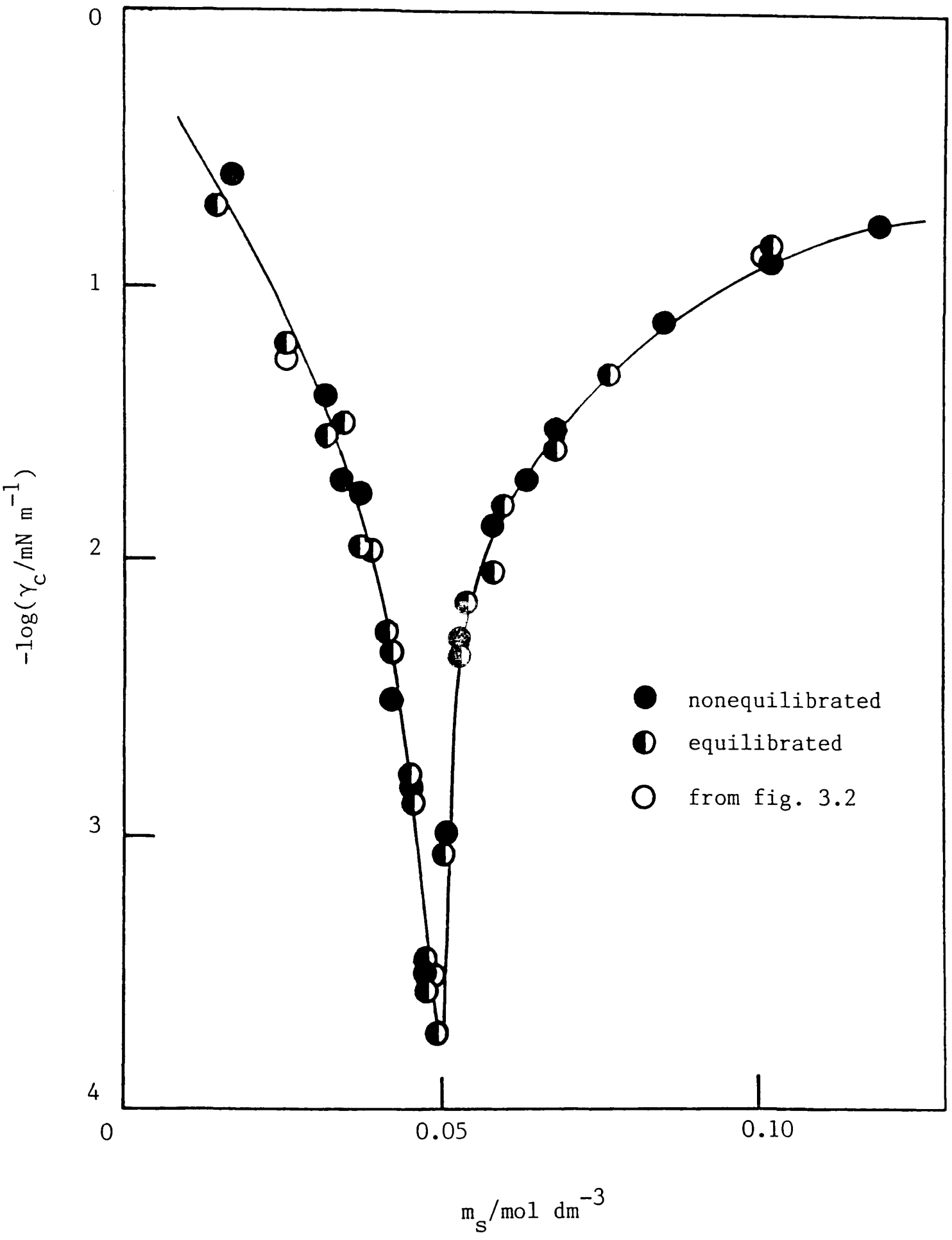

surfactant concentration. Mixtures were equilibrated using three concentrations of salt, one below (0.0171 mol dm^{-3} NaCl), one above (0.1027 mol dm^{-3} NaCl), and one equal (0.0512 mol dm^{-3} NaCl) to that necessary for minimum γ_c.

For distribution experiments in 0.0171 and 0.1027 mol dm^{-3} NaCl, solutions of various concentrations of AOT in heptane were agitated with equal volumes of aqueous salt solution and left to equilibrate. For 0.0512 mol dm^{-3} NaCl, two sets of experiments were done. In one, aqueous solutions of surfactant were shaken with heptane (2:1 water to oil by volume) and the resulting emulsions left for two weeks to separate. In addition, aqueous salt solutions were mixed with heptane solutions (3:1 by volume) containing various concentrations of AOT. Analysis for surfactant in aqueous and oil phases at equilibrium yielded the results in Table 3.2 and represented in Figure 3.4.

Reference to Figure 3.4a shows that at low m_s, as m_D in the system is increased surfactant resides totally in the aqueous phase which can be above or below the c.m.c. At higher m_s however, although the AOT remains entirely in the aqueous phase up to a concentration about equal to the c.m.c. expected in an aqueous phase saturated with alkane (but with no 'excess' alkane present), at concentrations greater than this, surfactant is also present in the alkane phase and middle phase, the aqueous phase concentration remaining constant (Figure 3.4b). The line for the results for 0.1027 mol dm^{-3} NaCl has a slope of unity indicating that all added surfactant above the c.m.c. resides in the oil phase; but for 0.0512 mol dm^{-3} NaCl substantial quantities of

Table 3.2

Distribution of AOT between aqueous NaCl and heptane at 25°C for three salt concentrations

(i) $m_s = 0.0171$ mol dm^{-3}

$[AOT]^{init.}_{oil}$ /mM	$[AOT]^{eqm.}_{aq.}$ /mM	$[AOT]^{eqm.}_{oil}$
0.211	0.203	
0.422	0.420	
0.632	0.630	
0.843	0.830	No surfactant was detected in any oil phase
1.054	1.040	
2.108	1.990	
10.540	10.260	
26.350	25.830	

(ii) $m_s = 0.1027$ mol dm^{-3}

$[AOT]^{init.}_{oil}$ /mM	$[AOT]^{eqm.}_{aq.}$ /mM	$[AOT]^{eqm.}_{oil}$ /mM	$K^{\dagger}$
0.052	0.050	0	0
0.104	0.113	0.002	0.02
0.207	0.203	0.002	0.01
0.311	0.225	0.084	0.37
0.415	0.226	0.172	0.76
0.520	0.236	0.310	1.31
1.040	0.248	0.860	3.47
2.070	0.254	1.935	7.62
2.590	0.254	2.480	9.76
3.110	0.266	2.985	11.22
5.190	0.246	5.130	20.85
10.370	0.269	10.290	38.25

(iii) $m_s = 0.0513$ mol dm^{-3}

$\left[\text{AOT}\right]_{\text{init.}}$ /mM	$\left[\text{AOT}\right]_{\text{aq.}}^{\text{eqm.}}$ /mM	$\left[\text{AOT}\right]_{\text{oil}}^{\text{eqm.}}$ /mM	$K^{\dagger}$
0.112	0.112	-	-
0.225	0.225	-	-
0.337	0.324	-	-
0.450	0.416	0.04	0.09
0.675	0.450	0.42	0.93
1.350	0.540	1.15	2.13
1.800	0.504	1.22	2.42
2.249	0.490	2.14	4.37
2.699	0.470	1.93	4.11
3.374	0.497	2.62	5.27
3.824	0.502	3.80	7.57
4.498	0.481	3.86	8.02
* 1.80	0.495	1.07	2.16
* 8.0	0.483	7.92	16.40
*20.0	0.491	21.40	43.60
*40.0	0.476	35.60	74.80

* AOT initially in heptane phase.

† K is defined as $\left[\text{AOT}\right]_{\text{oil}}^{\text{eqm.}} \Big/ \left[\text{AOT}\right]_{\text{aq.}}^{\text{eqm.}}$

Figure 3.4a Initial and equilibrium aqueous-phase concentrations of AOT in heptane-aq. NaCl systems at 25°C.

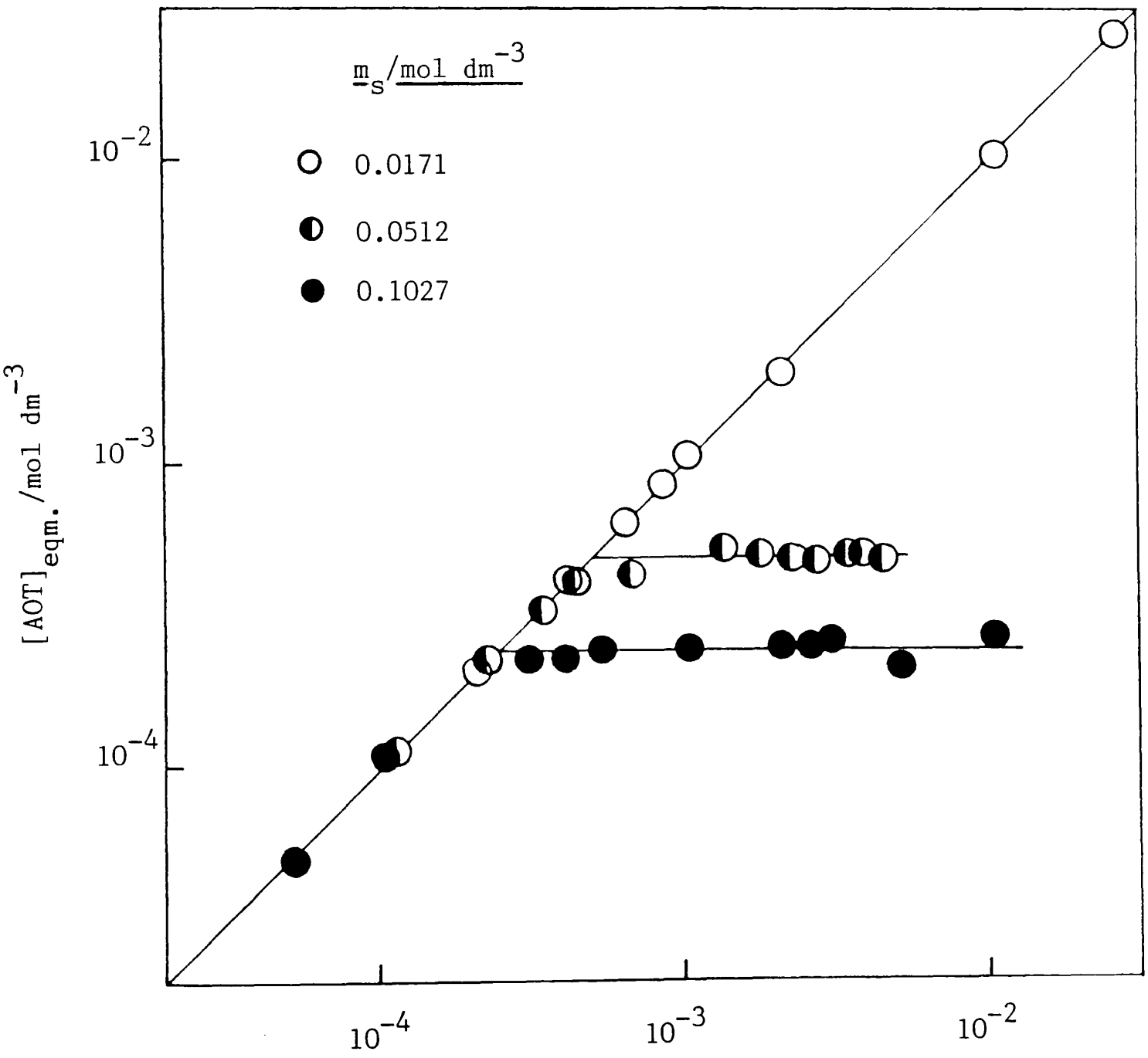

Figure 3.4b Initial and equilibrium heptane phase concentrations of AOT in heptane-aq.NaCl systems at 25°C.

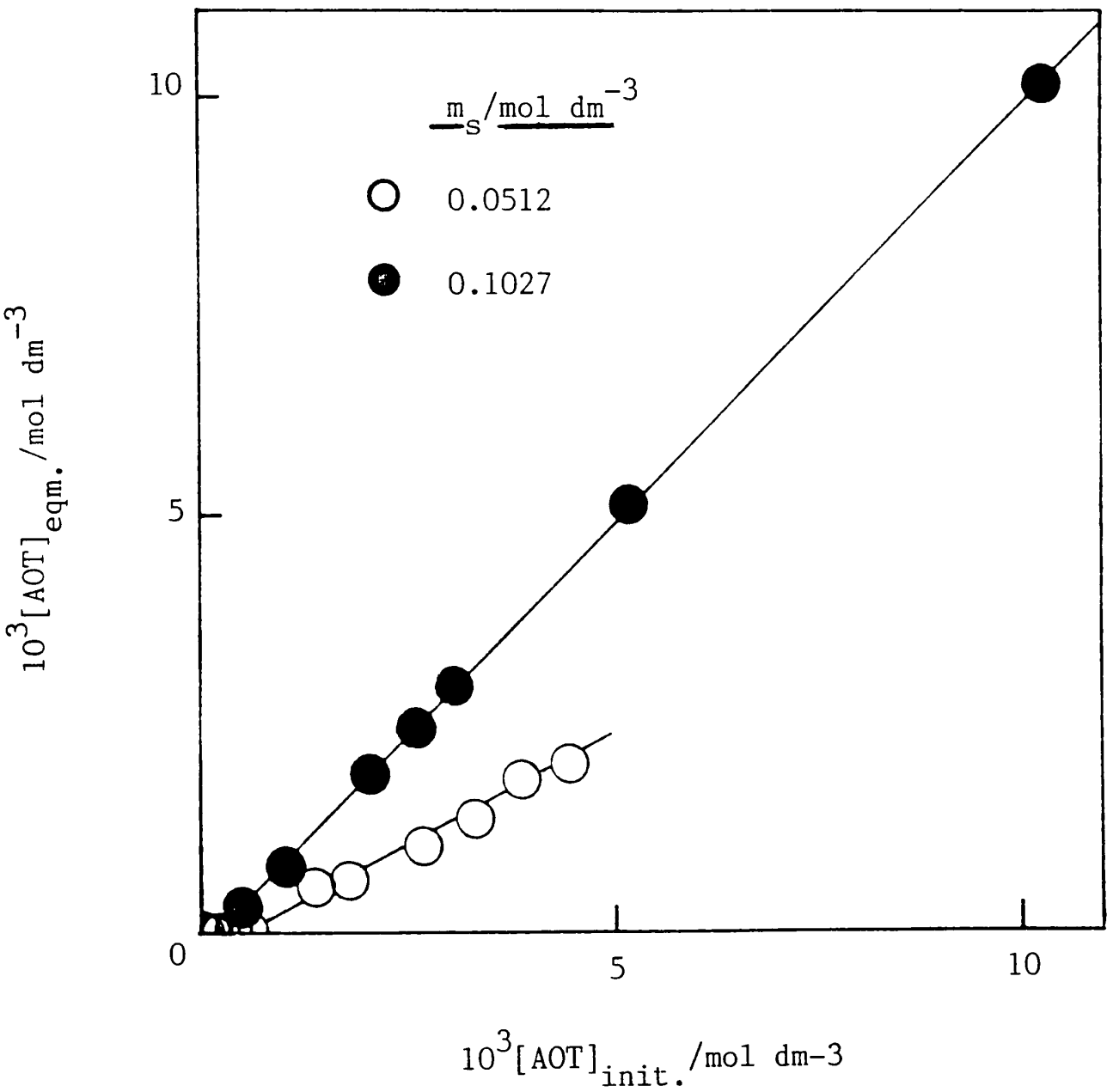

Slope of line through filled points is unity.

For m_s = 0.0171 mol dm^{-3} no surfactant detectable in heptane. The slope of less than unity through the open points indicates a loss of surfactant to a third, surfactant-rich phase.

surfactant also transfer to a middle phase. Under these conditions no micelles are detectable by light scattering in the aqueous phase. This has also been observed by Pouchelon *et al*;[98] if sufficient NaCl is present for aqueous phase concentrations initially above the c.m.c., surfactant transfers to the oil phase (and middle phase if present) leaving the equilibrium aqueous phase close to the c.m.c. The results obtained using the two equilibration procedures for 0.0512 mol dm^{-3} NaCl are in very good accord and since in one the surfactant was originally in the aqueous phase and in the other in the alkane, one may assume distribution equilibrium has been attained.

3.4.2 Equilibrium tensions and AOT concentration

The interfacial tensions between equilibrated 0.0512 mol dm^{-3} aqueous NaCl and oil phases are plotted in Figure 3.2 and show good agreement with tensions obtained from unprecontacted phases. The concentrations for which γ is falling are all below the c.m.c. in the aqueous phase. The tensions become constant at the c.m.c. Furthermore, the distribution ratio of surfactant between oil and water discussed by Chan and Shah[33] is seen to be an irrelevance. The tension attains the value γ_c just as the c.m.c. is reached, so here the distribution ratio K = (surfactant concentration in oil/surfactant concentration in water) is zero, and if surfactant then transfers to oil K increases as surfactant is added to the system while the tension remains constant. If conditions are such that surfactant does not transfer to oil then obviously K remains zero. In any event the condition such that

K = 1, stressed by Chan and Shah, depends on the concentration scales used.[101]

3.4.3 *Phase inversion*

It is well-known that surfactant distribution between phases is related to the type of coarse macroemulsion formed by agitation of oil + water + surfactant systems,[102] and this is exemplified by the present results. In oil-in-water (o/w) emulsions, surfactant resides in the continuous (water) phase whereas for water-in-oil (w/o) emulsions it resides predominantly in the oil phase. The conversion of one type of emulsion to the other is known as phase inversion and is readily detected by changes in conductivity of the emulsions. Because of the presence of salt in the aqueous phase, the electrical conductivity of the o/w emulsions is high (of the order of 1-2 mS cm^{-1} in the present case), whilst it is a factor of 10^2 to 10^3 lower for w/o emulsions. Thus the conductivity yields a quick indication of the emulsion type. However, the properties of emulsions are very dependent on (among other things) the phase volume ratio of oil:water and the surfactant concentration, and for this reason quantitative correlation between conductivity data, tensions, and distribution ratios has not been attempted.

Nonetheless, it has been confirmed that at low m_s (< 0.0512 mol dm^{-3} NaCl) the conductivity of emulsions formed with heptane from increasingly concentrated AOT solutions remains relatively high indicating that they are water continuous; all

the surfactant resides in the aqueous phase, which is above the c.m.c. (Figure 3.5). For higher m_s however, phase inversion from o/w to w/o emulsions occurs as surfactant transfer between phases takes place.

3.5 Salt concentration effects

3.5.1 Effect of salt concentration on distribution between phases

Pouchelon *et al.*[22] have studied the effect of increasing m_s on the phase behaviour and interfacial tensions in systems containing a micelle-forming anionic surfactant. For equilibrium, at low m_s they observe that the aqueous phase is an o/w microemulsion. At intermediate m_s three phases coexist, one being a 'middle phase' microemulsion (of unknown structure) in equilibrium with the aqueous and organic phases. At higher m_s a w/o microemulsion is in equilibrium with an aqueous phase. These authors have carried out detailed investigations into the nature of the phases in equilibrium and the tensions between them, but the situation is made more complex perhaps by the inclusion of butanol as cosurfactant. Similar findings are reported below for systems containing AOT in the absence of cosurfactant.

The minimum in γ_c with respect to salt concentration is related to the distribution of surfactant between phases. Distribution experiments were carried out for two oil:water ratios (1:1 and 1:3 by volume) with AOT originally in the heptane phase and varying concentrations of NaCl in the aqueous phase (Table 3.3). The results show that for $m_s < 0.045$ mol dm^{-3}, two

Figure 3.5 Effect of AOT on emulsion phase inversion in heptane-aq.NaCl systems at 25°C.

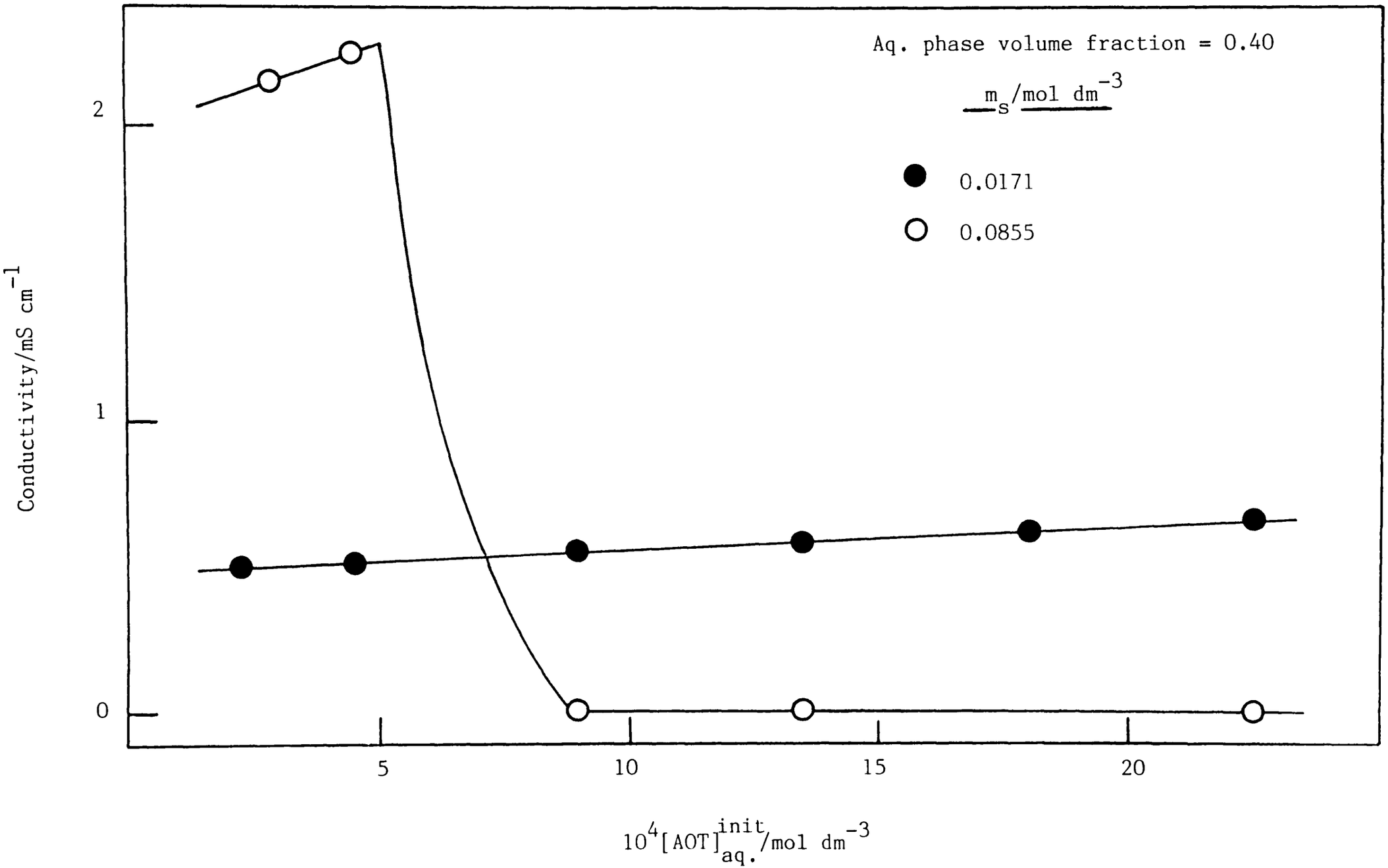

Table 3.3

Distribution of AOT between heptane and aqueous NaCl at 25°C as a function of salt concentration

m_s/mol dm^{-3}	$\left[AOT\right]^{eqm.}_{aq.}$ /mM	$\left[AOT\right]^{eqm.}_{oil}$ /mM	K
0	2.91	0.004	-
0.0171	2.90	0.16	-
* 0.0171	29.20	0.03	-
0.0342	2.37	0.04	-
* 0.0342	7.10	0.05	-
* 0.0428	1.30	0.46	0.3
0.0513	0.47	7.45	15.8
* 0.0513	0.47	15.50	33.0
* 0.0599	0.41	28.40	69.3
0.0684	0.36	8.62	23.9
* 0.0684	0.37	29.20	78.9
0.0856	0.31	8.86	28.6
0.1027	0.26	8.99	34.6
0.1198	0.24	9.18	38.2
* 0.1369	0.21	28.70	136.7
* 0.2053	0.15	29.60	197.3

---

* Oil to water volume ratio = 1:1, with $\left[AOT\right]^{init.}_{oil}$ = 30 mM.

The rest had $\left[AOT\right]^{init.}_{oil}$ = 10.12 mM, and volume ratio = 1:3.

clear phases exist at equilibrium. The lower aqueous phase contains all the detectable surfactant which is above the c.m.c. and we assume this to be a dilute o/w microemulsion. For m_s greater than 0.055 mol dm^{-3}, two clear phases also formed but now the majority of surfactant is found in the (upper) heptane phase, as a w/o microemulsion (see later). However, the aqueous phase concentration of AOT in equilibrium with the heptane phase was found to be close to its expected c.m.c. but yet devoid of micelles (as indicated by light scattering). At intermediate m_s (around 0.05 mol dm^{-3}), three phases formed. The upper organic and lower aqueous phases were optically clear and contained a concentration of AOT equal to the c.m.c., whilst the middle phase was quite viscous and 'milky' in appearance. Analysis showed it contained nearly all the surfactant in the system.

These findings are summarised in Figure 3.6a which shows the distribution of AOT (in aggregated form) between heptane and aqueous NaCl at 25°C. The filled points represent the % AOT in the heptane phase given by

$$\left\{[AOT]_{heptane}\ \phi_{heptane}\right\} / \left\{[AOT]_{ov} - \phi_{aq.}\ cmc\right\}$$

and the open points represent the % AOT in the aqueous phase given by

$$\left\{[AOT]_{aq} - cmc\right\}\ \phi_{aq.} / \left\{[AOT]_{ov} - \phi_{aq.}\ cmc\right\}$$

Here, $[AOT]_{ov}$ is the overall surfactant concentration in this system and the ϕ are phase volume fractions. The dotted line

the figure represents the loss to the middle phase obtained

Figure 3.6a Distribution of AOT (in aggregated form) between heptane and aqueous NaCl at 25°C.

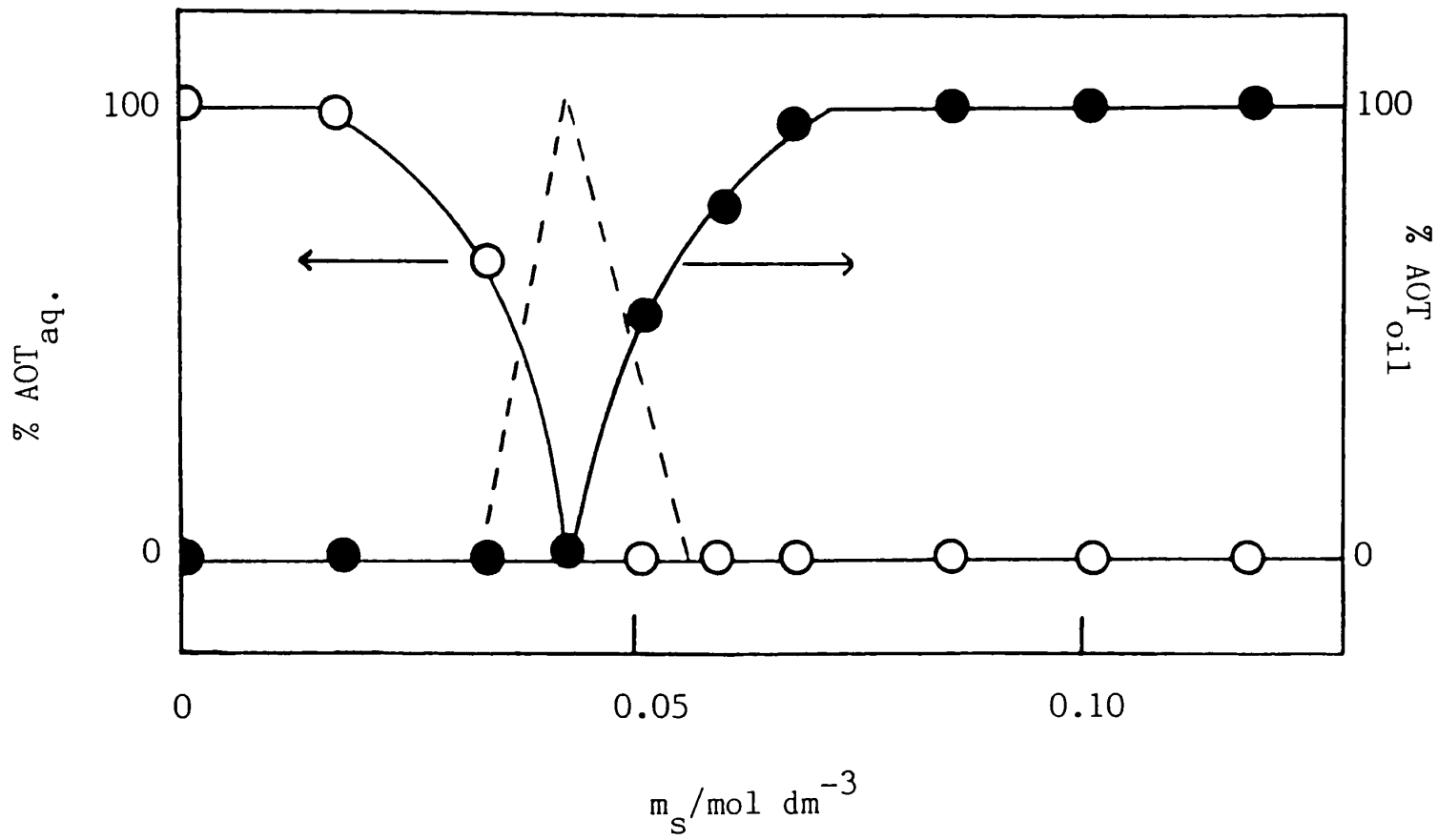

Figure 3.6b Conductivity of stirred emulsions versus m_s at 25°C.

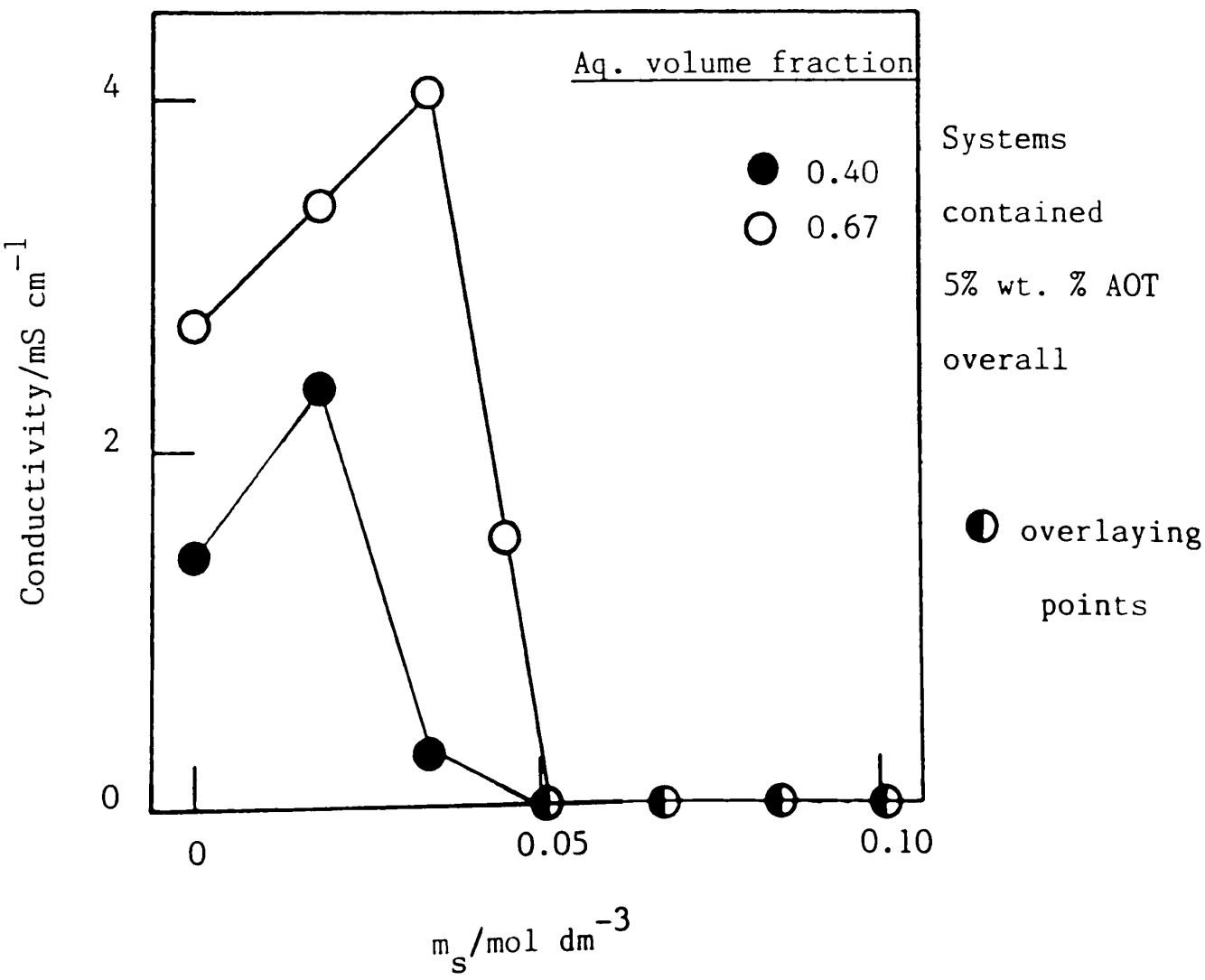

by mass balance. The equilibrium distribution expressed in this way is independent of the initial phase volume ratio. The c.m.c. has here been defined as the equilibrium aqueous phase concentration of surfactant at which aggregation occurs in the preferred phase.

As a backup to surfactant transfer experiments, the conductivities of emulsions formed in systems containing a fixed amount of AOT but increasing amounts of NaCl were measured, and are shown in Figure 3.6b. Phase inversion from o/w to w/o emulsions occurs as the salt increases, but the salt concentration at which it does so is found to depend on the phase volume ratio. At low m_s, the conductivity increases steadily with salt concentration, as may be expected with a continuous aqueous phase. At high m_s, the conductivity is lower than 0.1 mS cm^{-1} and essentially zero on the scale illustrated. In the inversion region the conductivity exhibits a sharp fall, but in some cases an intermediate value of the conductivity (equivalent to say 0.5 mS cm^{-1} on the graph) is observed. This 'non-catastrophic' drop indicates that the transition from complete water-external to complete oil-external emulsion occurs over a finite range of salt concentration. There is not enough evidence to decide about a structure of the emulsion around inversion on the basis of conductivity alone; it may be bicontinuous (aqueous/middle phase or middle phase/oil) or even tricontinuous. The picture is further complicated by the possibility of multicontinuity for the middle phase itself.[103]

3.5.2 *Equilibrium tensions and salt concentration*

A good test of whether conditions in the spinning-drop

tensiometer reach equilibrium or not is the agreement (or otherwise) of tensions between unprecontacted phases and those between equilibrated phases. In connection with the distribution work just discussed, interfacial tensions were determined between equilibrium phases as a function of m_s. In both two and three-phase régimes, a drop of the upper (alkane) phase was injected into the aqueous phase in the tensiometer and tensions remained unchanged from the start for periods of at least 2 h. It can be seen from the results in Figure 3.3 that the equilibrated and nonequilibrated tensions are in very good mutual agreement, thus confirming that conditions in the tensiometer reach quasi equilibrium, as mentioned earlier.

3.6 Origin of low interfacial tensions

An important inference from this agreement is that ultralow tensions can be attained between aqueous and organic phases in the absence of a middle phase. Presumably middle phase formation results from the low tension, as does the formation of the microemulsion. This conclusion is in sharp contrast to the claims of Puig *et al.*[30] (working with a similar system containing AOT) who believe that the presence of a third, surfactant-rich phase, which forms in situ between the aqueous and organic phases, is necessary to produce ultralow tensions. They note that aqueous preparations of AOT containing NaCl are turbid and contain liquid crystallites. On contacting with hydrocarbon, liquid crystallites containing hydrocarbon are supposed to form at the interface which lowers the tension. Our work however[104] demonstrates that visibly turbid aqueous solutions can be prepared

but that this turbidity disappears if the aqueous phase is equilibrated with an excess hydrocarbon phase. Equilibrium tensions are then in good agreement with those obtained for 'normal' preparations of AOT in aqueous NaCl, as discussed earlier.

It must be pointed out that for non-equilibrated systems (Figure 3.3), the tensions were low initially and became constant within 2-3 mins.. When the tension was very low however ($< 5 \times 10^{-3}$ mN m^{-1}) what appeared to be a thin coating of another phase formed around the oil drop, but with time this disappeared leaving a 'clean' oil-water interface. No such effect was observed in equilibrated systems. In any event, tensions (even when ultralow) were independent of the rotation speed of the capillary implying that the oil-water interface is fluid-like. In the work of Puig *et al.*,[30] the middle phase is said to be viscous and so presumably apparent interfacial tensions between a middle phase and oil or a middle phase and water would depend on the rotation speed.

The present work suggests that the monomers of surfactant adsorb at the macroscopic oil-water interface and that the micelles or microemulsion droplets in equilibrium with this monolayer are surface inactive. This proposition is given weight by recalling that oil-water interfacial tensions above the c.m.c. (γ_c) are independent of surfactant concentration, even though the concentration of the aggregates is changing (Figure 3.2). Also, the γ_c values are low ($< 10^{-1}$ mN m^{-1}) even in two-phase régimes and assume a constant value at precisely the c.m.c., where

but that this turbidity disappears if the aqueous phase is equilibrated with an excess hydrocarbon phase. Equilibrium tensions are then in good agreement with those obtained for 'normal' preparations of AOT in aqueous NaCl, as discussed earlier.

It must be pointed out that for non-equilibrated systems (Figure 3.3), the tensions were low initially and became constant within 2-3 mins.. When the tension was very low however ($< 5 \times 10^{-3}$ mN m^{-1}) what appeared to be a thin coating of another phase formed around the oil drop, but with time this disappeared leaving a 'clean' oil-water interface. No such effect was observed in equilibrated systems. In any event, tensions (even when ultralow) were independent of the rotation speed of the capillary implying that the oil-water interface is fluid-like. In the work of Puig *et al.*,[30] the middle phase is said to be viscous and so presumably apparent interfacial tensions between a middle phase and oil or a middle phase and water would depend on the rotation speed.

The present work suggests that the monomers of surfactant adsorb at the macroscopic oil-water interface and that the micelles or microemulsion droplets in equilibrium with this monolayer are surface inactive. This proposition is given weight by recalling that oil-water interfacial tensions above the c.m.c. (γ_c) are independent of surfactant concentration, even though the concentration of the aggregates is changing (Figure 3.2). Also, the γ_c values are low ($< 10^{-1}$ mN m^{-1}) even in two-phase régimes and assume a constant value at precisely the c.m.c., where

no aggregates exist anyway.

In connection with Figure 7 of reference 30, which shows the variation in tension with AOT concentration (in a system containing octane rather than heptane), the authors comment that below the AOT solubility limit interfacial tensions are higher than $\simeq 1$ mN m^{-1}. Above this limit, the tension is said to fall 'precipitously' to ultralow values ($< 10^{-2}$ mN m^{-1}). This implies that a new mechanism operates which separates the 'high' and 'low' tension régimes; this conclusion however may have been drawn from a lack of data points and the way in which the results are presented (i.e. as log γ vs log [AOT]). In our work, the so-called 'solubility limit' is defined as an aggregation point (c.m.c.) since aggregates are detected in either the aqueous or organic phase depending on conditions (see § 3.7 and 3.8). There is also found to be a continuous and smooth variation in tension from $\simeq 1$ mN m^{-1} to $< 10^{-3}$ mN m^{-1} with increasing AOT concentration (Figure 3.7). The slope of the tension curve in Figure 3.7 is, within experimental error, equal to the average slope from tensions of $\simeq 25$ mN m^{-1} down to near zero and so it is concluded that a monolayer of adsorbed surfactant is forming at the oil-water interface even at concentrations just below the c.m.c. where tensions are very low.

In SDS / toluene / butanol systems,[22] the interfacial tensions between the various equilibrium phases have been measured as a function of m_s. In summary, on increasing m_s, tensions between microemulsions (aqueous or middle phase) and organic phases, γ_{mo}, decrease whilst those between microemulsions (organic or middle

Figure 3.7 Log γ against ln[AOT] at heptane-aq.0.0512 mol dm^{-3} interface at 25°C.

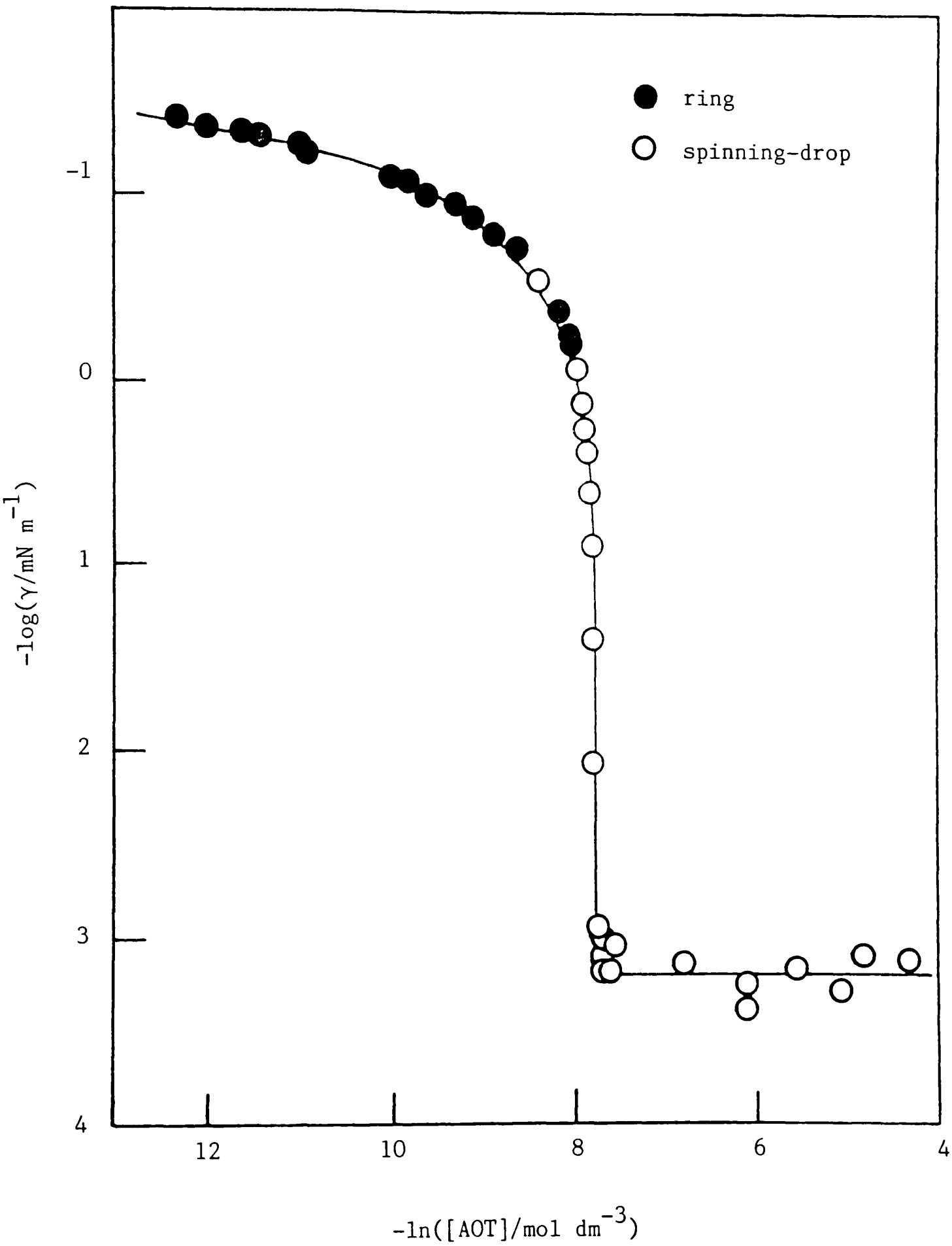

phase) and aqueous phase, γ_{mw}, increase. In two-phase régimes it was shown that the interfacial tension was independent of the droplet concentration in the microemulsion phase,[98] as in the present work, and its value was unchanged even when the microemulsion was replaced by its continuous phase. The (small) increase in γ_c with increasing AOT concentration observed by Puig *et al.*[30] may have been as a result of temperature drift in the tensiometer.

In the three-phase régime, Pouchelon *et al.*[22] demonstrate that the oil-water tension, γ_{ow}, remains equal to the higher of the other two tensions, so that $\gamma_{ow} < \gamma_{mo} + \gamma_{mw}$. They attribute the larger tension involving the middle-phase microemulsion to the presence of a surfactant layer possibly monomolecular; a thicker layer would rapidly resemble a microemulsion layer. For three fluid phases α,β, and δ in equilibrium, the general inequality derived by Widom[20]

$$\gamma_{\alpha\beta} < \gamma_{\alpha\delta} + \gamma_{\beta\delta}$$

holds, when the form of a droplet of the δ phase at the α-β interface is that of a lens, characteristic of a nonwetting situation.[20] Pouchelon *et al.*[22] report that the middle-phase microemulsion does not spread at the oil-water interface but instead forms a drop; this fully confirms the independence of the low value of γ_{ow} and the presence of the microemulsion phase.

3.7 Nature of equilibrium oil phases

3.7.1 Introduction

Under conditions where surfactant is detected in the heptane phase (i.e. above 0.05 mol dm^{-3} NaCl) water is also present. The concentration of water in equilibrium oil phases has been measured by Karl Fischer titrations both for varying surfactant concentration and increasing salt concentration (in the excess aqueous phase). In order that the determination of water be as accurate as possible, further distribution experiments were set up using higher concentrations of AOT. In all cases, aqueous salt solutions were shaken with heptane solutions containing AOT in a volume ratio of 1:1 and left to separate for a period of 1 week. All heptane phases were optically clear at equilibrium, and both surfactant and water analyses were carried out on them. The mole ratio of water to surfactant in the oil phase, designated R, is defined as

$$R = \frac{[H_2O]}{[AOT]}$$

Data are presented in Table 3.4. The errors in the concentrations represent the variation found from duplicate determinations. As seen, substantial quantities of water can be solubilised into the oil phase as surfactant transfers to it. For constant m_s, R is found, within experimental error, to be independent of oil phase surfactant concentration as seen in Figure 3.8a. On the other hand, R depends inversely on m_s

(Figure 3.8b). Similar R, m_s variation has been reported by Tosch *et al.*[105] for a system containing an organic sulphonate and alcohol cosurfactant. With reference to Figure 3.8a, it has been confirmed that the tension between equilibrated phases (for 0.0706 mol dm^{-3} NaCl) is also independent of AOT concentration.

Table 3.4

Values of R as a function of surfactant and salt concentration for AOT/aqueous NaCl/heptane/25°C

m_s/M	$[AOT]^{init.}_{oil}$ /mM	$[AOT]^{eqm.}_{oil}$ /mM	$[H_2O]^{eqm.}_{oil}$ /M	R
.0706	7.24	6.35 ± 0.15	0.41 ± 0.04	64.1 ± 7.8
.0706	36.2	34.80 ± 0.55	2.38 ± 0.04	68.4 ± 2.2
.0706	108.6	93.70 ± 1.8	6.48 ± 0.04	69.2 ± 1.8
.0706	181.0	136.80 ± 2.2	9.13 ± 0.02	66.7 ± 1.7
.0706	72.4	67.30 ± 1.1	4.65 ± 0.04	69.1 ± 1.7
.0605	72.4	61.50 ± 1.0	5.69 ± 0.04	92.6 ± 2.2
.0655	181.0	142.0	10.30 ± 0.15	72.5 ± 1.8
.0806	181.0	150.0	8.53 ± 0.06	56.9 ± 1.0
.0907	72.4	67.60 ± 1.1	3.12 ± 0.04	46.2 ± 1.3
.1008	72.4	68.80 ± 1.1	2.94 ± 0.04	42.7 ± 1.3
.1512	72.4	68.80 ± 1.1	2.12 ± 0.04	30.8 ± 1.1
.2016	72.4	71.0 ± 1.1	1.83 ± 0.04	25.2 ± 1.0
.252	181.0	163.2	4.01 ± 0.09	24.6 ± 0.8

Figure 3.8a Dependence of R on $[AOT]^{oil}_{eqm.}$ for an aqueous phase $m_s = 0.0706$ mol dm^{-3}

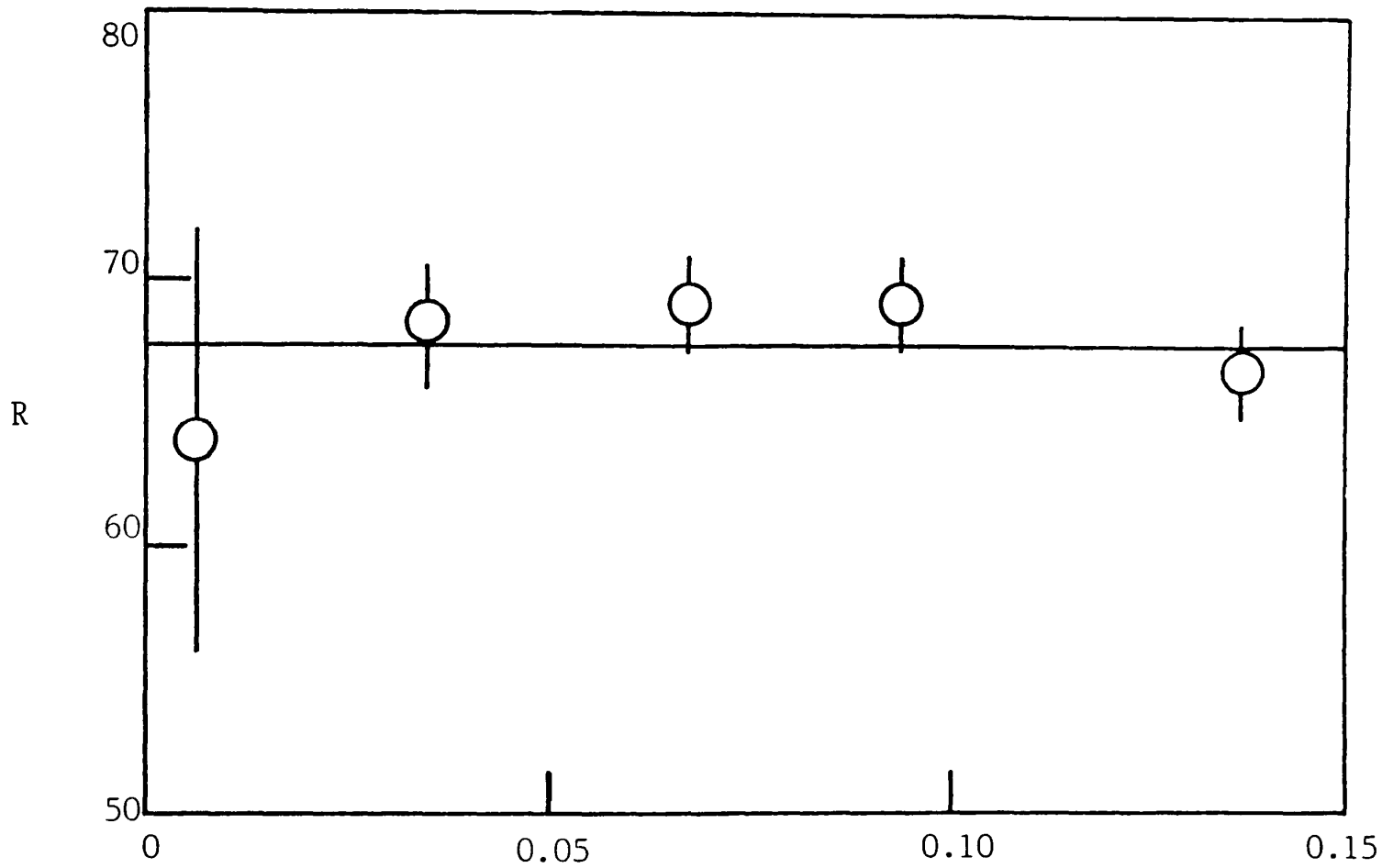

Figure 3.8b Variation of R with salt concentration at 25°C.

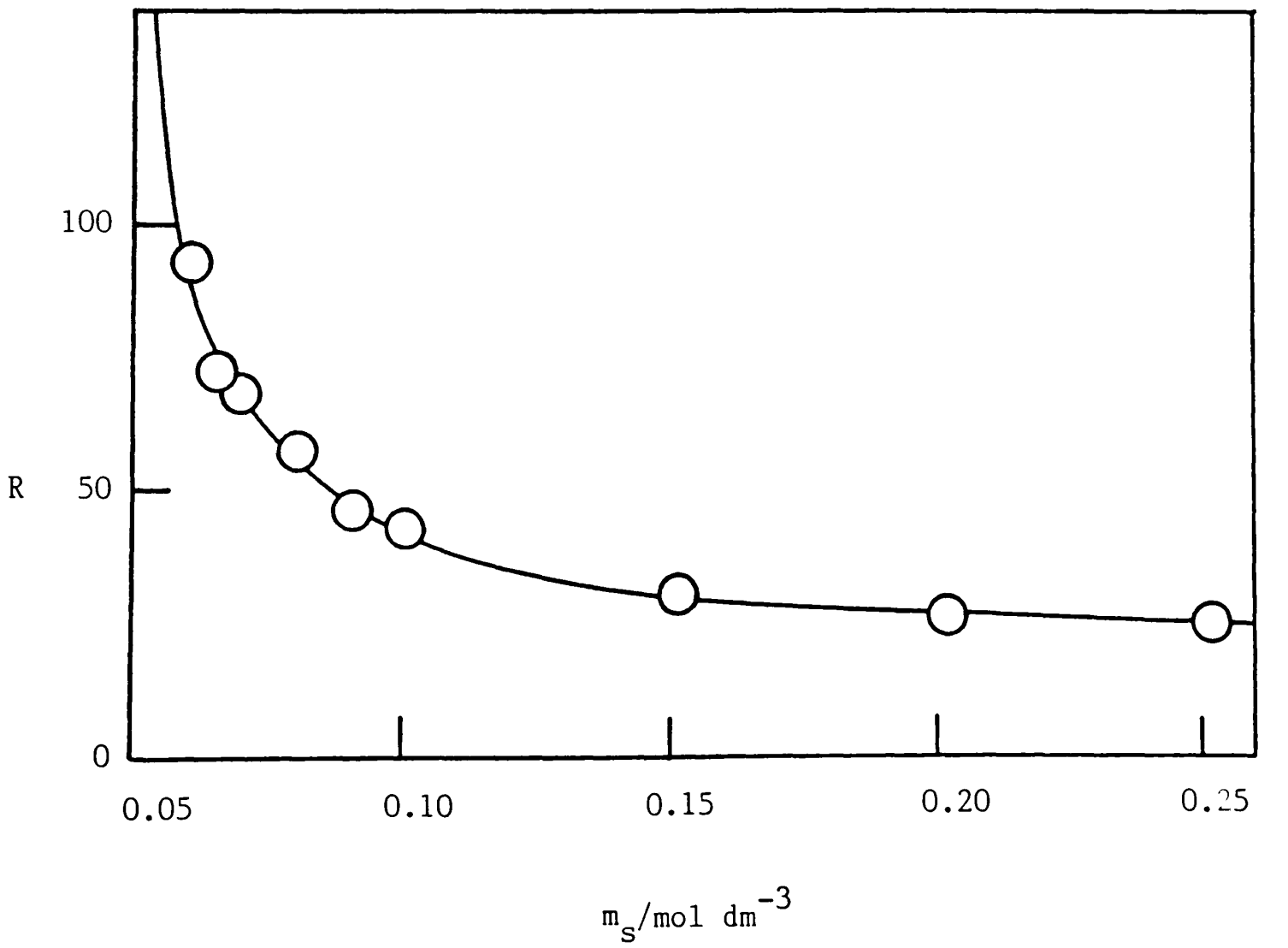

3.7.2 *Size of w/o microemulsion droplets*

Since surfactant is not detected in the oil phase below the c.m.c., one may suppose that when AOT is present it is in aggregated form. Further, since the oil phases are clear and water is only found in conjunction with surfactant, the implication is that the water is present as droplets coated with surfactant monolayers i.e. the oil phase is a water-in-oil microemulsion. The existence of microemulsion droplets is demonstrated by P.C.S. measurements.

Microemulsions similar to those obtained in equilibrium systems can be made up directly and then a range of R values is possible without phase separation occurring. The droplet concentration can be varied also. Water-in-oil microemulsions stabilised by AOT in heptane have previously been studied by both P.C.S.[106] and by small angle neutron scattering (S.A.N.S.).[107] The work reported here extends the droplet size range studied by Nicholson and Clarke.[106] Unlike previous studies, microemulsions have here been investigated in equilibrium with excess phases as well as 'made-up' samples.

As discussed in Chapter 2, the P.C.S. experiment measures the rate of movement of particles (i.e. droplets) in solution, which can be related to the diffusion coefficient D. The correlation length, ℓ, is related to D by the Stokes-Einstein relation[108]

$$\ell = \frac{kT}{6\pi\eta D}$$

where η is the solvent viscosity. In an 'ideal' system, each

droplet will move independently of all others and D does not vary with droplet concentration. In practice however particles do interact, restricting their motion so that D decreases with increasing concentration. The parameter ℓ contains a contribution from interdroplet interactions and can only be equated with the hydrodynamic radius, r_H, at infinite dilution of droplets.[106] The dependence of the correlation length on the hydrodynamic radius may be described by

$$\ell = \frac{r_H}{(1 + \alpha\phi_D)} \qquad (3.2)$$

where ϕ_D is the volume fraction of the dispersed phase (H_2O plus AOT) and α is an interaction parameter. For hard-sphere repulsive interactions, $\alpha = 1.5$, and attractive interactions are generally observed to reduce α.[109]

A reasonable estimate of the droplet size can be made on the assumption that the droplets are monodisperse spheres. From simple geometrical considerations,[110]

$$r_H = \frac{3RV_W}{A_D} + t \qquad (3.3)$$

in which V_W is the volume occupied by a water molecule in liquid water (0.03 nm^3) and A_D is the surface area per surfactant molecule at a droplet surface. It is assumed that all the surfactant is bound to the droplet surface. The hydrodynamic radius is expected to exceed the radius of the water core, r_c, by an amount t which is approximately the length of the surfactant

chains (see Figure 3.9). A value of t of 0.9 nm is estimated from geometrical models.

In the present work, ℓ has been determined for a range of ϕ_D and for various R values. The 'made-up' microemulsions were prepared by dissolving the surfactant in heptane (the solubility limit is above 0.3 mol dm^{-3}) and adding known volumes of water from a microlitre syringe. Clear microemulsions formed after shaking for 2-3 minutes. These systems are thermodynamically stable and the equilibrium sizes are established rapidly following dispersion. No salt was included in the 'made-up' samples, a point which will be discussed later. Both equilibrium and 'made-up' microemulsions were diluted with pure heptane. It is assumed that the droplet size does not vary significantly with droplet concentration, as indicated by neutron scattering data.[111]

The dependence of ℓ on ϕ_D for water/AOT/n-heptane microemulsions at 25°C for various R has been obtained and sample plots are shown in Figure 3.10a. At high volume fractions the P.C.S. profiles showed a marked deviation from a single exponential. The exponential sampling method of analysis revealed two distinct exponentials. The longer decay may be related to the cooperative motions of the droplets. However, at low and intermediate concentrations, where the deviations are relatively small (variance $< 15\%$), polydispersity is a strong possibility. Values of r_H (ℓ at $\phi_D = 0$) are plotted against R in Figure 3.10b, where results from references 106 and 107 are also included. It is clear from equation 3.3 that if A_D is constant, uch a plot should be linear and A_D can be obtained from the

Figure 3.9 Model structure for spherical water-in-oil microemulsion droplet

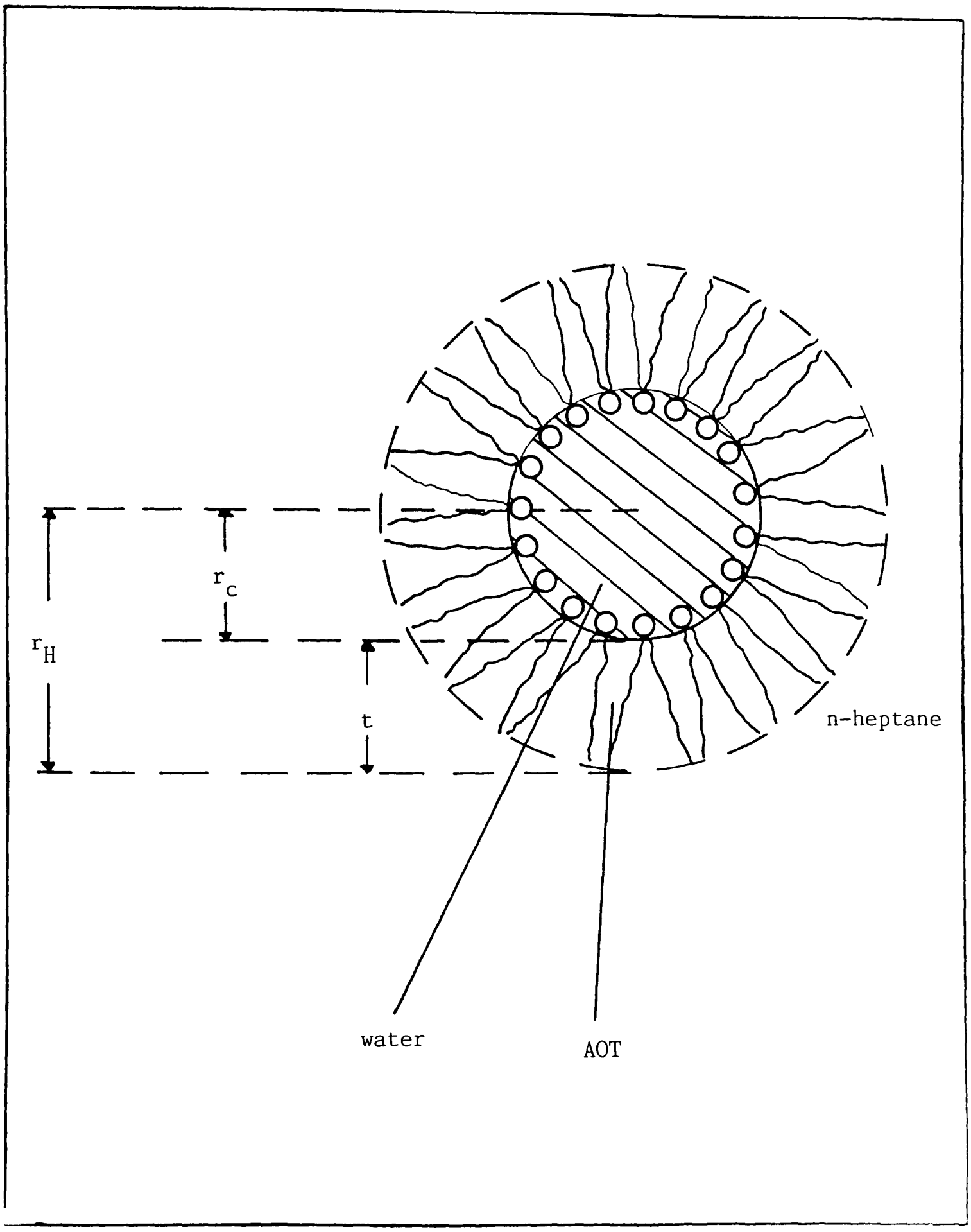

Figure 3.10a Variation of correlation length, ℓ, with droplet volume fraction, ϕ_D, for w/o microemulsions at 25°C.

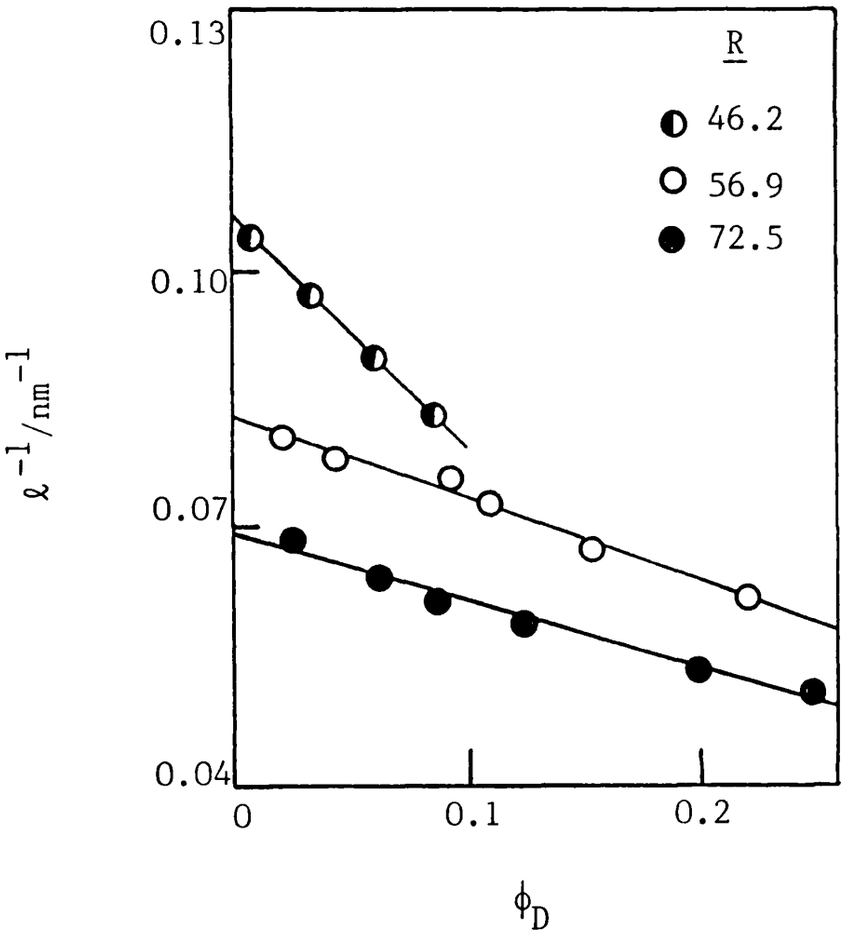

Figure 3.10b Dependence of hydrodynamic radius, r_H, on R at 25°C.

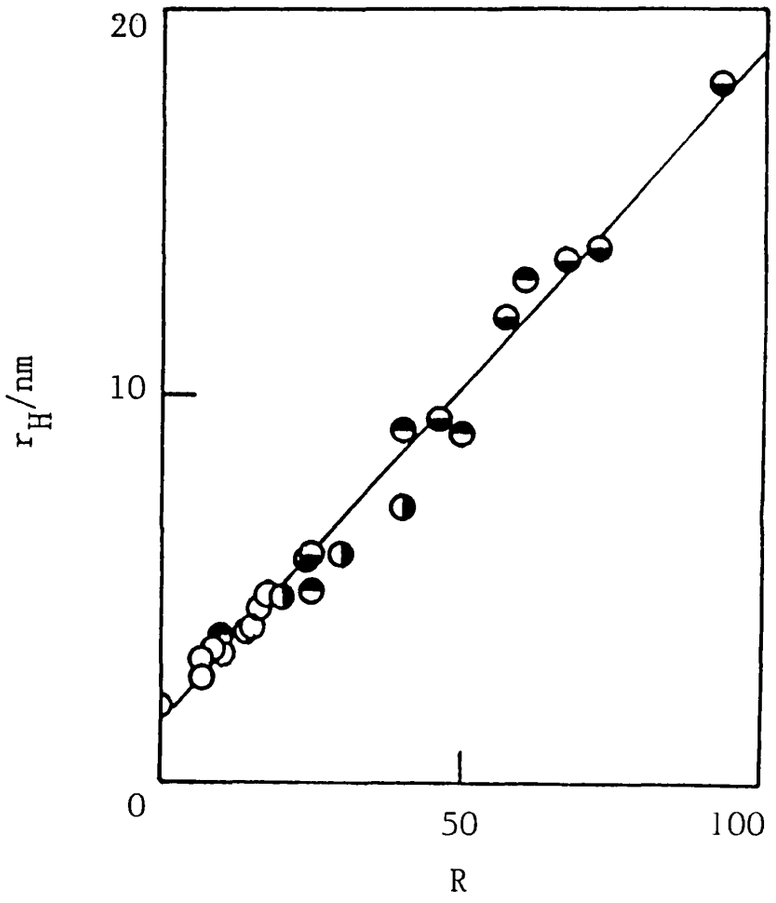

present work — made-up

present work — equilibrium

values from ref. 106

values of r_c from ref. 107 with 1.2 nm added.

slope. The intercept at R=0 gives a value for t. The data in Figure 3.10b are apparently linear and a linear least-squares fit of the (r_H, R) data gives A_D = 0.50 ± 0.03 nm^2 and t = 1.4 ± 0.1 nm. These values agree well with those from previous P.C.S. studies.[64] The results of the present investigation are summarised in Table 3.5.

Table 3.5

P.C.S. data relating to w/o microemulsions stabilised by AOT in n-heptane at 25°C.

Source of microemulsion	m_s/mol dm^{-3}	R	r_H/nm
'Made-up' (no salt)	-	10	3.56
		25	4.91
		40	9.03
		50	8.96
		60	13.00
In equilibrium with excess aqueous phase (containing salt)	0.252	24.6	5.74
	0.202	25.2	5.92
	0.091	46.2	9.41
	0.081	56.9	12.10
	0.071	66.7	13.60
	0.065	72.5	13.80
	0.060	92.6	18.17

As seen (Figure 3.10b) the results for the 'made-up' and equilibrium microemulsions fall on a common straight line implying A_D is constant. The value of A_D might be expected to change with R (or salt concentration) due to decreases in headgroup repulsions. The constancy of A_D may be attributed to the fact that the headgroup is large and the size is dictated by the packing of the ethyl groups of the chain region.[112] Experimental results on the same system[64] support this observation and this has contributed to the view that the systematic variation of R has a well-defined effect on the structure of the droplets. There is however increasing evidence to suggest that the assumptions made in deriving equation 3.3 are not justified and the linear relationship is a result of various competing factors which conceal the underlying complexity of the structural changes. For example, Robinson *et al.*[107] report that for larger R values (> 40) there are significant deviations from a linear relationship which they propose are due to the partitioning of surfactant between the interface and the oil medium.[113] They also present evidence to indicate that the spread in droplet size is much greater than has normally been assumed.

There appeared to be no systematic variation of α with R, an average being $\alpha = -2.0 \pm 0.5$. This may be indicative of net attractive forces between microemulsion droplets, as found by Nicholson and Clarke.[106] It is interesting that P.C.S. studies[64] of water-in-isooctane microemulsions stabilised by AOT have shown that the water solubilised in aggregates is held virtually

immobile when R is less than ≃ 10. Zulauf and Eicke[64] have suggested that for R values < 10, reverse micelles are formed where the water is highly structured in the aggregates by hydrogen bonds stabilised by the strong dipoles of the headgroup of the surfactant molecules. When the water content is larger (R > 10), water can be considered a pseudo-phase and a well-defined monolayer of surfactant separates the dispersed water in the core from the continuous oil phase. Whatever the structure of the aggregates, it is clear from this study that as the salt concentration in the aqueous phase increases beyond 0.05 mol dm^{-3}, the equilibrium interfacial tension γ_c between it and the w/o microemulsion increases as the size of droplets decreases. A fuller discussion of the relation between γ_c and the droplet size will follow later.

The hydrodynamic radius in systems containing excess dispersed phase is usually referred to as the equilibrium radius (corresponding to the actual curvature of the surfactant film). This radius is a compromise between that preferred by the film and increasingly smaller values due to entropy of dispersion effects. Only at this phase boundary is the film free to adopt this curvature. At other points in the phase diagram the natural curvature is constrained by the packing requirements dictated by the mixture composition. The actual film curvature of a particular surfactant is, of course, a function of salt concentration and temperature, among other things.

3.7.3 *Viscosity of w/o microemulsion droplets*

Information on the shape and/or solvation of microemulsion

droplets can be gleaned from a study of viscosities of microemulsions. This provides a useful complement to P.C.S. measurements since the method is relatively insensitive to droplet size.[108]

The specific viscosity, η_{sp}, of a solution (here microemulsion) is defined as $[(\eta-\eta_{solv})/\eta_{solv}]$ where η and η_{solv} are the viscosities of the solution and the solvent respectively. The intrinsic viscosity $[\eta]$ and Huggins coefficient k_H can give information on the nature of the droplets. Both are obtained from the concentration dependence of the reduced viscosity, η_{sp}/C, where C is the droplet concentration in g cm^{-3} of solution

$$\eta_{sp}/C = [\eta] + k_H[\eta]^2C \qquad (3.4)$$

The intrinsic viscosity is dependent on both droplet shape and solvation and for the present systems may be expressed as

$$[\eta] = w(\bar{V}_d + \delta\bar{V}_{solv}) \qquad (3.5)$$

The Simha factor, w,[114] is a shape parameter and is equal to 2.5 for spheres; its value increases with the axial ratio of the droplets. The quantities $\bar{V}_d$ and $\bar{V}_{solv}$ are the partial specific volumes of the droplets and solvent respectively. The parameter δ is the mass of solvent which can be considered to be solvating unit mass of the droplets. Theoretical estimates for the Huggins coefficient (k_H) in the case of hard spheres range from 0.7-0.8,[115] and interactions between droplets (repulsive or attractive) lead to an increase in this value.

In order that values of $\bar{V}_d$ may be derived and absolute viscosities η calculated from measured kinematic viscosities v_k (related through $\eta = v_k\rho$), measurement of the densities, ρ , of the microemulsions are also necessary. If w_{H_2O}, w_{solv} and w_{AOT} are the weight fractions of the subscribed species and V is the specific volume of the microemulsion, $V = w_{H_2O}\bar{V}_{H_2O} + w_{solv}\bar{V}_{solv} + w_{AOT}\bar{V}_{AOT}$ which rearranges to

$$\frac{V}{w_{solv}} = \bar{V}_d \frac{w_d}{w_{solv}} + \bar{V}_{solv} \qquad (3.6)$$

where $w_d\bar{V}_d = w_{H_2O}\bar{V}_{H_2O} + w_{AOT}\bar{V}_{AOT}$. The partial specific volume of the droplets can then be obtained from a plot of V/w_{solv} against w_d/w_{solv}.

For water-in-heptane microemulsions stabilised by AOT, the densities and kinematic viscosities were measured at 25 ± 0.1°C (see § 2.5) both as a function of R and of AOT concentration. Microemulsions were diluted by volume. The viscosities tabulated were all derived from at least four measurements of the outflow times through Ubbelohde viscometers. Occasionally, two viscosities were calculated for the same solution obtained with viscometers of differing bore. No differences between measurements were observed from which it may be concluded that the microemulsions undergo Newtonian flow.

Table 3.6 lists the derived specific viscosities from which plots of η_{sp}/C versus C (equation 3.4) were made (Figure 3.11). From such plots it can be shown that the Huggins coefficient

Table 3.6

Specific viscosities for AOT/water-in-heptane microemulsions at 25°C as a function of R and AOT concentration

R	[AOT]/mol dm^{-3}	η/cP	η_{sp}	10^2 C/g cm^{-3}	$(\eta_{sp}/C)/cm^3\ g^{-1}$
20	0.025	0.4245	0.0616	2.011	3.063
	0.050	0.4502	0.1257	4.023	3.124
	0.075	0.4810	0.2032	6.034	3.368
	0.100	0.5148	0.2870	8.046	3.567
	0.150	0.6006	0.5018	12.069	4.158
	0.180	0.6708	0.6775	14.483	4.678
30	0.025	0.4293	0.0690	2.461	2.804
	0.050	0.4633	0.1585	4.923	3.219
	0.075	0.5013	0.2483	7.384	3.363
	0.100	0.5426	0.3512	9.846	3.567
	0.150	0.6606	0.6520	14.769	4.415
40	0.025	0.4375	0.0932	2.911	3.202
	0.050	0.4766	0.1915	5.823	3.289
	0.075	0.5270	0.3178	8.734	3.634
	0.100	0.5866	0.4669	11.646	4.009
	0.150	0.7454	0.8640	17.469	4.945
	0.200	0.9915	1.4794	23.292	6.351
50	0.020	0.4347	0.0870	2.689	3.235
	0.050	0.4964	0.2414	6.723	3.591
	0.075	0.5671	0.4181	10.085	4.145
	0.100	0.6508	0.6274	13.446	4.666
	0.150	0.8956	1.2396	20.169	6.145
60	0.0125	0.4255	0.0640	1.906	3.358
	0.025	0.4525	0.1317	3.811	3.456
	0.050	0.5206	0.3018	7.623	3.959
	0.075	0.6081	0.5206	11.435	4.553
	0.100	0.7358	0.8401	15.246	5.510

Figure 3.11 Viscosities of w/o microemulsions at 25°C for various droplet concentrations C and R values.

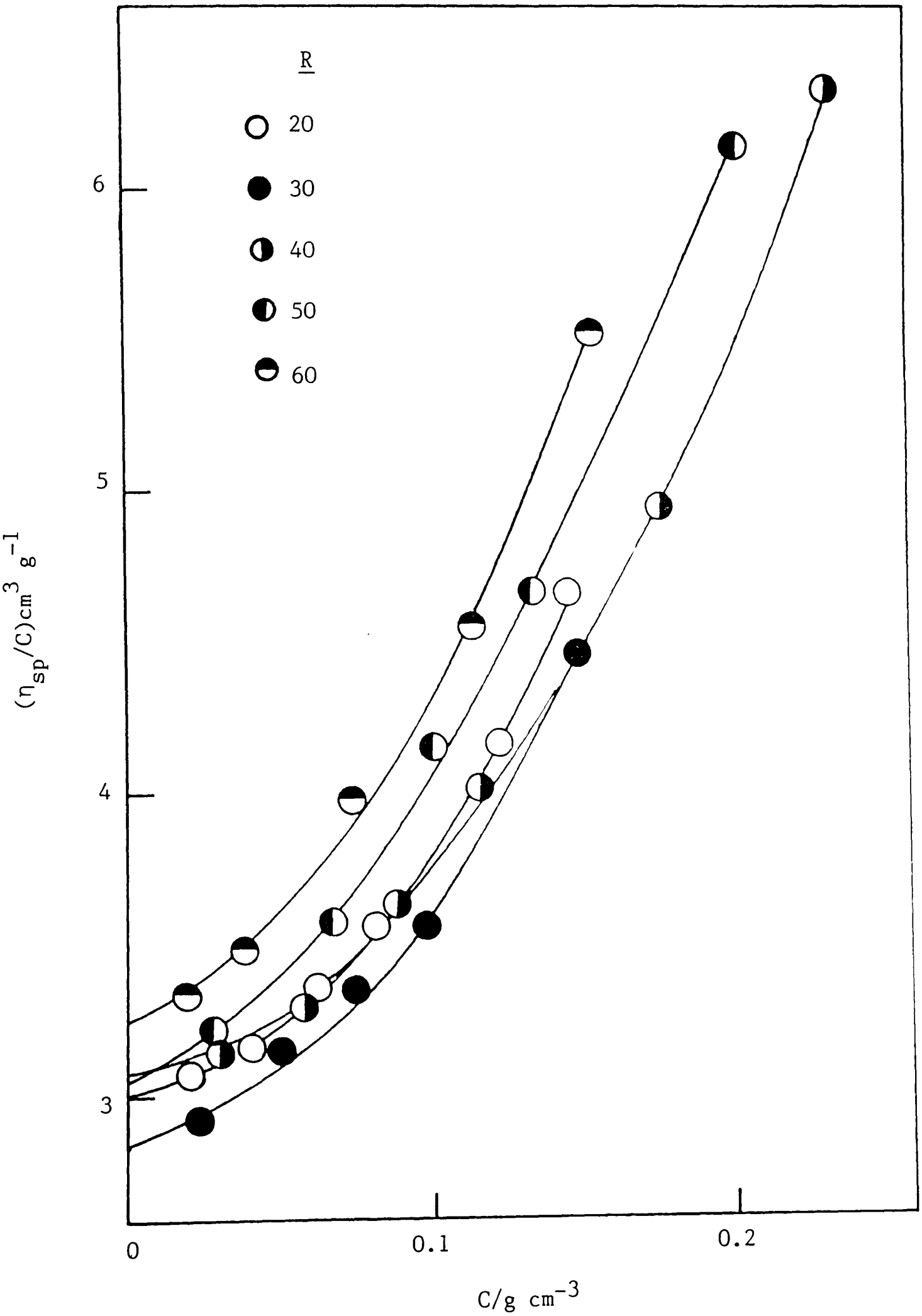

(k_H) varies with concentration. The data were therefore fitted to quadratic equations of the form

$$\eta_{sp}/C = [\eta] + aC + bC^2 \qquad (3.7)$$

where a and b are constants, so that k_H (at infinite dilution) = $a/[\eta]^2$. The densities were used to calculate values of $\bar{V}_d$. Plots according to equation 3.6. were accurately linear for all R values. No trend in $\bar{V}_d$ with R was apparent, an average value being 0.94 ± 0.01 cm^3 g^{-1}. Intercepts of such plots yielded $\bar{V}_{solv} = 1.47 \pm 0.01$ cm^3 g^{-1}, in agreement with measured densities.

Table 3.7 gives the derived values of the intrinsic viscosities and k_H (as $C \to 0$) for all microemulsions studied. Values of the Simha factor, w, obtained from equation 3.5 by assuming no solvation ($\delta = 0$) together with values of δ assuming spherical aggregates ($w = 2.5$) are also given.

Table 3.7

Solvation and Simha factors for w/o microemulsions in heptane stabilised by AOT at 25°C

R	$[\eta]/cm^3\ g^{-1}$	k_H ($C \to 0$)	w ($\delta = 0$)	δ($w = 2.5$)
20	3.01	0.12	3.20	0.18
30	2.85	0.39	3.03	0.14
40	3.11	0.09	3.31	0.21
50	3.03	0.64	3.22	0.18
60	3.28	0.20	3.49	0.25

Assuming $\delta = 0$, the values of w indicate axial ratios of 2.3 to 3.5.[116] Intuitively however, a more acceptable interpretation of the viscosity data is that the droplets are close to spherical in shape, rather than elliptical, and solvated by heptane. Similar conclusions have been drawn for microemulsions stabilised by AOT but using glycerol as dispersed phase.[117] An estimate of the molar ratio of solvent to surfactant at the interface of the droplets, N, may be obtained from the degree of solvation, since it can readily be shown that

$$\frac{\text{number moles surfactant}}{\text{per gram droplets}} = \frac{3\bar{V}_d}{N_A r_H A_D}$$

where N_A = the Avagadro constant. Also

$$\frac{\text{number moles solvent}}{\text{per gram droplets}} = \frac{\delta}{\text{molecular mass solvent}}$$

from which

$$N = \frac{N_A r_H A_D \delta}{300\ \bar{V}_d} \qquad (3.8)$$

The P.C.S. data yielded a value of $A_D = 0.50\ nm^2$ and the fitting equation $r_H/nm = 0.175\ R + 1.45$. Values of N calculated using equation 3.8 are 2 ± 1, i.e. approximately one heptane molecule is associated with every two surfactant molecules at the droplet surface. The penetration of alkane into the surfactant chain

region of the droplets is to be expected and will be discussed further in Chapter 7. Finally, values of k_H obtained (Table 3.7) clearly deviate from the hard-sphere value of $\simeq 0.7$. These are not reliable however due to the curved nature of plots like those in Figure 3.11 at low C.

3.8 Nature of equilibrium aqueous phases

It is normally assumed that at low salt concentrations, the aggregates present in the aqueous phase are small oil-in-water microemulsion droplets. This has been confirmed by small angle neutron scattering experiments, where sizes are given in the range 5-12 nm.[118] Very recent analyses in this laboratory[119] have characterised the aggregates in equilibrium aqueous phases for the AOT/heptane/aqueous NaCl system in terms of the ratio $R' = [\text{heptane}]_{aq}/[\text{AOT}]_{aq}$ using a titration technique.[120] It has been shown that for $m_s < 0.05$ mol dm^{-3}, R' increases with increasing m_s; simple model calculations, on the assumption of spherical droplets, yield aggregate radii of 0.2 nm for $m_s = 0$ rising to $\simeq$ 10 nm at $m_s = 0.045$. Time-resolved fluorescence studies[119] indicate that the radii depend linearly on R' and become larger as the phase inversion salt concentration is approached.

3.9 Possible structures of 'third'-phase

Whilst microemulsions coexisting with 'excess' oil or aqueous phases contain droplets of the dispersed medium, the structure

of the 'third'-phase microemulsion (in which the volume fraction of oil and water is comparable) is more complex. Experimental evidence obtained by means of ultracentrifugation[121] indicates, however that at the lower end of the salt concentration range, the middle phase contains droplets of oil-in-water while at higher concentrations the middle phase is oil continuous. A phase inversion must occur, at an intermediate salt concentration, from a water continuous to an oil continuous microemulsion. As a consequence, near this point, it is possible that the middle phase is composed of a constantly changing mosaic of regions of both kinds of microemulsion.

Several authors have proposed models to account for the experimentally observed features of the transition i.e. continuity of physical properties. Bicontinuous structures have been described as 'sponge-like',[122] mixtures of oil-in-water and water-in-oil microemulsions[123] and lamellar structures.[124] In all these, the surfactant is concentrated mainly at the internal surface between the oil and water regions and surface layers are assumed to be flexible. Since aggregate sizes increase as phase inversion is approached, the third-phase (often observed when ultralow tensions are produced) could be regarded as an 'infinite' aggregate in which the surfactant film is effectively planar and exhibits almost zero net curvature.

3.10 Geometrical approach to phase inversion

3.10.1 Introduction

It has long been appreciated that the molecular geometry of the surfactant molecule could be responsible for the phenomenon of

phase inversion and the type of emulsion formed. A simple yet useful approach to understanding results of the kind described is that discussed by Mitchell and Ninham[15] and earlier workers.[125] Droplet sizes have been calculated by considering (geometrically) the packing of surfactant chains of known length and volume in the droplet surface region. Surfactant behaviour is characterised in terms of a packing ratio, $P = v/a_h\ell$, where v and ℓ are the volume and length respectively of the hydrocarbon moiety and a_h is the effective cross-sectional area of the polar headgroup. The quantity v/ℓ which is the cross-sectional area of the chain, a_c, assumes an 'effective' value which includes penetration of alkane into the surfactant monolayers, and a_h includes a contribution from the hydration sheath around the headgroup. Thus P is essentially the ratio of the cross-sectional areas of the chain and headgroups. For $P < 1$, 'normal' structures are expected with the large headgroups on the outer side of a convex curved surface. These structures can take the form of spherical oil-in-water microemulsion droplets. For $P > 1$, inverted structures in the oil phase are predicted, in the form of water-in-oil droplets (or inverted micelles). When $P = 1$ (i.e. $a_h = v/\ell$), surfactant 'prefers' to be at a plane interface and it is argued that the tension of a plane oil-water interface (γ_c) assumes its minimum value, and the system will be at a phase inversion point. The third phase formed in the inversion region will be one in which surfactant monolayers exhibit almost zero net curvature. In macroscopic emulsions interfacial curvature is small, but the curvature of the surface of microemulsion droplets

is great. It may be assumed that in the latter case the curvature is the preferred curvature so that microemulsion droplet size may reflect in a relatively simple way the surfactant molecular geometry. Changes in a 'normal' system which serve to reduce a_h or increase v, bring the system closer to phase inversion and lead to a reduction in γ_c.

The packing ratio is affected by other factors (in addition to the salt concentration) including pH, temperature and the addition of amphiphilic compounds such as cosurfactants. Two of these factors will be discussed in later chapters.

3.10.2 *Molecular geometry and salt effects*

It has been shown that γ_c passes through a minimum as m_s is increased and that phase inversion and surfactant transfer between phases coincide with the occurrence of minimum γ_c. The effects are supposed to result from a reduction of lateral electrostatic repulsion and possibly hydration of surfactant headgroups caused by salt addition. In geometrical terms, a_h decreases and P increases.

The area per surfactant molecule, A_s, in a saturated film at a plane oil-water interface is expected to decrease with increasing m_s and assume an effectively constant value A_s^{ℓ} at the value of m_s corresponding to minimum γ_c. At low m_s, A_s should be governed mainly by the (large) headgroup area a_h since strong electrostatic repulsion operates between headgroups. At a planar interface the surfactant molecules can pack more and more closely until the headgroup area is reduced to that of the chain region.

The value of A_s^{ℓ} is expected to be determined by the size of the surfactant chains and by the degree of penetration of alkane into the monolayer; at a planar interface A_s^{ℓ} cannot be reduced below a_c (see Figure 3.12a).

These propositions may be tested by determining A_s (at the c.m.c.) as a function of m_s from plots of interfacial tension against $\ln m_D$ (examples of which are depicted in Figure 3.2) and the appropriate form of the Gibbs equation (equation 3.1). Values of A_s against m_s are shown in Figure 3.13. As seen, A_s falls sharply with m_s and the line in the figure is that described by the equation

$$A_s/nm^2 = 0.4237 \exp(-56.83\ m_s) + 0.722 \text{ (heptane)}$$

As predicted, A_s becomes effectively constant at $m_s \simeq 0.05$ mol dm^{-3} for the heptane-aqueous NaCl interface, corresponding to the salt concentration producing minimum in γ_c. The value of 0.72 nm^2 for A_s^{ℓ} will be discussed, in connection with values for other alkanes, in Chapter 7.

The results for the air-solution interface (Appendix I) are not immediately understandable. For this interface $A_s^{\ell} = 0.733$ nm^2, close to that for the heptane-solution interface, and larger than that for the interfaces involving the larger alkanes. This may be explained as folows. The volume v of the chain-region of an AOT molecule, calculated from the molar volume of ethylhexane (noting that a terminal CH_3 group is replaced by a CH_2 group in AOT) is 0.479 nm^3. Using molecular models, the chain length

Figure 3.12a Reduction of area per surfactant, A_s, at a plane interface.

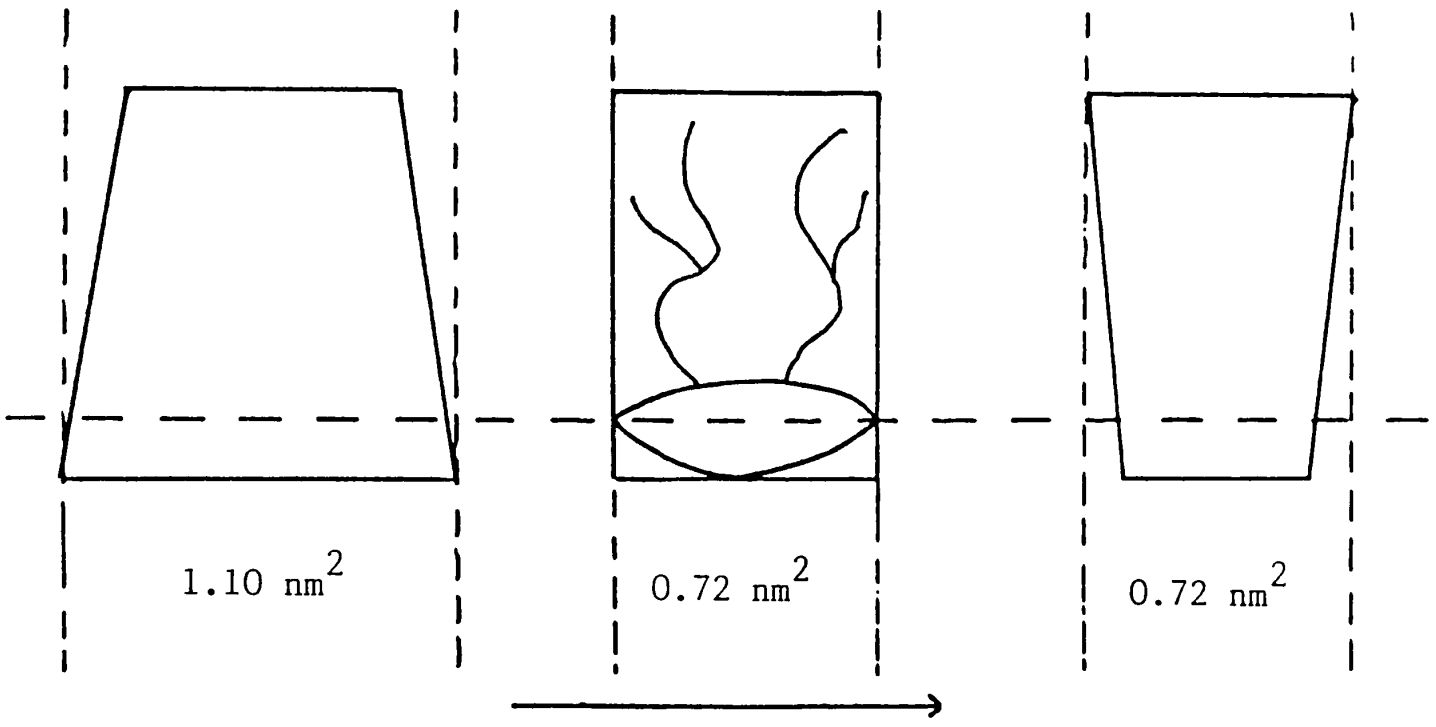

Figure 3.12b Enhanced packing at a convex water interface at high salt concentration

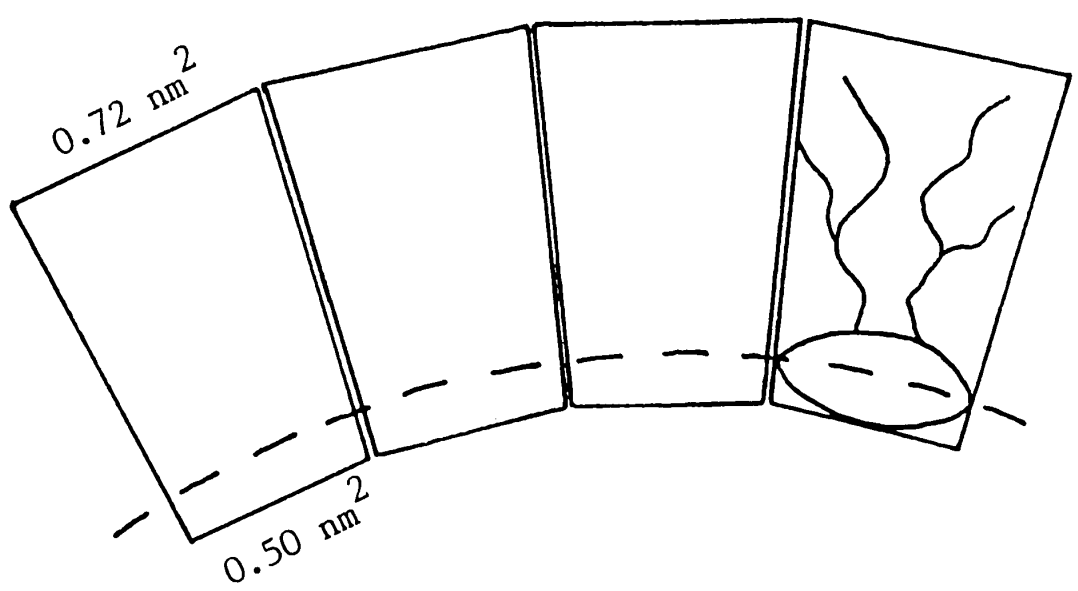

Figure 3.13 Variation of the saturated area per molecule with salt concentration for AOT at the heptane–solution interface at 25°C

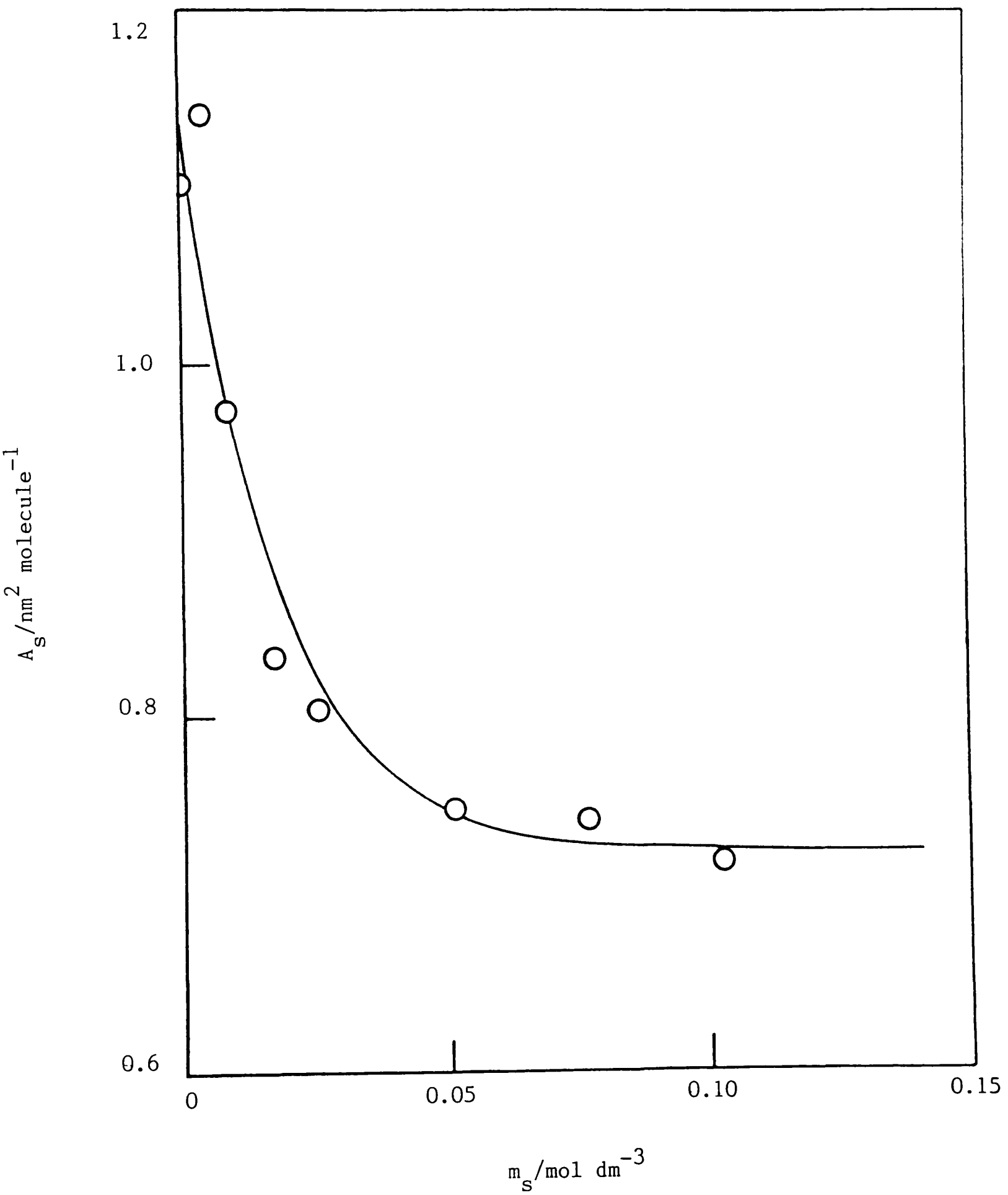

ranges from 0.65-0.90 nm, depending on conformation and so a chain cross-sectional area of between 0.74 and 0.53 nm^2 is expected. It would appear therefore that at the air-solution interface the AOT molecule adopts a conformation such that the chain length is minimised. This effect is presumably dominated by the unfavourable chain-air interactions in comparison with both intra- (i.e. CH_2-CH_2 in one chain) and inter-chain interactions. At the oil-solution interface favourable alkane-chain interactions serve to stabilise the extended conformations and thus can reduce the cross-sectional area.

3.10.3 *Comparison of area per surfactant molecule at plane and curved oil-water interfaces*

The value of A_s^{ℓ} of 0.72 nm^2 compares with A_D = 0.50 nm^2 for surfactant at a water droplet in a water-in-oil microemulsion. The microemulsions did not contain salt which suggests the posibility that in the distribution experiments little NaCl transfers to the oil phase. It is realised that the counterion concentration in microemulsion droplets is high (about 2 mol dm^{-3} for $r_H \simeq 6$ nm) and presumably constitutes swamping excess of salt, so A_s^{ℓ} and A_D should not differ on this count.

A possible explanation for the apparent reduction in suface area is a loss of surfactant from the surface of the droplets i.e. a distribution of surfactant between interface and continuous phase. The base catalysed degradation of AOT, where the concentration of surfactant inside the droplets is found

to be lower than expected for a given R value, gives credence to this hypothesis.[113] Equally important, the S.A.N.S. profiles show a marked polydispersity possibly due to 'dynamic' dimers and trimers of droplets in the system resulting in a reduction of the overall interfacial area.[107] A more likely alternative for the difference could arise as a result of the molecular geometry of AOT. Once aggregates form in the oil phase, the headgroup area may be further reduced at a curved interface by the addition of salt until its 'geometrical' size is reached ($\simeq$ 0.45 nm^2). Furthermore, if the geometrical size is smaller than that of the chains, the molecule can adopt a conical shape and pack more closely into a curved surface (Figure 3.12b).

The decrease in size of w/o microemulsion droplets with increasing m_s (Figure 3.8b) is due to the continued reduction in a_h at a curved interface. The value of 0.50 nm^2 represents the average area per molecule occupied over the range of m_s studied. The headgroup area at a microemulsion surface may be calculated as a function of m_s using the following model. If the nonpolar part of each AOT molecule is considered as a frustum of a cone of height t (the thickness of the chain region of the droplets) it can be shown that (Figure 3.14)

$$\frac{(a_c/4\pi)^{\frac{1}{2}} - (a_h/4\pi)^{\frac{1}{2}}}{t} = \frac{(a_h/4\pi)^{\frac{1}{2}}}{r_c}$$

from which $a_h = a_c r_c^2/(r_c + t)^2$. Taking t = 1.4 nm and a_c = 0.72 nm^2 found earlier, the change in a_h for different values of r_c (and hence m_s) is shown in Table 3.8. At high m_s, a_h approaches

Figure 3.14 Schematic representation of a surfactant molecule at the surface of a microemulsion droplet

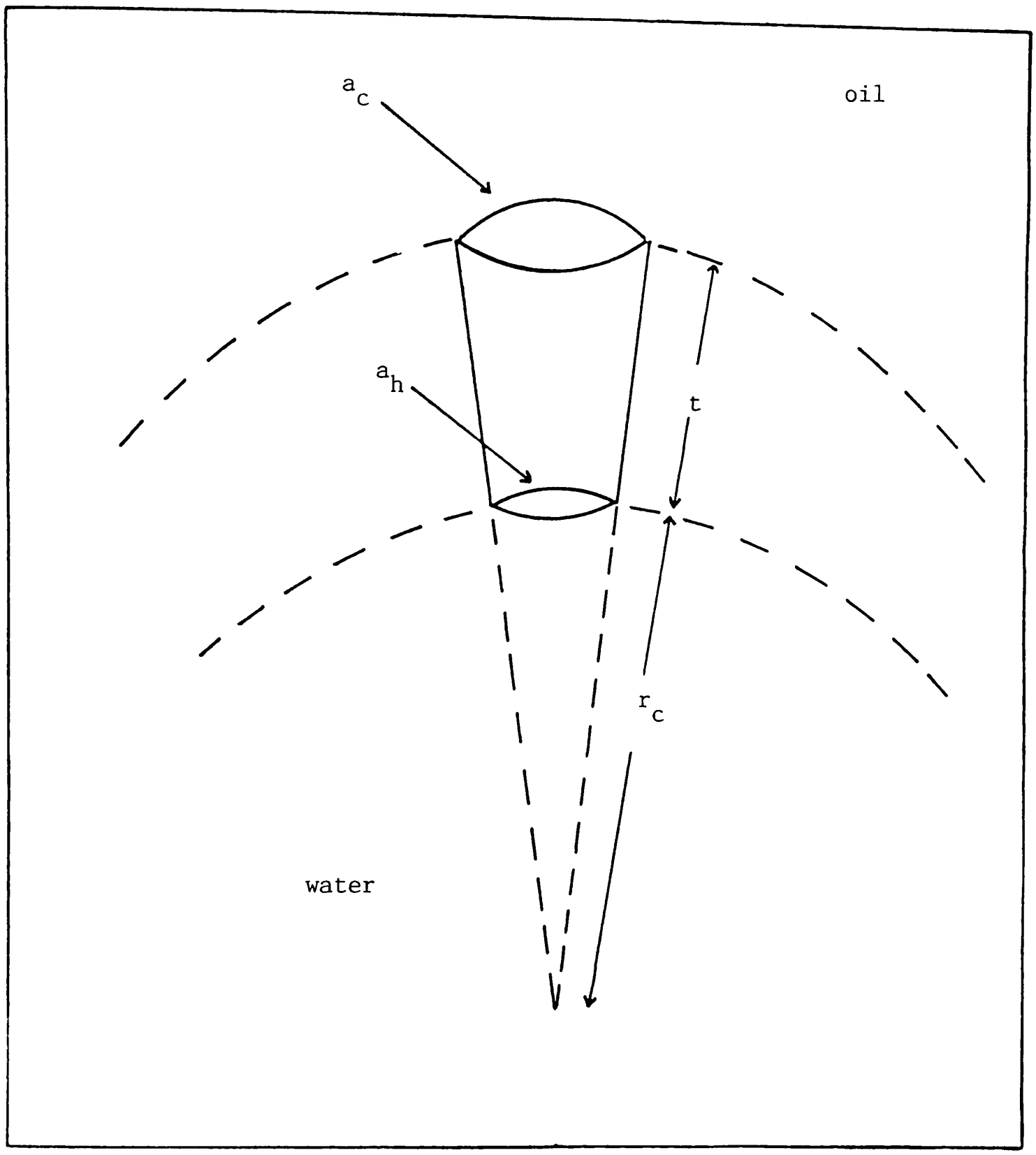

the molecular size of the headgroup where lateral repulsions are completely screened.

Table 3.8

Calculated variation of headgroup area with m_s at curved interface

m_s/mol dm^{-3}	R	r_c/nm	a_h/nm^2 molecule^{-1}
0.0605	92.6	16.8	0.613
0.0655	72.5	12.4	0.581
0.0706	66.7	12.2	0.579
0.0806	56.9	10.7	0.563
0.0907	46.2	8.0	0.521
0.1008	42.7	* 7.5	0.511
0.1512	30.8	* 5.4	0.454
0.2016	25.2	4.5	0.419
0.2520	24.6	4.3	0.410

* Values of r_c have been interpolated from the r_H, R plot shown in Figure 3.10b.

3.11 Relation between droplet size and interfacial tension

Several theoretical attempts have been made to predict low oil-water tensions when a surfactant layer is formed at the

interface, and when micelles or other structures are present in the equilibrium bulk phases.[126-130] In AOT/aqueous NaCl/heptane systems equilibrium sizes of droplets have been determined as a function of m_s. For oil droplets in water, values of $R'(= [\text{heptane}]_{aq}/[\text{AOT}]_{aq})$ versus salt concentration have been measured using a titration technique[120] and sizes calculated from measured aggregation numbers using time-resolved fluorescence studies.[119] In the case of water droplets in oil, sizes were measured using P.C.S. (§ 3.7.2). Radii are shown as a function of m_s in Figure 3.15 together with the corresponding γ_c values. As seen, the smaller the droplets, the higher the tension γ_c at the plane interface. The size of droplets tends to infinity as phase inversion and minimum γ_c occur.

The interfacial tension γ_d at the droplet surface is determined by the adsorption of surfactant from the bulk to the curved droplet surface. The interfacial tension γ_c between a microemulsion and the excess dispersed phase is similarly caused by the adsorption of surfactant at the interface which in this case is planar. Experimental data indicate that γ_c remains the same when the entire microemulsion is replaced by its continuous medium.[22] This means that the concentration of surfactant at the interface primarily affects the value of γ_c and that the presence of the droplets has at most only a secondary effect. Ruckenstein[126] argues, on the assumption that the concentration of surfactant is the same at the droplet and plane interfaces, γ_d and γ_c should differ only because the adsorbed layer is bent to a relatively

Figure 3.15 Variation of plane interfacial tension and microemulsion droplet radii with salt concentration (AOT-H_2O-heptane 25°C)

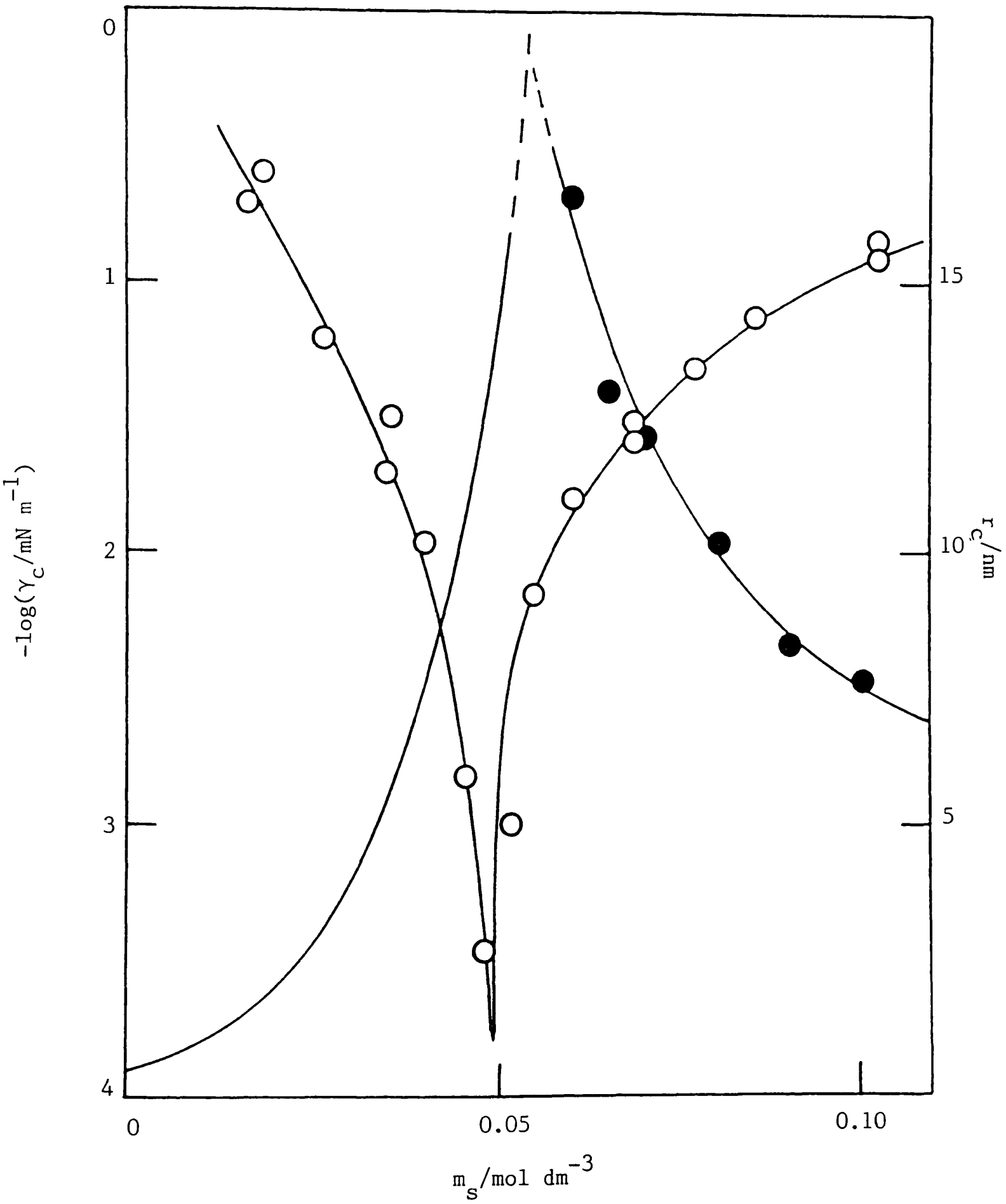

○ Interfacial tension

● w/o droplet radii (P.C.S.)

Full curve for o/w radii taken from results in ref. 119

large curvature in the former case. He and other authors[127,129] introduce a bending energy required to bend unit area of the interface. However, a second contribution to the tension arises from the increase in entropy of the system caused by dispersion of one phase in the other.

Bending effects arise because interaction between adjacent surfactant molecules is not uniform across the film i.e. adjacent headgroups interact differently from adjacent chains. The bending energy is primarily due then to the change in area per surfactant molecule between the inner and outer surfaces of the film. Most treatments concerned with deriving a relation between the tension γ_c and droplet size, lead to the conclusion that the tension should have an inverse dependence on the square of the droplet radius, of the form kT/L^2 where L is the droplet radius in two-phase regions and a characteristic size ξ for middle phase microemulsions. The data in Figure 3.15 suggest that this is approximately observed, although the find detail is not satisfied.

Calculations[127] show that dispersion reduces the droplet radius below its 'natural' or 'preferred' value; the increase in free energy in bending the film from its natural radius to a smaller value is counterbalanced by the simultaneous decrease in free energy of mixing due to an increase in the number of droplets. The basic result of these calculations is that the droplet radius in a two-phase microemulsion system is primarily a property of the interfacial film. The dispersion effect, although important, is secondary in nature. Nonetheless, the

precise value of γ_c is, of course, related to the size of the droplets which can be formed, since both (i.e. size and tension) are directly dependent on curvature properties.

In contrast, Langevin *et al.*[129] have separated the contributions to the plane interfacial tension into an entropic term γ_e (due to dispersion) and a term due to curvature effects, γ_b. The order of magnitude of the two tensions is shown to be the same and $\gamma_e \simeq \gamma_b \simeq kT/r^2$. Thus it can be noted that the tension depends ultimately on the droplet radius and not on droplet concentration (see Figure 3.3). Such conclusions are however very system dependent.[129]

The comments above summarise the current state of theoretical calculations in predicting low tensions. .They are preliminary to the development of a more rigorous approach to the relationship between interfacial tension and microemulsion droplet size. The nature of the problem is to develop a model for the dependence of the bending energy on salt concentration. A generalised model based on inter-droplet interactions of the hard-sphere type used in some treatments is unlikely to succeed since the behaviour of the real systems is far from that of hard spheres.

3.12 Salt effects in systems containing DHBS

In systems containing heptane-aqueous NaCl and DHBS, very similar behaviour with respect to tension changes and surfactant aggregation is observed as with AOT. In contrast however, DHBS has a very low solubility in water and does not reach a c.m.c. In the presence of NaCl however, the c.m.c. can be reduced to

below the solubility limit and micellisation occurs. Figure 3.16 shows that the onset of surfactant transfer to the oil and phase inversion are accompanied by minimum γ_c. The value of m_s at which this occurs is less than for AOT whilst the magnitude of the minimum tension is higher.[104]

The results of P.C.S. experiments for both 'made-up' and equilibrium w/o microemulsions yielded sizes that agree well. The value of A_D was 0.69 ± 0.02 nm^2, compared with 0.70 ± 0.01 nm^2 for A_s^{ℓ} at the planar interface. The reason for the similarity in these areas becomes apparent on inspection of a molecular model of DHBS indicating that an effective reduction of A_s at a curved surface is less likely than for AOT. The value of t was found to be 1.6 ± 0.2 nm close to the geometrical length of the molecule which is ≃ 1.3 nm. Although the differences between the two surfactant systems are of interest the deviation between them is reasonably small and the most important conclusion from the two studies is that the systems behave similarly. Both sets of data are consistent with a simple geometrical picture of the assemblies as spherical droplets whose sizes lie in a narrow distribution.

3.13 Salt effects in oil + water systems containing pure nonionic surfactants

The phase behaviour of oil + water systems containing nonionic surfactants of the type $C_{12}E_m$ (where E represents the oxyethylene group) is well documented.[19,131] The studies have mainly concentrated on the effect of temperature in such systems,

Figure 3.16 Interfacial tensions and surfactant distribution against m_s in the system DHBS-H_2O-heptane at 25°C

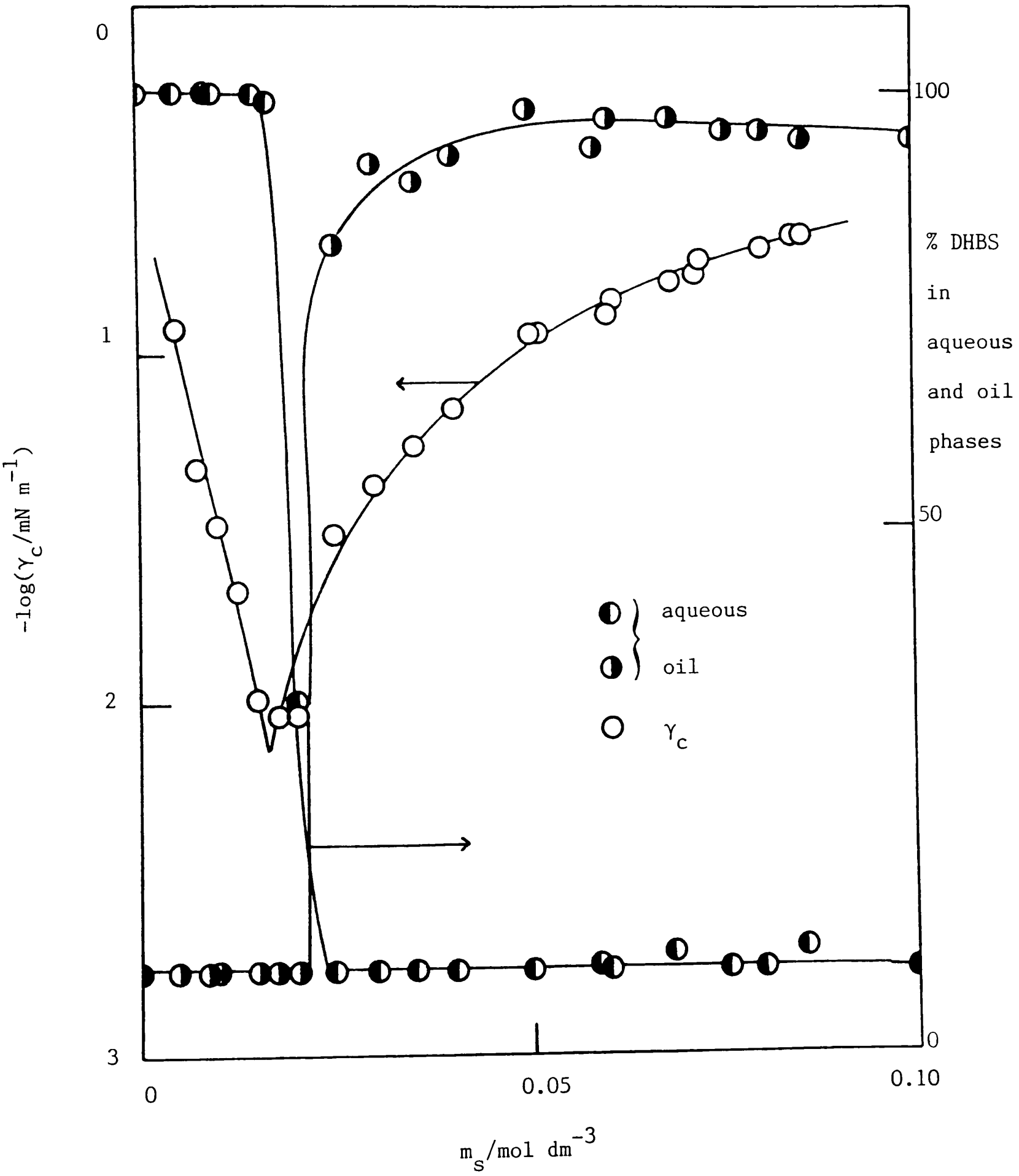

including detailed investigations around the phase inversion temperature. Very few reports however have appeared which relate to interfacial tensions or the effect of the presence of salt in these systems. Recently, Aveyard and Lawless[132] have presented data for the effects of changes in salt concentration and temperature on the interfacial tensions between alkane and aqueous phases containing various surfactants of the type $C_{12}E_m$. Results are discussed using a simple thermodynamic treatment. The work described below was designed to determine whether the interfacial tension minima with respect to salt concentration reported by Aveyard and Lawless are accompanied by surfactant transfer between phases and phase inversion, as is the case in systems containing ionic surfactants.

In systems containing anionic surfactants, it will be recalled that ultralow oil-water tensions can be obtained by injecting a drop of pure alkane into an aqueous surfactant solution at or above its c.m.c. If this procedure is adopted using $C_{12}E_m$ surfactants however, ultralow tensions do not result and it has been found necessary to dissolve the surfactant in the oil phase and at a high concentration ($\simeq 0.02$ mol dm^{-3}) relative to the aqueous phase c.m.c.[133] It has been ascertained that above a minimum concentration in the oil, the tension is independent of concentration (Figure 2 of reference 133). This is analogous to the constant γ_c with increasing concentration of anionic surfactant in the aqueous phase. Similarly, values of γ_c pass through a minimum as m_s is increased (Figure 3.17a).

Figure 3.17a Plot of γ_c against m_s for $C_{12}E_5$ + nonane + aq. NaCl at 31°C

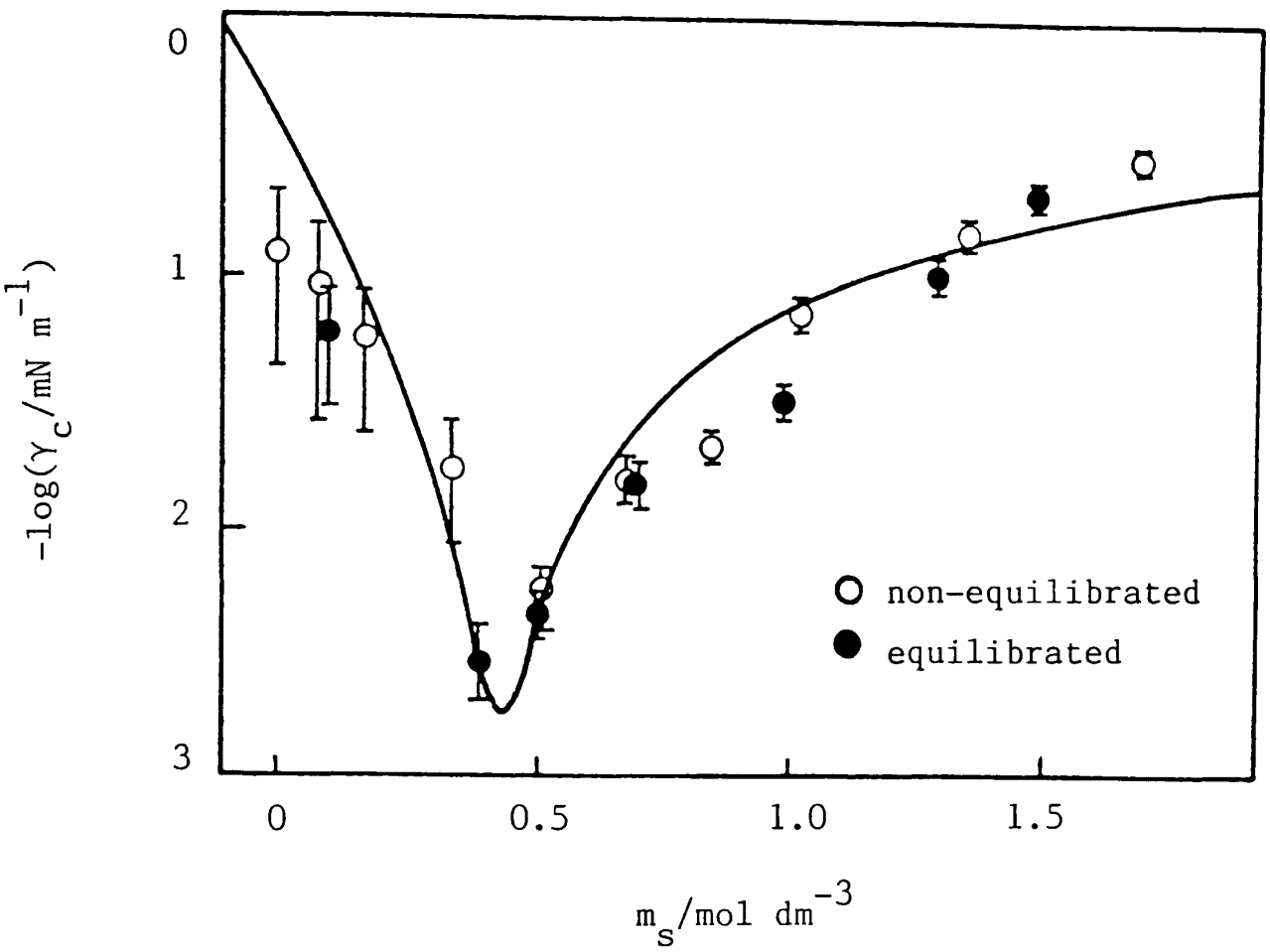

Figure 3.17b Distribution of $C_{12}E_5$ between phases against m_s

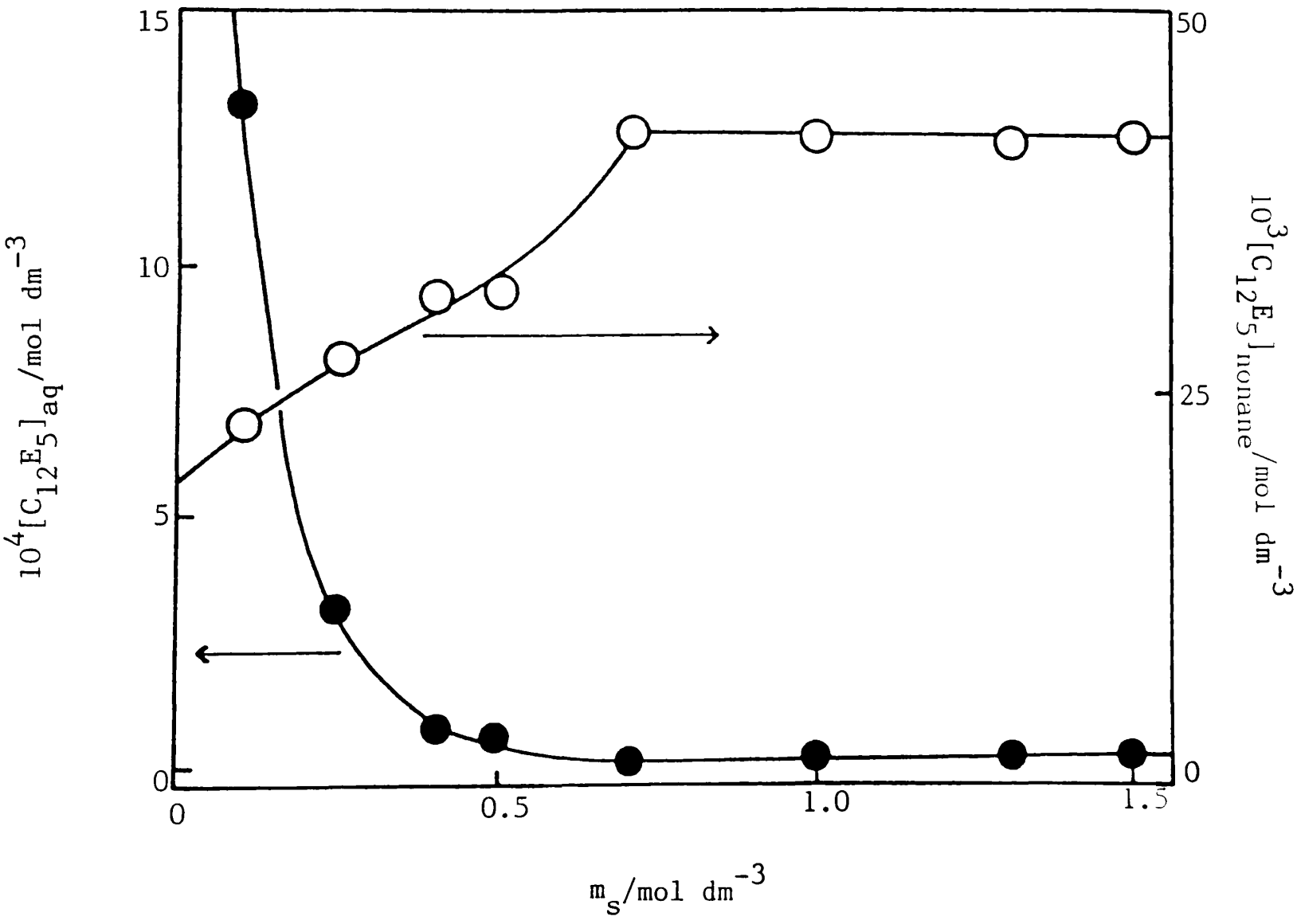

The striking difference between the minimum observed here and that obtained for AOT (Figure 3.3) is the much higher m_s needed to effect it.

The reason why relatively high oil phase concentrations of surfactant are required to obtain low γ is interpreted by noting that monomers of nonionic surfactant are expected to distribute largely in favour of alkane. This is to be expected from the nature of the surfactant and is consistent with the data of Manabe *et al.*[134] who studied similar materials but with shorter alkyl chains. As the surfactant concentration in the system is increased an aggregation point (c.m.c.) is reached either in the aqueous or oil phase depending on conditions (e.g. temperature and salt concentration). The c.m.c. condition corresponds to a high concentration in the oil phase and a low concentration in the aqueous phase. Above the c.m.c., the activity of the monomer remains essentially constant and since it is this which adsorbs at an interface, the tension also remains constant.

The effect of salt concentration on the distribution of a fixed total amount of $C_{12}E_5$ between water and nonane at 31°C has been studied in connection with the occurrence of the minimum in γ_c depicted in Figure 3.17a. One volume of 0.043 mol dm^{-3} $C_{12}E_5$ in nonane was shaken with five volumes of aqueous solution containing various concentrations of NaCl. Surfactant concentrations in each phase were determined spectrophotometrically (see § 2.4.2). Results from these experiments are shown in Figure 3.17b. For m_s of 0.4 and 0.5 mol dm^{-3} three phases were present at equilibrium. For all other values of m_s, two clear

phases formed. At low m_s, the aqueous and alkane phase concentrations are high, but as m_s increases the aqueous phase concentration falls to a low and almost constant value, approximately equal to reported c.m.c. values,[135] and the oil phase concentration rises to a high plateau value.

From a knowledge of the distribution of monomeric surfactant, it may be concluded that at low m_s, the aqueous phase surfactant concentration is high and an o/w microemulsion is present in equilibrium with an excess oil phase containing a high concentration of monomers. As m_s is increased surfactant transfers to the oil phase and forms aggregates (in the form of w/o microemulsion droplets) in equilibrium with monomers at high concentration. The surfactant concentration in the excess aqueous phase falls to a level close to the c.m.c. that would be observed in the absence of excess oil phase.

The above propositions are supported by P.C.S. results obtained for the equilibrium phases. At low m_s, P.C.S. indicated that small aggregates were present in aqueous phases; none of the oil phases exhibited any correlation function over a range of sample times appropriate for aggregate radii from <1 to 250 nm. At high m_s, however, no structure was found in the aqueous phases but the nonane phases exhibited light scattering typical of small w/o microemulsion droplets.

The interfacial tensions between equilibrated phases are shown in Figure 3.17a as a function of m_s. The agreement between these and tensions from phases not originally at equilibrium is

good. In both pre-equilibrated and non-equilibrated systems, the tension varied in an oscillatory fashion with time with a period of $\simeq$1 min. The oscillations continued, about the same mean γ_c, for periods of up to 4 h. This effect (not observed for anionic surfactants) could arise as a result of the slower rate of diffusion of nonionic surfactants to and from the interface. Injecting an oil drop into the spinning-drop apparatus causes it to elongate and its surface area increases. This leads to an increase in tension if the surface concentration of surfactant is not maintained. In turn, this would tend to cause a contraction of the drop, giving an increase in surface concentration and a concomitant fall in tension. Elongation of the drop would then occur and the process could be repeated.

From the foregoing discussion, it may be concluded that as surfactant concentration in a system is increased, the tension is lowered until the onset of aggregation in the preferred phase and then remains constant at a value of γ_c. A similar kind of tension variation has been reported by Crook *et al.*[136] With increasing m_s, surfactant transfer between phases occurs around the condition for minimum γ_c, which also corresponds to the phase inversion of the coarse emulsions formed by agitation of aqueous and oil phases. The type of macroemulsion formed corresponds to the type of microemulsion which exists at equilibrium.

Acknowledgements

The author thanks Dr. J. Mead for his collaboration in obtaining the data in Figure 3.10, and similarly Mr. S. Clark for those in Figure 3.11.

Chapter Four

CHAPTER 4

THERMODYNAMIC TREATMENT FOR SALT EFFECTS IN SYSTEMS CONTAINING IONIC AND NONIONIC SURFACTANTS

4.1 Introduction

Aveyard *et al.*[133,137] have given a thermodynamic treatment for micelle-forming surfactants (both ionic and nonionic) which relates to a single interface. It is not relevant therefore when a liquid crystalline film intervenes between oil and aqueous phases and two interfaces exist.[14,30] Ruckenstein[138] has treated similar systems to those of interest here but no simple equations which demonstrate how a tension minimum can occur are given. Recently, Ruckenstein and Beunen[139] have proposed the possibility that tension minima observed with respect to salt concentration (at high salt concentration with nonionic surfactant) can arise as a result of the change in sign of the surface excess of surfactant at the oil-water interface. This could mean that at high salt concentrations (say around 1 mol dm^{-3} NaCl), when the interfacial tension is still very low (say 10^{-2} - 10^{-1} mN m^{-1}), the surface excess of surfactant is negative. The thermodynamic treatment presented below leads to an alternative and one believes more likely explanation of tension minima in systems containing nonionic or anionic surfactant and 1:1 electrolyte.

4.2 Thermodynamic formulation for variation of γ_c - with salt concentration in systems containing anionic surfactant

4.2.1 Derivation of general expression for $d\gamma/d\ln m_{Na}$

Consider a system containing oil (o), water (w) and a 1:1 electrolyte (NaCl) having a common cation (Na^+) with an anionic surfactant whose anion is designated D. The variation of the oil-water tension γ with surfactant molarity m_D is taken to be as shown in Figure 4.1, where the constant γ attained at the c.m.c. for a given salt concentration and temperature (points A and B) is designated γ_c. In systems where the aqueous phase surfactant concentration is initially greater than the c.m.c., the oil-water tension in the equilibrated system is γ_c.

Figure 4.1

Schematic representation of γ against $\ln m_D$ for two salt concentrations

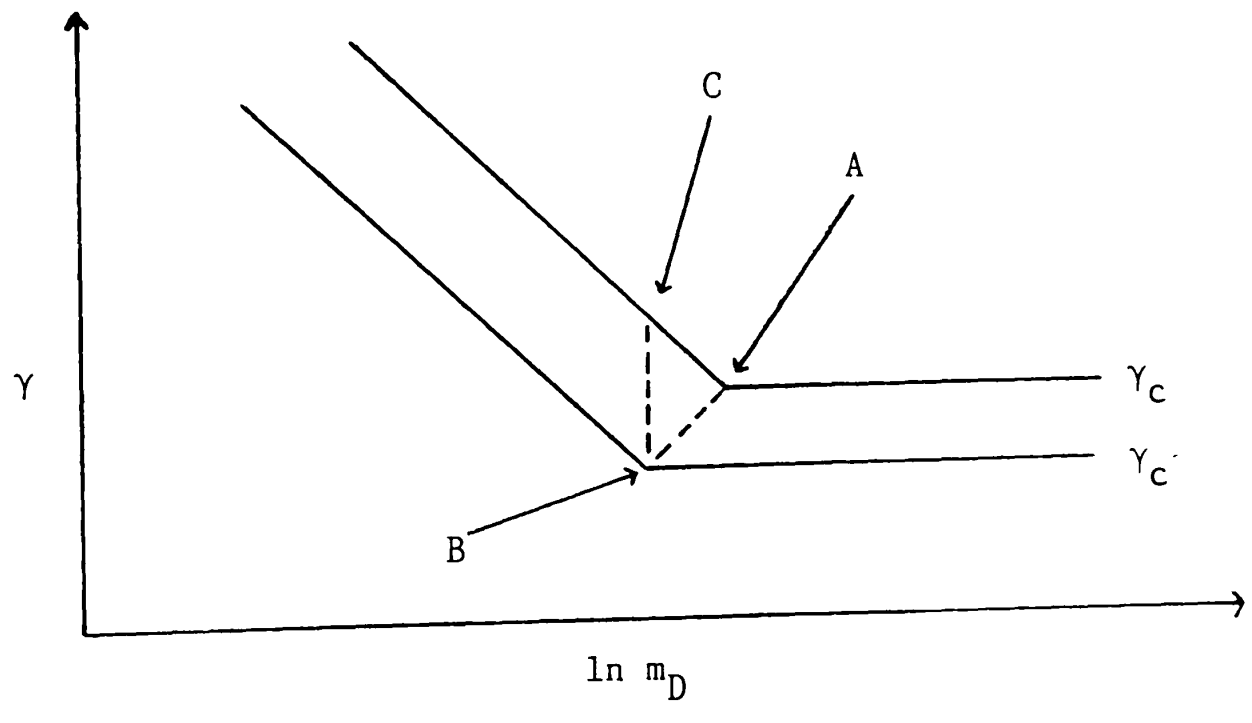

For variations in salt concentration, γ_c can pass through a minimum and is frequently ultralow. The object of the present treatment is to obtain an expression for $d\gamma_c/d\ln[salt]$ and to show under what circumstances this quantity can change sign. Interest is also in identifying the important factors associated with the tension minimum.

The changes in γ_c between points A and B (Figure 4.1) brought about by addition of salt at constant temperature is given by

$$\frac{d\gamma_c}{d\ln m_{Na}} = \left(\frac{\partial\gamma}{\partial\ln m_{Na}}\right)_{D,T} + \left(\frac{\partial\gamma}{\partial\ln m_D}\right)_{Na,T} \cdot \frac{d\ln m_D}{d\ln m_{Na}} \qquad (4.1)$$

where the signs on the ions have been omitted for clarity. The terms in parentheses on the right-hand side of equation 4.1 can be obtained from the Gibbs equation, which for constant pressure is

$$-d\gamma = \sum_i \Gamma_i \, d\mu_i + S_u^\sigma \, dT \qquad (4.2)$$

where the Γ_i are surface excesses.

If the Gibbs convention for the surface is employed and the dividing plane is chosen such that the surface excess of water is zero, the other Γ are relative adsorptions and the excess entropy per unit area of surface, S_u^σ, is the relative surface entropy.[140] For the systems of interest, it can be shown that an analagous form of equation 4.2 exists if the Guggenheim model is used, except that the Γ_i are total surface concentrations. lso, since as shown later Γ_i are either very small (Γ_{Cl}) or very

large (Γ_D, Γ_{Na}), the distinction between excess and total concentrations becomes unimportant.

At and below the aqueous phase c.m.c., one may suppose there are negligible amounts of water and surfactant in the oil and hence neglect the term in dμ (oil). Assuming no hydrolysis of the surfactant occurs, terms in H^+ and OH^- may be omitted so that at constant T equation 4.2 becomes

$$-d\gamma = RT\,(\Gamma_{Na}\,d\ln a_{Na} + \Gamma_D\,d\ln a_D + \Gamma_{Cl}\,d\ln a_{Cl}) \qquad (4.3)$$

where a denotes molar activity. Thus

$$\frac{-1}{RT}\left(\frac{\partial\gamma}{\partial\ln m_{Na}}\right)_{D,T} = \Gamma_{Na} + \Gamma_{Na}\left(\frac{\partial\ln f_{Na}}{\partial\ln m_{Na}}\right)_{D,T} + \Gamma_D\left(\frac{\partial\ln f_D}{\partial\ln m_{Na}}\right)_{D,T}$$

$$+ \Gamma_{Cl}\left[\frac{m_{Na}}{m_{Cl}} + \left(\frac{\partial\ln f_{Cl}}{\partial\ln m_{Na}}\right)_{D,T}\right] \qquad (4.4)$$

where m are molar concentrations and f molar activity coefficients.

4.2.2 *Treatment taking* $\Gamma_{Cl} = 0$

In systems similar to those of present interest, there is experimental evidence that Γ_{Cl} is very small and negative,[43] as might be expected for a surface containing a monolayer of anionic surfactant. For the present, assuming Γ_{Cl} is effectively zero, or electroneutrality in the interface, $\Gamma_{Na} = \Gamma_D$. The case where

Γ_{Cl} is not zero will be considered later. Therefore equation 4.4 may be written

$$\frac{-1}{RT}\left(\frac{\partial\gamma}{\partial \ln m_{Na}}\right)_{D,T} = \Gamma_D\left[1 + 2\left(\frac{\partial \ln f_{\pm}^{NaD}}{\partial \ln m_{Na}}\right)_{D,T}\right] \qquad (4.5)$$

where $f_{\pm}^{NaD}$ is the mean ionic activity coefficient of the surfactant in the presence of the supporting electrolyte, which here is present in large excess. It is reasonable to assume that $f_{\pm}^{NaD} = f_{\pm}^{NaCl}$, after Tajima.[43]

The second term in parentheses in equation 4.1 can also be obtained from equation 4.3 assuming as before that $\Gamma_{Cl} = 0$, and is given as

$$\frac{-1}{RT}\left(\frac{\partial\gamma}{\partial \ln m_{D}}\right)_{Na,T} = \Gamma_D\left[1 + 2\left(\frac{\partial \ln f_{\pm}^{NaD}}{\partial \ln m_{D}}\right)_{Na,T}\right] \qquad (4.6)$$

In the special case of interest here, m_D = c.m.c. in the presence of solubilised alkane. As previously mentioned, the c.m.c. is defined as the aqueous phase concentration of surfactant at which surfactant aggregation occurs in the preferred phase. Also, for a large excess of salt, the term $f_{\pm}^{NaD}$ is determined by the salt and so one may assume that $\partial \ln f_{\pm}^{NaD}/\partial \ln m_D$ is negligible. Combination of equations 4.1, 4.5 and 4.6 yields

$$\frac{-d\gamma_c}{d \ln m_{Na}} = RT\Gamma_D\left[1 + 2\left(\frac{\partial \ln f_{\pm}^{NaCl}}{\partial \ln m_{Na}}\right)_{D,T} + \frac{d \ln cmc}{d \ln m_{Na}}\right] \qquad (4.7)$$

where changes in $f_{\pm}^{NaD}$ have been taken to be equal to changes in $f_{\pm}^{NaCl}$. The salt concentration is equal to m_s, whereas m_{Na}, the total counterion concentration, is equal to the salt concentration plus c.m.c. For many surfactants it is found that $d\ln cmc/d\ln m_{Na}$ is constant.

Inspection of equation 4.7 shows that for minimum γ_c

$$2\left(\frac{\partial \ln f_{\pm}^{NaCl}}{\partial \ln m_{Na}}\right)_{D,T} + \frac{d\ln cmc}{d\ln m_{Na}} = -1 \qquad (4.8)$$

Both terms on the left-hand side of equation 4.8 have negative values. For sodium chloride in water at 25°C, the maximum value of $-2(\partial \ln f_{\pm}^{NaCl}/\partial \ln m_{Na})$ is $\simeq 0.18$[141] (Figure 4.2). Unless $-d\ln cmc/d\ln m_{Na}$ is at least $\simeq 0.82$ no minimum in γ_c appears possible using sodium chloride as electrolyte. For example, the reported variation of the c.m.c. of sodium dodecyl sulphate with salt gives $d\ln cmc/d\ln m_{Na} \simeq -0.67$ and so this surfactant is not expected to give a minimum in γ_c (see later).

From the foregoing discussion, it appears that whether or not a minimum tension is observed with respect to salt concentration depends on the magnitude of $d\ln cmc/d\ln m_{Na}$. When a minimum does occur, the activity coefficient term is an important factor in determining the salt concentration at which it does so. In general terms, the form of the γ_c against salt concentration curves arise from the competing effects on the tension when salt is added. At constant m_D, salt addition lowers

Figure 4.2a Plot of $\ln f_{\pm}$ against m_{Na} obtained using data from ref. 141 for NaCl at 25°C.

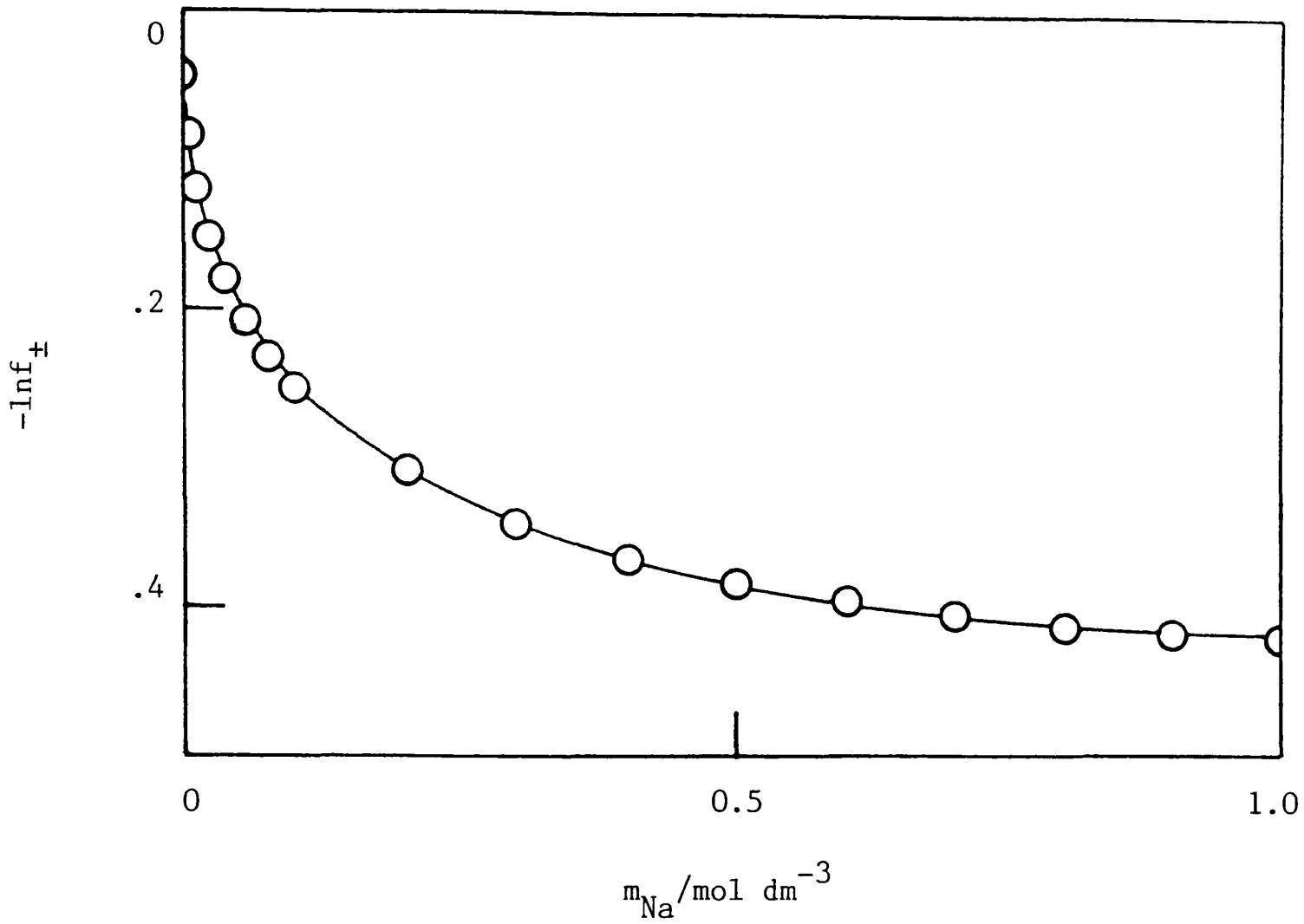

Figure 4.2b Plot of $d\ln f_{\pm}/d\ln m_{Na}$

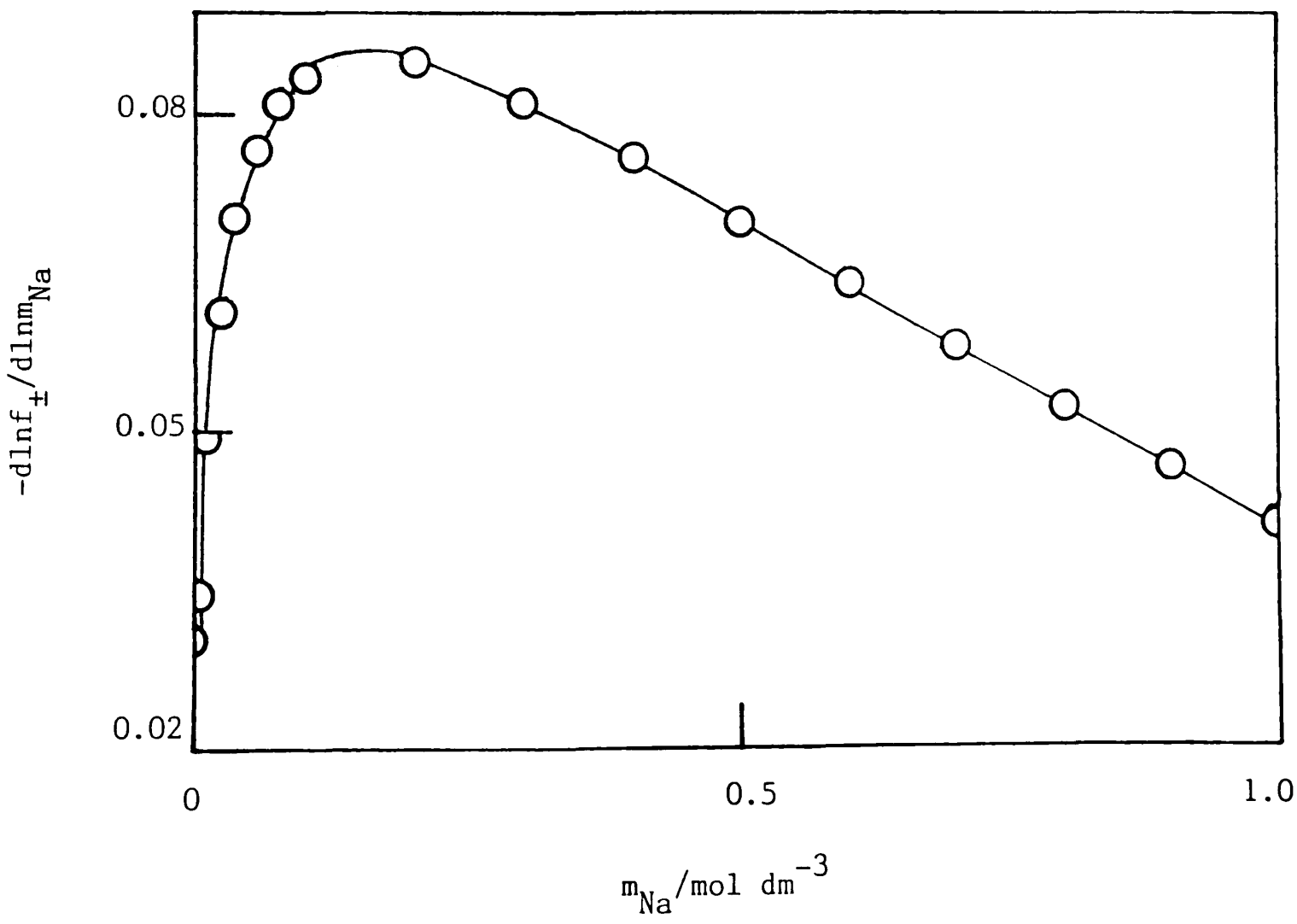

γ according to equation 4.5. On the other hand, m_D is reduced leading, at constant salt concentration, to an increase in γ, (Figure 4.1).

The form of the γ_c against [salt] curves predicted by equation 4.7 may be obtained by integration of equation 4.7 with respect to $\ln m_{Na}$. At constant Γ_D and T this produces

$$-\gamma_c = RT\Gamma_D \left(\ln m_{Na} + 2\ln f_{\pm}^{NaCl} + \ln cmc\right) + B \qquad (4.9)$$

where B is an integration constant. Values of $f_{\pm}^{NaCl}$, from reference 141, were fitted to a cubic in $\ln m_{Na}$:

$$2\ln f_{\pm}^{NaCl} = -6.83 \times 10^{-4}(\ln m_{Na})^3 - 0.025(\ln m_{Na})^2 - 0.278\ln m_{Na} - 1.017 \qquad (4.10)$$

Furthermore

$$\ln cmc = \left(\frac{d\ln cmc}{d\ln m_{Na}}\right) \cdot \ln m_{Na} + a \qquad (4.11)$$

where a is a constant, so that equation 4.9 becomes

$$\gamma_c = -RT\Gamma_D \left[-6.83 \times 10^{-4} (\ln m_{Na})^3 - 0.025 (\ln m_{Na})^2 + \left(0.722 + \frac{d\ln cmc}{d\ln m_{Na}}\right) \ln m_{Na}\right] + B' \qquad (4.12)$$

where $B' = -B - aRT\Gamma_D$, and is the tension at $m_{Na} = 1$ mol dm^{-3}.

Equation 4.12 shows that the form of the γ_c curves will be determined primarily by the values of Γ_D and the c.m.c. term. For the purposes of illustration, Γ_D is taken as constant with value of 2.31×10^{-6} mol m^{-2} (corresponding to an area per

surfactant molecule of ≃ 0.72 nm^2, which would be appropriate for AOT). As seen earlier (§ 3.3.1), Γ_D decreases at low salt concentrations but below that for which minimum γ_c is predicted however. By arbitrarily setting $B' = 1$ mN m^{-1}, the curves generated by equation 4.12 for three values of $dlncmc/dlnm_{Na}$ are shown in Figure 4.3. Curve (a) for $dlncmc/dlnm_{Na} = -0.70$ (similar to that for SDS for example) has no minimum. A shallow minimum is observed for a value of -0.80 (curve b); however for $dlncmc/dlnm_{Na} = -0.85$, a very sharp minimum in tension is predicted at low salt concentration ($m_{Na} \simeq 0.06$ mol dm^{-3}), similar to that measured for AOT/heptane/aq. NaCl systems.

To test how well equation 4.12 fits the experimental data for the AOT/heptane/aq. NaCl system requires very careful determination of the variation of c.m.c. with m_{Na}. Critical micelle concentrations have been determined tensiometrically and taken as the aqueous surfactant concentration at which γ just attains the constant value γ_c. Experimentally, aqueous surfactant solutions were diluted (by weight) using the appropriate salt concentration. Interfacial tensions were measured by injecting pure heptane into the spinning-drop tensiometer, equilibrium being attained within a matter of minutes. Examples of such tension data are shown in Figure 4.4a.

The variation of c.m.c. with salt concentration is described by

$$lncmc = -0.855\ lnm_{Na} - 10.29 \qquad (4.13)$$

nd is depicted in Figure 4.4b. In the distribution studies,

Figure 4.3 Curves predicted by equation 4.12.

Γ_D is taken as 2.31×10^{-6} mol m^{-2} and

$B' = 1$ mN m^{-1}.

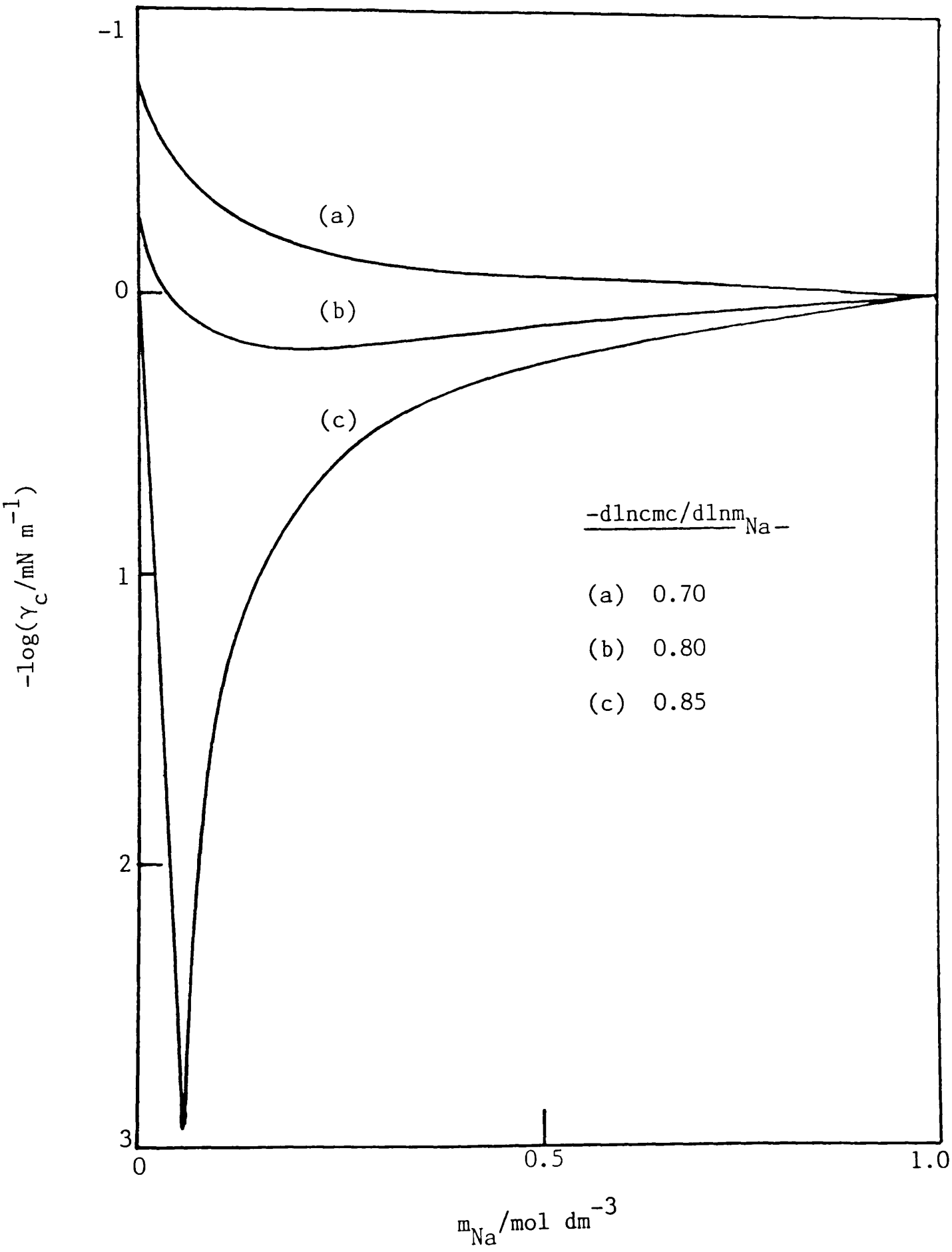

Figure 4.4a Tensiometric determination of the c.m.c. of AOT in the presence of NaCl and excess heptane phase at 25°C.

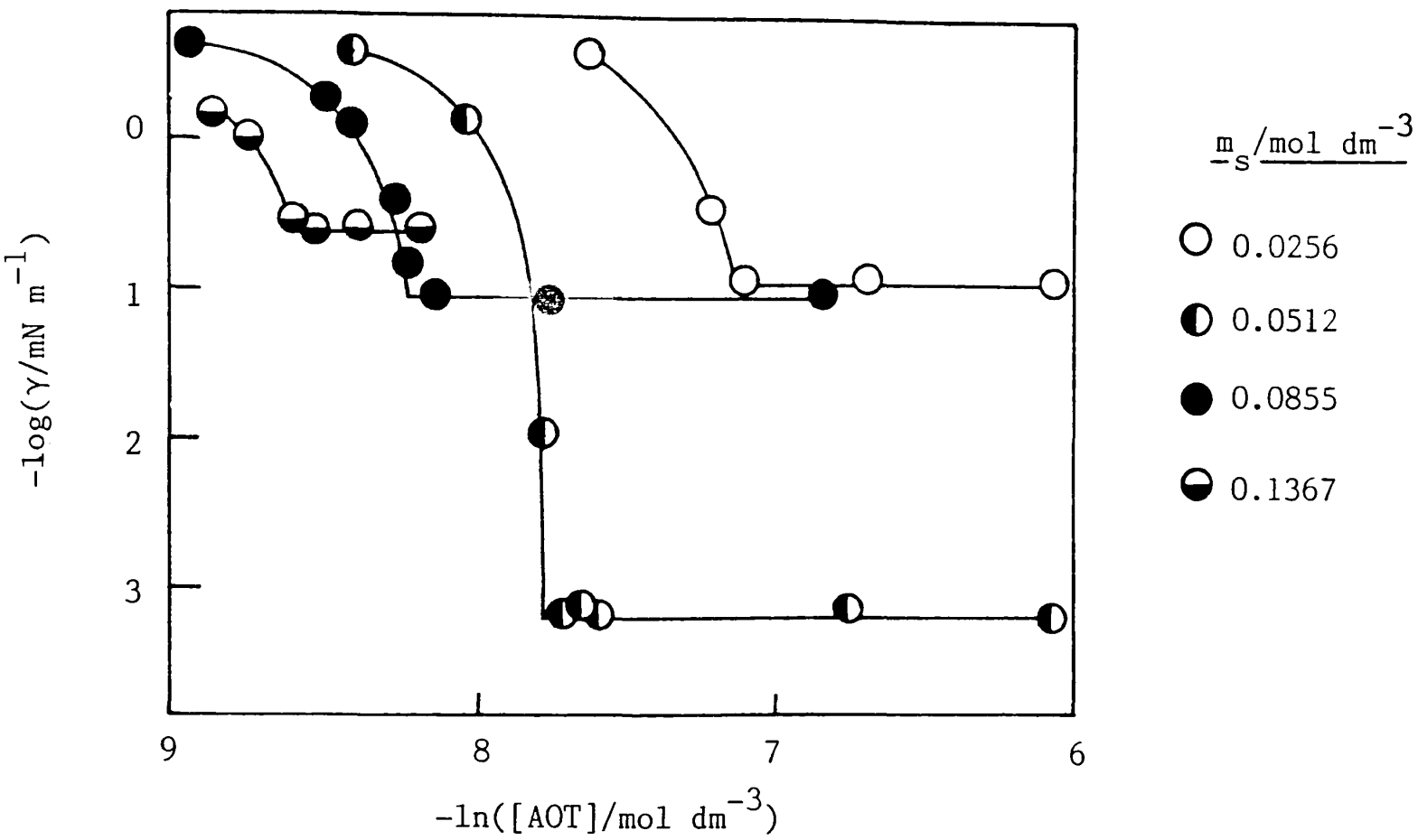

Figure 4.4b Dependence of c.m.c. on total counterion concentration.

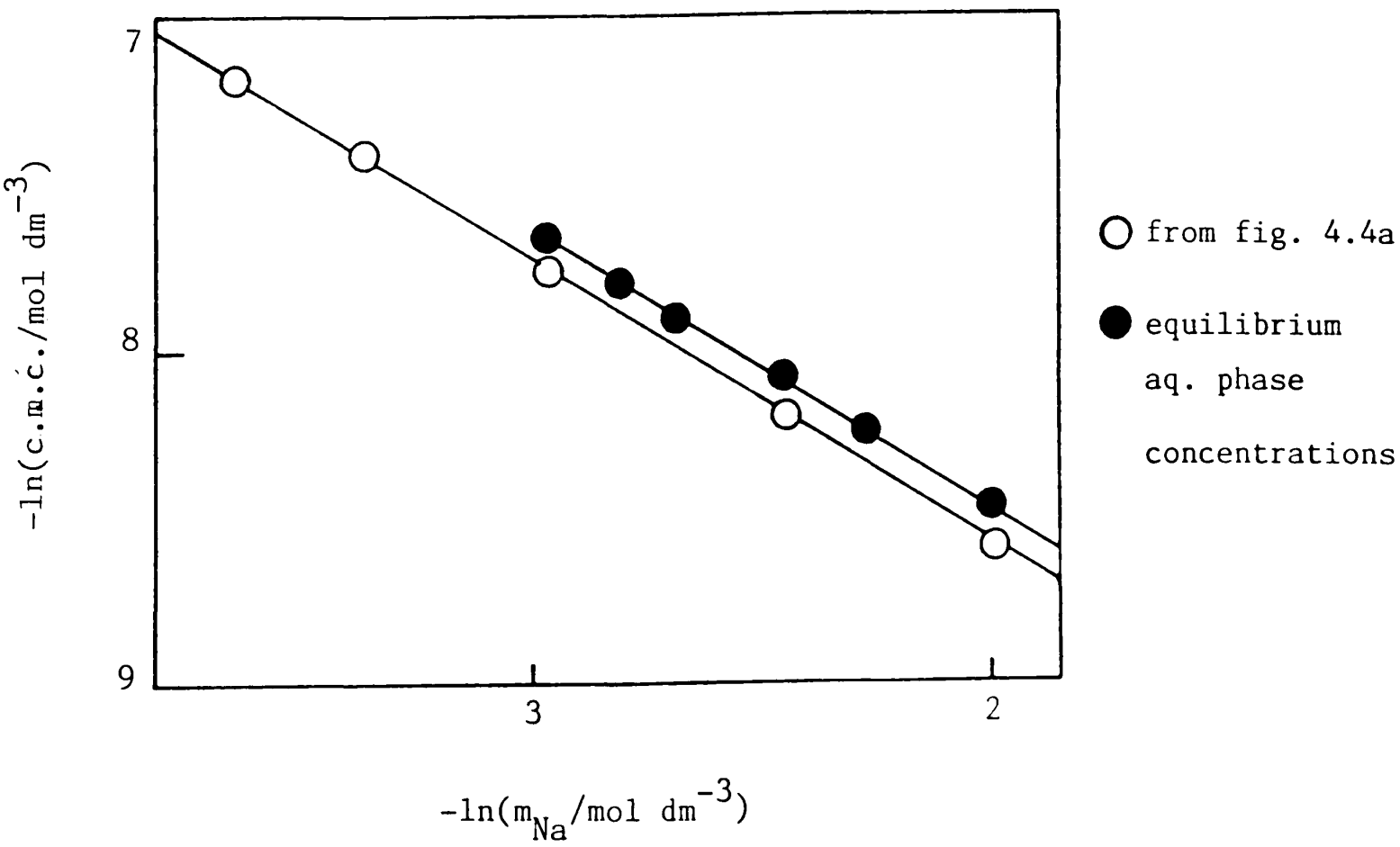

equilibrium concentrations of AOT in aqueous solution were determined as a function of m_s. It was found that AOT concentrations were ≃ 10% higher than the c.m.c. values determined tensiometrically and yet no micelles were detectable by P.C.S. The γ values determined in spinning-drop experiments appear to be equilibrium values (Figure 3.3) and so there is no ready explanation for this discrepancy. A similar observation has been observed by Cazabat *et al.*.[34] Despite this, a linear relation exists between ln (equilibrium aqueous phase concentration of AOT) and $\ln m_{Na}$ (Figure 4.4b), the slope of the line being equal within experimental error to $d\ln cmc/d\ln m_{Na}$. Hence the analysis involving this term in unaffected.

The full curve in Figure 4.5 is obtained from equation 4.12 with a value of $B' = 1.101$ mN m^{-1} and $\Gamma_D = 2.31 \times 10^{-6}$ mol m^{-2}. The magnitude of B' only affects the horizontal position of the minimum tension and has been chosen to give the fit shown. As seen, agreement between experimental tensions and the curve predicted by equation 4.12 is satisfactory, both in terms of the shape of the curve and the salt concentration for minimum γ_c. There are however significant discrepancies which are possibly associated with the assumption that Γ_{Cl} is zero, and this is now explored further.

4.2.3 *Treatment including Γ_{Cl} term*

Equation 4.4 may be rearranged to give

$$\frac{-1}{RT}\left(\frac{\partial\gamma}{\partial \ln m_{Na}}\right)_{D,T} = \Gamma_{Na}\left[1+\left(\frac{\partial \ln f_{Na}}{\partial \ln m_{Na}}\right)_{D,T}\right]+\left(\frac{\partial \ln f_{Cl}}{\partial \ln m_{Na}}\right)_{D,T}\left(\Gamma_D+\Gamma_{Cl}\right) + \Gamma_{Cl}\cdot\frac{m_{Na}}{m_{Cl}} \qquad (4.14)$$

Figure 4.5 Variation of γ_c with m_s at 25°C. The full line is obtained using equation 4.12 with $B' = 1.101\ mN\ m^{-1}$

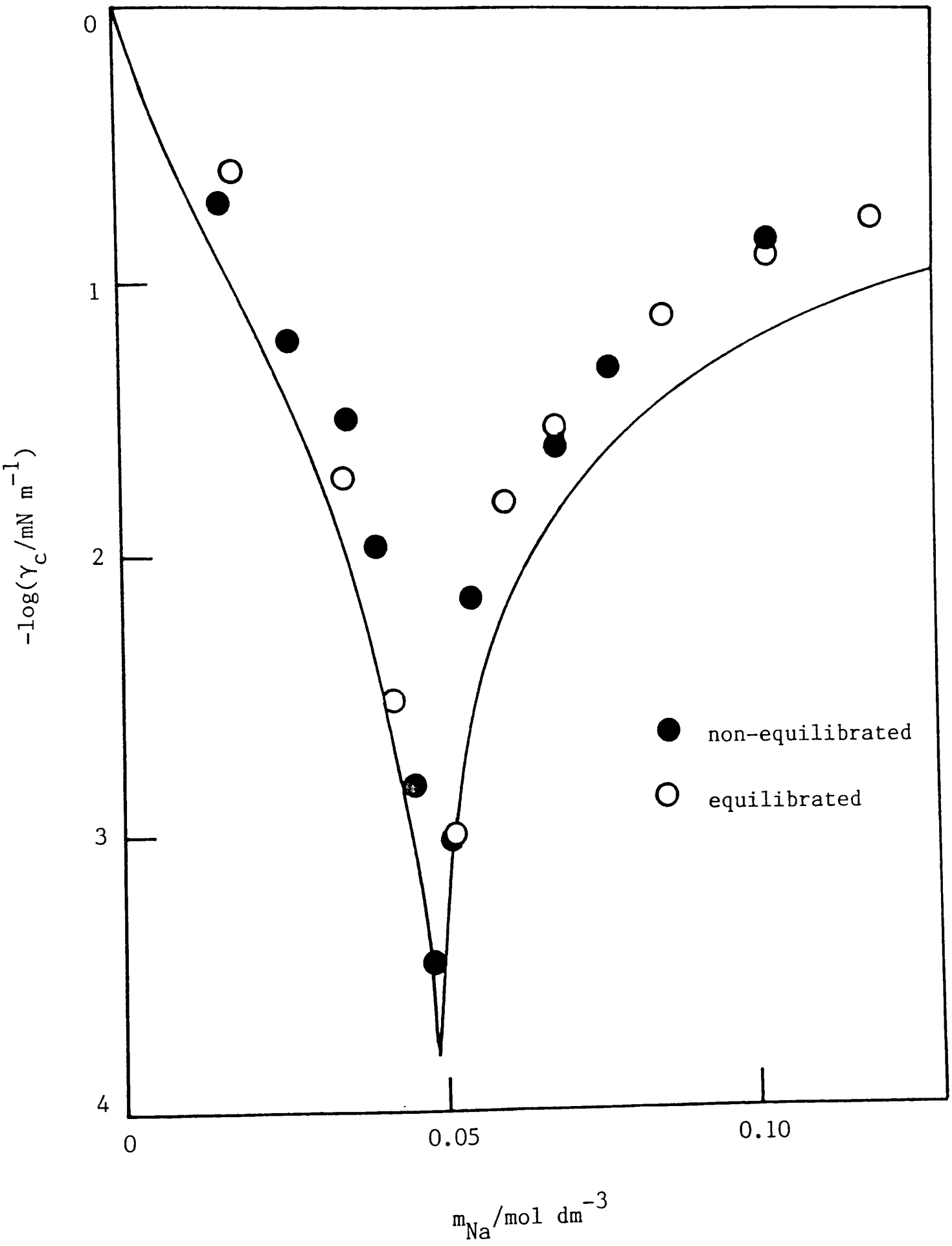

Noting that for electroneutrality in the surface, $\Gamma_D + \Gamma_{Cl} = \Gamma_{Na}$, simplifies to

$$\frac{-1}{RT}\left(\frac{\partial\gamma}{\partial \ln m_{Na}}\right)_{D,T} = \Gamma_{Na}\left[2\left(\frac{\partial \ln f_{\pm}^{NaCl}}{\partial \ln m_{Na}}\right)_{D,T} + 1\right] + \Gamma_{Cl}\frac{m_{Na}}{m_{Cl}} \qquad (4.15)$$

Further from equation 4. 3,

$$\frac{-1}{RT}\left(\frac{\partial\gamma}{\partial \ln m_D}\right)_{Na,T} = \Gamma_D - \Gamma_{Cl}\left(\frac{m_D}{m_{Cl}}\right) \qquad (4.16)$$

Combination of equations 4.1, 4.15 and 4.16, noting that m_D = cmc, then yields

$$\frac{-d\gamma_c}{d\ln m_{Na}} = RT\Gamma_D\left\{1 + 2\left(\frac{\partial \ln f_{\pm}^{NaCl}}{\partial \ln m_{Na}}\right)_{D,T} + \frac{d\ln cmc}{d\ln m_{Na}} + \frac{2\Gamma_{Cl}}{\Gamma_D}\left[1 + \left(\frac{\partial \ln f_{\pm}^{NaCl}}{\partial \ln m_{Na}}\right)_{D,T}\right]\right\} \qquad (4.17)$$

Further insight into the significance of a minimum in γ_c can be obtained from this equation by noting that Hall[142] has shown that

$$\frac{-d\ln cmc}{d\ln m_{Na}} = \left(1 - \alpha_m\right) + \left(2-\alpha_m\right)\left(\frac{\partial \ln f_{\pm}^{NaCl}}{\partial \ln m_{Na}}\right) \qquad (4.18)$$

Here α_m is the effective micellar degree of dissociation, defined as twice the negative adsorption of coions and surfactant monomer per micellar surfactant ion. One can similarly define a

degree of dissociation α_p of surfactant in a monolayer at a plane surface as $-2\Gamma_{Cl}/\Gamma_D$, noting that the surface excess of surfactant ions not in the adsorbed monolayer will be negligible in the presence of swamping electrolyte. It can be appreciated that by setting $\Gamma_{Cl} = 0$ (the approximation used earlier) one is assuming that the monolayer is completely associated. In the context of the approximation this was justified but Γ_{Cl} can be slightly negative[43] and so slight dissociation of the monolayer occurs. Then combination of equations 4.17 and 4.18 leads to

$$\frac{-d\gamma_c}{d\ln m_{Na}} = RT\Gamma_D \left\{ \left[1 + \left(\frac{\partial \ln f_{\pm}^{NaCl}}{\partial \ln m_{Na}} \right)_{D,T} \right] (\alpha_m - \alpha_p) \right\} \qquad (4.19)$$

Inspection of this latter equation reveals the interesting result that a minimum in γ_c is obtained for the salt concentration such that the degree of dissociation of surfactant in the micelle and the plane oil-water interface are equal. On the low salt concentration side of the minimum, $\alpha_m > \alpha_p$ and it is known that micelles are present in the aqueous phase in this salt concentration régime. On the high salt concentration side, however, micelles are absent in the aqueous phase. Since a monolayer at a plane interface is almost completely associated ($\alpha_p \simeq 0$), for micelles to exist in water α_m would need to be negative. Physically, this implies that the anionic micelle would have to take on a positive charge. It can thus be understood that surfactant 'prefers' to transfer to the oil phase at higher salt concentrations.

The balancing factors associated with the micellar surface and the plane monolayer at minimum γ_c will be seen again in the case where temperature is varied rather than the salt concentration.

4.2.4 *Calculation of* α_m *and* α_p

Rearrangement of equation 4.18 shows that α_m is given by

$$\alpha_m = \left\{ 1 + 2\left(\frac{\partial \ln f_{\pm}^{NaCl}}{\partial \ln m_{Na}}\right) + \frac{d\ln cmc}{d\ln m_{Na}} \right\} \Bigg/ \left\{ 1 + \left(\frac{\partial \ln f_{\pm}^{NaCl}}{\partial \ln m_{Na}}\right) \right\} \quad (4.20)$$

and so α_p, obtained from equation 4.19, is

$$\alpha_p = \left[\alpha_m + \frac{1}{RT\Gamma_D}\left(\frac{d\gamma_c}{d\ln m_{Na}}\right)\right] \Bigg/ \left(1 + \frac{\partial \ln f_{\pm}^{NaCl}}{\partial \ln m_{Na}}\right) = \frac{-2\Gamma_{Cl}}{\Gamma_D} \quad (4.21)$$

Thus both Γ_{Cl} and α_p may be calculated using the experimental (γ_c, m_{Na}) values. As shown earlier (§ 3.10.2),

$$(10^2/\Gamma_D)/nm^2 \text{ molecule}^{-1} = 42.37 \exp.(-56.83\ m_{Na}) + 72.2 \quad (4.22)$$

Further the (γ_c, $\ln m_{Na}$) data are fitted by

$$\gamma_c/mN\ m^{-1} = 1.843 + 1.210\ \ln m_{Na} + 0.19905\ (\ln m_{Na})^2 \quad (4.23)$$

Table 4.1 gives the values of α_m calculated from equation 4.20 and α_p obtained from equations 4.21-4.23. The same data are represented in Figure 4.6a. Both α_m and α_p are very small, of comparable magnitude, and of opposite sign. Thus, although Γ_{Cl} is indeed very small (Figure 4.6b) it is not negligible in the context.

The important observation is that α_m and hence α_p are both zero at $m_{Na} \simeq 0.05$ mol dm^{-3} where minimum γ_c is observed. This is why the curve generated by equation 4.12 (Figure 4.5) for which it was assumed that Γ_{Cl} (and α_p) were zero, gives the minimum at the correct salt concentration.

Table 4.1

Values of degrees of dissociation as a function of m_s

m_s/mol dm^{-3}	α_m	$10^6\Gamma_D$/mol m^{-2}	α_p	$10^6\Gamma_{Cl}$/mol m^{-2}	Γ_{Cl}/Γ_D
0.027	0.0213	2.085	-0.0245	0.026	0.012
0.033	0.0139	2.146	-0.0150	0.016	0.007
0.041	0.0064	2.200	-0.0063	0.007	0.003
0.050	-0.0011	2.236	0.0020	-0.002	-0.001
0.061	-0.0076	2.260	0.0110	-0.012	-0.005
0.074	-0.0130	2.273	0.0208	-0.024	-0.011
0.091	-0.0185	2.280	0.0305	-0.035	-0.015

4.3 Thermodynamic formulation for variation of γ_c with salt concentration in systems containing nonionic surfactant

Consider a system comprising a water-insoluble oil (alkane say), an aqueous solution containing a 1:1 electrolyte (designated S)

Figure 4.6a Variation of α_m and α_p with Na^+ concentration

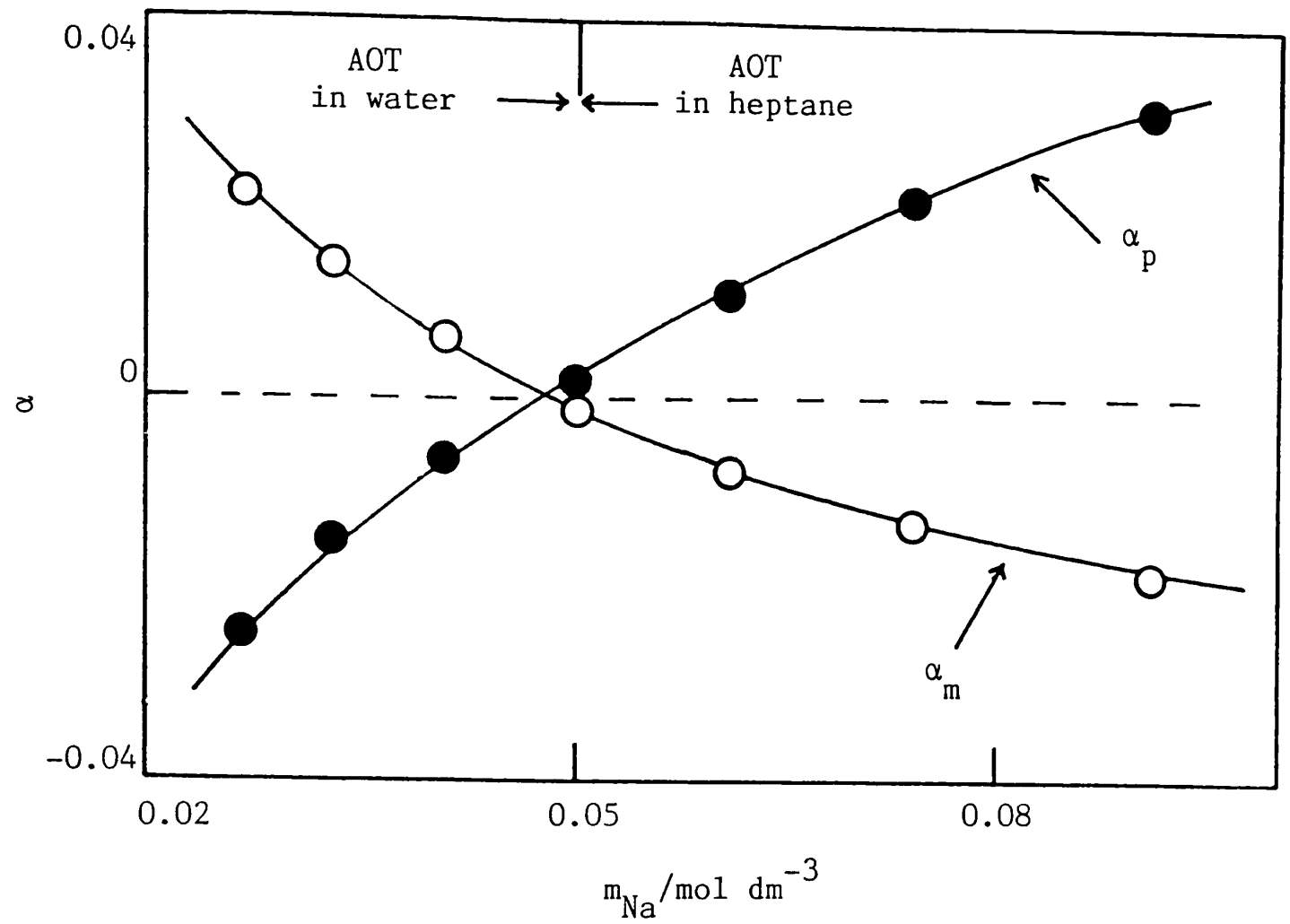

Figure 4.6b Γ_{Cl} and Γ_D as a function of Na^+ concentration

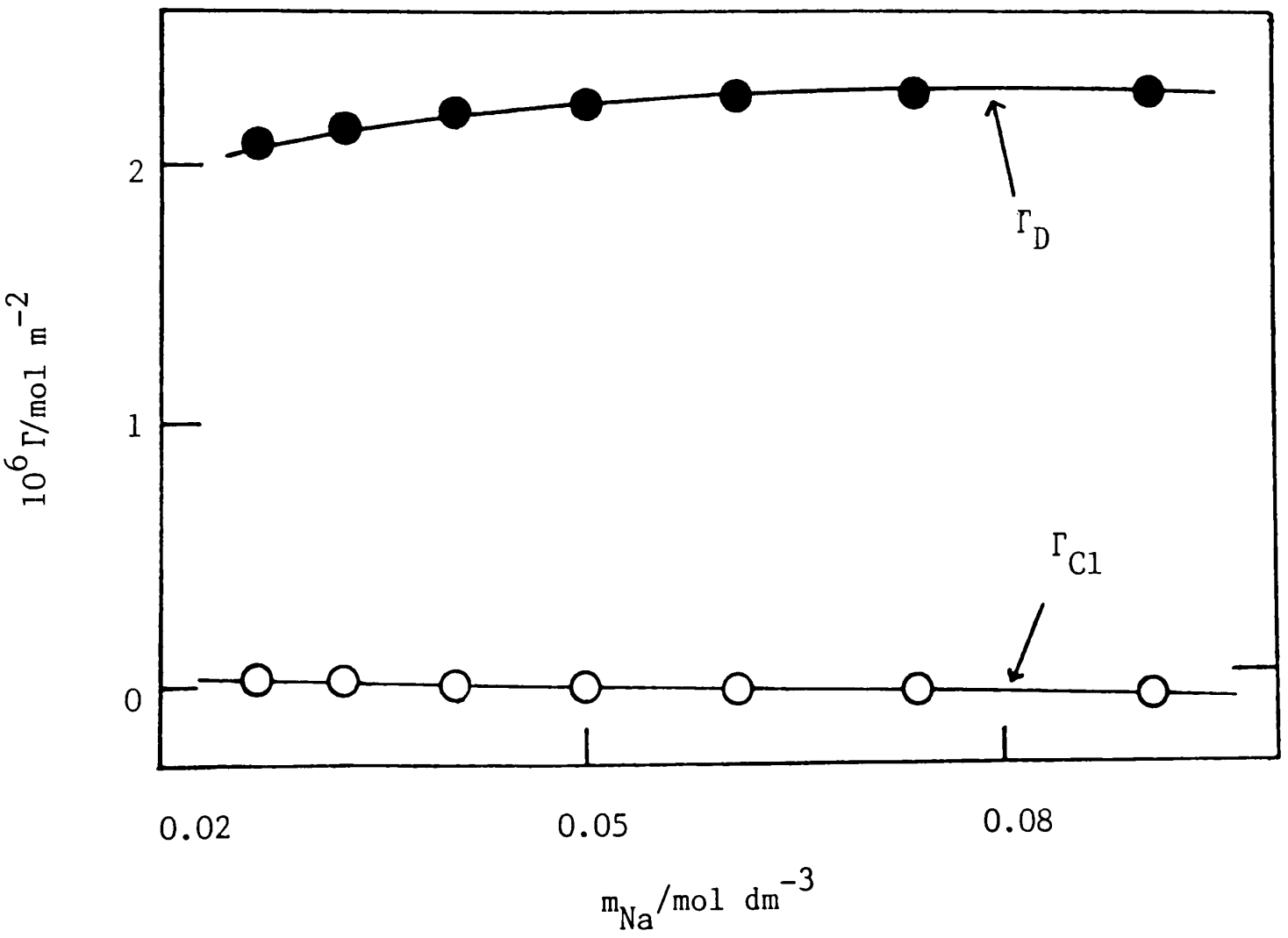

and a nonionic surfactant D distributed between the phases. With reference to Figure 4.1, the tension difference between points A and B, which are at the c.m.c. for salt concentrations $m_{S,1}$ and $m_{S,2}$, respectively, is given by the sum of the differences in tension between points A and C and between points C and B, i.e.

$$d\gamma_c = \left(\frac{\partial\gamma}{\partial \ln m_D}\right)_{S,T} .d\ln m_D + \left(\frac{\partial\gamma}{\partial \ln m_S}\right)_{D,T} .d\ln m_S \qquad (4.24)$$

Employing the Gibbs convention for the interface and noting that for electroneutrality, $\Gamma_{Na} = \Gamma_{Cl} = \Gamma_S$, it can be shown that

$$\frac{-1}{RT}\left(\frac{\partial\gamma}{\partial \ln m_S}\right)_{D,T} = \Gamma_D\left(\frac{\partial \ln f_D}{\partial \ln m_S}\right)_{D,T} + 2\Gamma_S\left[1 + \left(\frac{\partial \ln f_{\pm}^{NaCl}}{\partial \ln m_S}\right)_T\right] \qquad (4.25)$$

Furthermore, by assuming that concentrations of D (i.e. $m_D \leqslant$ c.m.c.) do not significantly affect $f_{\pm}^{NaCl}$ and that f_D does not vary with m_D (i.e. the surfactant is in infinitely dilute solution),

$$\frac{-1}{RT}\left(\frac{\partial\gamma}{\partial \ln m_D}\right)_{S,T} = \Gamma_D \qquad (4.26)$$

Combination of equations 4.24 - 4.26, noting that in the case of interest $\gamma = \gamma_c$ and m_D = c.m.c., yields

$$\frac{-d\gamma_c}{dm_S} = 2.303\ RT\Gamma_D\left[\left(\frac{\partial \log f_D}{\partial m_S}\right)_{D,T} + \frac{d\log cmc}{dm_S}\right] + \frac{2RT\Gamma_S}{m_S}\left[1 + \left(\frac{\partial \ln f_{\pm}^{NaCl}}{\partial \ln m_S}\right)_{D,T}\right] \qquad (4.27)$$

The quantity $d\log f_D/dm_S$ is frequently constant up to m_S = 1 or 2 mol dm^{-3} and is the 'salting constant' k_S for the surfactant monomer in solution.[143] Positive values correspond to 'salting-out' and negative values to 'salting-in'. It can be split into additive contributions for the nonpolar chain, k_{np}, and for the polar headgroup, k_p.[144] The term $d\log cmc/dm_S$ is also known to be constant for a number of nonionic surfactants[145] and is equal to $(k_m - k_S)$, where k_m is the salting constant for the monomer in the micelle.[146] The quantity k_m is assumed to arise mainly from the effect of salt on the polar group i.e. $k_m \simeq k_{p,m}$.

Equation 4.27 reveals the possibility of a minimum in γ_c with respect to m_S without Γ_D changing sign. For a salted-out monomer such that $k_S > |d\log cmc/dm_S|$, the term in Γ_D is positive for positive Γ_D. Sodium chloride is likely to be desorbed at an oil-water interface[79] so the term in Γ_S will be negative since $|\partial \ln f_{\pm}^{NaCl}/\partial \ln m_S| < 1$. The magnitude of the positive term in Γ_D can vary through variations in Γ_D with m_S, and the negative term in Γ_S can vary through changes in Γ_S/m_S and the term in $f_{\pm}^{NaCl}$. Thus the sign of $d\gamma_c/dm_S$ can change, leading to a minimum in γ_c, if the terms in Γ_D and Γ_S are finely balanced.

Consider what can be deduced from the position of the minimum in the γ_c against m_S curve. In the system $C_{12}E_5$/nonane/aq. NaCl/31°C (see Figure 3.17), minimum γ_c occurs at $m_S \simeq 0.5$ mol dm^{-3}. If Γ_D at this salt concentration is taken equal to the value for zero salt, $\Gamma_D = 3.3 \times 10^{-6}$ mol m^{-2}.[147] The value of $d\log cmc/dm_S$ may be taken as -0.41 dm^3 mol^{-1}, obtained

for $C_{12}E_6$ in the absence of alkane (as estimated from Figure 1 of reference 145). The value of Γ_S is taken as -0.83×10^{-7} mol m^{-2}, the value for 0.5 mol dm^{-3} NaCl in contact with decanol.[148] The interface with decanol may not be too dissimilar to that containing a monolayer of nonionic surfactant.

At m_S = 0.5 mol dm^{-3}, it can be seen that equation 4.27 becomes

$$2.303\Gamma_D\left(k_S + \frac{d\log cmc}{dm_S}\right) = 2.303\Gamma_D k_{p,m} = \frac{-2\Gamma_S}{0.5}\left[1 + \left(\frac{\partial \ln f_{\pm}^{NaCl}}{\partial \ln m_S}\right)_{D,T}\right] \quad (4.28)$$

Using this, k_S is 0.45 and $k_{p,m}$ = 0.04. If these values are reasonable, this indicates that the effect which salt has on the c.m.c. is mainly a result of the salting-out of the monomer from solution.

An alternative form of equation 4.27 is

$$\frac{d\gamma_c}{dm_S} = 2.303\ RT\Gamma_D\ (k_p' - k_m) \quad (4.29)$$

where $k_p' = \frac{-2\Gamma_S}{2.303\Gamma_D m_S}\left(1 + \frac{\partial \ln f_{\pm}^{NaCl}}{\partial \ln m_S}\right)$ may be regarded as a salting coefficient for a surfactant molecule in the monolayer at the plane oil-water interface and k_m as before is that for a monomer in an aggregate. It is clear from equation 4.29 that if γ_c is to pass through a minimum with respect to m_S, either or both of k_p' and k_m must vary with m_S. Since $k_m = k_S + d\log cmc/dm_S$ = 0.45-0.41, its value is the small difference between two large

numbers each of which is usually taken to be constant. Taking the data for the decanol-solution interface[148] as being appropriate, values of k_p' can be obtained as a function of m_S. It is then found that the values of k_m required to reproduce the (γ_c, m_S) data for $C_{12}E_5$/nonane (§ 3.13) are as shown in Figure 4.7. The striking point is that k_p' is constant over a wide range of m_S (the variation at low m_S possibly resulting from experimental errors) whereas k_m varies between 0.08 and 0.02 up to m_S = 1.5 mol dm^{-3}. To accommodate this change however, each of k_S and dlogcmc/dm_S need only vary by less than 5%, which is almost certainly within the experimental error on these quantities. From Figure 4.7, since k_p' is almost constant, the variation in γ_c with m_S results largely from the variation in k_m. The sizes of aggregates formed will be expected to vary with salt concentration, becoming larger as phase inversion is approached (§ 3.11) and changes in k_m presumably result from changes in the mean curvature of the aggregates.

4.4 Comparison of salt effects in systems containing anionic and nonionic surfactants

It is possible to obtain a simple form of equation 4.27 which gives a fuller insight into the origins of the tension minima and highlights the similarities and differences in salt effects in ionic and nonionic surfactant systems. According to Hall[142] for variations at the micelle point, at constant T and P,

$$\sum_i (n_i + n_i^+)\, d\mu_i = 0 \qquad (4.30)$$

Figure 4.7 Variation of k_p and k_m with salt concentration for nonionic surfactant system

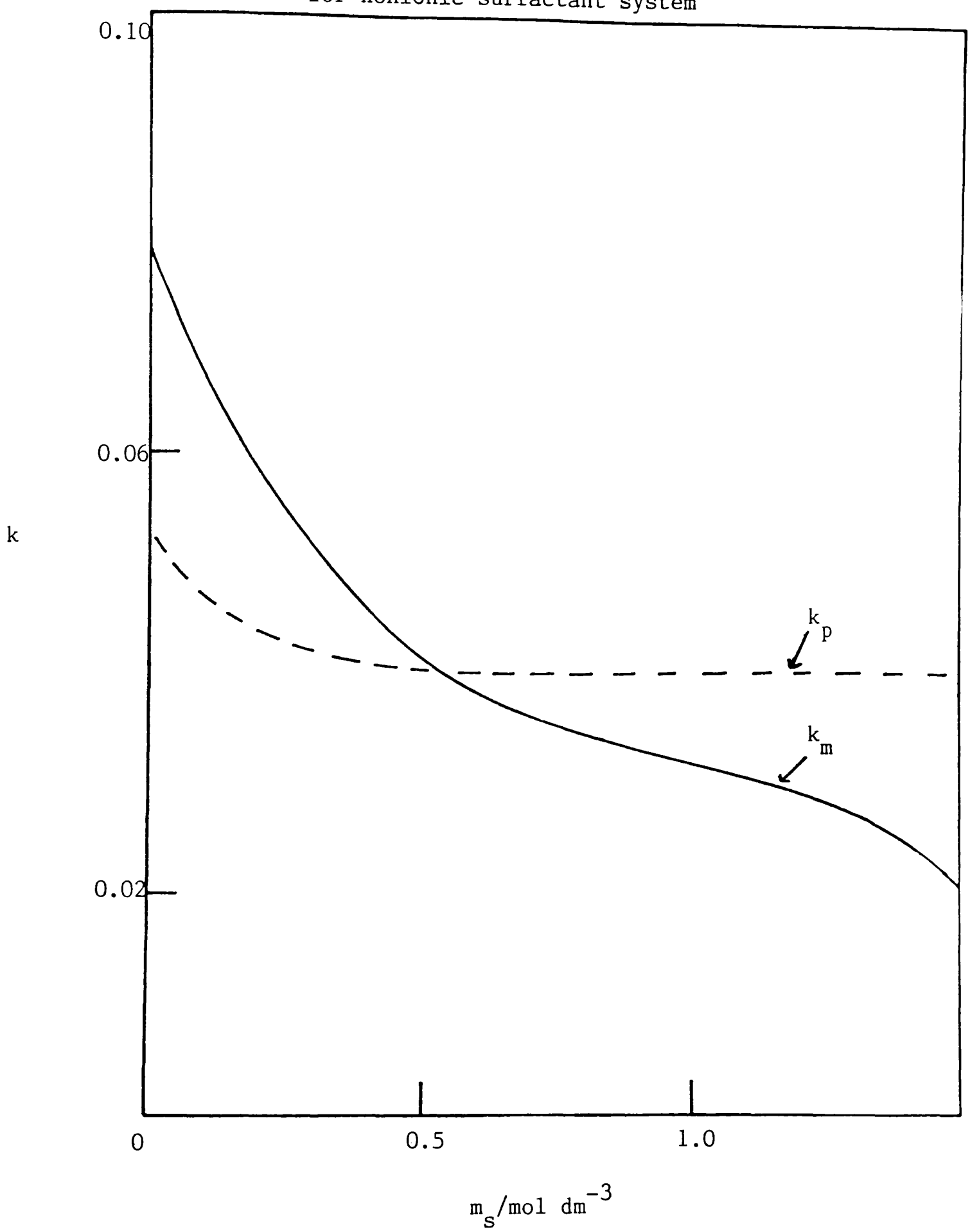

where n_i = number of molecules of i in a micelle

n_i^+ = number of molecules of i adsorbed per micelle

μ_i = chemical potential of the electrically neutral species

For systems of present interest, equation 4.30 becomes

$$n_D \, d\mu_D + n_S^+ \, d\mu_S = 0 \qquad (4.31)$$

For a plane interface, choosing a dividing surface such that the surface excess of water is zero and assuming $d\mu$ (oil) $\simeq$ 0, the Gibbs equation for constant T is

$$-d\gamma_c = \Gamma_D \, d\mu_D + \Gamma_S \, d\mu_S \qquad (4.32)$$

where Γ are surface excesses. Combination of equations 4.31 and 4.32 gives

$$\frac{d\gamma_c}{d\mu_S} = \Gamma_D \left(\frac{n_S^+}{n_D} - \frac{\Gamma_S}{\Gamma_D} \right) \qquad (4.33)$$

which, noting that for a 1:1 electrolyte $d\mu_S = 2RTd\ln m_S f_\pm$, may be expressed

$$\frac{d\gamma_c}{d\ln m_S} = 2RT\Gamma_D \left[\left(\frac{n_S^+}{n_D} - \frac{\Gamma_S}{\Gamma_D} \right) \left(1 + \frac{d\ln f_\pm^{NaCl}}{d\ln m_S} \right) \right] \qquad (4.34)$$

For an anionic surfactant NaD in the presence of a supporting electrolyte with a common cation, NaCl, equation 4.19 may be

written as[132]

$$\frac{d\gamma_c}{d\ln m_{Na}} = 2RT\Gamma_D\left[\left(\frac{\Gamma_{Cl}^{m}}{\Gamma_D^{m}} - \frac{\Gamma_{Cl}}{\Gamma_D}\right)\left(1 + \frac{d\ln f_{\pm}^{NaCl}}{d\ln m_{Na}}\right)\right] \qquad (4.35)$$

in which m_{Na} is the total counterion concentration, and terms in Γ^m arise from the degree of dissociation α_p of a surfactant monolayer in an aggregate. The similarity between equations 4.34 and 4.35 is obvious. Equation 4.35 describes the variation of γ_c with total counterion concentration ($\simeq m_S$) in terms of the desorption of the salt anion at plane and micelle surfaces. In the case of the nonionic surfactant systems however (equation 4.34), it is the desorption of the electroneutral salt which appears. The shape of the (γ_c, m_S) curves results in both cases from a delicate balance of salt or ion desorption from micelle and plane interfaces. The very different salt concentration required to give minimum γ_c for ionic and nonionic surfactant systems is presumably a result of the different nature of the desorption processes. In the case of anionic surfactants, the salt anion is repelled electrostatically from the surfactant monolayers, whereas the desorption of salt from films of nonionic surfactant is likely to result from the exclusion of the strongly solvated cations from the surface.[149]

Chapter Five

CHAPTER 5

EFFECT OF TEMPERATURE VARIATION IN OIL + WATER SYSTEMS CONTAINING AOT

5.1 Introduction

As mentioned earlier, a second important external variable afecting behaviour in oil + water + surfactant systems is the temperature. The solution behaviour of AOT + isooctane + water mixtures as a function of temperature, T, has been investigated by Kunieda and Shinoda.[99] At constant surfactant and salt concentrations, they find that at low T, AOT dissolves largely in the oil phase and forms reversed micellar solution in equilibrium with excess water. At higher T, AOT is dissolved in the water phase which is in equilibrium with excess oil. A three-phase region composed of water, oil and surfactant phases exists at intermediate T; the surfactant phase is known to dissolve a large amount of oil and water and is bluish-white in appearance. The type of emulsion formed by a mixture of oil, water and a surfactant (i.e. water continuous o/w or oil continuous w/o) may be predicted by Bancroft's rule.[150] This states that the continuous component of the emulsion tends to be the one in which the surfactant is most soluble. Since the emulsion types change above and below the three-phase region, this is known as phase inversion. Normally phase inversion occurs over a narrow range of T called the hydrophile-lipophile

balance (HLB) temperature range since it is here that the surfactant has equal affinities for the oil and water.

In order to understand the phase behaviour close to the three-phase region, the changes of volume fractions of respective phases in the vicinity of the HLB temperature range have been studied.[99] At temperatures corresponding to the onset of the HLB range, surfactant phase is separated from oil phase containing aggregated surfactant, which changes to a near pure oil phase on increasing T. Conversely, a mutual dissolution process occurs between surfactant phase and water phase, and the latter changes to an aqueous surfactant solution. The composition of the surfactant phase thus changes from oil-rich to water-rich with increasing T. At higher T the surfactant phase disappears and a normal micellar solution exists in equilibrium with an excess oil phase.

Very few studies involving anionic surfactants have dealt with the effects of temperature on the interfacial tension.[151] The present work is aimed at investigating these effects in systems containing AOT. The primary data are given in Appendix II.

5.2 Effect of temperature on γ_c-

As with salt concentration, m_s, the c.m.c. tension, γ_c, can pass through a sharp minimum with respect to T. Figure 5.1 indicates that the temperature T^* for minimum γ_c is very sensitive to the value of m_s; T^* increases with increasing m_s. In

periments leading to these results, a drop of pure heptane was

Figure 5.1 Variation of γ_c with temperature for AOT-heptane aq. NaCl systems

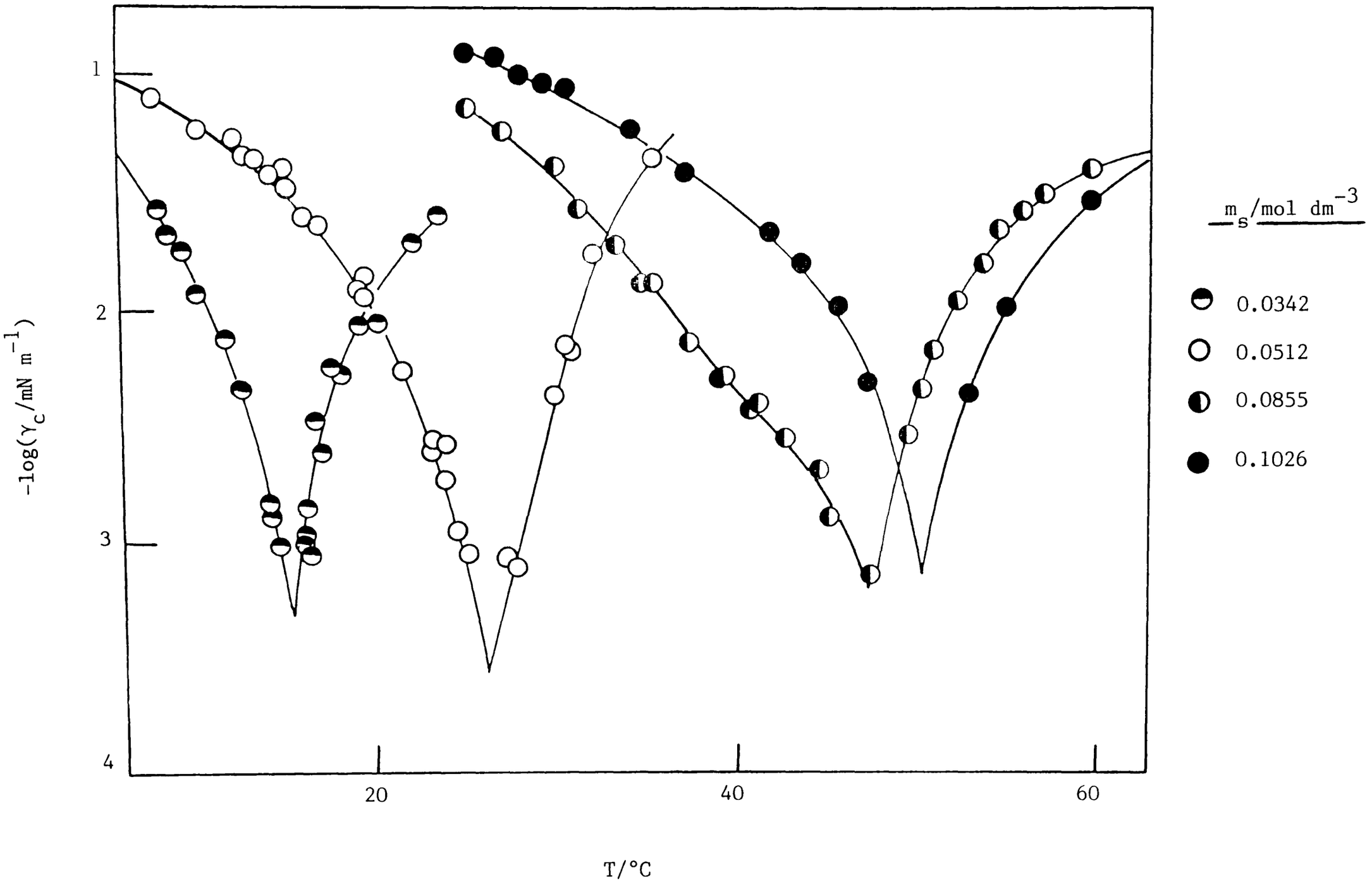

injected into the spinning-drop capillary containing aqueous AOT solution above the c.m.c. In some cases, the temperature was increased in $\simeq 2°C$ intervals after stabilisation of the drop diameter had occurred ($\simeq$ 10 min). The tensions so measured were in good agreement with those in which the temperature was lowered. At temperatures close to T^*, the oil drops frequently became unstable, breaking into smaller droplets; in this case drops were rejected. In calculating the tension, the variation in the densities of aqueous salt solutions and heptane with T was taken from values quoted in reference 74.

Low interfacial tensions have also been determined in various other connections for systems where the surfactant is at or above the c.m.c. in the aqueous phase. For example, experiments have been performed in which AOT is initially present in both oil (octane) and water and determined tensions as a function of T (Figure 5.2). For the four highest concentrations of AOT in oil, the points lie on a common curve and have not been differentiated for reasons of clarity. The tension is again independent of surfactant concentration above a certain value. However, below this value (corresponding to $\simeq 2 \times 10^{-4}$ mol dm^{-3} in 0.0855 mol dm^{-3} NaCl) the tension shows a marked increase; this observation is linked to the occurrence of a c.m.c. in the aqueous phase.

5.3 Surfactant transfer and interfacial tensions for salt concentration and temperature variation

Distribution experiments were performed by equilibrating solutions of increasing m_s at two other temperatures. Heptane

Figure 5.2 Effect of initial oil-phase surfactant concentration on tensions for the system AOT + octane + aq. 0.0855 mol dm^{-3} NaCl.

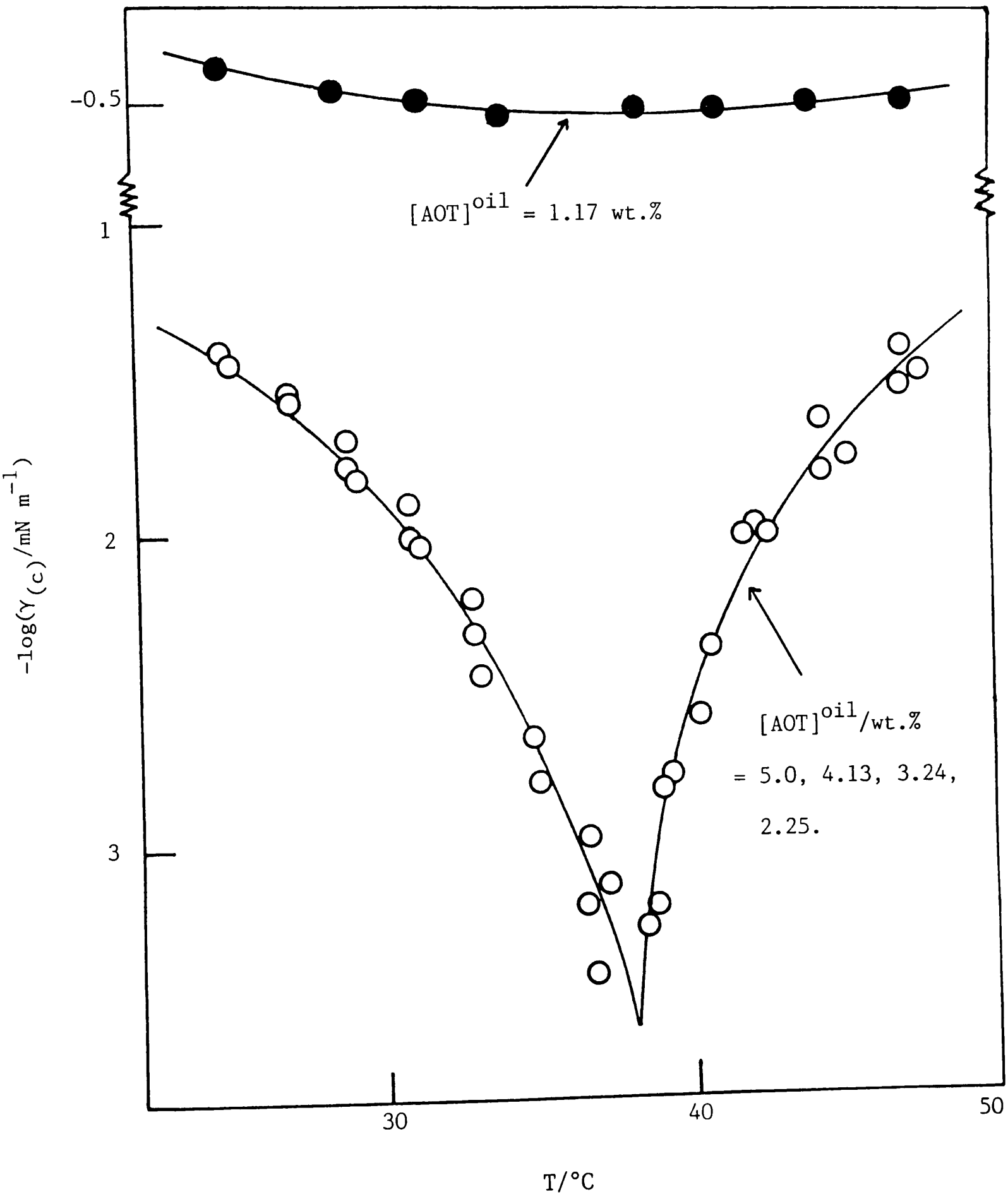

phases containing AOT (0.05 mol dm^{-3}) were agitated with aqueous NaCl solutions (phase volume ratio 1:1) and left to separate in a thermostat for a week; temperatures of 10°C and 40°C were studied. Surfactant concentrations were determined in the usual way and the results are presented in Figure 5.3, where those for 25°C are included for comparison. At low m_s the surfactant is all in the aqueous phase which is above the c.m.c. As m_s is increased, transfer of surfactant to the alkane occurs and the aqueous phase is left close to its expected c.m.c. At higher T, higher salt concentrations are needed to effect surfactant transfer to the oil. The shape of the distribution curve for 10°C is different to that for 25 and 40°C. The distribution at 10°C has possibly not reached equilibrium since the rate of the transfer (from oil) is presumably slower. Indeed, emulsions had to be centrifuged at ≃10,000 r.p.m. for 30 mins. in order to obtain separate phases.

The corresponding tension variation with m_s is seen (Figure 5.4) to be entirely consistent with the distribution work; the minima in γ_c occur as surfactant begins to transfer to the oil phase.

5.4 Phase inversion with respect to temperature

It is well-known that both salt concentration and temperature affect the type of emulsion formed on agitating mixtures of oil, water and surfactant.[152] Emulsion type is readily characterised by conductivity. However, although phase inversion temperature ranges (PIR) are often quoted, it should be stressed that they

Figure 5.3 Distribution of AOT (in aggregated form) between heptane and aqueous NaCl

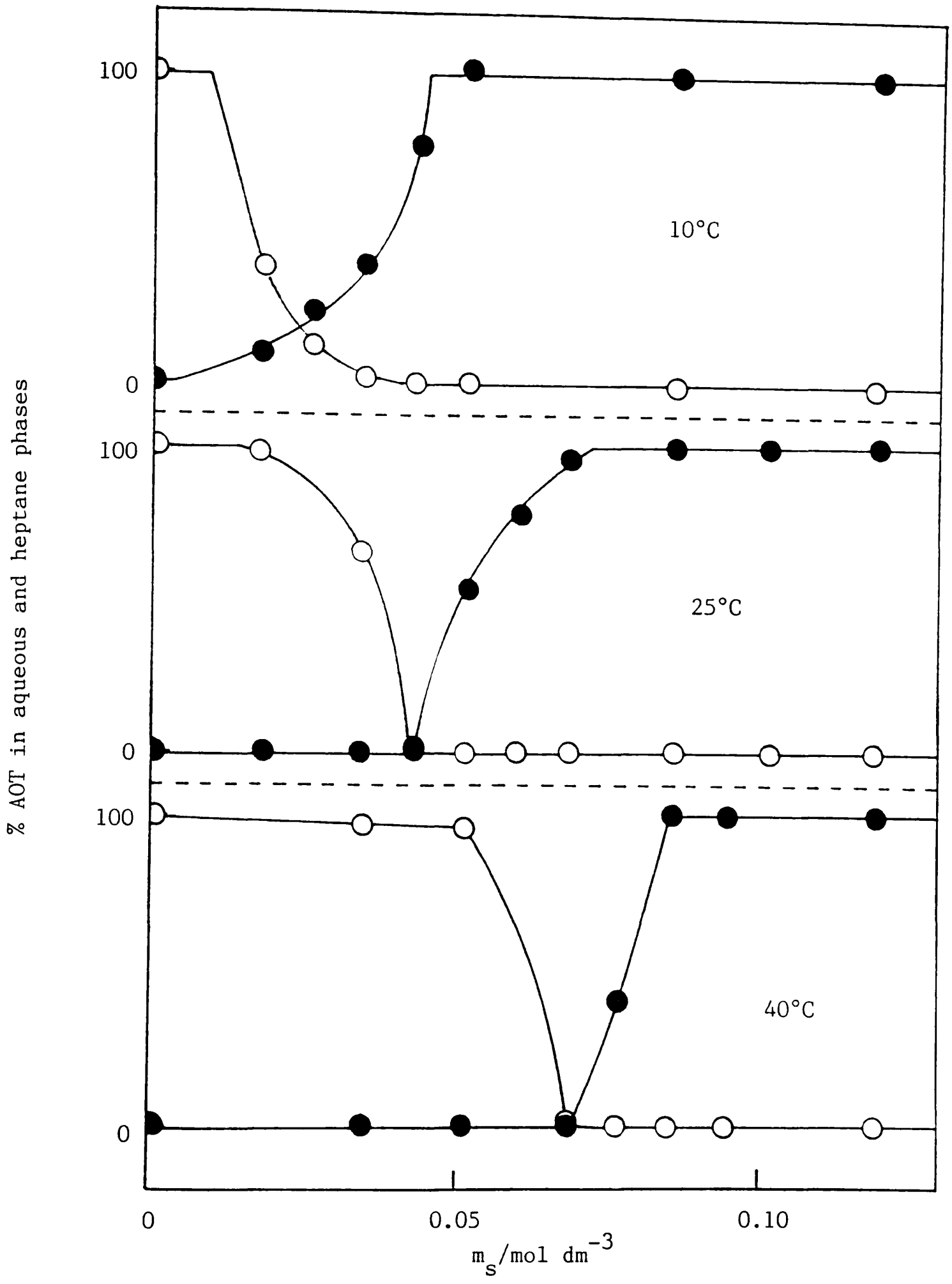

○ % AOT aqueous phase

● % AOT heptane phase

Figure 5.4 Minima in γ_c with respect to m_s for AOT-heptane-aq. NaCl systems at three temperatures

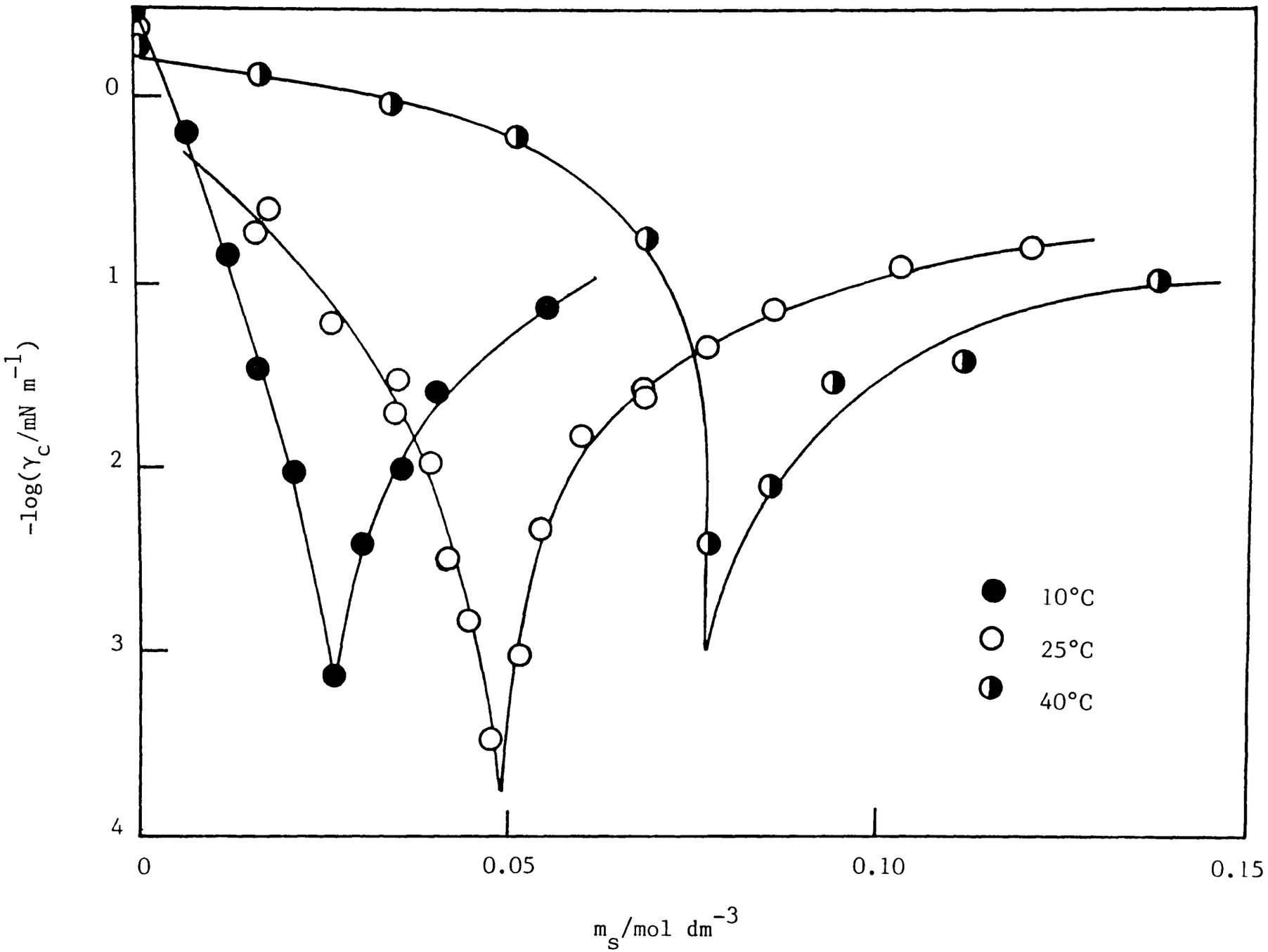

are dependent on the overall composition of the system. Thus, for a fixed overall concentration of surfactant, the phase inversion range depends on the volume fraction of water, ϕ . This is illustrated in Figure 5.5a where the effect of ϕ on the PIR in the heptane-water-0.0684 mol dm^{-3} NaCl system containing 5 wt. % AOT is shown. Here, ϕ is defined as (vol. aq. phase/vol. aq. + vol. oil phases). An increase in T can lead to inversion from w/o to o/w emulsions. The former, which have oil as the continuous phase, exhibit low conductivity, whereas for the latter the conductivity is high. Decreasing ϕ causes inversion at higher T.

If emulsion droplets are considered as non-interacting, monodisperse hard spheres, an assembly of them should occupy no more than 74% of the total volume of the system. At a volume fraction of $\phi > 0.74$, the droplets would have to be packed more densely than is possible and hence deform. In the present work, experiments showed that below $\phi = 0.05$ emulsions were w/o, and above $\phi = 0.78$ were o/w, at all T between 10 and 80°C. These two values of ϕ represent critical values beyond which no inversion is possible. The simple packing hypothesis is invalidated since, in general, emulsion droplets are neither resistant to deformation nor are they of equal size.[153]

Effects of both m_s and T on conductances of emulsions are shown in Figure 5.5b for $\phi = 0.40$. The occurrence of a broader phase inversion range as m_s increases is evident and is in accord with the findings of Kunieda and Shinoda,[99] and the tension plots

Figure 5.5a Effect of ϕ on the PIR in the heptane-water-0.0684 mol dm^{-3} NaCl system containing 5 wt.% AOT.

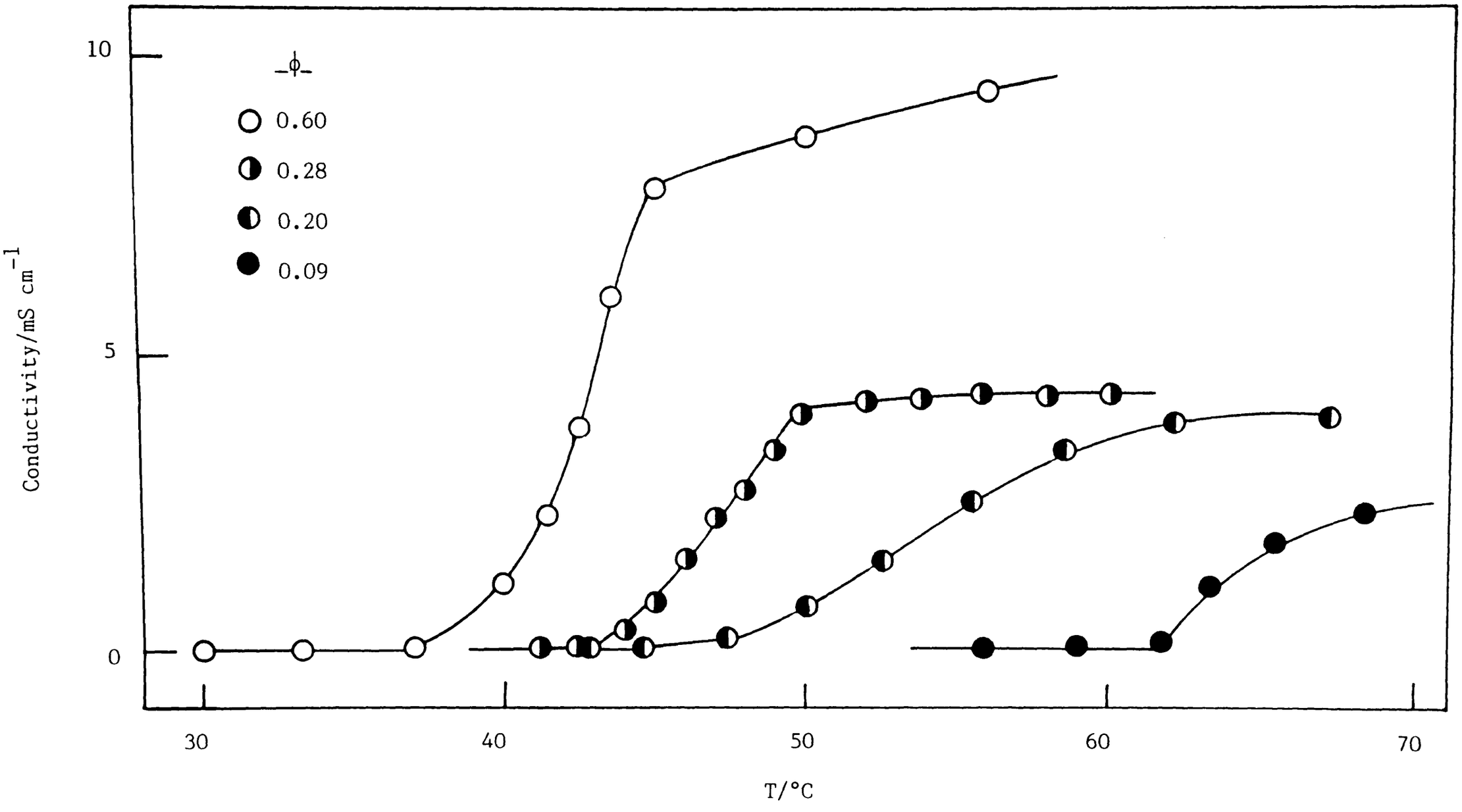

Figure 5.5b Conductivity of stirred emulsions as a function of temperature for various salt concentrations (Systems contained 5 wt.% AOT overall; aqueous phase volume fraction = 0.40).

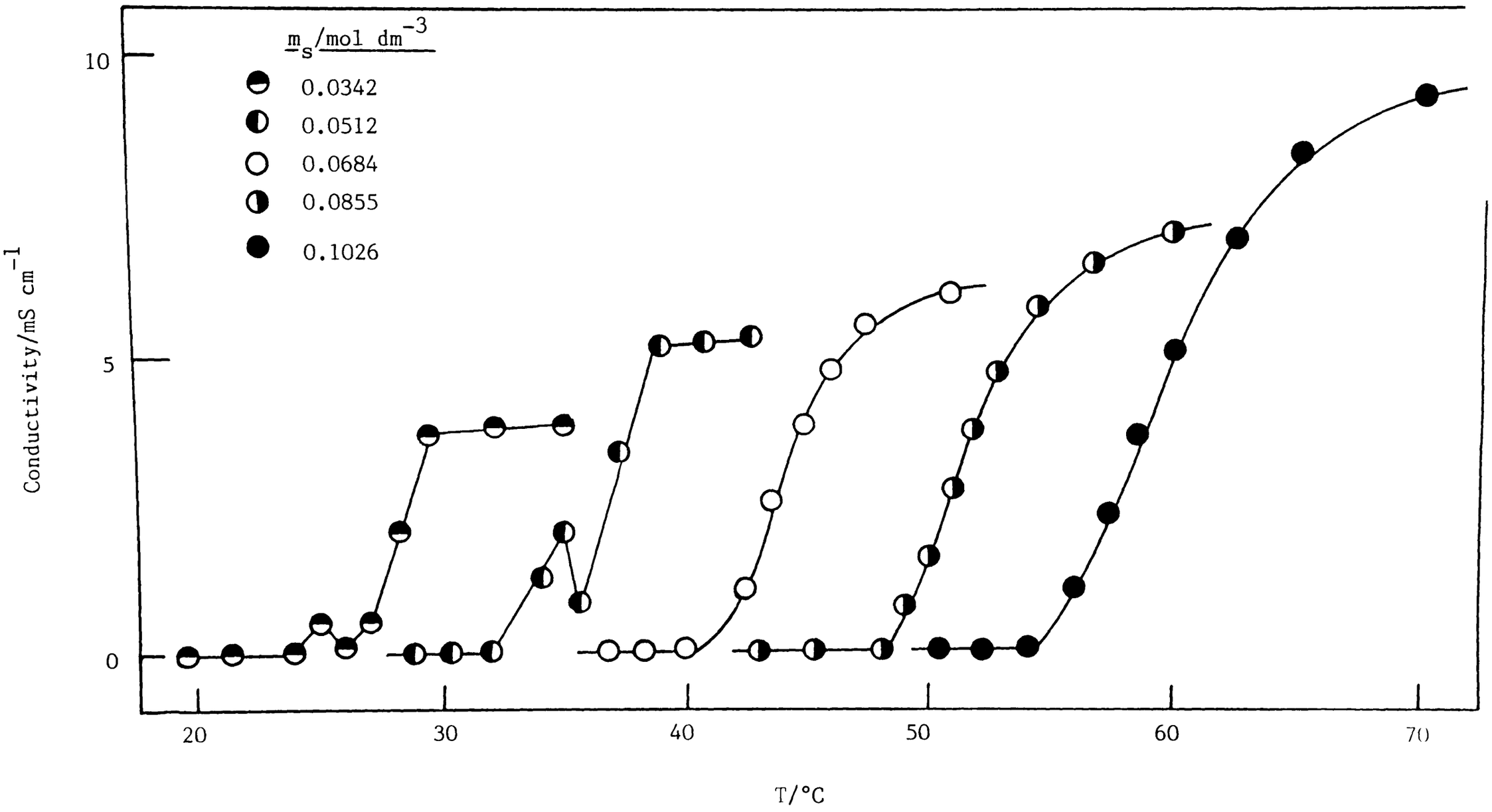

of Figure 5.1. Phase inversion with respect to temperature is again accompanied by a minimum in γ_c. As seen (§ 4.2.4), as m_s is increased, the degree of dissociation of surfactant in the micelle, α_m, is decreased and when $\alpha_m = 0$ surfactant transfers to the alkane phase. It can be appreciated from Figure 5.3 that for a given m_s, surfactant resides in the oil at low T and transfers to the aqueous phase at higher T, and one may suppose that α_m becomes more positive with increasing T. Thus, increases in m_s and T affect α_m in opposite senses and it can be appreciated why the temperature corresponding to minimum tension increases as the salt concentration is increased.

5.5 Temperature effects on 'effective' surfactant geometry

In terms of the 'geometrical' approach,[15] the effect of temperature on $v/a_h\ell$ is difficult to predict in any simple way. However, the observed phenomena for ionic surfactants may be accounted for if one assumes $v/a_h\ell$ decreases with T. This may occur for a number of reasons. An increase in T might increase the value of ℓ since the chains become more flexible and probably elongate. Alternatively, increasing the temperature may reduce the alkane penetration (and hence v/ℓ) of the chain region of the surfactant monolayer. But it is not known whether the dominant effect for this is an entropic one (due to chain mixing) or an enthalpic one. A more plausible explanation appears to be that increasing T is likely to increase the degree

of counterion dissociation of the surfactant film (see above) since ion-binding is an exothermic process. The resulting increased mutual headgroup repulsion favours positive curvature and o/w microemulsion formation.

Acknowledgement

The author is indebted to Mr. S. Clark for the measurements leading to the data presented in Figure 5.5a.

Chapter Six

CHAPTER 6

THERMODYNAMIC DESCRIPTION OF TEMPERATURE EFFECTS IN ANIONIC SURFACTANT SYSTEMS

6.1 Derivation of the expression for $d\gamma_c/dT$

It is convenient here[137] to adopt the 'surface-phase' model for the interface[37] in which total quantities (denoted by superscript s) for the surface appear rather than the excess quantities of the Gibbs approach. It is supposed as before (§ 4.2.1) that the oil (o) and water (w) are immiscible.

Figure 6.1

Origin of minimum γ_c- with respect to T

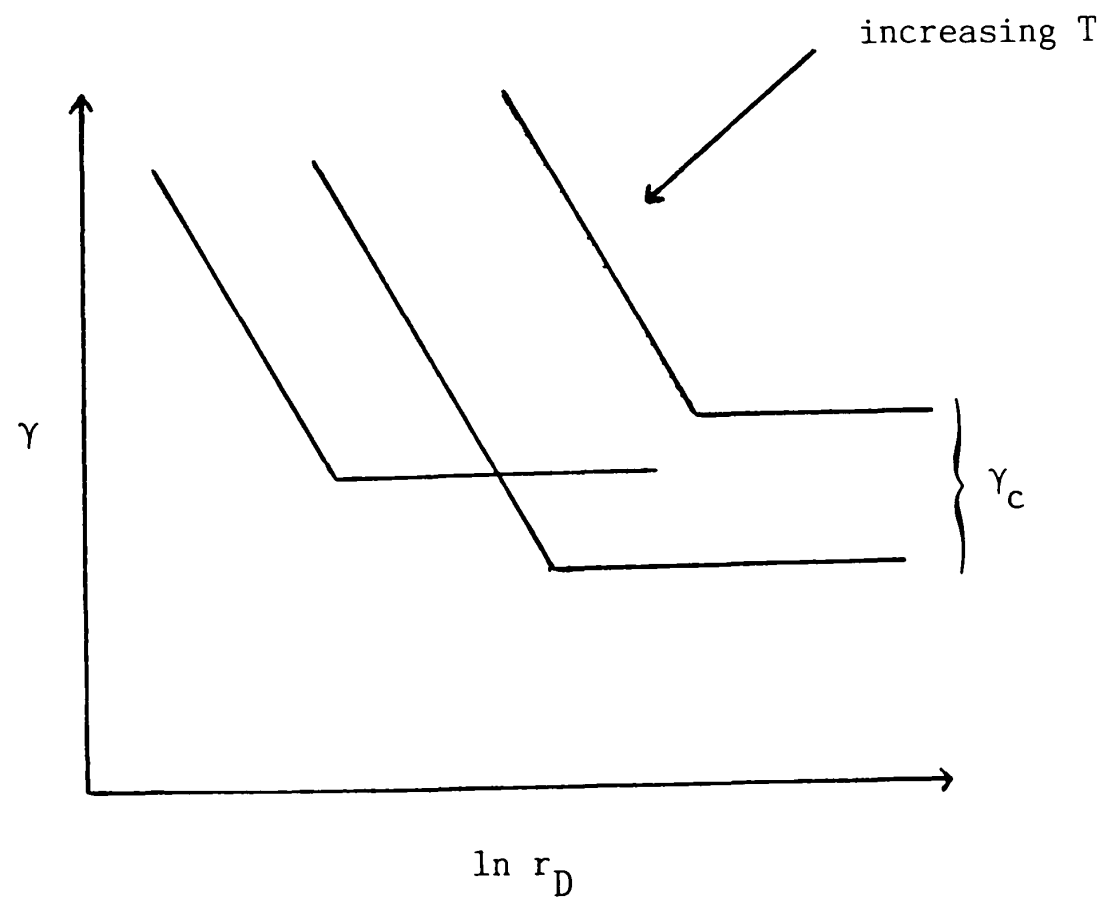

With reference to Figure 6.1, we may write for changes in γ_c with T

$$\frac{d\gamma_c}{dT} = \left(\frac{\partial\gamma}{\partial T}\right)_{r_D} + \left(\frac{\partial\gamma}{\partial \ln r_D}\right)_T \cdot \frac{d\ln r_D}{dT} \qquad (6.1)$$

where r_D is the surfactant-solvent mole ratio in a solution of D.[37] For simplicity, consider only the limb of the γ_c against T curve corresponding to the situation where surfactant (D) is present entirely in the aqueous phase. The salt (s) under these conditions will also be entirely in the aqueous phase.

The Gibbs equation for this system is

$$-d\gamma = S_u^s dT + \sum_i \Gamma_i^s d\mu_i \qquad (6.2)$$

where $\sum_i$ denotes summation over all i components and S_u^s is the entropy of unit area of surface; the surfactant and salt are considered as the electrically neutral species (D and s). The $d\mu$ are given by[37]

$$d\mu_D = -S_D dT + \left(\frac{\partial\mu_D}{\partial r_D}\right) dr_D + \left(\frac{\partial\mu_D}{\partial r_s}\right) dr_s \qquad (6.3)$$

$$d\mu_s = -S_s dT + \left(\frac{\partial\mu_s}{\partial r_D}\right) dr_D + \left(\frac{\partial\mu_s}{\partial r_s}\right) dr_s \qquad (6.4)$$

$$d\mu_w = -S_w dT + \left(\frac{\partial\mu_w}{\partial r_D}\right) dr_D + \left(\frac{\partial\mu_w}{\partial r_s}\right) dr_s \qquad (6.5)$$

and for the pure oil

$$d\mu_o = -S_o dT \qquad (6.6)$$

where the S_i are partial molar entropies in bulk solution and r_s is the salt-solvent mole ratio in a solution of s. For a constant concentration of salt the terms in dr_s are zero, and for very dilute solutions of surfactant in a swamping concentration of salt, terms in $d\mu_s/dr_D$ and $d\mu_w/dr_D$ may be neglected.

Combination of equations 6.2 - 6.6 yields

$$-d\gamma = dT\,(S_u^s - \Sigma\Gamma_i^s S_i) + \Gamma_D^s(\partial\mu_D/\partial r_D)dr_D \qquad (6.7)$$

The first term on the right-hand side of equation 6.1 may be derived from equation 6.7 as

$$\left(\frac{\partial\gamma}{\partial T}\right)_{r_D} = -\left(S_u^s - \sum_i \Gamma_i^s S_i\right) \qquad (6.8)$$

and the second term has previously been derived as

$$\left(\frac{\partial\gamma}{\partial \ln r_D}\right)_T = -RT\Gamma_D^s \qquad (6.9)$$

Substitution of equations 6.8 and 6.9 into equation 6.1, noting that r_D corresponds to the c.m.c., gives

$$\frac{d\gamma_c}{dT} = -\left(S_u^s - \sum_i \Gamma_i^s S_i\right) - RT\Gamma_D^s\left(\frac{d\ln cmc}{dT}\right) \qquad (6.10)$$

for the variation in γ_c with T.

6.2 Origin of tension minima with respect to T

Further insight into the origins of the tension minima with respect to temperature may be obtained by noting that, to a good

approximation, $-RT\ (d\ln cmc/dT) = \Delta S_m$, the molar entropy change on forming micelles at the c.m.c., given by[142]

$$\Delta S_m = S_m - \sum_i N_i S_i \qquad (6.11)$$

where S_m is the entropy of micelles containing one mole of surfactant and N_i is the number of moles of the i'th component in the micelles ($N_D = 1$). As a result, equation 6.10 may be written

$$\frac{d\gamma_c}{dT} = -(S_u^s - \sum_i \Gamma_i^s S_i) + \Gamma_D^s \Delta S_m \qquad (6.12)$$

which demonstrates that the shape of the γ_c against T curve is determined by the relative magnitudes of the entropy of surface formation per unit area (which contains Γ_D^s moles of surfactant) and the entropy of micelle formation per Γ_D^s moles of surfactant. At the temperature T^* corresponding to minimum γ_c

$$(S_u^s - \sum_i \Gamma_i^s S_i) = \Gamma_D^s \Delta S_m$$

that is, the entropy of transferring a mole of D (with the other associated species) to the plane oil-water interface becomes equal to the molar entropy of micelle formation. Thus, phase inversion and minimum γ_c are attained, as in the case where the salt concentration is varied, when there is some equivalence between the plane oil-water interface and curved aggregates.

6.3 Entropy changes accompanying formation of aggregates and plane interface

Equation 6.12 can be written

$$\frac{d\gamma_c}{dT} = -(S_u^s - \sum_i \Gamma_i^s S_i) + \Gamma_D^s (S_m - S_D - \sum_j N_j S_j) \qquad (6.13)$$

from which

$$\Gamma_D^s S_m - S_u^s = \sum_j S_j(\Gamma_D^s N_j - \Gamma_j^s) + d\gamma_c/dT \qquad (6.14)$$

where $\sum_j$ denotes summation over all components other than surfactant D, treated as the electrically neutral species. The significance of equations 6.13 and 6.14 and of $d\gamma_c/dT$ can be understood as follows. To form unit area of interface, $(\Gamma_D^s + \Sigma\Gamma_j^s)$ mol must be transferred from the appropriate bulk phases to interface, assuming for simplicity that a given component is present in only one of the bulk phases. The entropy change for this process is $(S_u^s - \Gamma_D^s S_D - \sum_j \Gamma_j^s S_j)$. To form micelles containing Γ_D^s mol surfactant, $(\Gamma_D^s + \sum_j \Gamma_D^s N_j)$ mol are transferred from bulk and the entropy change is $(\Gamma_D^s S_m - \Gamma_D^s S_D - \sum_j \Gamma_D^s N_j S_j)$. It can be seen that the term $\Sigma(\Gamma_D^s N_j - \Gamma_j^s)$ in equation 6.14 arises from the difference in composition of interface and micelles; Γ_D^s mol is associated with $\sum_j \Gamma_j^s$ mol j at the interface and with $\sum_j \Gamma_D^s N_j$ in micelles. If now material is removed from unit area of interface and the Γ_D^s mol surfactant are transferred to micelles, $\sum_j(\Gamma_D^s N_j - \Gamma_j^s)$ mol are removed from the bulk phase where the entropy is given by $\sum_j S_j(\Gamma_D^s N_j - \Gamma_j^s)$. The overall entropy change for the transfer is therefore $\Gamma_D^s S_m - S_u^s - \sum_j S_j(\Gamma_D^s N_j - \Gamma_j^s)$, which as equation 6.14 shows is simply $d\gamma_c/dT$. At the temperature T^* corresponding to minimum γ_c, this entropy change is zero as a result of the equality

$$\Gamma_D^s S_m - S_u^s = \sum_j S_j (\Gamma_D^s N_j - \Gamma_j^s)$$

For $T > T^*$ where $d\gamma_c/dT > 0$ and aggregates are in the aqueous phase,

$$S_u^s < \Gamma_D^s S_m - \sum_j S_j(\Gamma_D^s N_j - \Gamma_j^s) \qquad (6.15)$$

In other words, for normal structures to exist in water the interfacial entropy S_u^s must be less positive than the entropy of the micelles containing the same amount of surfactant less the entropy in bulk of the $\sum_j(\Gamma_D^s N_j - \Gamma_j^s)$ mol taken up by the aggregates from bulk. The inequality (equation 6.15) is reversed for $T < T^*$ where inverted aggregates form in the oil phase.

6.4 Application to experimental data

The temperature variation of γ_c for the system consisting of heptane in contact with micellar AOT in 0.0855 mol dm^{-3} NaCl is shown in Figure 5.1. At all temperatures the AOT is above its c.m.c. and T^* is $\simeq 47°C$. For $T > T^*$, where surfactant is present only in the aqueous phase, the data have been fitted by the equation

$$\gamma_c/mN\ m^{-1} = 4.9873 - 0.2824\ T + 5.265 \times 10^{-3}T^2 - 3.2207 \times 10^{-5}T^3$$

In order to obtain numerical values for the entropy terms occurring in equation 6.12, it is necessary to determine the variation of the c.m.c. with T (equation 6.10). As with salt concentration, the c.m.c. is taken as the aqueous phase concentration of surfactant where the tension just begins to increase from the constant value γ_c. Such tension changes are shown in Figure 6.2a for 4 temperatures. For T above 35°C it was

'ensiometric determination of c.m.c. at various T

for AOT-heptane-aq. 0.0855 mol dm^{-3} NaCl systems

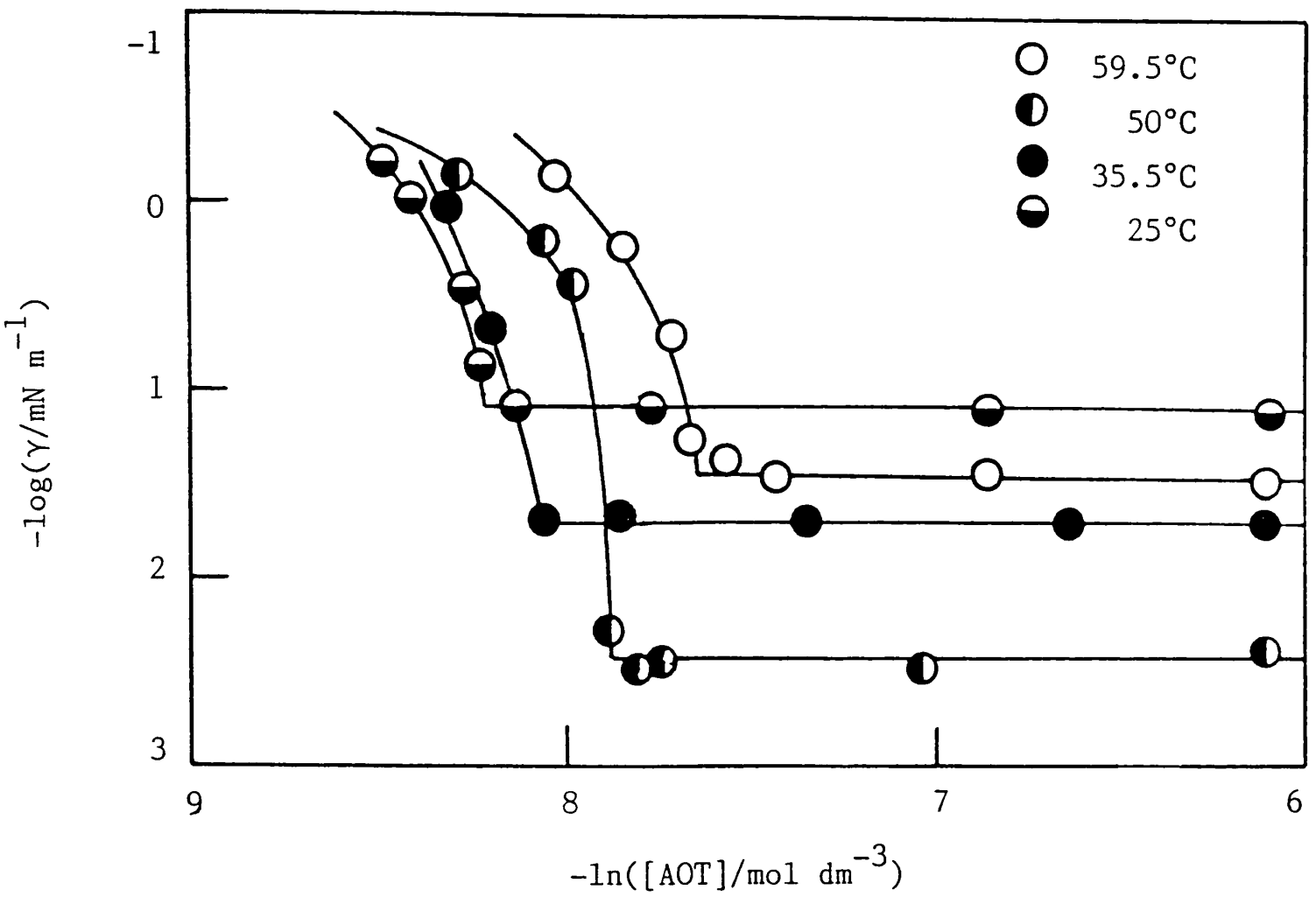

Figure 6.2b Variation of c.m.c. of AOT in heptane-aq.0.0855 mol dm^{-3} NaCl system with temperature

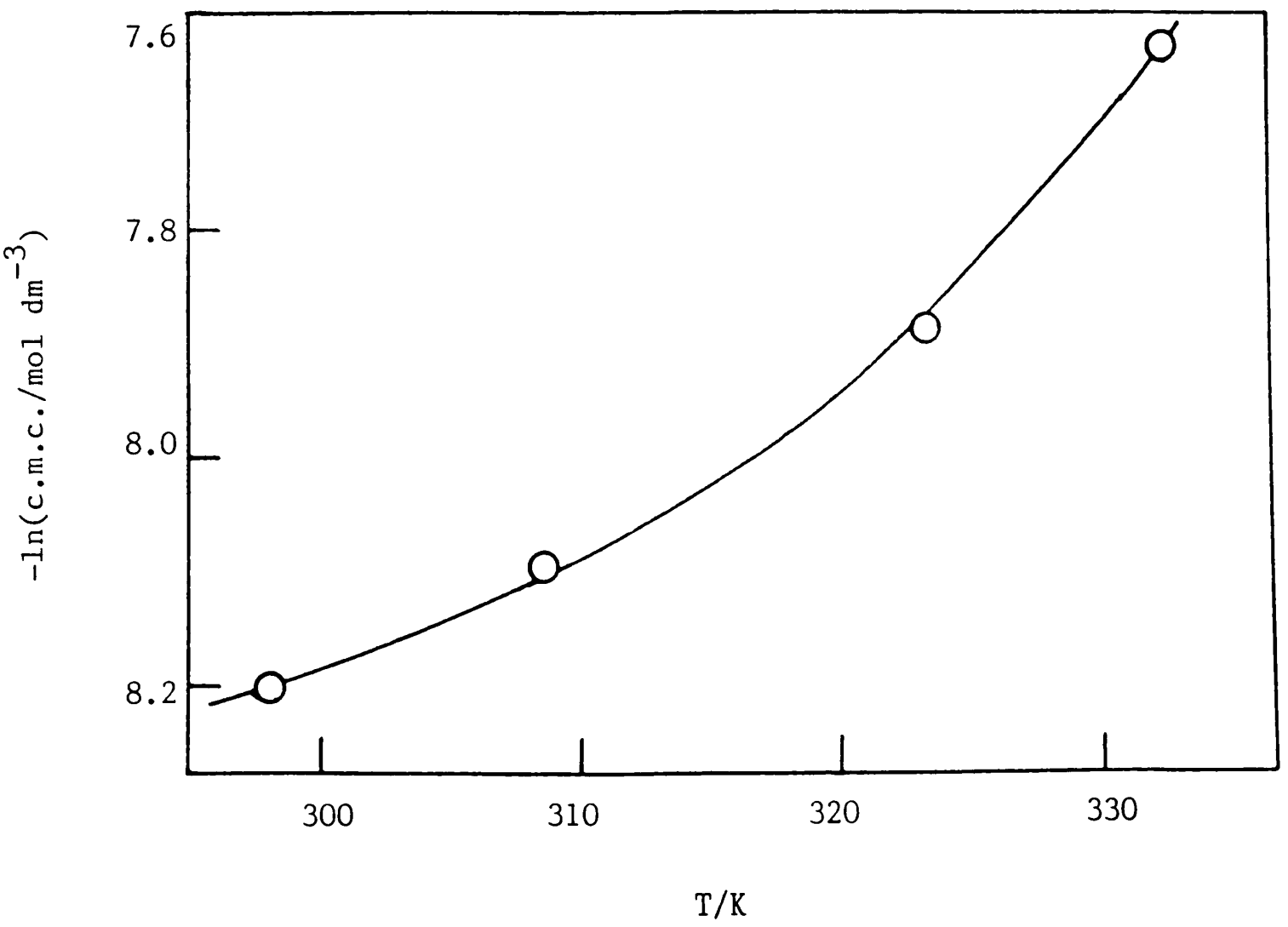

necessary to degas the aqueous solutions by causing them to foam. As a check, AOT concentrations were determined by titration for stock solutions; it was concluded that foaming caused negligible changes in surfactant concentration.

In Figure 6.2b, lncmc is plotted against T; the plot is curved and the data are well fitted by the equation

$$\ln(\text{cmc/mol dm}^{-3}) = -62.3889 + 0.5947T - 2.1803 \times 10^{-3}T^2 + 2.6671 \times 10^{-6}T^3$$

which is represented by the full line in Figure 6.2b. Values of $\Gamma_D^s \Delta S_m$ obtained from dlncmc/dT and taking $\Gamma_D^s = 2.31 \times 10^{-6}$ mol m^{-2} (which is equivalent to 0.72 nm^2 $molecule^{-1}$) are shown in Table 6.1, for $T > T^*$. These have been used to calculate values of $\Delta S_u^s = (S_u^s - \sum_i \Gamma_i^s S_i)$ using equation 6.12. Table 6.1 shows that $d\gamma_c/dT$ is only 2 or 3% of the magnitude of $\Gamma_D^s \Delta S_m$ and ΔS_u^s, which are thus almost equal. It follows that the tension minimum with respect to temperature arises from a very fine balance between the entropies of surface and micelle formation.

It would be difficult to draw any rigorous conclusions from the values or the sign of ΔS_u^s. This quantity is associated with all the species present and since it is negative, the presence of the interface clearly imposes some order on the system.

Table 6.1

Entropies of micelle and surface formation

in the system AOT/heptane/aq. 0.0855 mol dm^{-3} NaCl System *

T/K	323.2	326.5	330.0	332.5
$10^6 \, d\gamma_c/dT$	2.71	4.39	3.88	2.07
$-10^4 \, \Gamma_D^s \Delta S_m$	1.30	1.49	1.70	1.87
$-10^4 \, \Delta S_u^s$	1.27	1.45	1.66	1.84

* All units are J m^{-2} K^{-1}

Chapter Seven

CHAPTER 7

VARIATION IN OIL TYPE IN SYSTEMS CONTAINING AOT

7.1 Introduction

The variable of alkane chain length, N, is different in kind to that of salt concentration or temperature; when N is changed so is one component of the system and variation of γ_c with N is less readily treated thermodynamically than variation with m_s and T. Nonetheless, recent work by Chen *et al.*[154] using a double-chained cationic surfactant indicate that microemulsions exhibit a high degree of oil specificity and the role of the oil in prescribing droplet curvature becomes dramatically obvious.[155] Earlier work by Wade *et al.*[25] introduced the concept of equivalent alkane carbon number (E.A.C.N.) to explain interfacial tension minima with respect to 'mixed' and aromatic oils. Although useful in an empirical sense, no insight into the role of the oil in these systems was gained. The work presented below (and listed in Appendix III) is directed at understanding more fully what effect the oil has on 'effective' surfactant molecular geometry in the first case for n-alkanes and then for other oils.[156]

7.2 Systems containing n-alkanes

7.2.1 Tension minima, surfactant transfer and phase inversion with respect to N

As with salt concentration (m_s) and temperature, minima in γ_c can be effected by changing the alkane chain length, N. Figure 7.1 shows the effect on γ_c of injecting different pure alkanes into a spinning capillary containing micellar AOT. The position of the minimum will be seen later to depend on m_s. To determine if the expected transfer of surfactant accompanies the minimum tension, the distribution of AOT above the c.m.c. between aqueous NaCl and a range of n-alkanes at 25°C has been determined. Aqueous solutions of AOT (0.02 mol dm^{-3}) and NaCl (0.0684 mol dm^{-3}) were shaken with alkanes of N = 6-15. The aqueous:oil phase volume ratio was 5:1 in all cases. All mixtures were allowed to equilibrate at 25°C for 1 week and the phases separated by centrifugation at ≃ 18,000 r.p.m. for 30 mins. The concentrations of AOT in the two major phases were determined and the results are shown in Figure 7.2a.

For N < 9, much of the surfactant is in the alkane and from earlier work using heptane (Chapter 3) and unpublished results from this laboratory,[157] it is assumed the oil phases are dilute w/o microemulsions and that the surfactant concentration in the aqueous phases is approximately equal to the c.m.c. For N > 10 surfactant is largely in the aqueous phase above the c.m.c. The trend is in accord with the findings of Chen *et al.*[154] that

Figure 7.1 Variation of γ_c with alkane chain length N for AOT at the alkane-aq. 0.0684 mol dm^{-3} NaCl interface at 25°C.

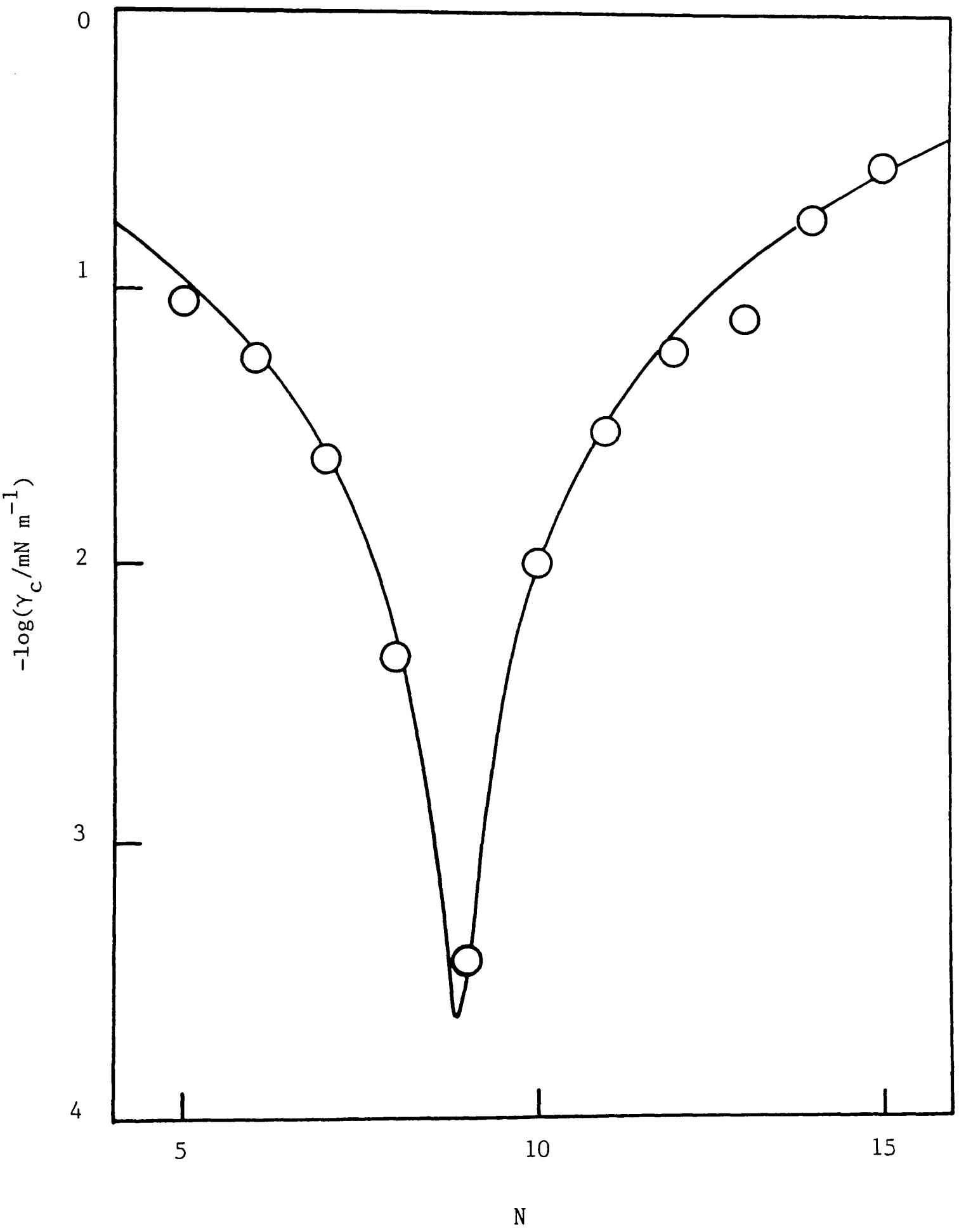

a Distribution of AOT (in aggregated form) between aq. 0.0684 mol dm^{-3} NaCl and n-alkanes at 25°C.

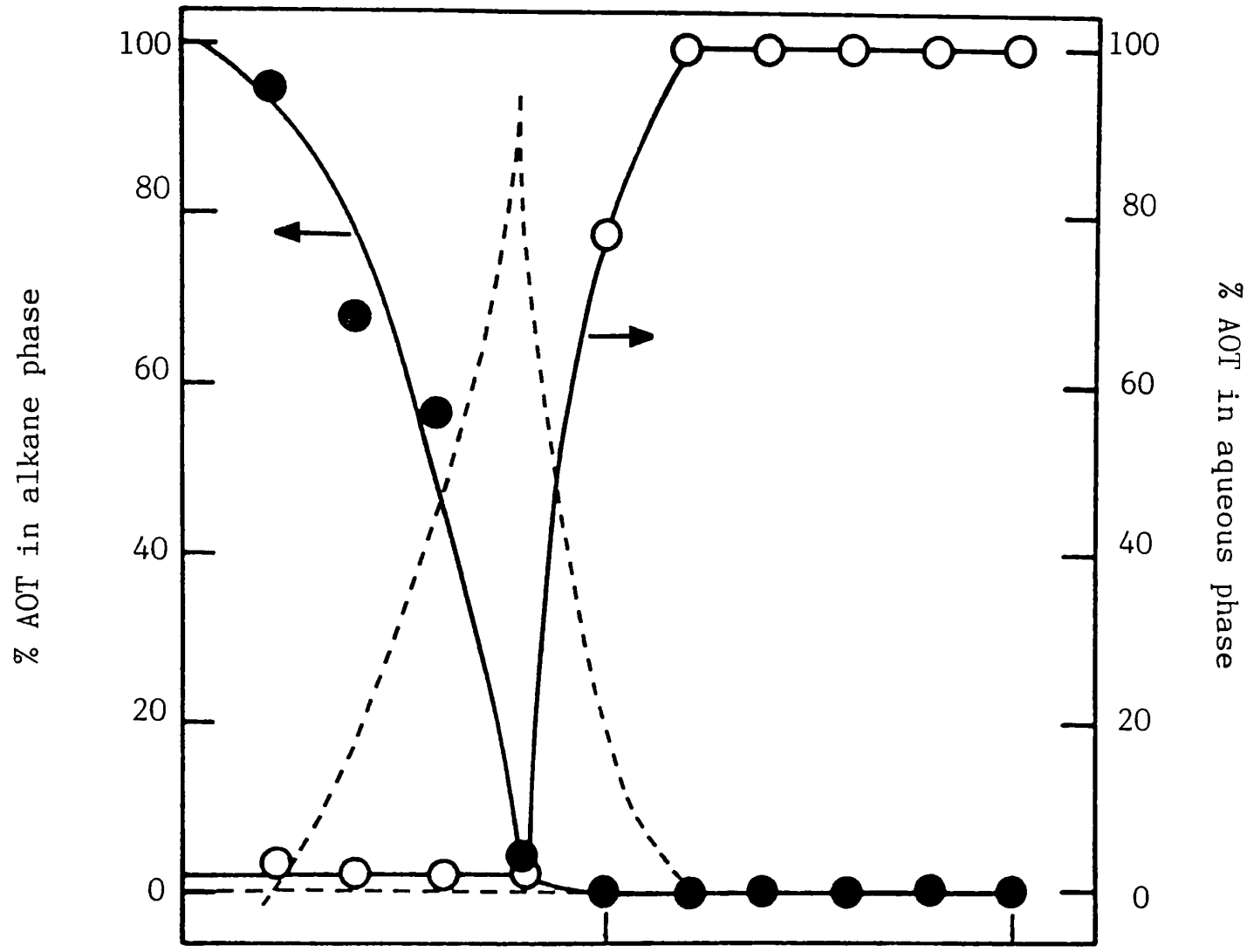

Figure 7.2b Conductivity of emulsions formed on stirring alkanes (N) with 0.05 mol dm^{-3} AOT in aq. 0.684 mol dm^{-3} NaCl at 25°C.

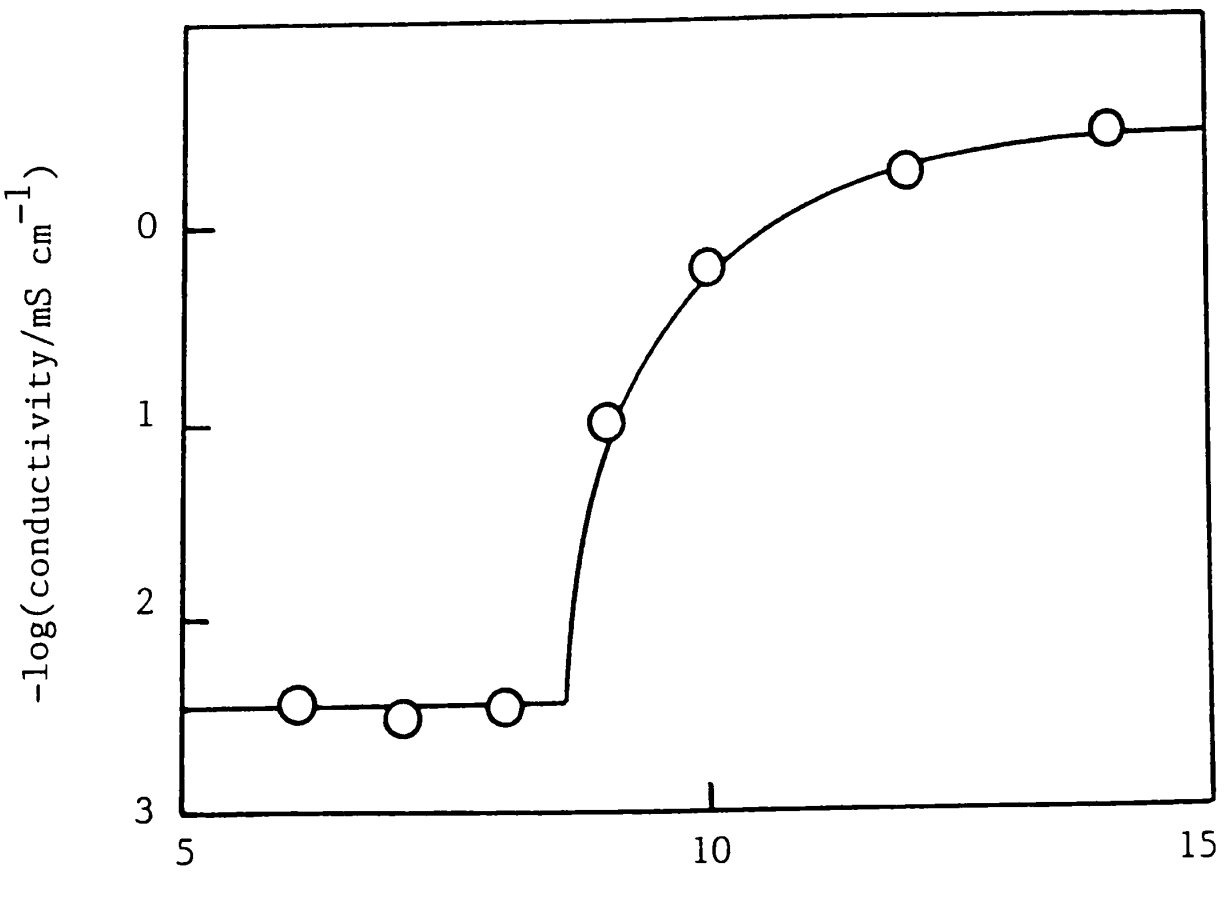

for lower N surfactant tends to exist as inverted structures in the oil phase. In the region of N = 9 much of the AOT is present in a surfactant-rich phase, as shown by mass balance and represented by the dotted line in Figure 7.2a. That phase inversion also occurs around N = 9 (for the same salt concentration) can be seen from the conductivities of the coarse emulsions depicted in Figure 7.2b. For N < 9, the low conductivity indicates the continuous phase is alkane i.e. the emulsion is of the w/o type. The conductivities rise sharply for N > 9 indicating emulsion inversion to the o/w type. As can be seen from both Figures 7.1 and 7.2 then, minimum γ_c, surfactant transfer and phase inversion are observed for N = 9, in this salt concentration.

7.2.2 *Experimental and predicted (γ_c, $\underline{m}_s$) curves*

Effects of salt have been discussed in detail previously (Chapters 3 and 4). It has been shown that for a given N, γ_c passes through a minimum as m_s is increased. The equation relating γ_c and m_{Na} (the total counterion concentration) was given for constant temperature as (§ 4.2.3)

$$\frac{-d\gamma_c}{d\ln m_{Na}} = RT\Gamma_D \left\{ 1 + 2\left(\frac{\partial \ln f_{\pm}^{NaCl}}{\partial \ln m_{Na}}\right)_D + \frac{d\ln cmc}{d\ln m_{Na}} + \frac{2\Gamma_{Cl}}{\Gamma_D}\left[1 + \left(\frac{\partial \ln f_{\pm}^{NaCl}}{\partial \ln m_{Na}}\right)_D \right] \right\} \quad (7.1)$$

$$= RT\Gamma_D \left\{ \left[1 + \left(\frac{\partial \ln f_{\pm}^{NaCl}}{\partial \ln m_{Na}}\right)_D \right] \left[\alpha_m - \alpha_p \right] \right\} \quad (7.2)$$

It was shown that, where heptane is the oil, $\Gamma_{Cl} = 0$ for

$m_s = m_s^*$ (γ_c = minimum) but not for other m_{Na}. If however Γ_{Cl} is assumed to be zero for all m_{Na}, the predicted (log γ_c, m_{Na}) curve has the minimum at the correct m_{Na} but deviations exist between predicted and experimental γ_c on either side of this salt concentration. Nonetheless, the correct general features are given when Γ_{Cl} is set equal to zero and if this is done, and Γ_D is supposed constant, equation 7.1 can be written

$$\gamma_c = -RT\Gamma_D \left\{ -6.83 \times 10^{-4} (\ln m_{Na})^3 - 0.025 (\ln m_{Na})^2 + \left[0.722 + \frac{d\ln ncmc}{d\ln m_{Na}} \right] \ln m_{Na} \right\} + B' \qquad (7.3)$$

where B' is an integration constant.

Experimentally, the value of m_s for which minimum γ_c is observed depends markedly on N as can be seen for the (γ_c, m_{Na}) curves shown in Figure 7.3a. It can be appreciated from equation 7.1 (assuming $\Gamma_{Cl} = 0$) that the shift in the position of minimum γ_c is associated with different values of $d\ln ncmc/d\ln m_{Na}$ for different N. For a given N this term is known to be constant. A series of curves generated by equation 7.3 using slightly different values of $d\ln ncmc/d\ln m_{Na}$ are shown in Figure 7.3b; the series closely resembles that observed experimentally. It must be recalled however that these curves are produced assuming Γ_D is constant; it is known (see later) that Γ_D varies with m_s and so the fine details of the plots may not be in accord with experiment as a consequence of this.

Figure 7.3a Experimental results for variation of γ_c with Na^+ concentration for AOT against n-alkanes at 25°C.

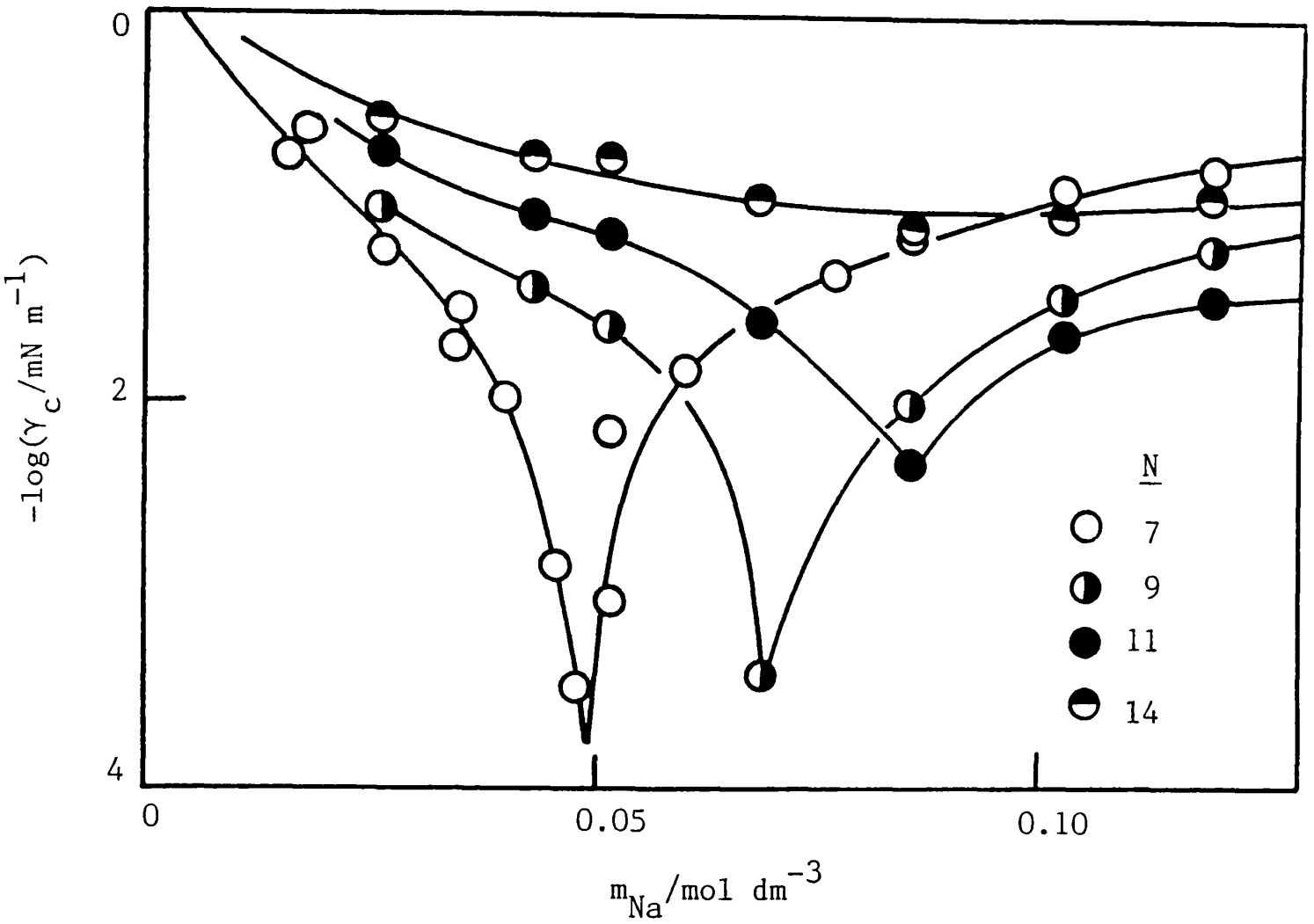

Figure 7.3b Curves generated by equation 7.3 for different values of $dlncmc/dlnm_{Na}$.

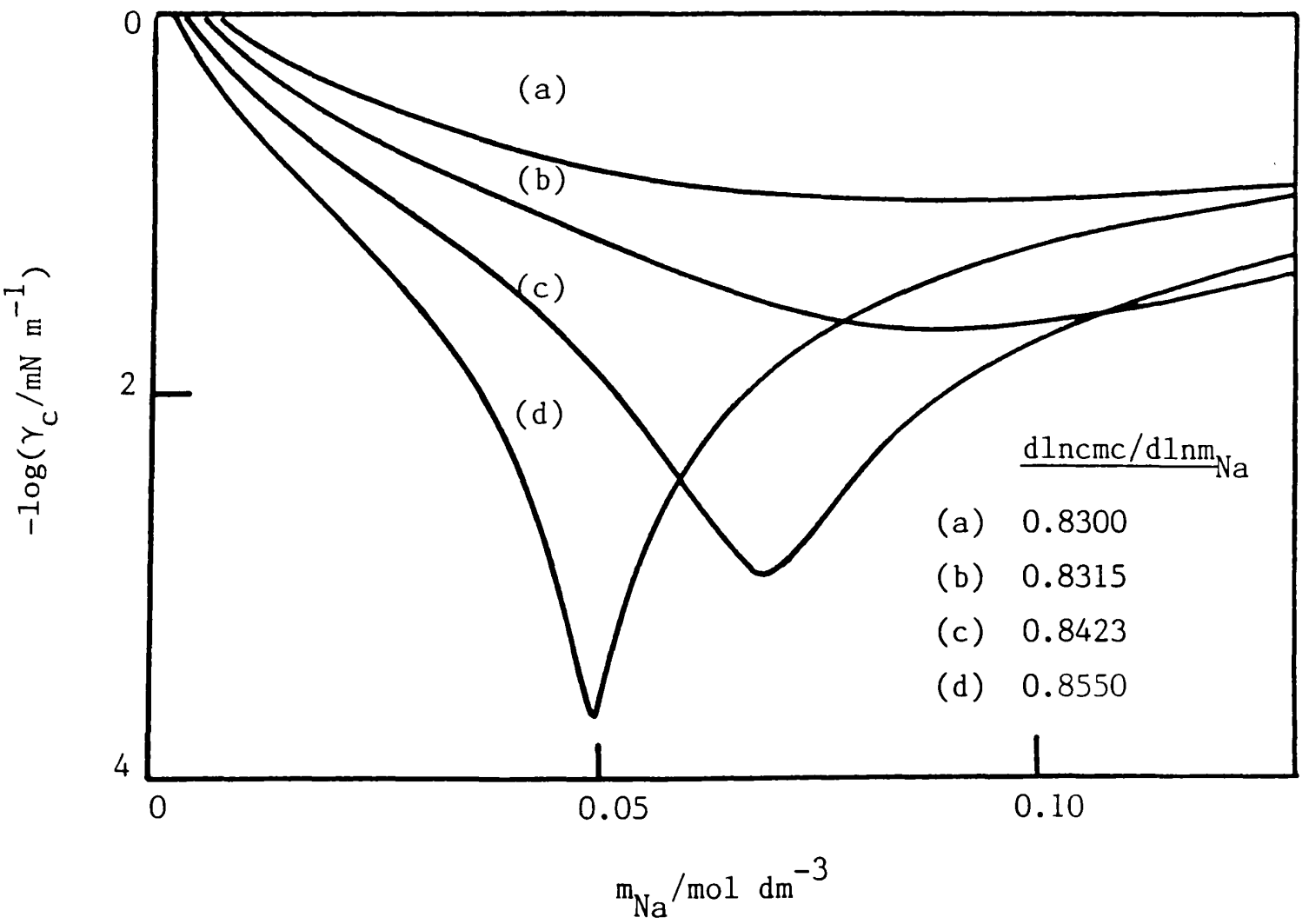

Previously (§ 4.2.2) it was found, using heptane, that $d\ln cmc/d\ln m_{Na} = -0.855$. In addition, c.m.c.'s have been determined tensiometrically in the presence of tetradecane. Interfacial tension - surfactant concentration plots of the type shown in Figure 7.4a were used to determine the c.m.c. at various values of m_s. All tensions are from spinning-drop experiments. The plot of $\ln cmc$ versus $\ln m_{Na}$ is rectilinear (Figure 7.4b) yielding a value for $d\ln cmc/d\ln m_{Na} = -0.832$. As expected from equation 7.1 and Figure 7.3a this is slightly lower than the value for the system containing heptane. To give the minimum γ_c at the value of m_s shown in Figure 7.3a (= 0.089 mol dm^{-3}), $d\ln cmc/d\ln m_{Na}$ for the tetradecane system would have to be -0.830.

Interestingly, it can be seen from Figure 7.3a that the value of the minimum γ_c increases with N for N > 9. The work of Kahlweit and Strey[158] using pure nonionic surfactants offers an explanation for this effect. From a variety of water-oil-surfactant phase diagrams they conclude that the phase behaviour of a ternary system is determined by its 'distance' from a tricritical point. With systems close to the tricritical point, the three-phase region is small. Correspondingly the three-phase alkane interval is narrow and the interfacial tension between the phases low. With increasing distance from the tricritical point, the three-phase region increases as does the interfacial tension. Thus tricritical points in such systems may be regarded as kinds of pivot points from which the phase behaviour evolves. If one wishes to have a large three-phase region and a wide alkane

Figure 7.4a Tensiometric determination of the c.m.c. of AOT in the presence of NaCl and excess tetradecane phase at 25°C.

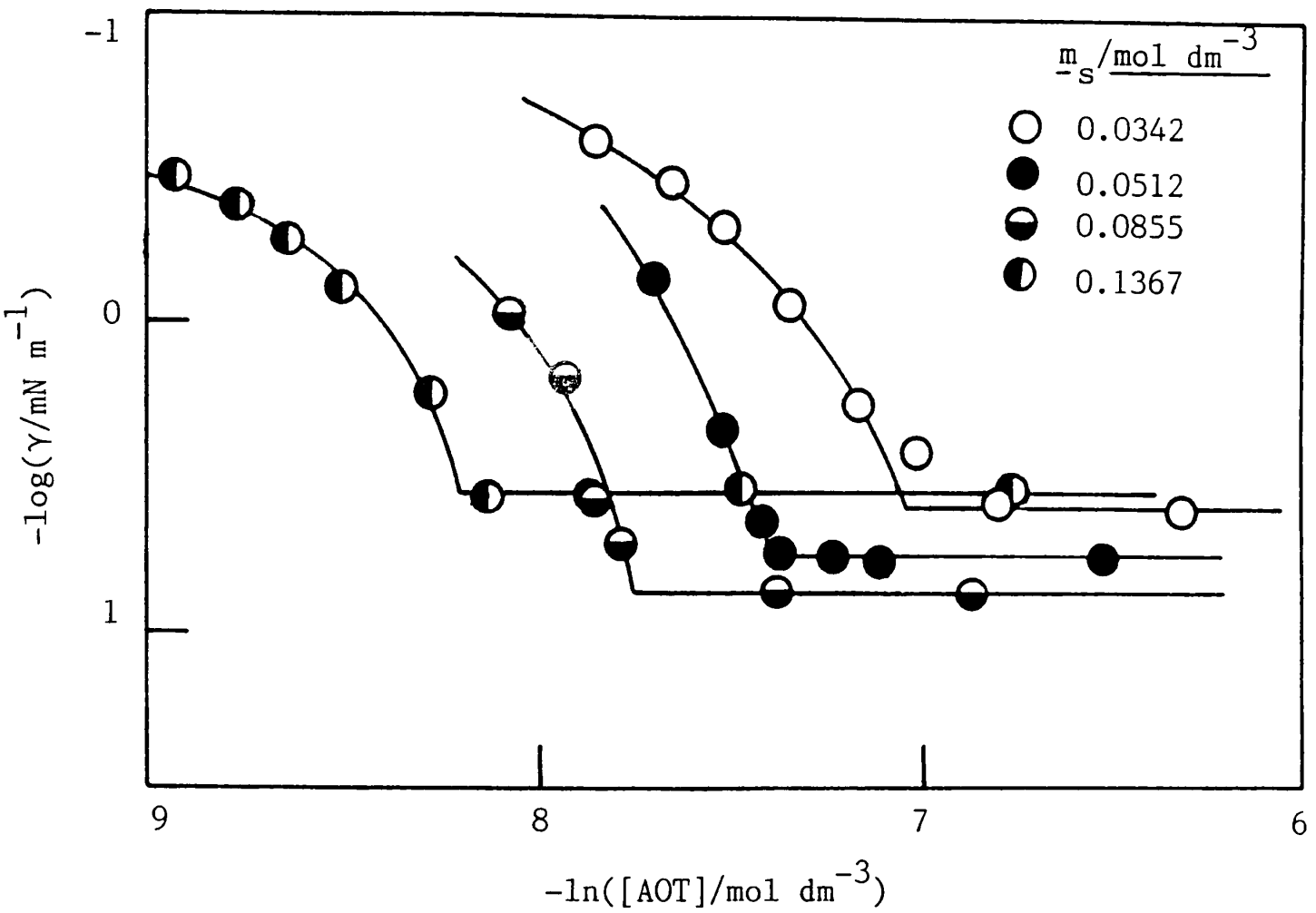

Figure 7.4b Dependence of c.m.c. on total counterion concentration at 25°C.

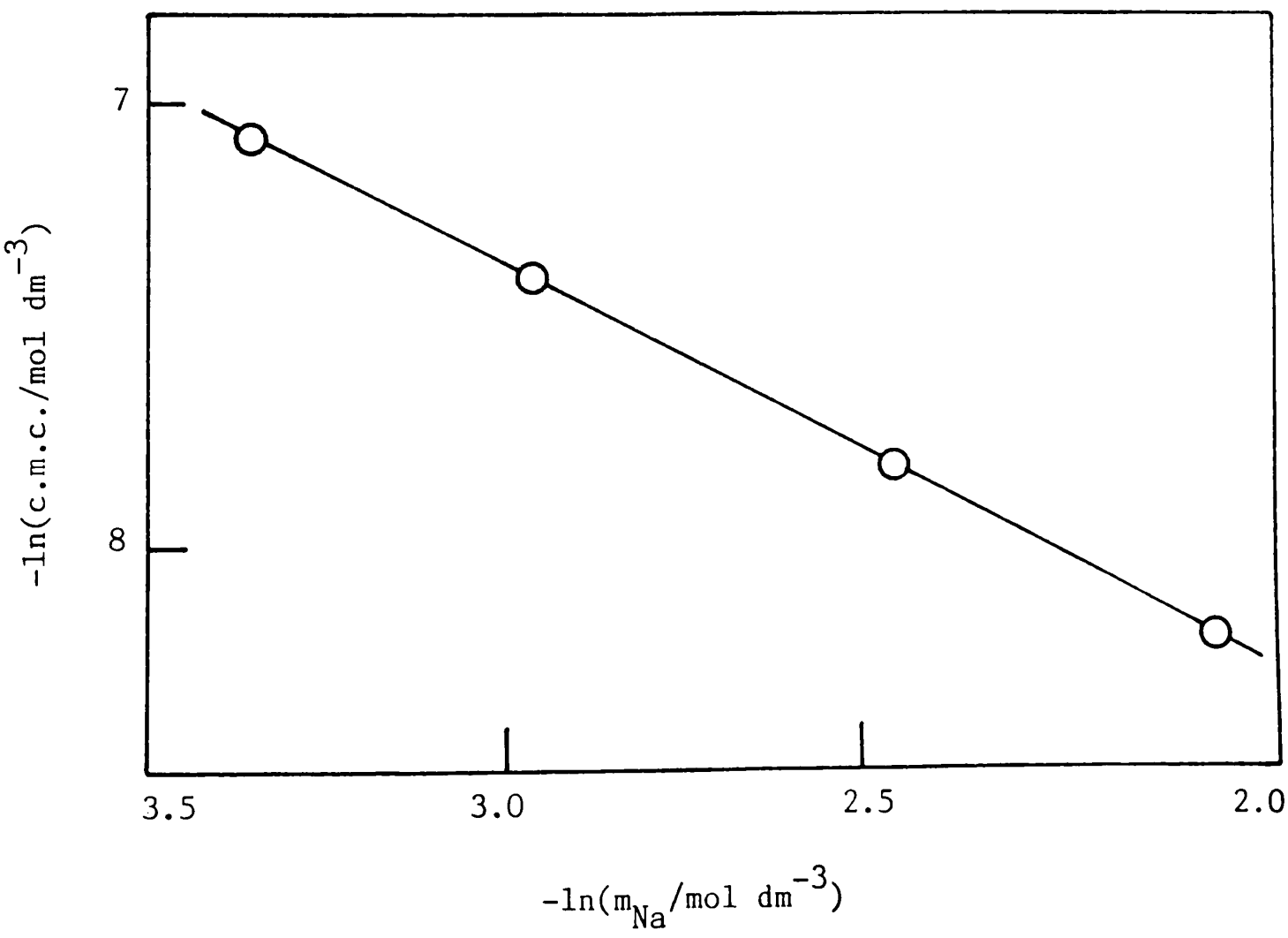

(or temperature) interval, one has to pay with relatively high interfacial tensions. Hence, for a given oil and a given temperature the problem is to optimise these properties by choosing the appropriate surfactant or combination of surfactants.

The salt concentration at which minimum tension is observed depends on N; this gives rise to a minimum in γ_c with respect to N as can be appreciated by reference to Figure 7.5. Minima with respect to m_s for three values of N are represented in Figure 7.5a; in Figure 7.5b the γ_c corresponding to a fixed m_s (represented in Figure 7.5a by the vertical dashed line) are plotted against N. Although, as depicted, γ_c for N_1 and N_3 are equal it is clear from Figure 7.5b that $d\gamma_c/d\ln m_{Na}$ at the selected value of m_s is positive for alkane N_1 and negative for alkane N_3. It follows from equation 7.2 that, assuming α_p is relatively unaffected by N, α_m must be greater for larger N. For small N, where $d\gamma_c/d\ln m_{Na}$ is positive, $\alpha_m < \alpha_p$, implying if $\alpha_p \simeq 0$ that α_m is negative. Physically this indicates that surfactant transfers to the oil phase leaving the aqueous phase devoid of micelles (see Figure 7.2a).

7.2.3 *Effects of N on 'effective' surfactant geometry*

From the geometrical approach put forward by Mitchell and Ninham,[15] the effect of alkane chain length on phase inversion may be understood in terms of the degree of oil penetration into the chain region of surfactant monolayers. Penetration increases the effective value of v (i.e. swells the chain region) and gives an increase in P. Experiments on the solubility of hydrocarbons

Figure 7.5 Origin of a minimum in γ_c with respect to N

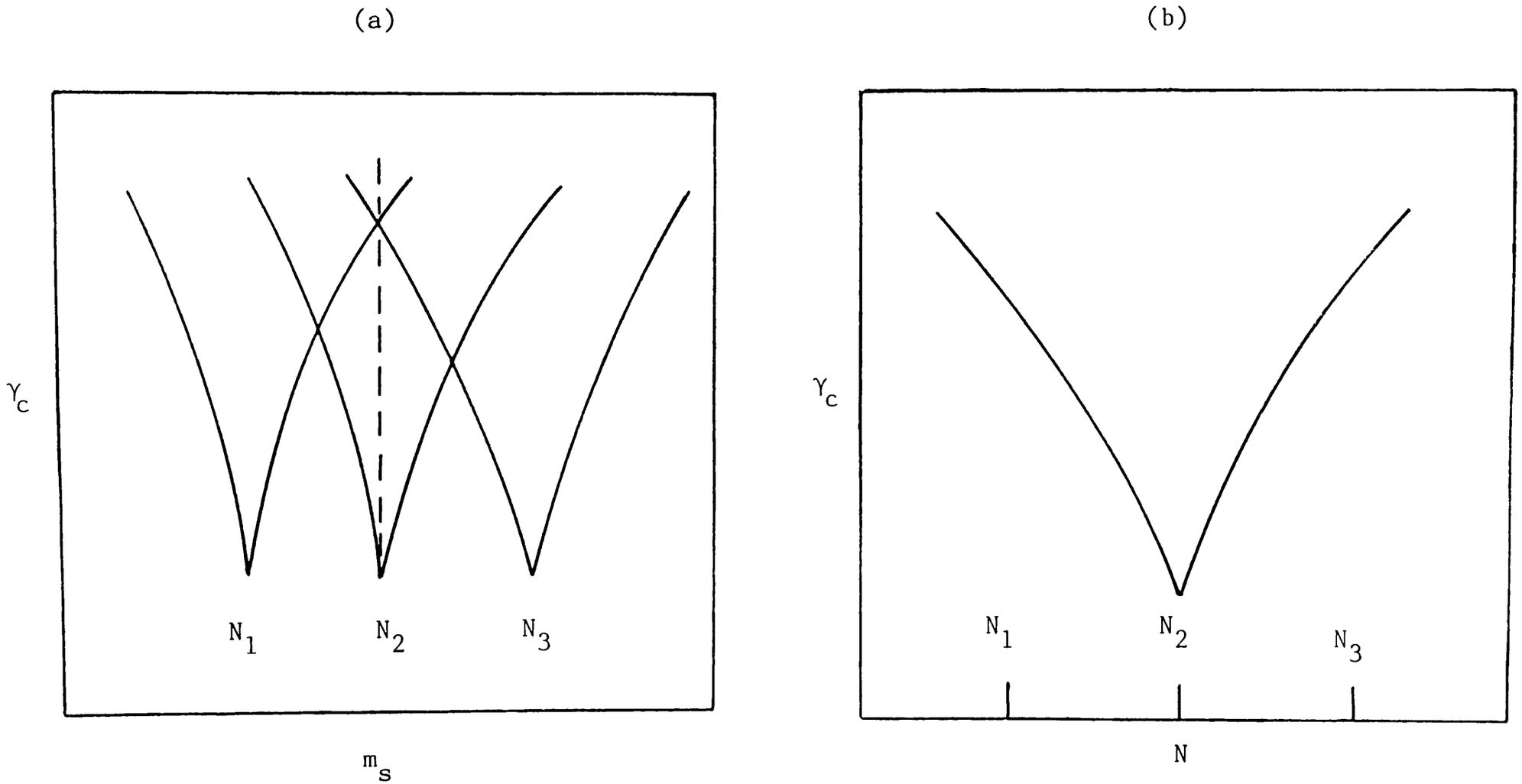

in lipid lamellar phases[159] suggest that smaller alkanes penetrate into the surfactant layers more strongly than larger homologues. Thus shorter chain alkanes tend to induce inverted surfactant structures i.e. w/o microemulsions; one would expect that if a series of alkanes were used such that phase inversion of an oil + water + surfactant system occurred within this range, a minimum in γ_c would also result. From the experiments discussed by Gruen[159] it is seen that decane swells the hydrocarbon layer of a glycerol monoleate black film to double its thickness (from 2.4 to 4.8 nm). Experimentally it is known that the headgroup area remains constant. Thus the volume per surfactant molecule doubles and so $v/a_h\ell$ also doubles. With longer chain hydrocarbons, $v/a_h\ell$ changes less markedly e.g. for hexadecane by a factor of 4/3.

The way in which the shape and curvature of surfactant aggregates change as phase inversion conditions are approached has also been discussed in terms of a statistical mechanical model by Mukherjee *et al.*[36] The main feature of their approach is the description of the spherical o/w interface by a lattice model of the hydrocarbon region of the surfactant film at the droplet surface. This region contains the hydrocarbon chains of surfactant (which are assumed to be fully extended) as well as oil molecules taken up by the film (which are assumed to be completely flexible). With this model of the chain region and with the surfactant polar groups taken as hard discs occupying a surface, the theory provides a simple description of bending

effects and hence droplet size. The theory predicts how oil chain length affects microemulsion behaviour. Basically, different chain lengths lead to different free energies of mixing in the hydrocarbon region of the film and it is concluded that shorter alkanes penetrate more effectively than do longer chain homologues.

The geometrical ideas discussed earlier (Chapter 3) imply that the area per ionic surfactant molecule, A_s, in a saturated film at a plane oil-water interface should be governed by the headgroup area a_h at low m_s. Alkane penetration into surfactant chain regions may also play a part as discussed below. The area A_s should fall with increasing m_s and assume an effectively constant value A_s^{ℓ} for m_s which corresponds to minimum γ_c. The value of A_s^{ℓ} is expected to be determined by the size of the surfactant chains and by the degree of penetration of alkane into the monolayer, and so should be higher in the presence of the shorter chain alkanes.

To test these ideas, values of A_s as a function of m_s have been determined in systems containing dodecane (in addition to those using heptane, § 3.10.2). Plots of γ against $\ln m_D$, examples of which are depicted in Figure 7.6a, were used to calculate A_s values (at the c.m.c.) using the appropriate form of the Gibbs equation (see § 1.3). The A_s are plotted against m_s in Figure 7.6b and listed in Table 7.1; A_s falls exponentially with m_s and the line in the figure is obtained from the fitting equation (for 0.01 mol dm^{-3} < m_s < 0.14 mol dm^{-3})

$$10^2 \, A_s/nm^2 = 39.76 \exp.(-52.12 \, m_s) + 64.1$$

ation of γ with aqueous phase concentration of AOT at the dodecane-aq. NaCl interface at 25°C.

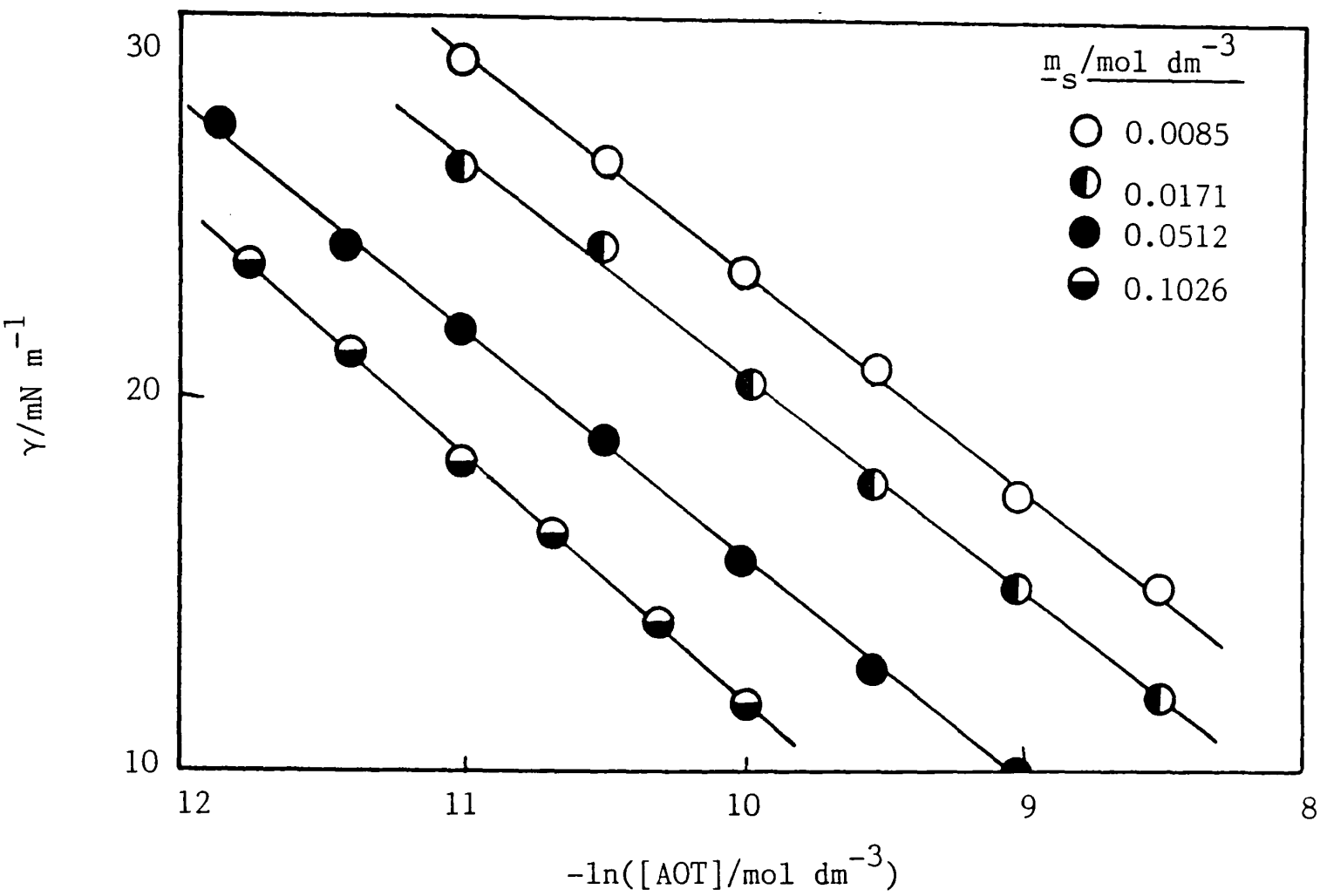

Figure 7.6b Saturated areas A_s against salt concentration for AOT at the dodecane-solution interface at 25°C.

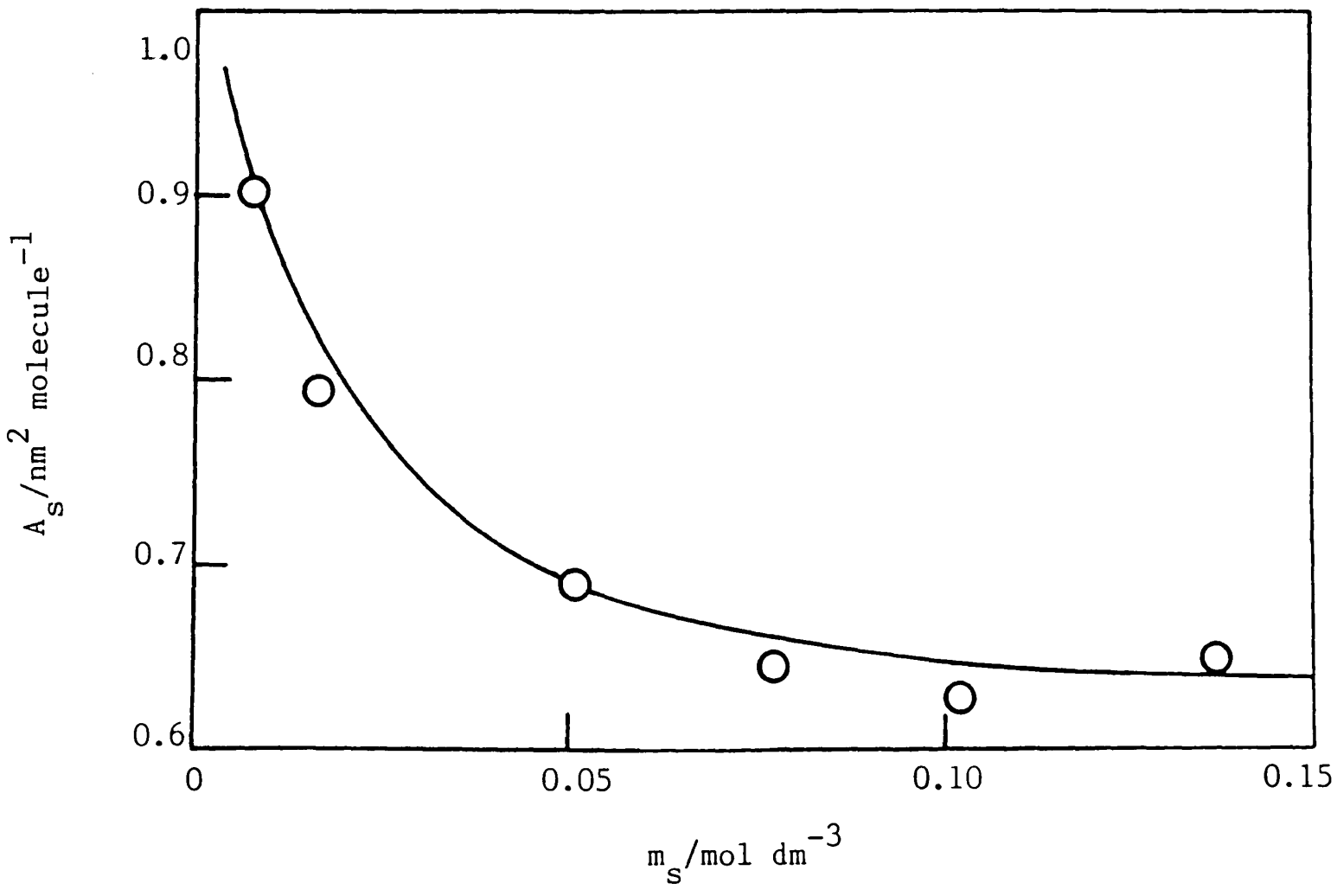

Table 7.1

Values of A_s versus m_s for AOT adsorbed at the dodecane-aqueous NaCl interface at 25°C

m_s/mol dm^{-3}	A_s/nm^2 $molecule^{-1}$
0.0085	0.90 ± 0.02
0.0170	0.79 ± 0.01
0.0513	0.69 ± 0.01
0.0770	0.64 ± 0.01
0.1026	0.63 ± 0.01
0.1370	0.65 ± 0.01

As predicted, A_s becomes effectively constant in the correct range of m_s; it is also seen that A_s^{ℓ} is achieved at higher m_s for dodecane than for heptane (0.085 mol dm^{-3} and 0.05 mol dm^{-3} NaCl respectively, see Figure 3.13). In addition, A_s^{ℓ} values have been determined (for m_s = 0.103 mol dm^{-3}, corresponding to w/o systems in all alkanes) for systems containing other alkanes, from tension plots like those in Figure 7.7a. It is seen (Figure 7.7b and Table 7.2) that A_s^{ℓ} falls smoothly with increasing N. It thus appears that the geometrical approach provides a satisfactory empirical description of the way in which salt and alkane cause the inversion of surfactant type accompanying minima in γ_c.

Figure 7.7a γ against ln AOT for various alkanes for aq. 0.1026 mol dm^{-3} NaCl at 25°C.

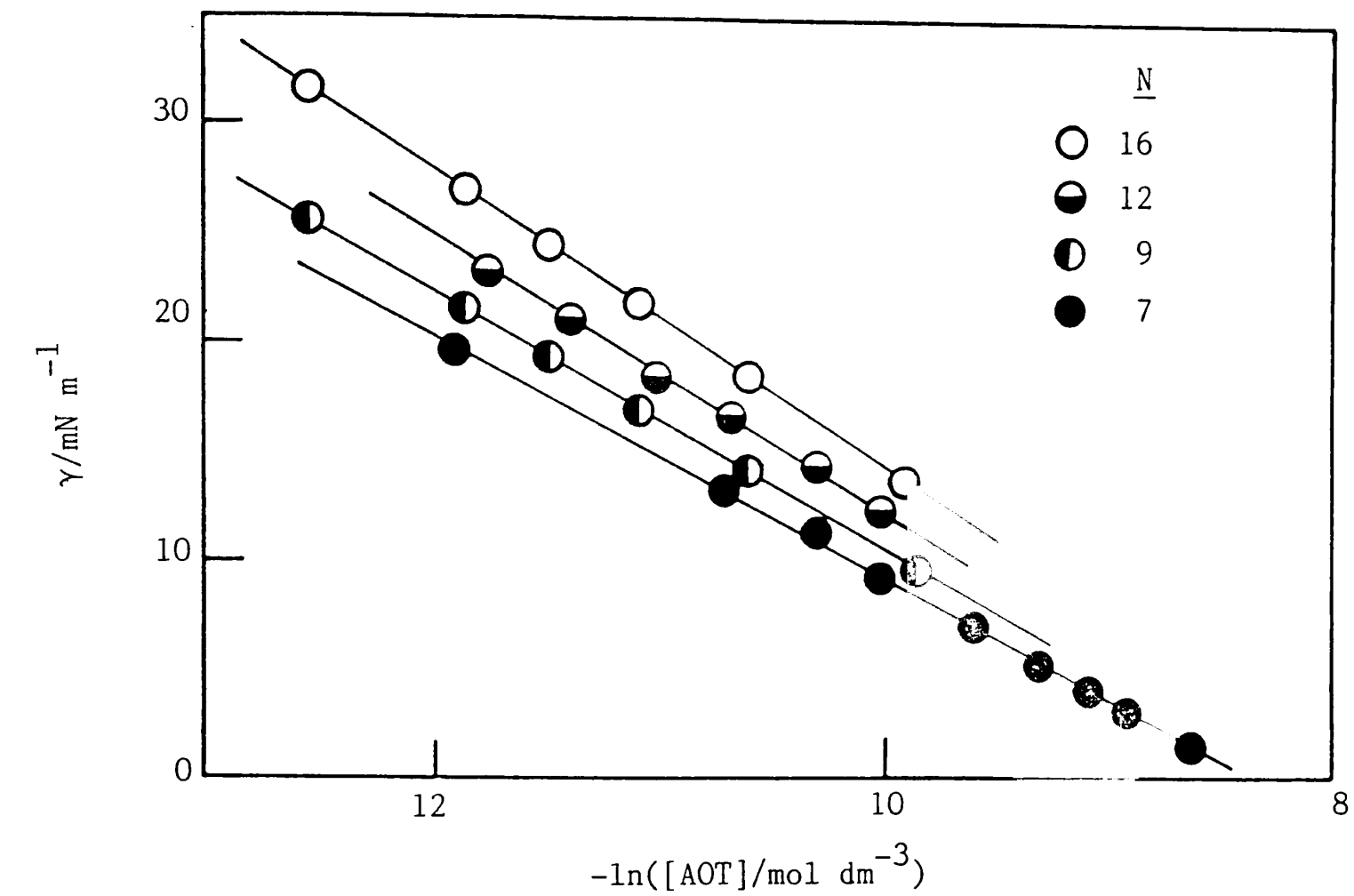

Figure 7.7b Variation of limiting area with N for AOT at 25°C.

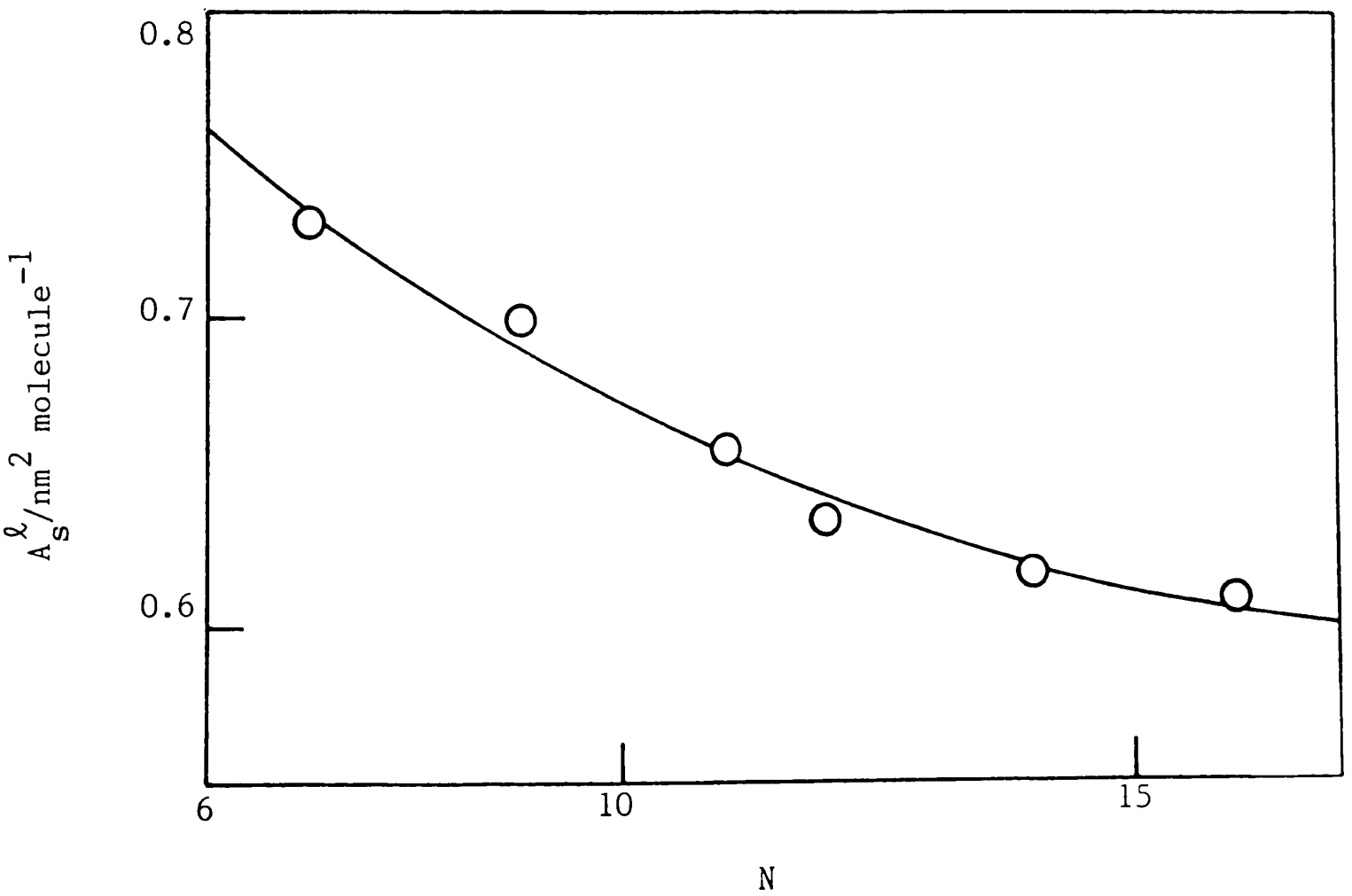

Table 7.2

Effect of alkane on A_s^{ℓ} values for AOT at 25°C

N	A_s^{ℓ}/nm^2 molecule^{-1}
7	0.722
9	0.698
11	0.656
12	0.641
14	0.616
16	0.608

7.3 Systems containing other oils

The properties of systems containing highly penetrating oils are of very great interest. Chen *et al.*[154] report that the minimum amount of water needed for w/o microemulsion formation using cyclohexane is much less than for hexane in systems containing the double-chained cationic surfactant didodecyldimethylammonium bromide. They explain this in terms of the greater degree of oil penetration into surfactant chains using cyclohexane. Kahlweit *et al.*,[160] working with short chain nonionic surfactants, present phase diagrams which show that the position and width of three-phase intervals (with respect to temperature) are very dependent on the oil type. The

results below represent a preliminary study into the effect of different oils on surfactant behaviour.

In order to study the influence of the nature of the oil, the following three hydrocarbons have been selected as representative : (i) n-heptane as a normal alkane, (ii) cyclohexane as a cyclic alkane, and (iii) toluene as an aromatic hydrocarbon. The hydrophobicity (as measured by solubility in water) of these oils decreases in the same order. An estimate of the degree of penetration of oils into surfactant monolayers is provided by measurement of the effective chain cross-sectional area (A_s^{ℓ}). Tensions(γ) are shown in Figure 7.8a as a function of $\ln m_D$ for AOT in 0.103 mol dm^{-3} NaCl in contact with each of the three oils at 25°C. The salt concentration is above that needed for minimum γ_c (m_s^*) so that the A_s values obtained from these data are limiting values A_s^{ℓ}, and are 0.738 (heptane), 0.802 (cyclohexane) and 0.898 (toluene) nm^2 $molecule^{-1}$. It appears from this that penetration increases in the order heptane < cyclohexane < toluene. It is therefore expected, for example, that using toluene as the oil phase should cause phase inversion at lower m_s^* than if heptane is used. The plots of γ_c versus m_s shown in Figure 7.8b confirm that this is indeed the case. Values of m_s^* for mixtures of heptane and toluene fall between those for the two pure components.

Interesting work reported by Martin and Magid[80] is concerned with the conformational and dynamic properties of AOT w/o microemulsions, studied by ^{13}C n.m.r. Their results lead to the

Figure 7.8a γ against ln AOT for aq. 0.1026 mol dm^{-3} NaCl at 25°C and three oils.

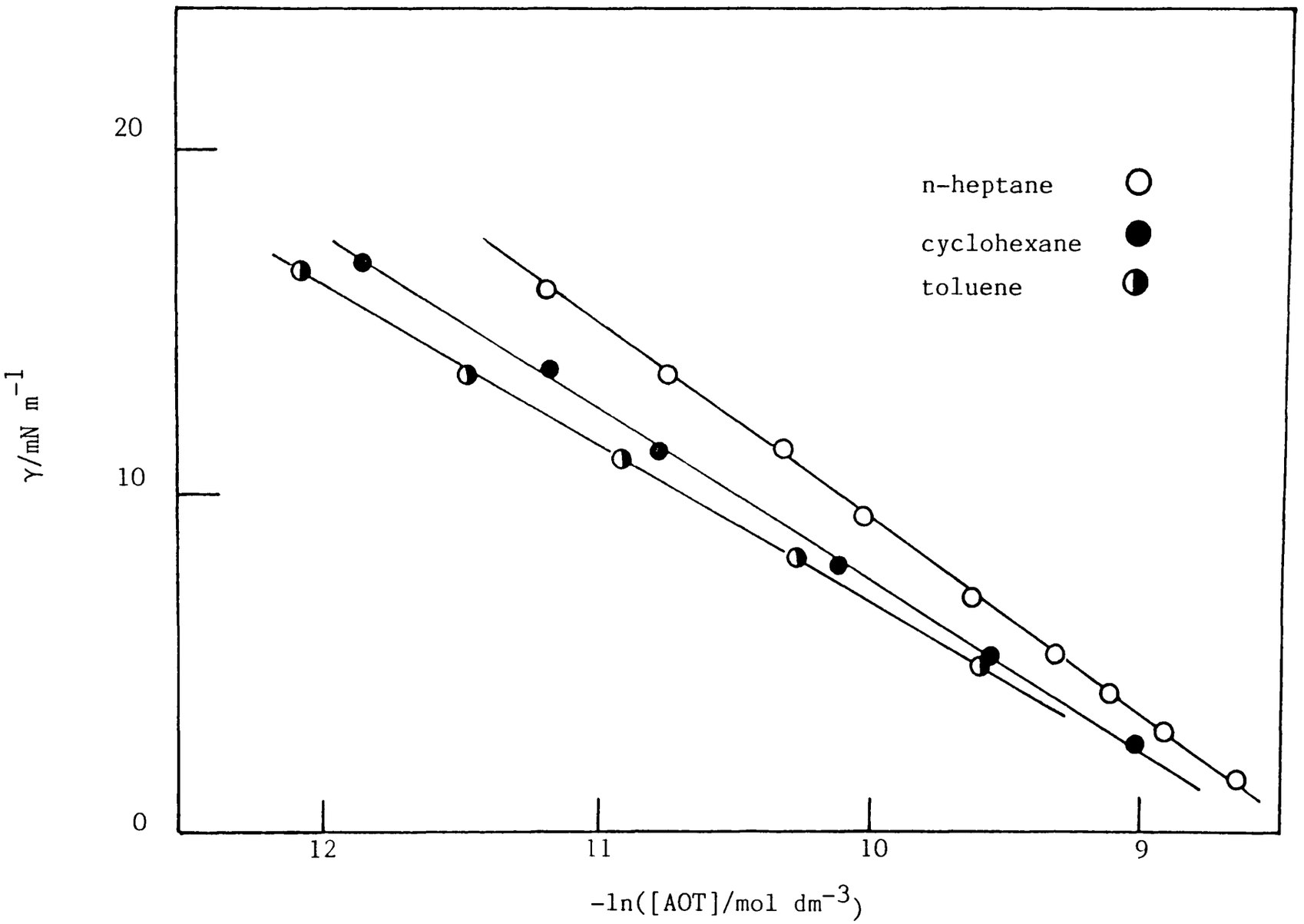

Figure 7.8b Variation of γ_c with m_s for AOT at 25°C adsorbed at interfaces with heptane, toluene and mixtures.

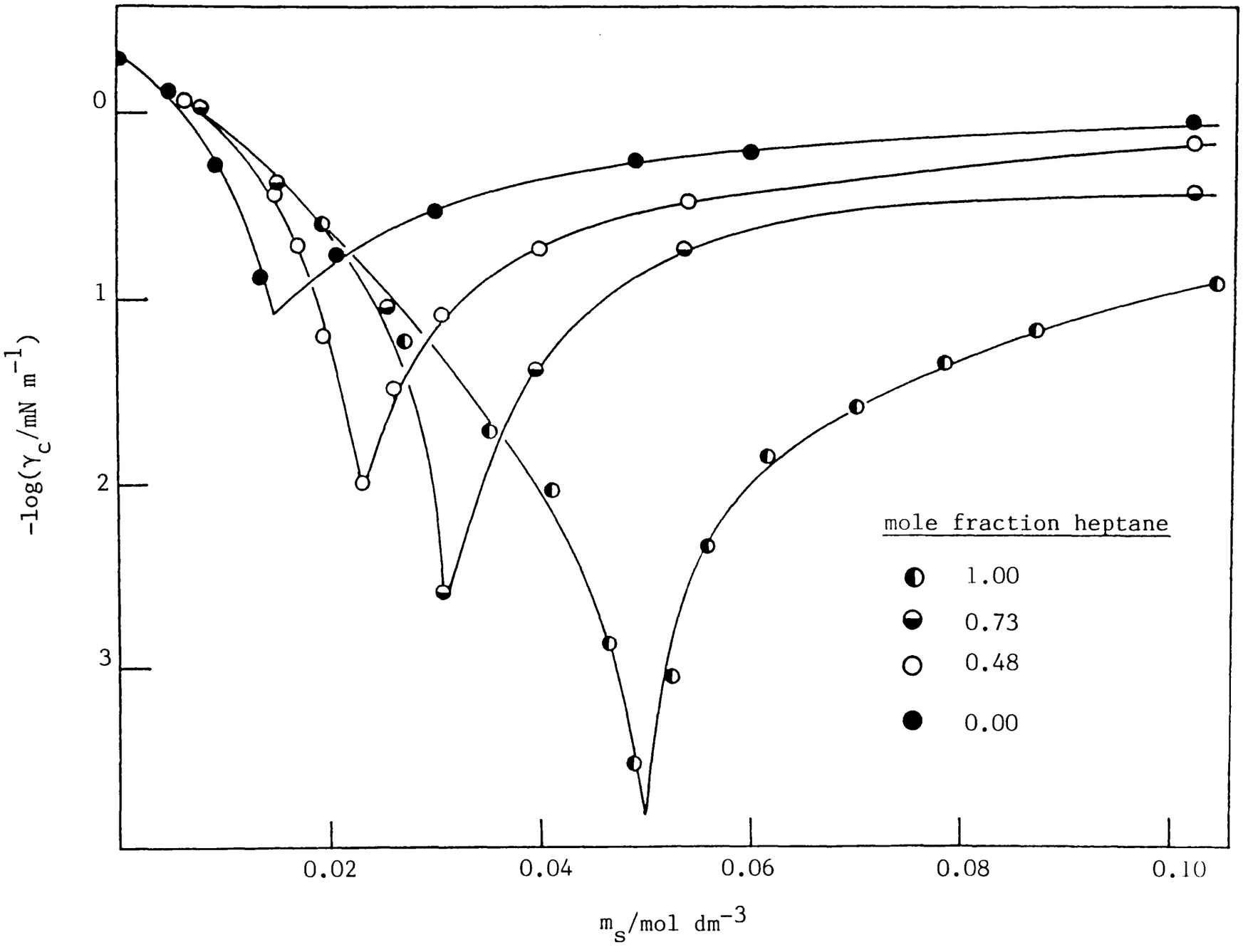

proposition that a benzene oil phase intercalates the AOT hydrocarbon chains while in cyclohexane the voids at the oil-water interface are filled by the chains of the hydrocarbon themselves. They attempt to rationalise the observed penetrating abilities of the two oils by considering their solvent properties. Due to the nonpolar nature of these oils, any interaction with the AOT headgroups should be due to dipole-induced dipole interactions. The polarisability parameter for benzene is larger than for cyclohexane, benzene occupies the smallest volume per mole and has a slight hydrogen-bonding tendency. When these factors are combined with the mutual solubilities of each oil and water,[161] it is claimed that a convincing argument is made for solvent penetration into AOT microemulsions decreasing from benzene to cyclohexane. However, no mention is made about the adsorption of the oil to the interface and a more detailed study is required, probably including a consideration of the entropies of mixing of the oils with the surfactant hydrocarbon chains, in order to understand fully the reasons for the differing degrees of oil penetration.

Acknowledgements

The author is indebted to Mr. S. Clark and Dr. J. Mead respectively, for some of the results presented in Figures 7.6a and 7.7a.

Chapter Eight

CHAPTER 8

ADDITION OF COSURFACTANTS TO SYSTEMS CONTAINING AOT

8.1 Introduction

Ionic surfactants often require the use of a second surface-active material called cosurfactant to form microemulsions with oil and water, and the emphasis has been on medium chain length alkanols and occasionally amines e.g. references 162, 163. As pointed out by Overbeek *et al.*[32] it is common for a surfactant to reach a solubility limit or aggregation point (c.m.c.) before very low interfacial tensions are attained. When such is the case however, it may be possible to reduce the tension further by addition of a cosurfactant. The preceding chapters have demonstrated that in alkane + aqueous NaCl systems containing AOT, low tensions and microemulsion formation can occur in the absence of a cosurfactant. This chapter reports an investigation into minima in γ_c brought about by addition of n-alkanols to the system. Results are discussed in terms of the effective molecular geometry of the surfactant and cosurfactant, and a thermodynamic treatment of the effect of cosurfactant is developed.[156] All primary data are given in Appendix IV.

8.2 Experimental data for n-alkanol addition

8.2.1 Effects of n-dodecanol concentration on γ_c

In terms of the geometrical description of Mitchell and Ninham of surfactant aggregation, the presence of an alkanol in a surfactant film can affect the operative values of both v (effective volume of hydrocarbon chain) and a_h (cross-sectional area of surfactant headgroup). Adsorption of alkanol results in the screening of the repulsions between surfactant headgroups (thus lowering a_h for the surfactant) and may act in such a way as to allow oil uptake (thus increasing v). Thus, depending on alkanol chain length, the addition of cosurfactant can cause an increase or a decrease in the parameter P (= $v/a_h\ell$), and hence in γ_c.

As discussed earlier (§ 3.10.2), for AOT, a_h can be larger than the chain area a_c (at low m_s where lateral headgroup repulsion within a monolayer is strong), or smaller than a_c (high m_s where the repulsion is sufficiently screened). Addition of a cosurfactant (e.g. n-dodecanol) for which $a_c > a_h$ is expected to affect the system in different ways, depending on whether, for the surfactant a_h is greater or smaller than a_c. For low values of m_s (where $P < 1$), dodecanol should, at small concentrations, mix in the monolayer producing mean a_c and a_h values which are more nearly equal, reducing the tendency of the plane monolayer to bend and hence reducing γ_c. At higher concentrations of cosurfactant in a monolayer however, a mismatch between mean

a_h and a_c is expected to reappear and γ_c should rise. At high m_s, (greater than that, m_s^*, causing minimum γ_c), the area a_c for the surfactant exceeds a_h and addition of cosurfactant to the film merely serves to increase the mismatch, and so γ_c is expected only to rise.

That these effects can be realised in practice is clearly demonstrated by the results in Figure 8.1. Figure 8.1a depicts the variation of γ_c with m_s (for NaCl at 25°C) in the absence of dodecanol (as shown previously in Figure 3.3). Three values of m_s (0, 0.017 and 0.043 mol dm^{-3}) have been chosen which are less than m_s^* (= 0.062 mol dm^{-3} at 30°C) and two values (0.068 and 0.1027 mol dm^{-3}) greater than m_s^*. Using these salt concentrations, dodecanol (dissolved in the heptane phase) has been added progressively in each case. The five curves of γ_c versus dodecanol activity (see later) are shown in Figure 8.1b. For $m_s < m_s^*$ minima are observed, which move to lower alkanol activity as m_s is increased. At the activity corresponding to minimum γ_c phase inversion occurs and surfactant transfers to the oil phase (as determined experimentally by surfactant analysis). The two curves for $m_s > m_s^*$ show no minimum, the tension only rising with cosurfactant activity. It is concluded that the simple geometrical picture outlined above appears to be reasonable in these systems.

In experiments leading to the data shown in Figure 8.1b, a solution of dodecanol in heptane was injected into the aqueous surfactant in the spinning-drop tensiometer; the two phases were not pre-equilibrated. Since dodecanol distributes strongly in

Figure 8.1a Effect of m_s on γ_c in absence of dodecanol at 25°C. Arrows denote m_s values represented in Figure 8.1b.

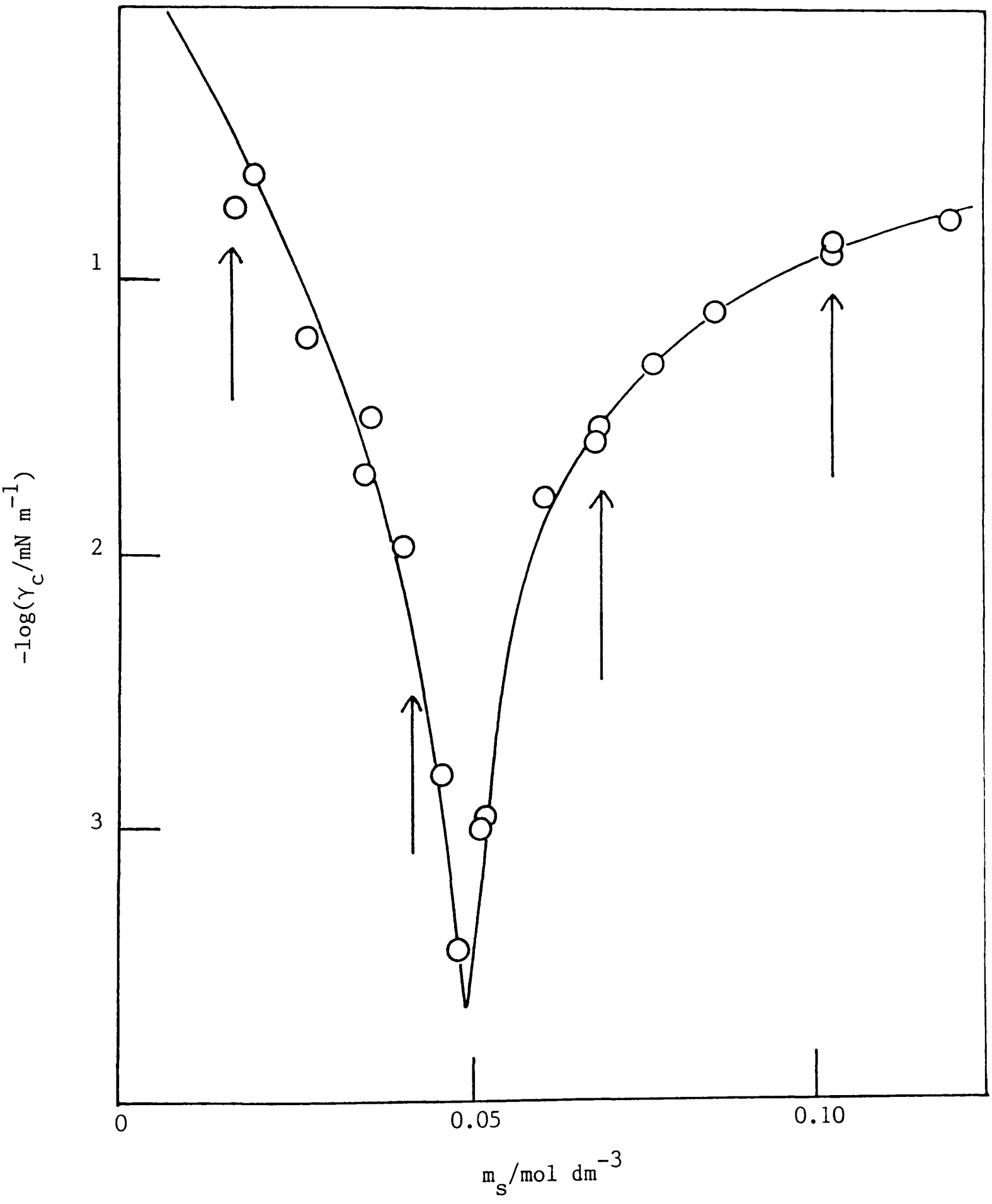

Figure 8.1b Variation of γ_c for AOT with the activity a_A of dodecanol in heptane at 30°C for various m_s.

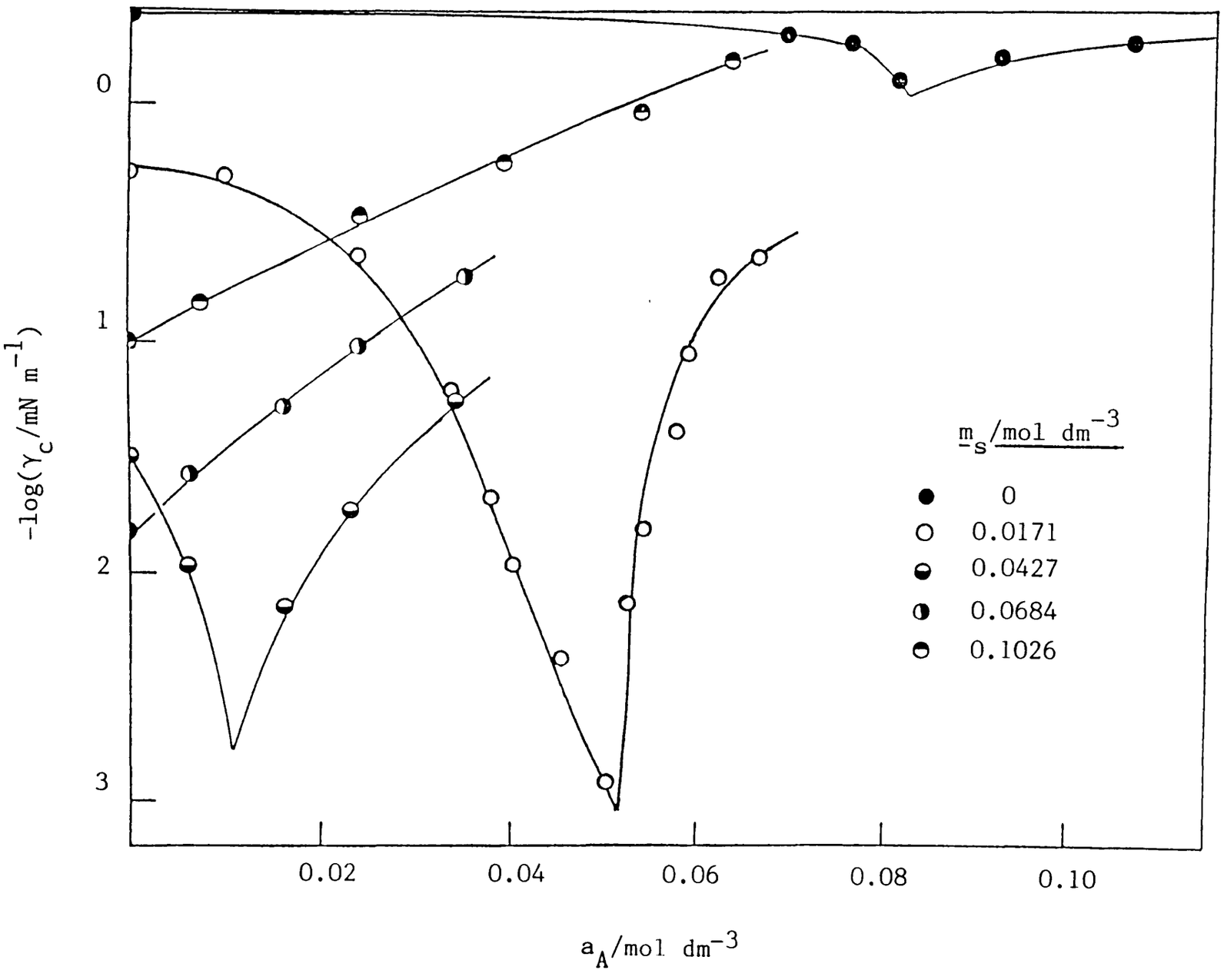

favour of the oil phase in pure oil-water systems,[101] the concentration in the oil phase is not therefore expected to be reduced significantly by loss to water. Some alkanol will however be incorporated into surfactant aggregates (see later). Accordingly, surfactant concentrations only about 10% above the c.m.c. have been used so that all alkanol concentrations used (typically 10^{-2} mol dm^{-3} in oil) greatly exceed the concentrations of aggregated surfactant ($\simeq 10^{-4}$ mol dm^{-3}), and so the alkanol activity is unlikely to be significantly affected by solubilisation. Further, for a fixed concentration of alkanol in oil, the γ_c tension is independent of AOT concentration (up to about 10 x c.m.c.) and so solubilisation does not appear to result in complications.

8.2.2. Addition of n-alkanols of varying chain length

It is predicted by the theory of Mukherjee *et al.*[36] that the effect of cosurfactant should depend upon cosurfactant chain length. Since the alkanol chain length affects a_c for the alkanol, shorter chain length alkanols would be expected to be less efficient than dodecanol in promoting phase inversion. In conformity with this, it is found that the reduction in γ_c is smaller (for a given mole fraction in heptane) the shorter the alkanol chain (Figure 8.2). Indeed, hexanol leaves γ_c unchanged and pentanol gives an increase. Loss of these two alkanols to the aqueous phase in the tensiometer may be more significant than for the higher alkanols, but since they do not lower the tensions this is not a problem in the context.

Figure 8.2 Variation of γ_c with mol fraction x_A of various alkanols in heptane at 30°C; $m_s = 0.0171$ mol dm^{-3}.

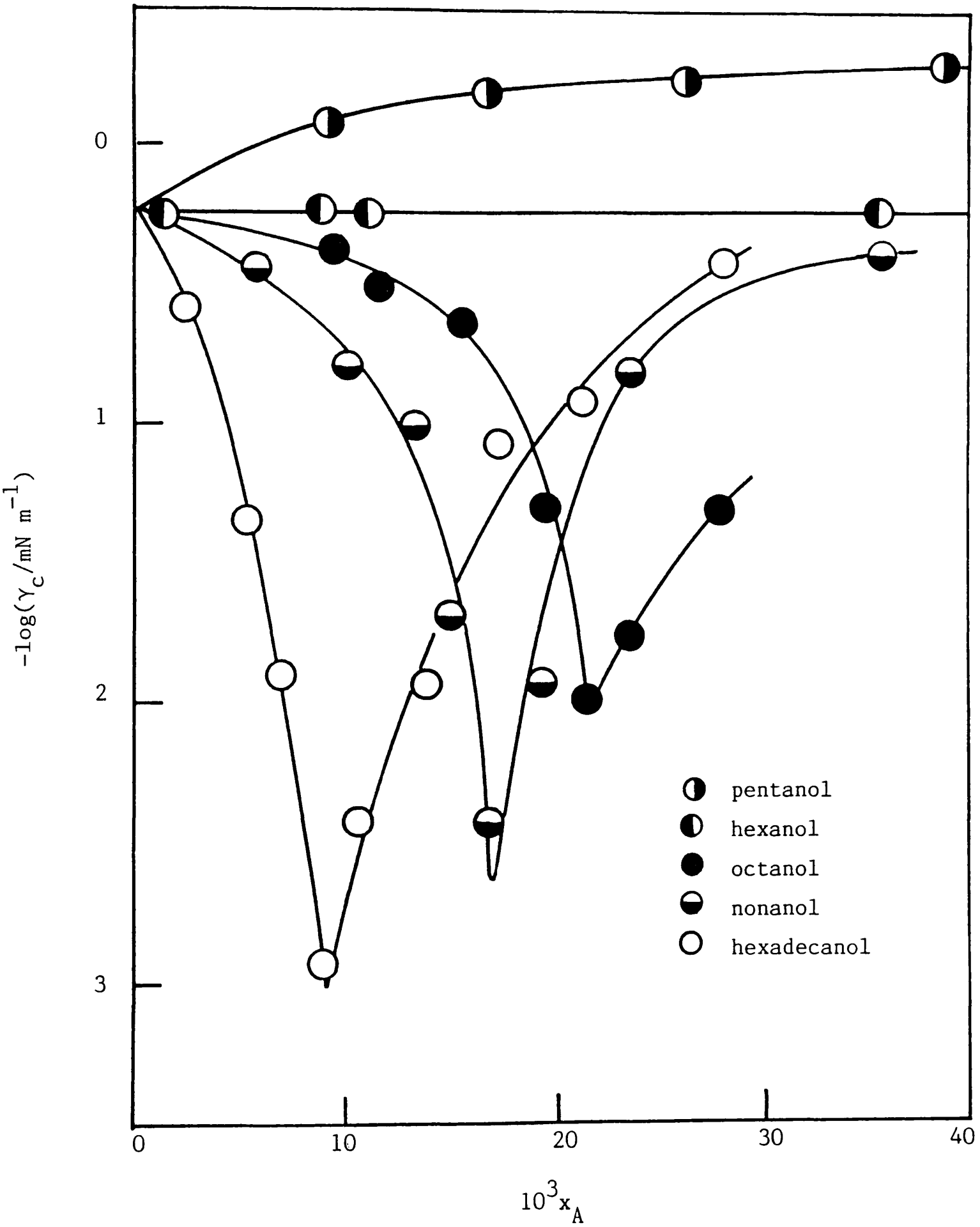

8.3 Thermodynamic treatment of effect of cosurfactant

8.3.1 *Derivation of expression for variation of* γ_c *with alkanol activity*

The Gibbs equation for systems at constant T containing an oil soluble cosurfactant and an aqueous phase containing an ionic surfactant and salt may be written

$$-d\gamma = \sum_i \Gamma_i d\mu_i + \Gamma_o d\mu_o + \Gamma_A d\mu_A \qquad (8.1)$$

where the Γ_i are surface excess concentrations for the ionic species (relative to that of water $\Gamma_w = 0$), Γ_o that for the oil and Γ_A for the cosurfactant. Since the concentration of alkanol in oil will be small ($\simeq 10^{-2}$ mol dm^{-3}), to a good approximation $d\mu_o = 0$ and the term in Γ_o may be neglected. The species to be considered are therefore Na, D (surfactant), Cl and A (cosurfactant).

With reference to Figure 8.3a which depicts the possible variation of the interfacial tension with surfactant concentration at various alkanol concentrations (leading to the minimum in γ_c shown in Figure 8.3b), changes in γ are written

$$-d\gamma = \left(\frac{\partial\gamma}{\partial \ln m_D}\right)_{m_A} .d\ln m_D + \left(\frac{\partial\gamma}{\partial \ln a_A}\right)_{m_D} .d\ln a_A \qquad (8.2)$$

The activity a_A is included rather than concentration m_A since the alkanols are present in alkane at concentrations where activity coefficients f_A differ significantly from unity as a

Figure 8.3 Origin of minimum γ_c with respect to cosurfactant concentration.

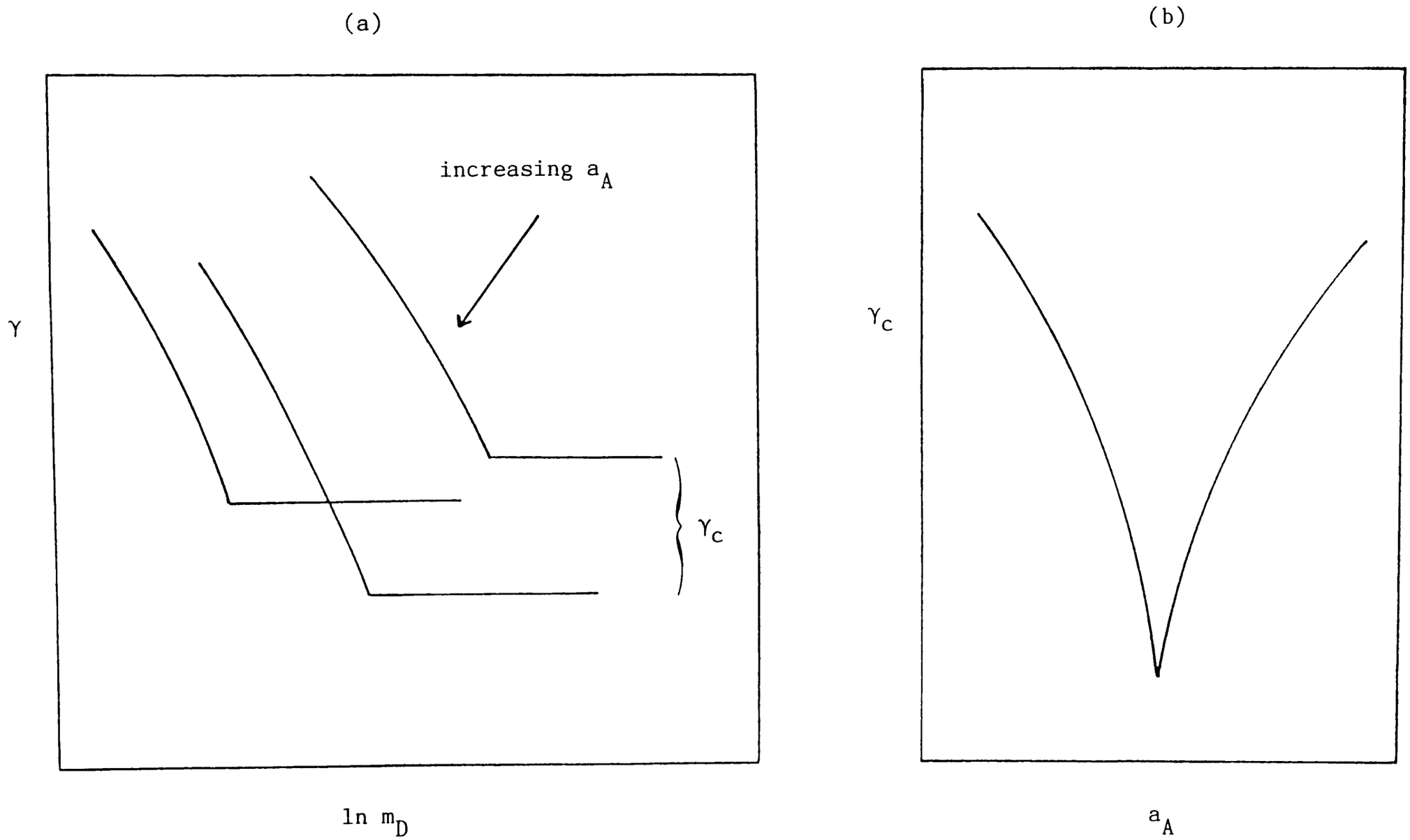

result of autoassociation through hydrogen-bonding.[164] The concentrations in the aqueous phase, m_A (aq), at distribution equilibrium will be very small so that the aqueous solutions can be regarded as ideal and so $d\ln m_{A\ (aq)} = d\ln a_A = d\ln m_A f_A$, where m_A is the oil phase concentration. From the Gibbs equation 8.1, it is readily shown that, in the presence of swamping electrolyte, to a good approximation

$$\left(\frac{\partial\gamma}{\partial \ln m_D}\right)_{m_A} = -RT\Gamma_D \qquad (8.3)$$

and

$$\left(\frac{\partial\gamma}{\partial \ln a_A}\right)_{m_D} = -RT\Gamma_A \qquad (8.4)$$

At the c.m.c., from equations 8.2-8.4

$$\frac{d\gamma_c}{d\ln a_A} = -RT\left[\Gamma_A + \Gamma_D \cdot \frac{d\ln cmc}{d\ln a_A}\right] \qquad (8.5)$$

Equation 8.5 describes the variation in γ_c with cosurfactant activity in terms of the surface excesses of surfactant and cosurfactant and the change in c.m.c. brought about by cosurfactant addition. The sign of $d\ln cmc/d\ln a_A$ is expected to be negative i.e. the term in Γ_D is negative. Since Γ_A is positive, the possibility of an extreme γ_c is seen.

Further insight into the origins of tension minima with respect to alkanol activity may be gained by noting that Hall[142] has shown that for an ionic surfactant in supporting aqueous electrolyte in the presence of a sparingly soluble solubilised additive (e.g. long chain alkanol),

$$-\frac{d\ln cmc}{d\ln m_{A\ (aq)}} = \frac{N_A}{N_D} \qquad (8.6)$$

where the N are average numbers of molecules per micelle. In the systems presented here the aggregates can be in either the aqueous or the oil phase, depending on conditions, and alkane is also present. But the alkane activity may be assumed to remain constant (see earlier) and so equation 8.6 is still valid. From equations 8.5 and 8.6, it is seen that

$$\frac{d\gamma_c}{d\ln a_A} = -RT\left[\Gamma_A - \Gamma_D \cdot \frac{N_A}{N_D}\right] \qquad (8.7)$$

The quantity Γ_A is the number of moles of alkanol in an area of surface containing Γ_D mol surfactant; $\Gamma_D N_A/N_D$ is the number of moles of alkanol in micelles containing Γ_D mol surfactant. Thus $(\Gamma_A - \Gamma_D N_A/N_D)$ is an excess of alkanol (associated with Γ_D mol surfactant) in the plane surface over that in micelles. Clearly when $\Gamma_A/\Gamma_D = N_A/N_D$, γ_c is minimum (where $a_A = a_A^*$). Thus, as in the case of the (γ_c, m_s) and (γ_c, T) curves (Chapters 4 and 6), it is seen that minimum γ_c occurs when there is some kind of equivalence between the plane oil-water interface and the aggregates in equilibrium with the interface, in this case the mole ratio of cosurfactant to surfactant. The equivalence is presumably arrived at by the increase in aggregate size as phase inversion and minimum γ_c are approached. The third surfactant-rich phase often observed could be regarded as an 'infinite' aggregate in which the surfactant film is effectively planar.

8.3.2 *Numerical analysis of experimental data*

In order to calculate values of N_A/N_D by use of equation 8.7 both Γ_D and Γ_A are required at various alkanol concentrations. Values of Γ_D at the c.m.c. have been determined from (γ, $\ln m_D$) data (examples of which are shown in Figure 8.4a), obtained in the presence of 8 different concentrations of dodecanol (using equation 8.3). From these same data surface pressures (lowerings of γ), π, of alkanols have been extracted as a function of a_A for various m_D, sample results being shown in Figure 8.4b. The value of π is equal to the tension without alkanol less the tension with alkanol, at the same m_D. From this, Γ_A have been determined (using equation 8.4) and hence Γ_A at the c.m.c. by extrapolation. Activity coefficients of dodecanol in heptane have been assumed to be the same as those for dodecanol in octane.[164] The data in reference 164 were obtained using both an infrared (i.r.) absorbance method and vapour pressure osmometry. Results are for 'dry' systems (i.e. no water present); however it has been confirmed (using i.r.) that the activity coefficient remains unchanged when a dry solution is brought to equilibrium with excess water. Values of Γ_D and Γ_A at the c.m.c. for 8 alkanol activities in heptane at 30°C are given in Table 8.1.

Values of the c.m.c. have also been obtained tensiometrically as a function of alkanol activity and these are plotted in Figure 8.5. Because changes in the c.m.c. caused by alkanol are small, values of N_A/N_D cannot be reliably calculated by the use of equation 8.6. Instead the values of Γ_A/Γ_D, $1/RT\Gamma_D$ and γ_c

Figure 8.4a Variation of γ for the heptane-0.0171 mol dm^{-3} NaCl interface with m_D for various mol fraction activities a_A of dodecanol.

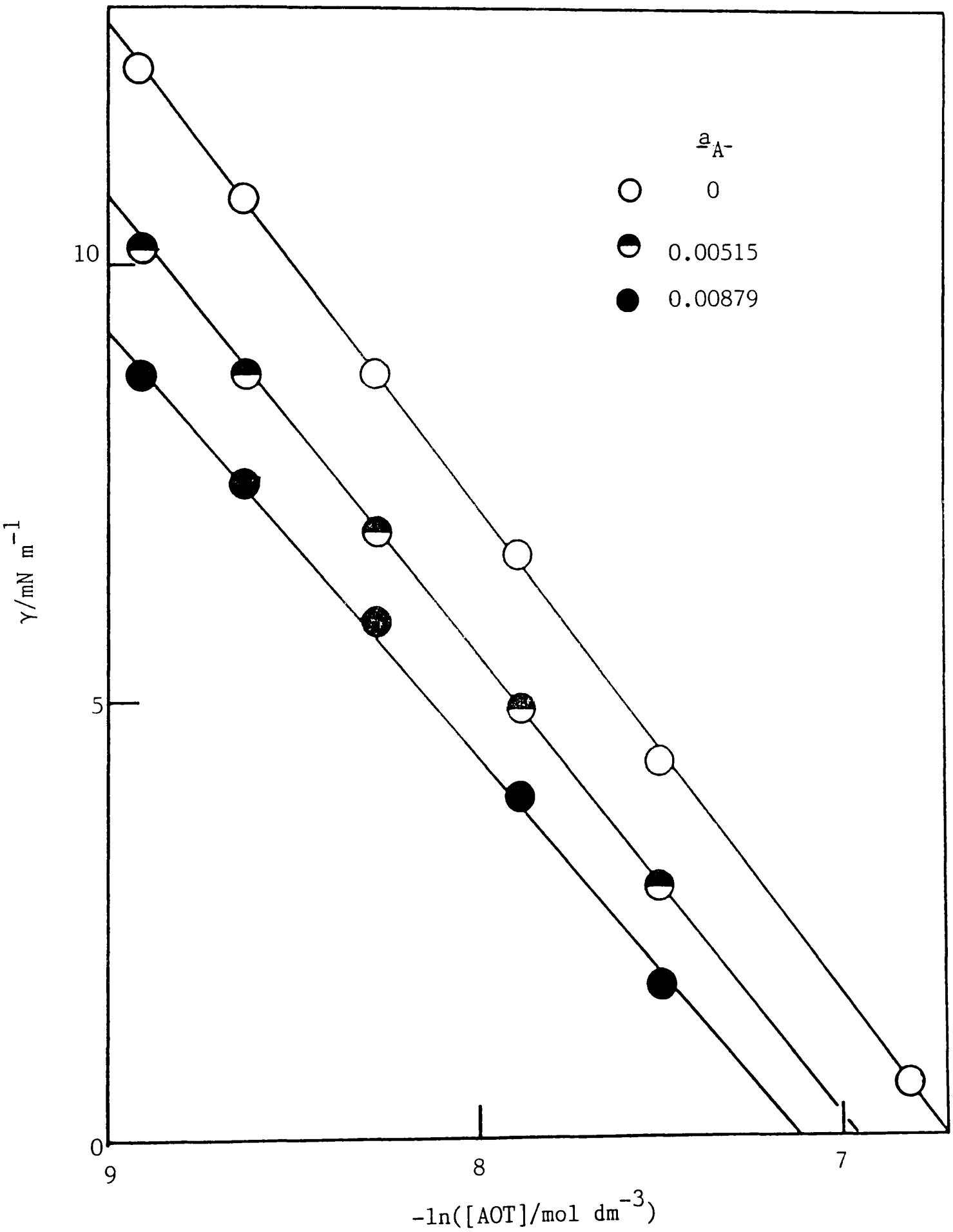

Figure 8.4b Surface pressure π of dodecanol as a function of a_A for various aqueous concentrations of AOT.

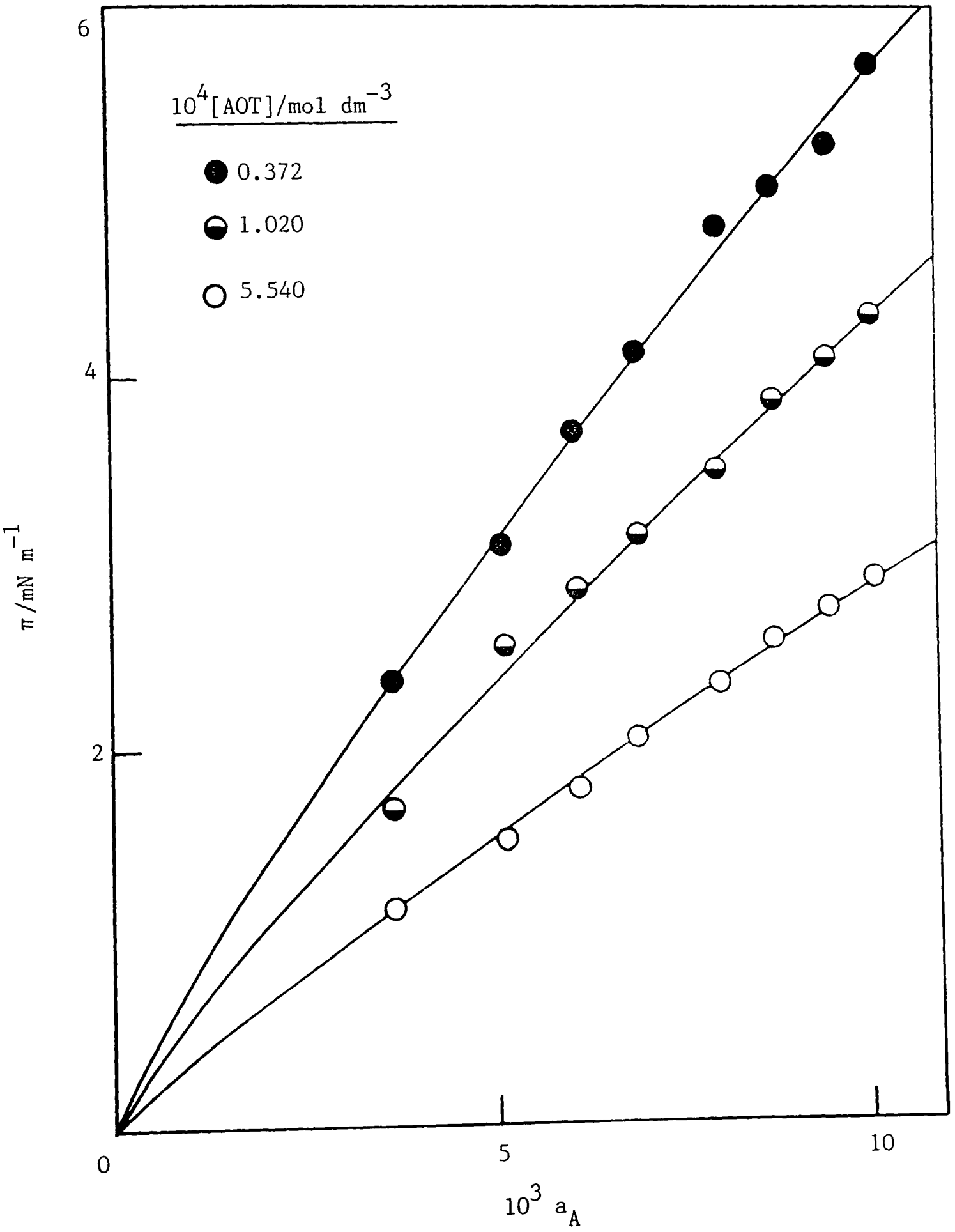

Table 8.1

Interfacial concentrations of AOT and dodecanol at the heptane/0.017 mol dm^{-3} NaCl interface as a function of mol fraction activity, a_A, of dodecanol in heptane at 30°C

$10^3 a_A$	$10^6 \Gamma_D$/mol m^{-2}	$10^7 \Gamma_A$/mol m^{-2}	Γ_A/Γ_D
0	2.10	0	0
3.66	2.05	2.91	0.14
5.15	1.99	4.09	0.21
6.13	1.95	5.08	0.26
6.95	1.91	5.68	0.30
8.07	1.87	7.03	0.38
8.79	1.85	7.59	0.41
9.51	1.82	8.22	0.45
10.12	1.78	9.02	0.51

were fitted to equations in terms of alkanol activity, and values of N_A/N_D then determined by use of equation 8.7.

The full lines shown in Figures 8.1b (for 0.017 mol dm^{-3} NaCl) and 8.6 were drawn using the fitting equations (respectively)

$$\gamma_c = 10^{-(1.94\times10^6 a_A^{2.767}+0.3128)} + 10^{-(225.73\ln a_A+24.967(\ln a_A)^2+510.8)} \qquad (8.8)$$

(for $a_A \leqslant a_A^*$) (for $a_A > a_A^*$)

Figure 8.5 Variation of the c.m.c. of AOT at 30°C with dodecanol activity in heptane -aq. 0.0171 mol dm^{-3} NaCl systems.

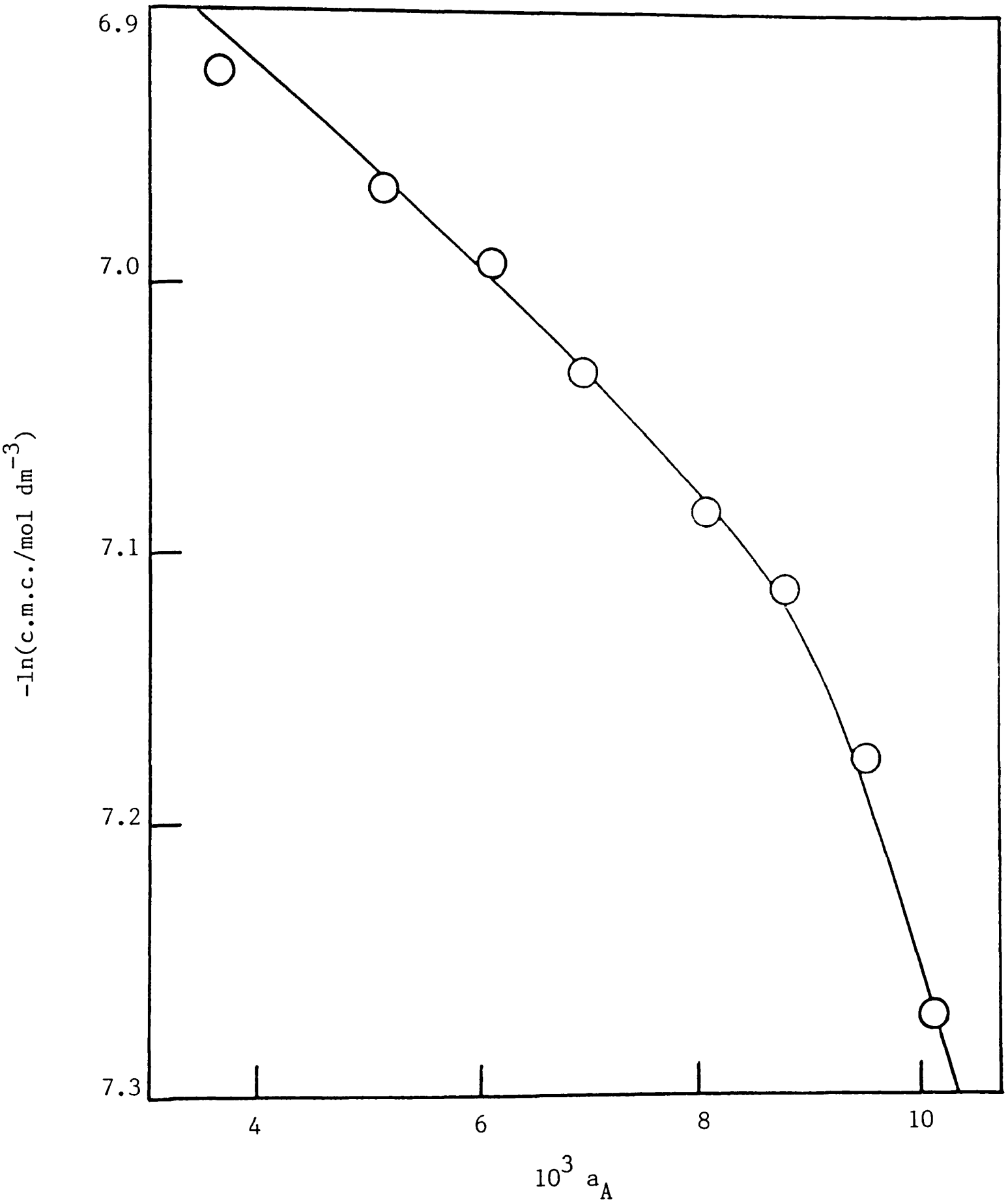

Points are experimental. The full line is obtained as described in the text.

and

$$\Gamma_A/\Gamma_D = 182.6\ a_A^{1.286} \tag{8.9}$$

Values of Γ_D were also fitted by

$$1/RT\Gamma_D = 0.02796\ \ln a_A + 0.3481 \tag{8.10}$$

By rearrangement of equation 8.7 and substitution of equations 8.8 - 8.10, values of N_A/N_D were calculated from equation 8.11:

$$\frac{N_A}{N_D} = 182.6a_A^{1.286} + (0.02796\ \ln a_A + 0.3481) - \left[1.236 \times 10^{(6.6872-1.94 \times 10^6 a_A^{2.767})} a_A^{2.767} - (1151\ln a_A + 519.9) \times 10^{-(225.731\ln a_A + 24.967(\ln a_A)^2 + 510.8)}\right] \tag{8.11}$$

The ratios N_A/N_D and Γ_A/Γ_D are plotted as a function of alkanol activity in Figure 8.6. At low a_A, $\Gamma_A/\Gamma_D > N_A/N_D$ implying that the aggregates in water contain a smaller proportion of alkanol than the plane interface. At high a_A, $N_A/N_D > \Gamma_A/\Gamma_D$, and at a_A corresponding to minimum γ_c, the two ratios are equal at 0.36, i.e. minimum γ_c is given for a monolayer in which there are about 3 AOT molecules to one alkanol. The mole fraction of alkanol in the inverted structures rises sharply with increasing a_A.

Although, as mentioned N_A/N_D cannot be reliably calculated

Figure 8.6 Molar ratios of dodecanol to AOT at 30°C as a function of dodecanol activity, a_A, in heptane.

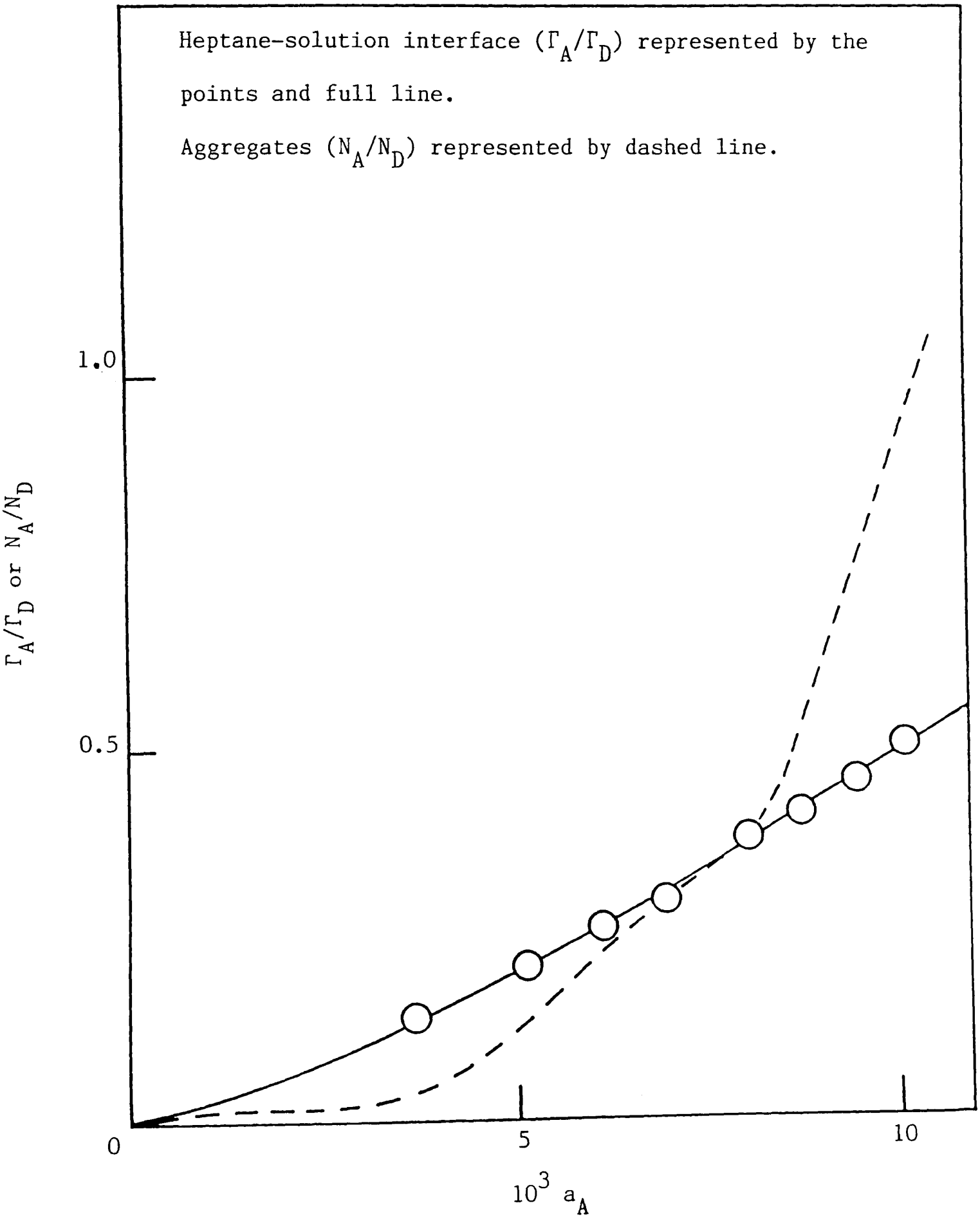

from c.m.c. values, it can nevertheless be demonstrated that the results in Figure 8.5 are consistent with the rest of the data. Integration by parts of equation 8.7 yields

$$\ln cmc = \frac{-\gamma_c}{RT\Gamma_D} - \int \frac{\Gamma_A}{\Gamma_D} \, d\ln a_A + \int \gamma_c \frac{d(1/RT\Gamma_D)}{d\ln a_A} \, d\ln a_A \qquad (8.12)$$

The integrals have been evaluated using the fitting equations given earlier; details of the numerical analysis are given in Appendix IV. The full line in Figure 8.5 is obtained after the suitable choice of a value for an integration constant, which only affects the vertical position but not the shape of the line. As seen, the line follows closely the experimental c.m.c. values.

The consistency of the simple geometrical approach with the preceding data is readily demonstrated. In a mixed surfactant-cosurfactant film giving minimum γ_c, the average headgroup area is expected to be equal to the average chain area (a_c) so that

$$\Gamma_D \, a_{h,D} + \Gamma_A \, a_{h,A} = \Gamma_D \, a_{c,D} + \Gamma_A \, a_{c,A} \qquad (8.13)$$

At the condition for minimum γ_c,

$$\Gamma_A/\Gamma_D = (a_{h,D}-a_{c,D})/(a_{c,A}-a_{h,A}) \qquad (8.14)$$

Reasonable estimates of the four areas are: $a_{c,D} = 0.72$ nm^2 (the value of A_s^{ℓ} in the heptane system), $a_{h,D} = 0.82$ nm^2 (the value

of A_s for m_s = 0.017 mol dm^{-3}, see § 3.3.1; presence of alkanol may of course alter $a_{h,D}$ but, if so, the magnitude of the change is unknown), $a_{c,A}$ = 0.28 nm^2 (the cross-sectional area of a single alkyl chain[165]), and $a_{h,A}$ = 0.05 nm^2 (an estimate of the area of the OH group). Substituting these values into equation 8.14 yields Γ_A/Γ_D = 0.43, close to the value of 0.36 shown in Figure 8.6.

Acknowledgement

The author thanks Dr. J. Mead for the results in Figure 8.4 and assistance with fitting the data referred to in this chapter.

Chapter Nine

CHAPTER 9

EFFECTS OF SALT AND COSURFACTANT ADDITION IN OIL + WATER SYSTEMS CONTAINING THE SINGLE-CHAIN SURFACTANT SDS

9.1 Introduction

It is well-known[32,34] that microemulsions can be formed (and by inference low oil-water tensions achieved) in systems containing a single chain anionic surfactant (e.g. sodium dodecyl sulphate) if a cosurfactant is also present. This chapter reports a study of systems containing SDS both in the presence and absence of cosurfactant.[166] The primary data are listed in Appendix V. Overbeek *et al.*[32] briefly describe the behaviour of systems containing SDS with n-pentanol as the cosurfactant. Pentanol however distributes fairly evenly between nonpolar oils and water,[101] and relatively high aqueous and oil phase concentrations are required to produce ultralow tensions. In order to simplify matters octanol has been used here as cosurfactant; this distributes much in favour of the oil phase and lower aqueous phase concentrations at least are required to give the desired lowering of tensions. Since alkanols associate through H-bonding in dilute solutions in nonpolar oils[164] it has been necessary to determine activity coefficients of octanol in solution in cyclohexane at 30°C.

9.2 Systems in the absence of cosurfactant

9.2.1 Effect of salt concentration on γ_c

Interfacial tensions have been obtained at 30°C as a function of SDS concentration, m_D, for various salt concentrations in the heptane/water system (Figure 9.1a). The constant tensions, γ_c, are not low (between about 4 and 7 mN m^{-1}) for salt concentrations up to 0.20 mol dm^{-3} and they do not pass through a minimum (Figure 9.1b). Using the appropriate form of the Gibbs equation (see § 1.3) linear portions of the $\gamma/\ln m_D$ curves yield values of Γ_D from which the area per SDS molecule in a saturated monolayer, A_s, may be calculated. Table 9.1 lists the variation in A_s with m_s, which is small compared with the AOT system (Table 3.1). In terms of the molecular geometry of SDS one supposes the absence of a minimum in γ_c is a result of the different magnitudes of a_h and a_c. Although addition of salt reduces a_h (as seen from the values of A_s in Table 9.1) by reducing the electrostatic repulsion between headgroups in the monolayer, and possible their hydration, apparently a_h is not reduced below a_c. In order to achieve a matching of (mean) a_h and a_c it is necessary to introduce into the monolayer a cosurfactant for which $a_c > a_h$. Use of an oil (e.g. cyclohexane) which strongly penetrates the chain region of the surfactant film should also serve to make a_h and a_c more nearly equal.

Figure 9.1a Heptane-aq.NaCl interfacial tensions as a function of SDS concentration, m_D at 30°C.

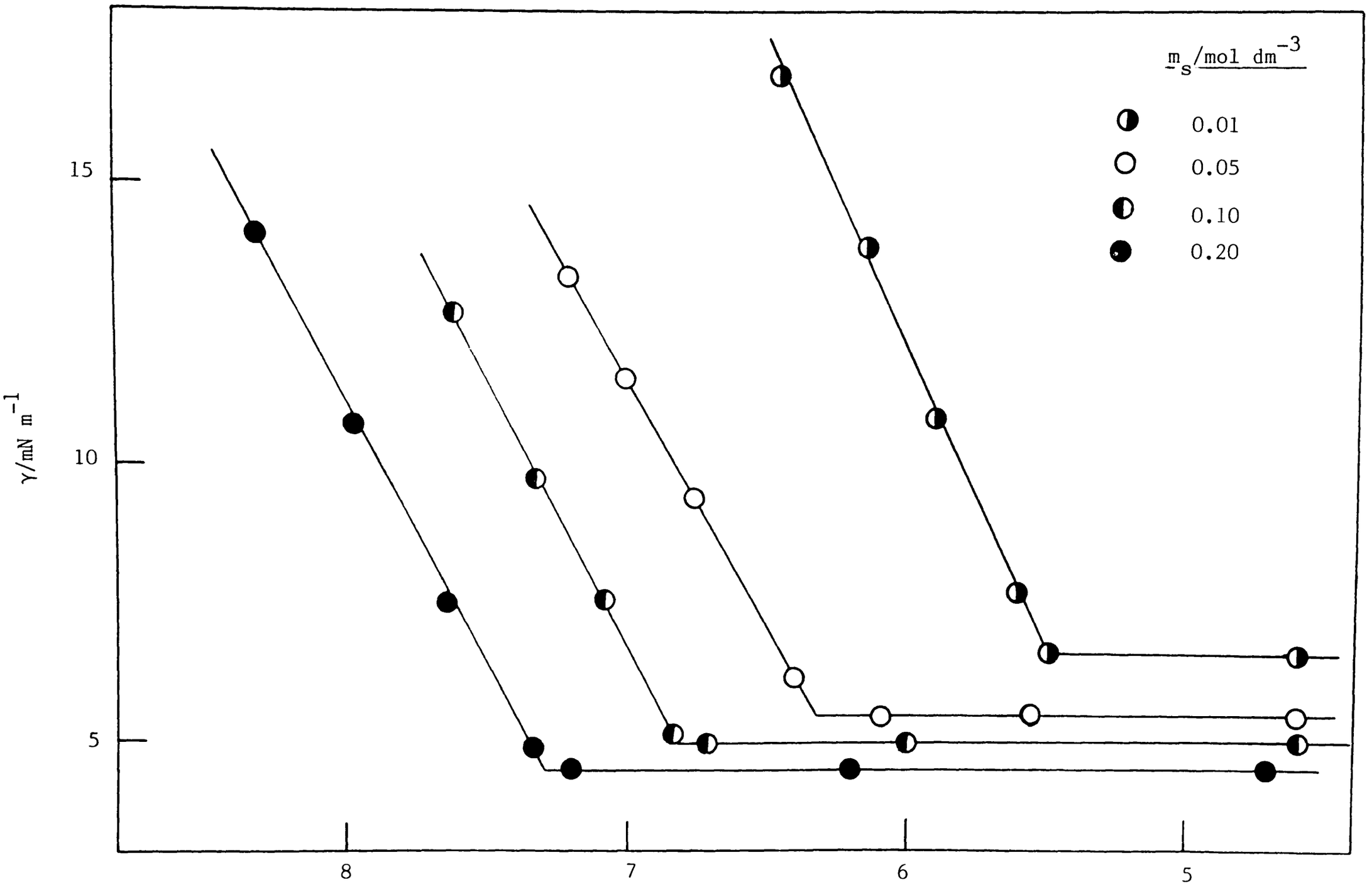

Figure 9.1b Variation of γ_c with m_{Na} for SDS in heptane-aq. NaCl systems at 30°C.

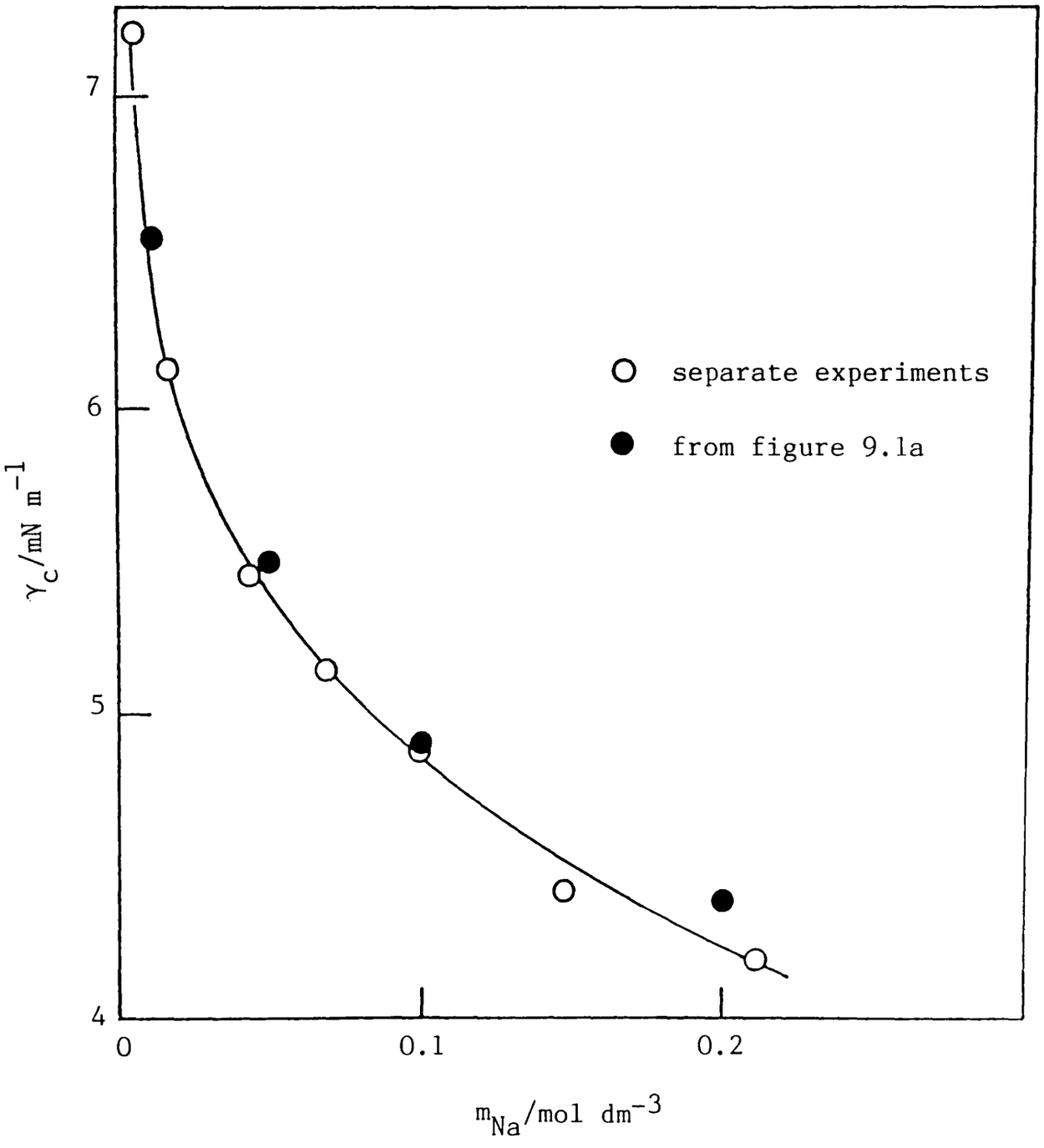

Table 9.1

Variation of A_s with m_s for SDS at the heptane/aq. NaCl interface at 30°C

m_s/mol dm^{-3}	0.01	0.05	0.10	0.20
A_s/nm^2 molecule^{-1}	0.49_6	0.47_6	0.42_8	0.43_8

9.2.2 Application of theory for salt effects

It was shown in § 4.2.3 that γ_c is related to m_{Na} (the total sodium ion concentration) by

$$\frac{-d\gamma_c}{d\ln m_{Na}} = RT\Gamma_D \left\{ 1 + 2\left(\frac{\partial \ln f_{\pm}^{NaCl}}{\partial \ln m_{Na}}\right)_{D,T} + \frac{d\ln cmc}{d\ln m_{Na}} + \frac{2\Gamma_{Cl}}{\Gamma_D}\left[1 + \left(\frac{\partial \ln f_{\pm}^{NaCl}}{\partial \ln m_{Na}}\right)_{D,T}\right]\right\} \qquad (4.17)$$

As mentioned earlier (p.106) Γ_{Cl} is expected to be small and negative and for the moment the term in Γ_{Cl} in equation 4.17 will be neglected. The c.m.c. can be obtained, as a function of salt concentration, from the data in Figure 9.1a, and a plot of $\ln cmc$ versus $\ln m_{Na}$ is given in Figure 9.2a. It is linear and of slope -0.69, close to that obtained from the data of Williams *et al.*[167] in systems without alkane present. In the range of m_s studied, $2(\partial \ln f_{\pm}^{NaCl}/\partial \ln m_{Na})$ is in the region of -0.12 to -0.18, and it can be appreciated from equation 4.17 (assuming $\Gamma_{Cl} = 0$)

Figure 9.2a Variation of c.m.c. of SDS with m_{Na} in systems containing NaCl.

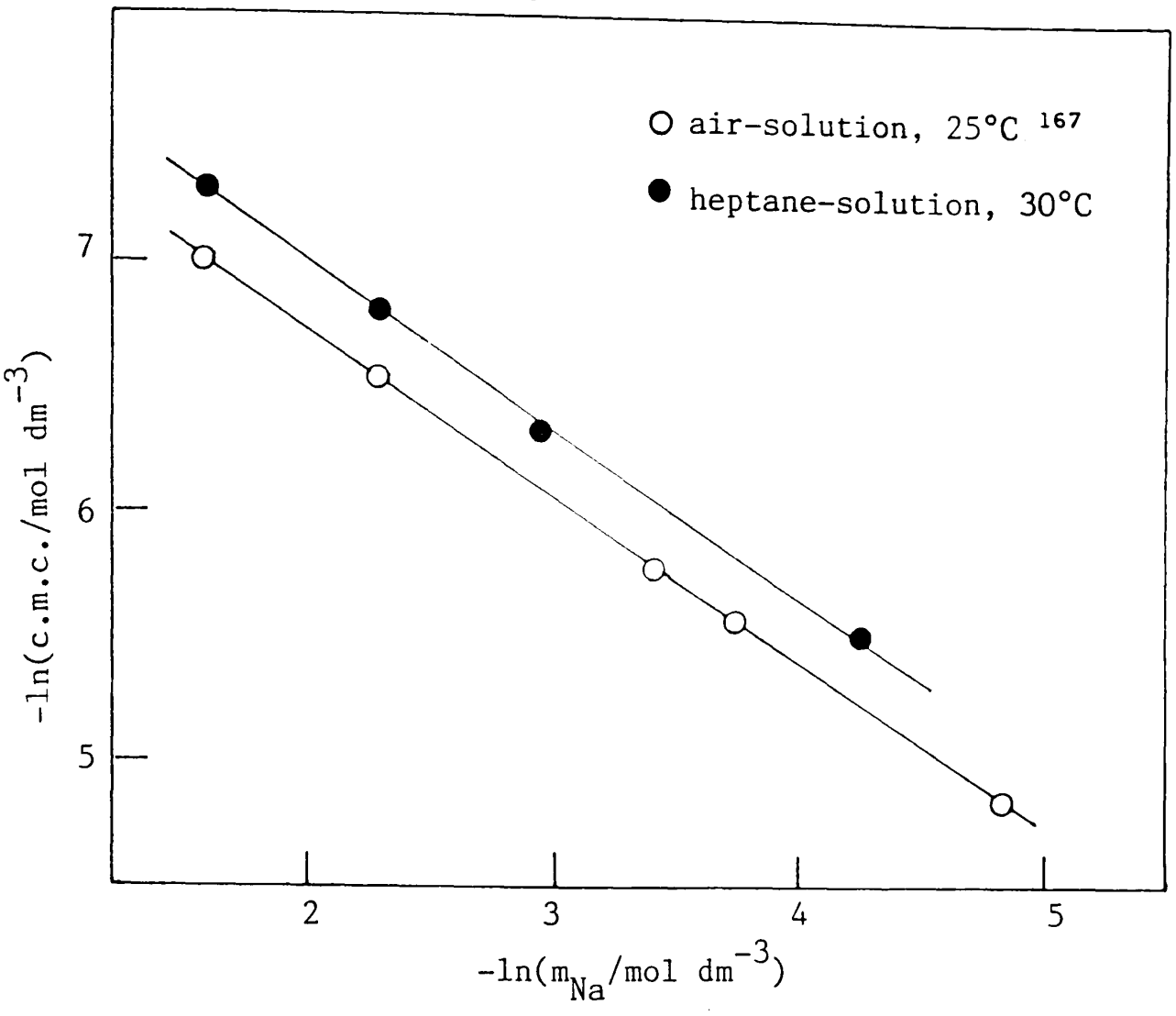

Figure 9.2b Variation of Γ_D and Γ_{Cl} at the interface between aq. NaCl and heptane at 30°C with m_{Na}.

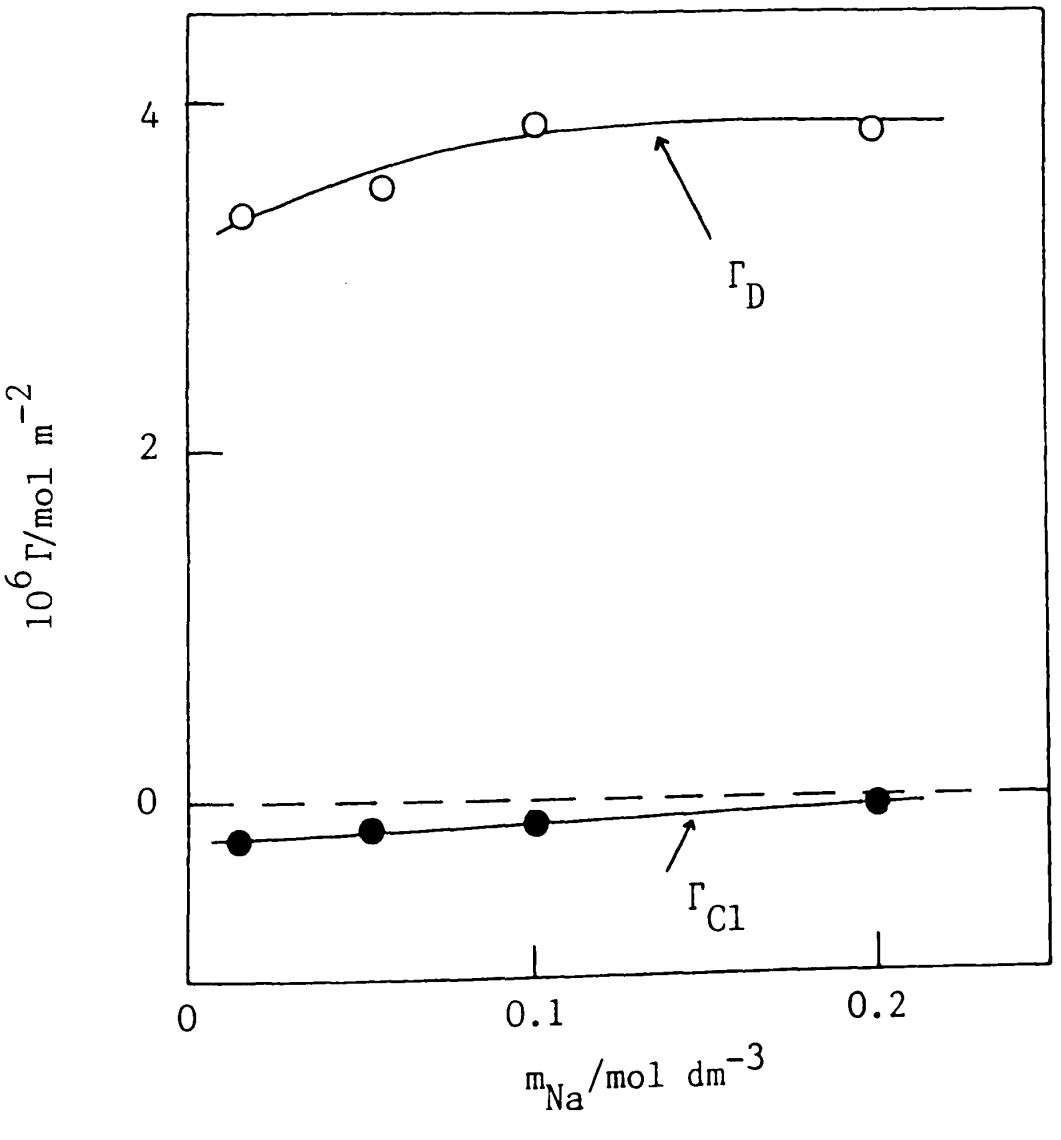

that $d\gamma_c/dlnm_{Na}$ will not be zero, and hence γ_c is not expected to pass through a minimum value. This is as observed in Figure 9.1b.

It is possible to calculate Γ_{Cl} using equation 4.17 from a knowledge of $d\gamma_c/dlnm_{Na}$, Γ_D and $dlncmc/dlnm_{Na}$. Values of Γ_{Cl} obtained in this way are shown in Figure 9.2b as a function of the salt concentration. As expected they are small (relative to Γ_D) and negative. Reassuringly, the Γ_{Cl} values obtained in this way are similar in magnitude to those determined by Tajima using a different approach.[43]

9.3 Effects of cosurfactant

9.3.1 Minima in γ_c with respect to alkanol concentration

Overbeek *et al.*[32] have reported a limited set of γ versus lnm_D data for the SDS/cyclohexane/0.3M NaCl system in the presence of pentanol as cosurfactant. Values of γ_c were not presented but we have determined γ_c in equilibrated systems containing pentanol and a minimum with respect to pentanol concentration is produced (Figure 9.3). Pentanol distributes roughly evenly between aqueous and oil phases so that the concentration (or activity) of cosurfactant is high in both phases around the condition for minimum γ_c. It has been convenient in connection with the thermodynamic analysis presented later however to use a cosurfactant which is at low concentration in at least one phase.

It has been possible by addition of dodecanol to the heptane phase to produce a minimum in γ_c with respect to alkanol

Figure 9.3 Variation of γ_c in the SDS-cyclohexane-aq. 0.3 mol dm^{-3} NaCl system at 30°C with pentanol concentration.

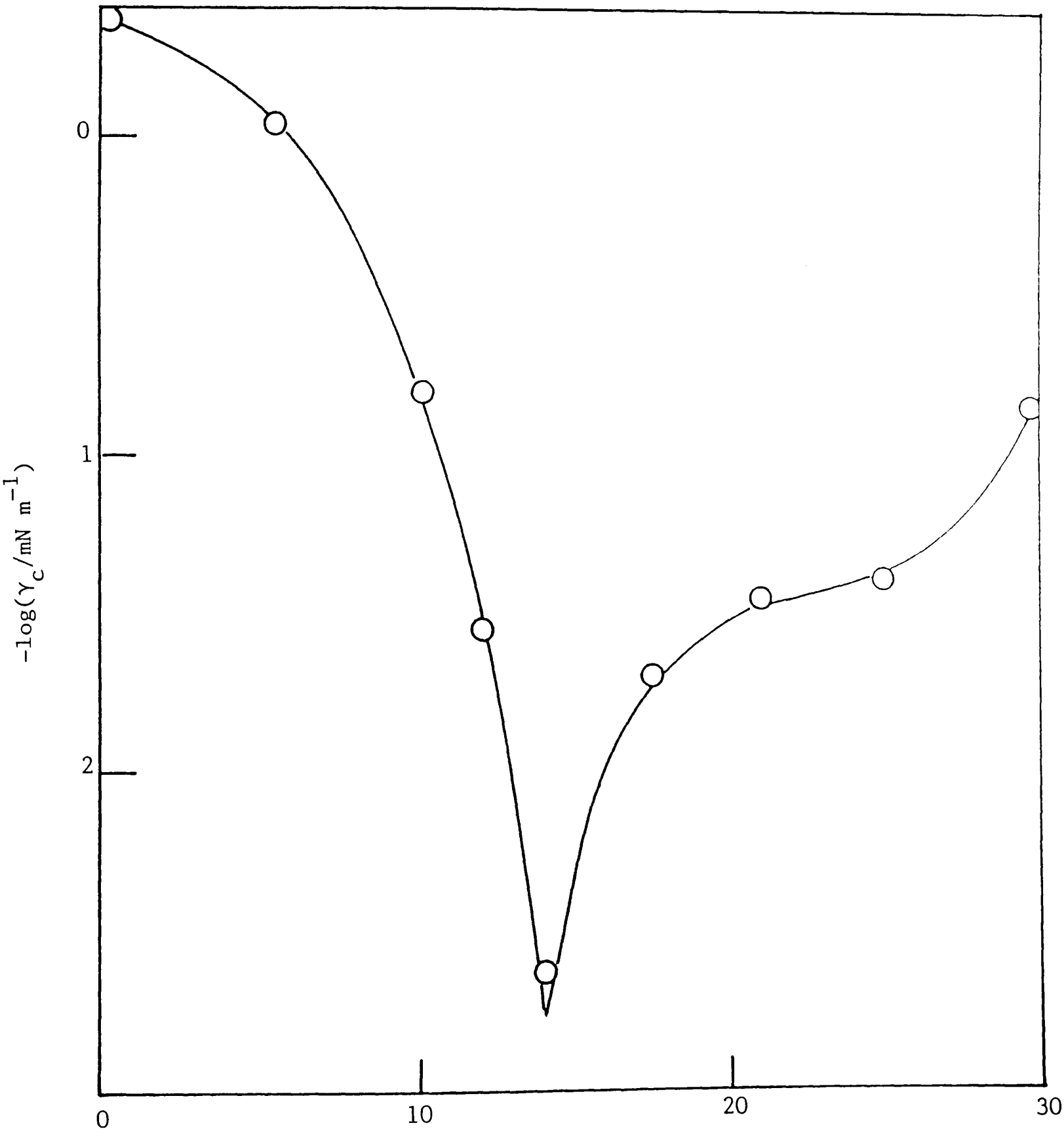

Threee volumes of aqueous phase were brought to equilibrium with one volume of oil phase; the γ_c refer to the equilibrium systems.

concentration, using a high salt concentration (m_s = 0.1 mol dm^{-3}) as shown in Figure 9.4a (open points). The alkanol activity required for minimum γ_c (0.075 mol dm^{-3}) is about the same as that ($\simeq$ 0.08 mol dm^{-3}) in the worst case (i.e. for m_s = 0) using AOT (Figure 8.1b, filled points). It may be that a higher m_s (> 0.1 mol dm^{-3}) would mean a lower dodecanol activity is necessary to produce a minimum though this seems unlikely since A_s ($\equiv a_h$) for SDS is broadly constant for 0.1 < m_s < 0.2 mol dm^{-3} as already seen (Table 9.1).

For the reasons discussed earlier, the concentration of cosurfactant required to give minimum γ_c should be reduced if a strongly penetrating oil is used. A series of experiments at 30°C have therefore been performed using cyclohexane. In the presence of SDS and dodecanol however, tensions were unreproducible and so octanol was subsequently used as the cosurfactant.

Octanol is more soluble in water than is dodecanol and although the solubility is still very low, the oil to water volume ratio in a spinning-drop experiment is very small. We have therefore determined the thermodynamic distribution ratio K(= activity octanol in cyclohexane/activity octanol in 0.3 mol dm^{-3} NaCl) by measuring equilibrium aqueous phase concentrations (assumed equal to activities) tensiometrically. Various concentrations of octanol in cyclohexane were shaken with aqueous phases containing 0.3 mol dm^{-3} NaCl (but no surfactant) in a volume ratio of 1:10. Surface tensions of the equilibrated aqueous phases were determined by the ring method and compared

Figure 9.4a Effects of alkanol activity, a_A, on γ_c in systems containing SDS at 30°C.

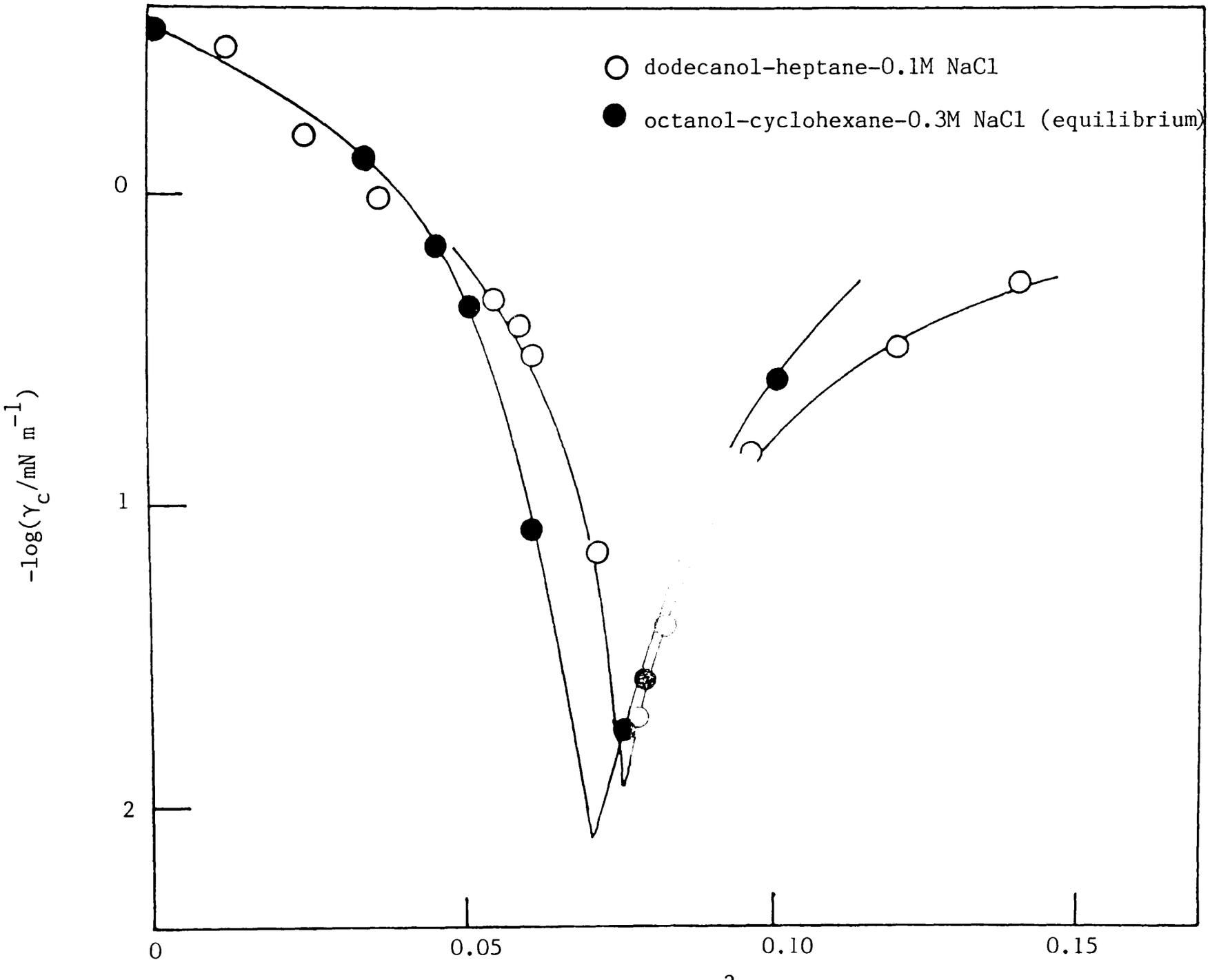

with those from solutions containing known amounts of octanol (which had been saturated with cyclohexane). Oil phase concentrations at equilibrium were then obtained by mass balance and converted to activities using the activity coefficients referred to later. Oil phase activities obtained from a series of distribution experiments are plotted against equilibrium aqueous phase concentrations in Figure 9.5; the plot is rectilinear giving $K \simeq 160$. In Figure 9.4b, γ_c data are shown for the SDS/cyclohexane/0.3 mol dm^{-3} NaCl system as a function of octanol activity in cyclohexane, using both equilibrated and non-equilibrated phases. As seen, the differences are appreciable, but entirely ascribable to octanol distribution subsequent to injection of the cyclohexane phase into the spinning-drop tensiometer when non-equilibrated phases are used.

In the event, the activity of cosurfactant required to produce minimum γ_c in the dodecanol/heptane/0.1 mol dm^{-3} NaCl and the octanol/cyclohexane/0.3 mol dm^{-3} NaCl systems are very similar (Figure 9.4a). This presumably arises since dodecanol is a more effective cosurfactant than octanol (see § 8.2.2) but at the same time cyclohexane is a more penetrating oil than heptane (see § 7.3). The different salt concentrations used are unlikely to produce any differences since both are high in the context.

9.3.2 *Surfactant distribution and phase inversion*

In systems containing SDS and octanol, it has been confirmed that minimum γ_c with respect to alkanol activity occurs in the

Figure 9.4b Values of γ_c against a_A in SDS-octanol-cyclohexane-aq. 0.3 mol dm^{-3} NaCl systems at 30°C.

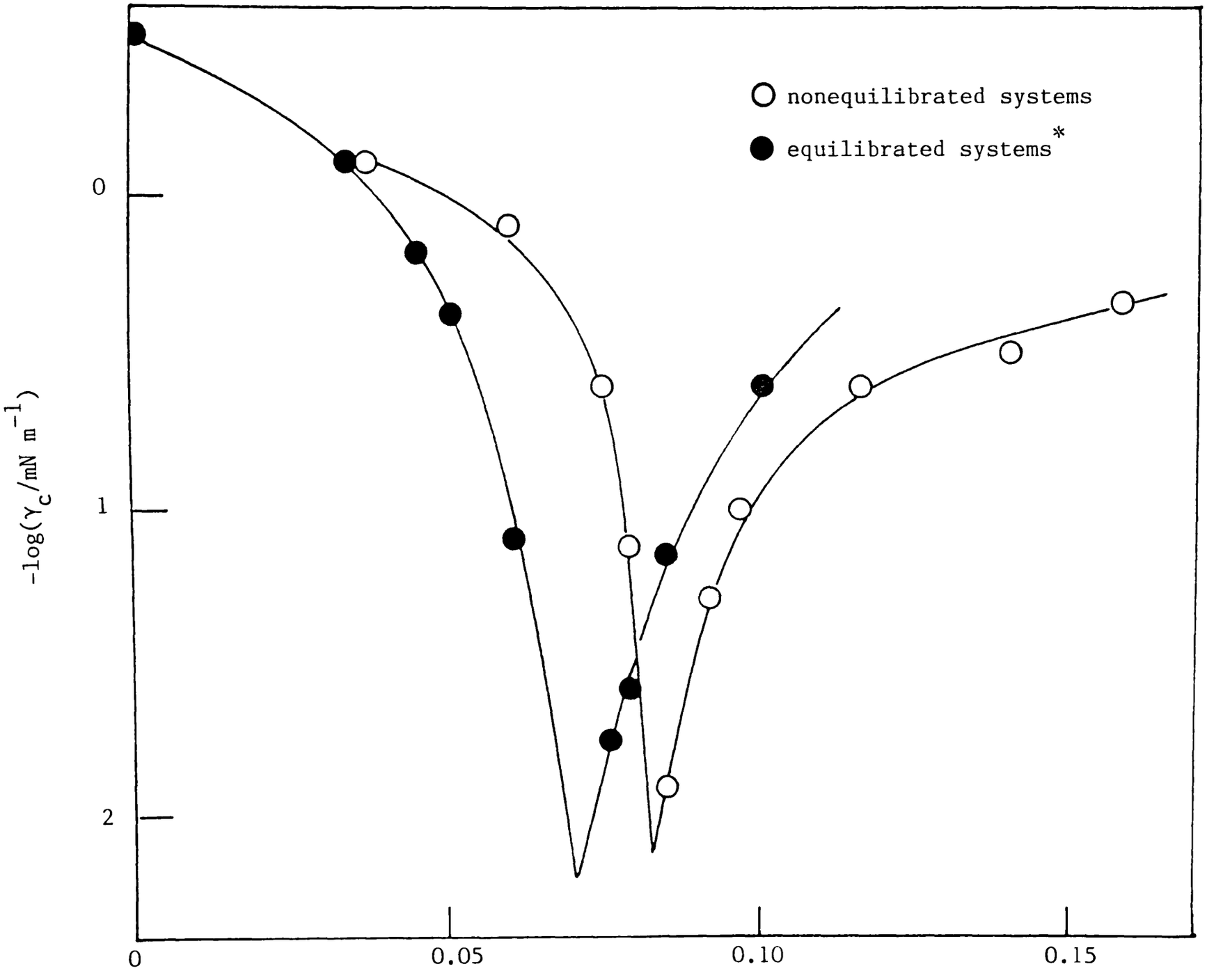

* Two volumes of oil phase (containing cosurfactant) were equilibrated with one of aqueous phase (containing surfactant)

Figure 9.5 Equilibrium distribution of octanol between cyclohexane and aq. 0.3 mol dm^{-3} NaCl at 30°C.

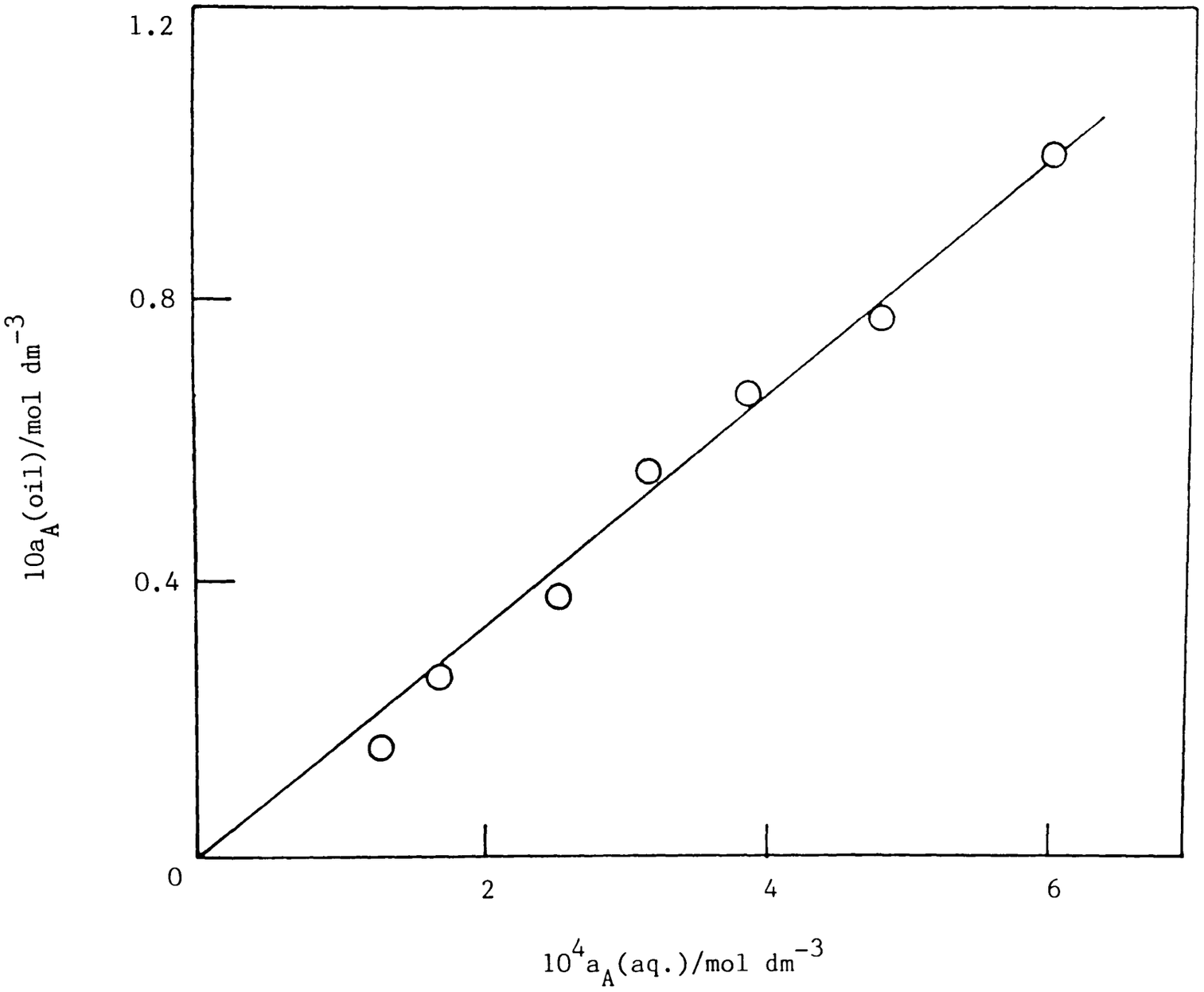

region where there is marked transfer of SDS from the aqueous to the oil phase. In the same region the conductance of the coarse emulsions formed by agitation of the systems falls, indicating a change from water continuous (o/w) to oil continuous (w/o) emulsions (Figure 9.6). All the data shown in Figure 9.6 are for pre-equilibrated phases. In the case of the distribution work one volume of 2×10^{-3} mol dm^{-3} SDS in 0.3 mol dm^{-3} aqueous NaCl was shaken with two volumes of cyclohexane solution containing varying concentrations of octanol. The conductivity data relate to exactly the same system and so a direct comparison may be made.

It is noteworthy that SDS transfers to some extent to the octanol solution in cyclohexane even below its aggregation point (Figure 9.6a) where in a system without alkanol it would be entirely in the aqueous phase. We attribute this to a mixed solvent effect since alkanol concentrations are quite high. This has meant that in measuring tensions (including those below the c.m.c.) all systems had to be pre-equilibrated and equilibrium SDS concentrations in the aqueous phase determined (see later). A further observation in connection with Figure 9.6a is that in the (broad) region where the aqueous phase SDS concentration is falling a third phase also forms.

9.3.3 *Determination of activity coefficients*

There are strong deviations from ideal solution behaviour in solutions of alkanols in nonpolar solvents, even at high dilution, as result of auto-association of alkanol through

Figure 9.6a Distribution of SDS and emulsion conductance as a function of (initial) octanol concentration in cyclohexane at 30°C.

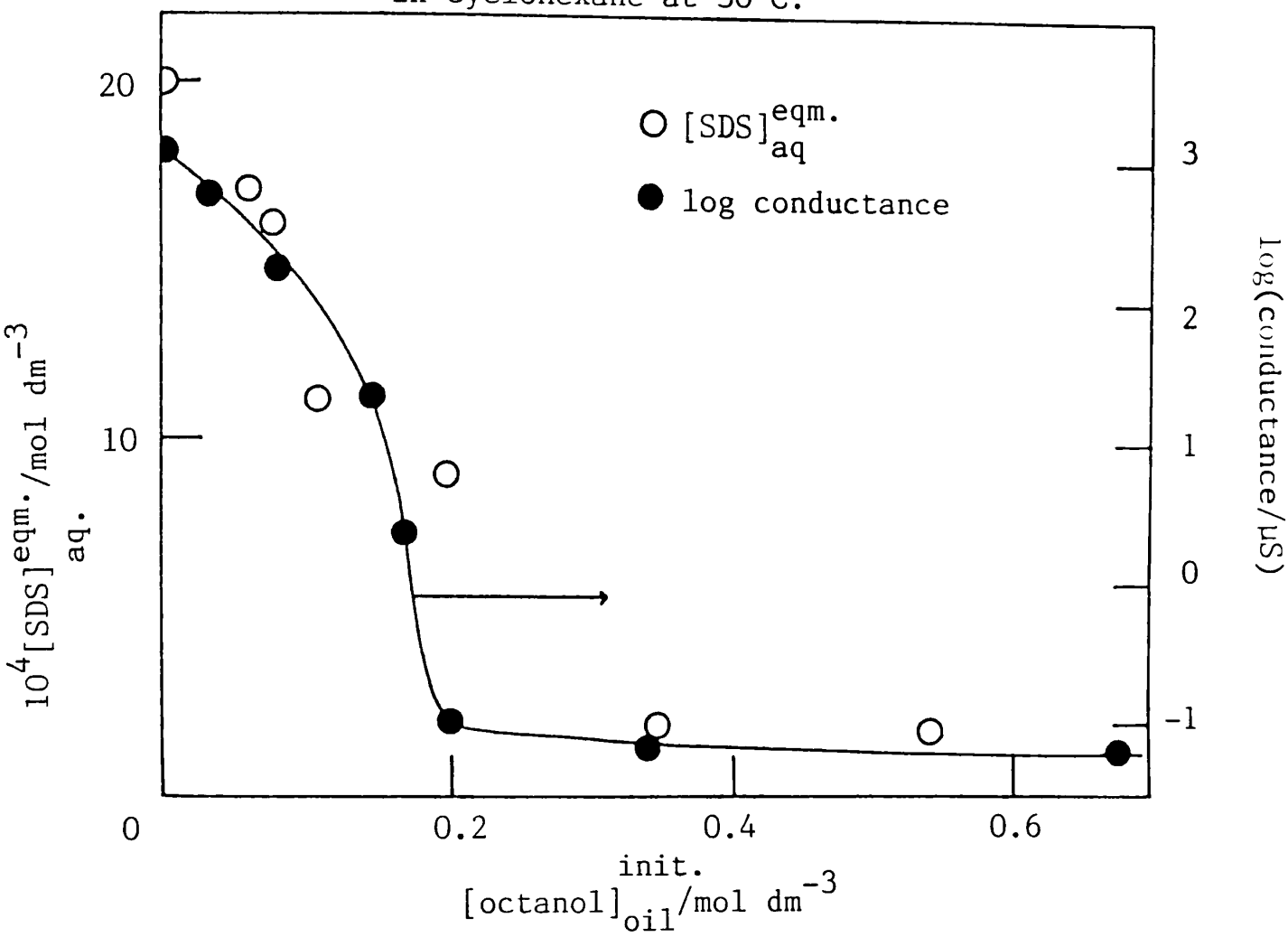

Figure 9.6b Tensions, γ_c and emulsion conductance as a function of (initial) octanol concentration in cyclohexane at 30°C.

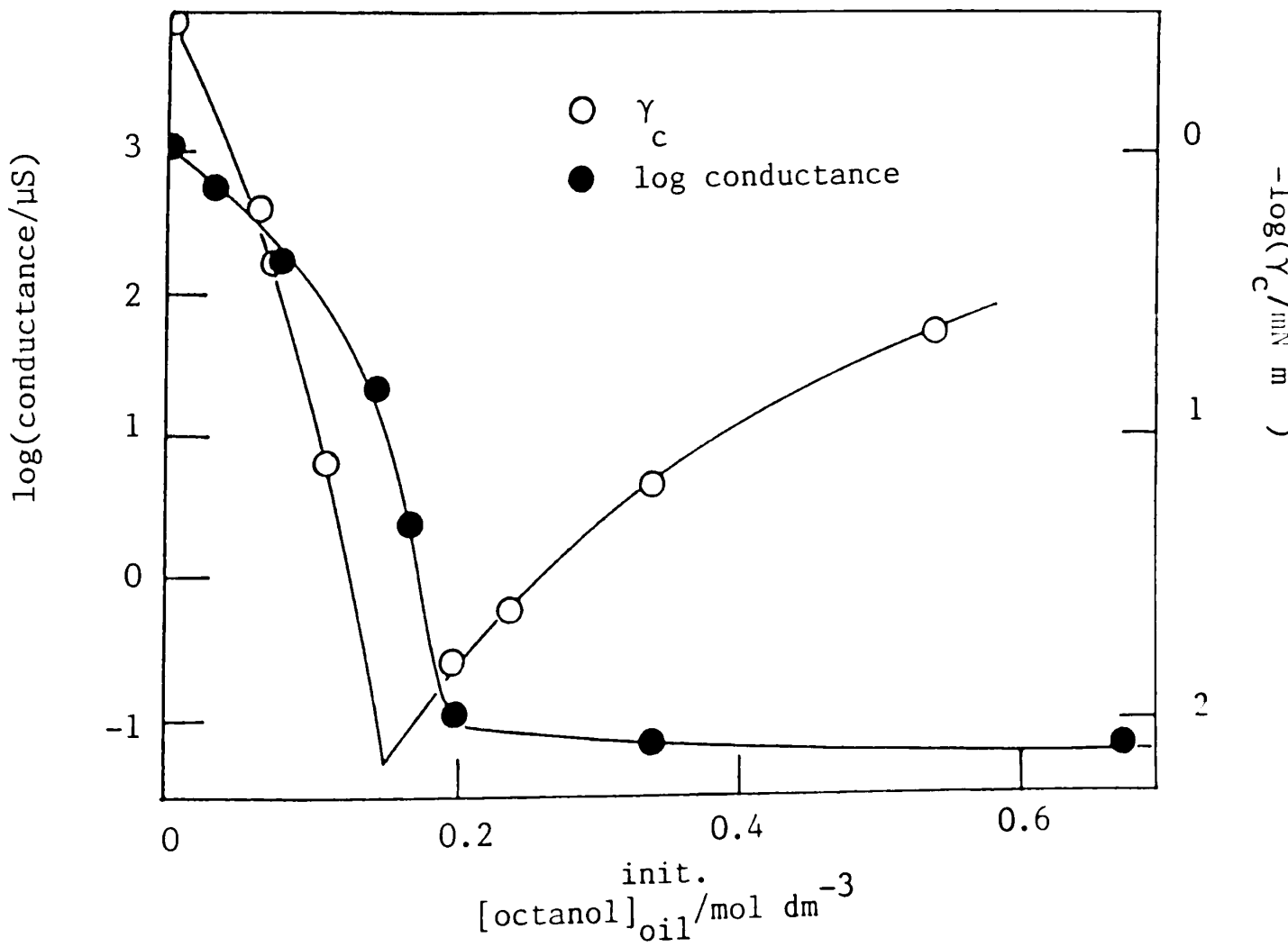

intermolecular hydrogen bonding.[164] Here an infrared absorbance method has been used to determine activity coefficients, as described in detail elsewhere.[164] The rational activity coefficient, f_2, of solute 2 in solvent 1 is defined by

$$\mu_2 = \mu_2^{\ominus} + RT\ln f_2 x_2$$

where μ_2 is the chemical potential and $\mu_2^{\ominus}$ the standard chemical potential of the solute, and x_2 its mole fraction. There is a choice of two reference states (i.e. states where $f_2 = 1$). In the present work, where dilute solutions are studied, the unsymmetrical reference state is appropriate. This state is that of an ideal solution at infinite dilution of component 2 in component 1.

In the infrared method the activity coefficient of the solute is measured by the determination of the fraction, α, of monomeric solute molecules present in the solution. It has been shown,[168] using the unsymmetrical reference system, that $\alpha = f_2/f_1$. In dilute solutions $f_1 \rightarrow 1$ (as $x_1 \rightarrow 1$) so that for such a system, to a good approximation, $\alpha = f_2$ and it is assumed that the associated species once formed behave ideally. The absorbance, A', of a solution of alkanol in alkane is related to the molar absorptivity, ε, by[169]

$$A' = \log_{10} (I_o/I) = \varepsilon cd \qquad (9.1)$$

where I_o is the intensity of incident light on a solution of molarity, c, in a cell of path length, d cm, and I is the

intensity of the transmitted light. The fraction, α, of monomeric species in a solution at a molarity c for molecules which associate through the OH group is given by [169]

$$\alpha = \varepsilon/\varepsilon_o \qquad (9.2)$$

where ε_o is the molar absorptivity of the OH group in the monomeric species and ε is the apparent molar absorptivity determined by use of equation 9.1.

Absorbances at 1.3605 μm ($A'_{1.36}$) of solutions of octanol in cyclohexane at 30°C were measured using a Pye Unicam SP 700 spectrophotometer, fitted with a circulating thermostat, and 2 cm path length infrasil silica cells. The wavelength 1.3605 μm corresponds to the maximum absorption of the OH group in unassociated alkanol molecules (monomers) in cyclohexane. A broad band at higher wavelengths is due to OH groups involved in H-bonding and is absent in dilute solutions. By determining $A'_{1.36}$ at low alkanol concentrations (< 0.02 mol dm^{-3}) where absorbance is a linear function of concentration, ε_o can be determined.

Values of f_2 have been obtained using absorbance data in Figure 9.7a; from these data (see inset where results for dodecanol in octane at 30°C[164] are shown for comparison) a value of ε_o of 1.72 $dm^3\ mol^{-1}\ cm^{-1}$ is obtained. The activity coefficients, which are well represented by

$$f_2 = 0.8409 \exp(-7.159\ c) + 0.17$$

Figure 9.7a Absorbance, $A'_{1.36}$, as a function of octanol concentration in cyclohexane at 30°C.

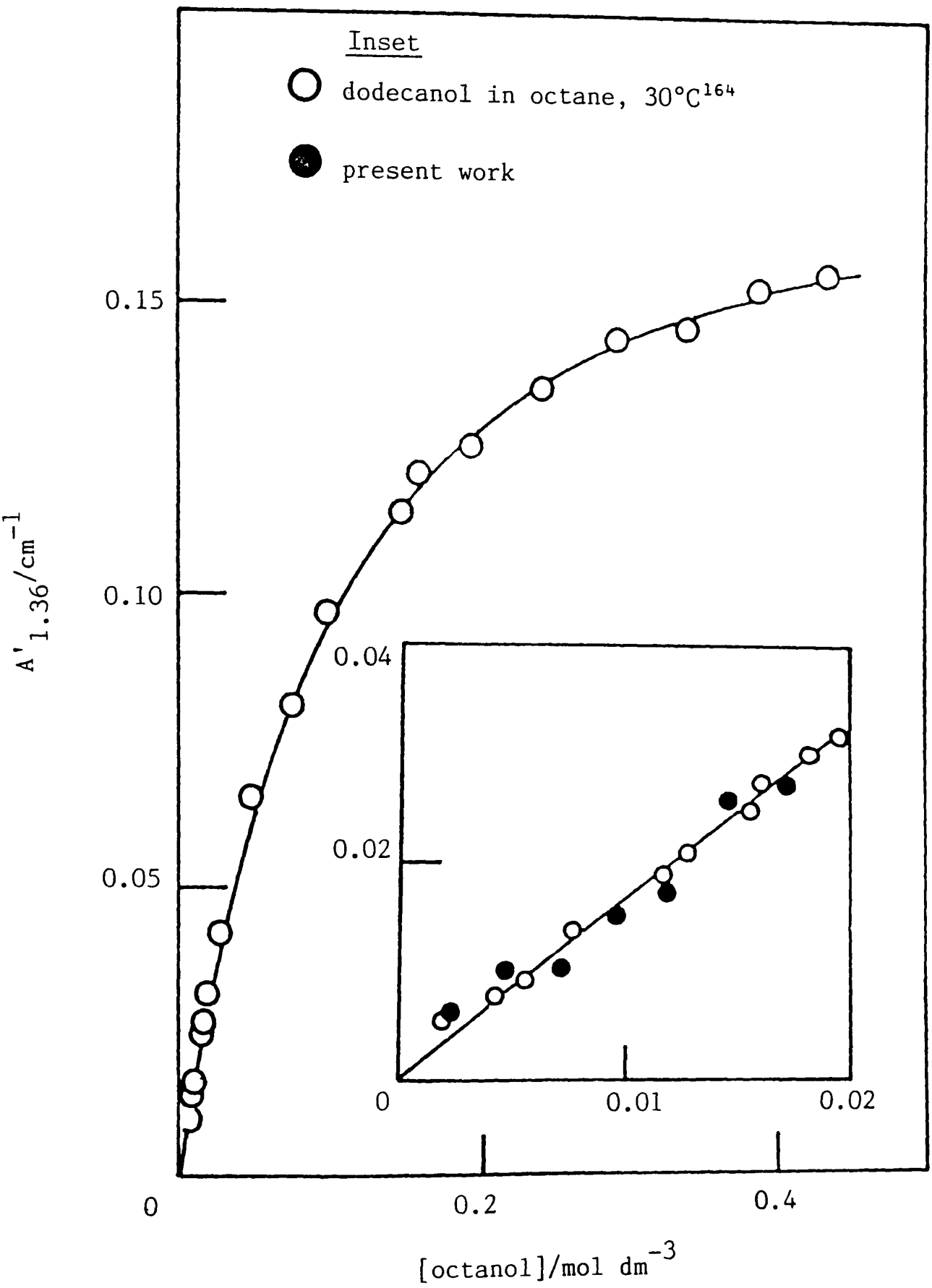

for octanol concentrations up to 0.5 mol dm^{-3}, are shown in Figure 9.7b together with those for dodecanol in octane. Also indicated are mean ratios of monomer to formal alkanol concentration (equivalent to our $A'_{1.36}/\varepsilon_o c$) for a series of n-alkanols (propanol through to octanol) in isooctane at 25°C obtained by Anderson *et al.*[170] using a vapour pressure method. It appears that f_2 is not very dependent on alkanol chain length or the precise structure of the nonpolar oil. The assumption that $f_1 = 1$ becomes less secure at higher alkanol concentrations and the values of f_2 correspondingly less reliable.

It has been confirmed that f_2 remains unchanged when a 'dry' solution is brought to equilibrium with excess water. Subsequently, we further assume that the presence of surfactant aggregates does not affect f_2 significantly. It is recognised, of course, that in systems of interest some alkanol will be incorporated into the aggregates but the overall alkanol to aggregated surfactant mole ratio is always very high.

9.3.4 Thermodynamic treatment of effect of cosurfactant on γ_c.

It has been shown earlier (§ 8.3.1) that the variation of γ_c with alkanol activity, a_A (= cf_2), is given by

$$\frac{d\gamma_c}{d\ln a_A} = RT\Gamma_D \left(\frac{N_A}{N_D} - \frac{\Gamma_A}{\Gamma_D} \right) \qquad (8.7)$$

where N are average numbers of molecules per aggregate. The ratio N_A/N_D is given by[142]

$$\frac{-d\ln cmc}{d\ln a_A} = \frac{N_A}{N_D} \qquad (8.6)$$

Figure 9.7b Activity coefficients, f_2, as a function of alkanol concentration, m_A.

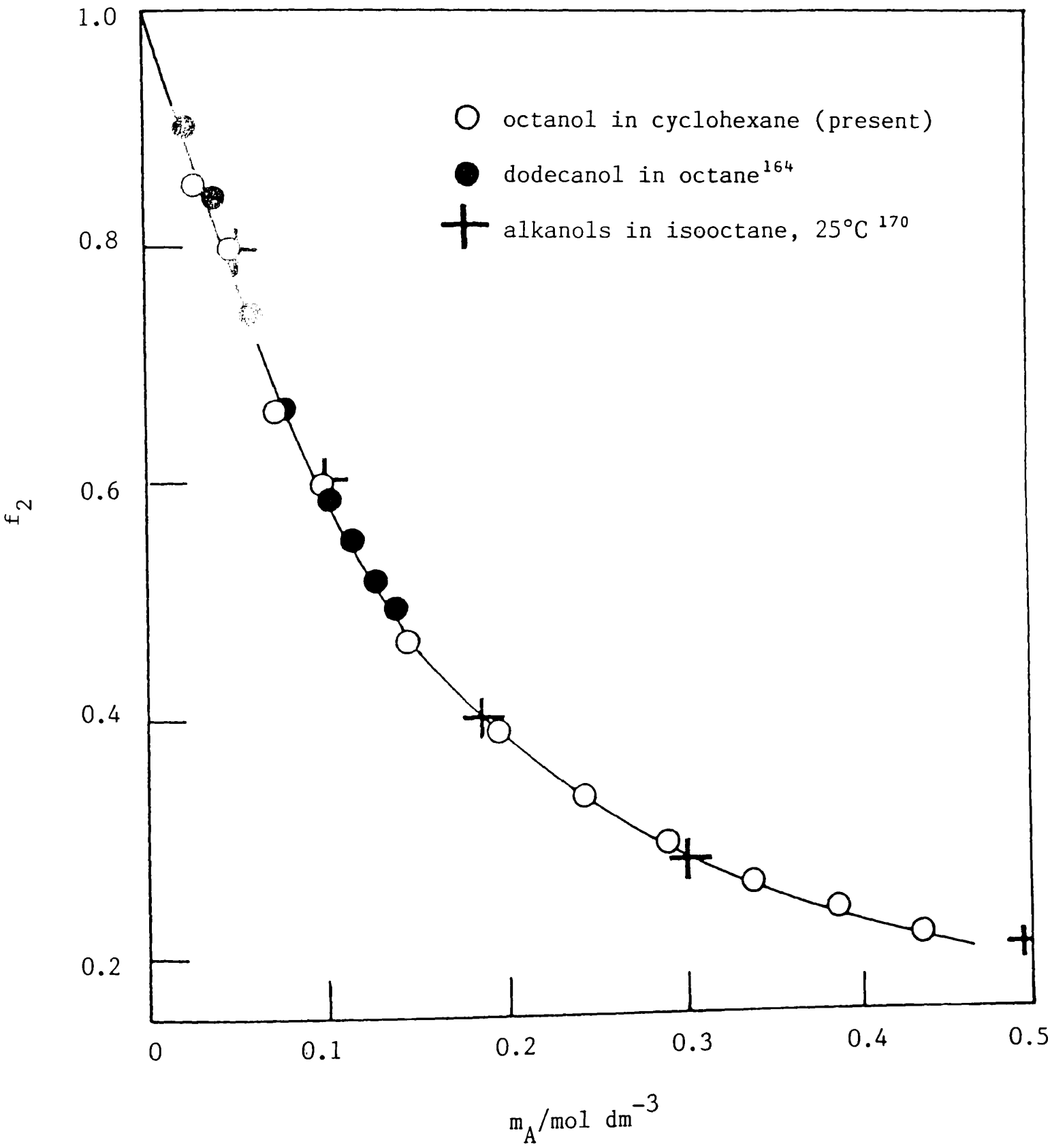

In our systems the aqueous phase is in equilibrium with excess oil phase so the aggregates (when present in the aqueous phase) contain solubilised oil. However, if the chemical potential of the oil remains unchanged with respect to alkanol concentration, equation 8.6 may still be expected to hold, at least when the aggregates are present in the aqueous phase. It is seen (equation 8.7) that minimum γ_c is obtained when interfacial and micellar compositions are equal with respect to surfactant and cosurfactant. A similar conclusion has been arrived at recently by Rosen and Murphy[171] for systems containing two surfactants. If values of $d\ln cmc/d\ln a_A$, Γ_D and $d\gamma_c/d\ln a_A$ are known, Γ_A can be obtained by use of equations 8.6 and 8.7 and hence values of Γ_A/Γ_D calculated as a function of a_A and the value for minimum γ_c interpolated. Alternatively, Γ_A/Γ_D can be calculated using equation 8.7 and compared with N_A/N_D for a_A where aggregates form in the aqueous phase.

In the present work values of the aggregation points (c.m.c.'s) and of Γ_D have been determined tensiometrically. As mentioned (§ 9.3.2) all tension measurements were on equilibrium systems. Two volumes of a fixed concentration of octanol in cyclohexane were equilibrated with one volume of aqueous 0.3 mol dm^{-3} NaCl containing increasing amounts of SDS. The aqueous phase concentration of SDS at equilibrium, $(m_D, aq)eq$, was determined and plots of γ against $\ln(m_D, aq)eq$ for various a_A are shown in Figure 9.8a. Because of the tedious nature of the experiments only a limited number of data points have been obtained, which renders the values of Γ_D calculated from these plots somewhat imprecise.

Figure 9.8a Variation of γ with equilibrium aq. phase concentration of SDS in octanol-cyclohexane-0.3 mol dm^{-3} NaCl systems at 30°C.

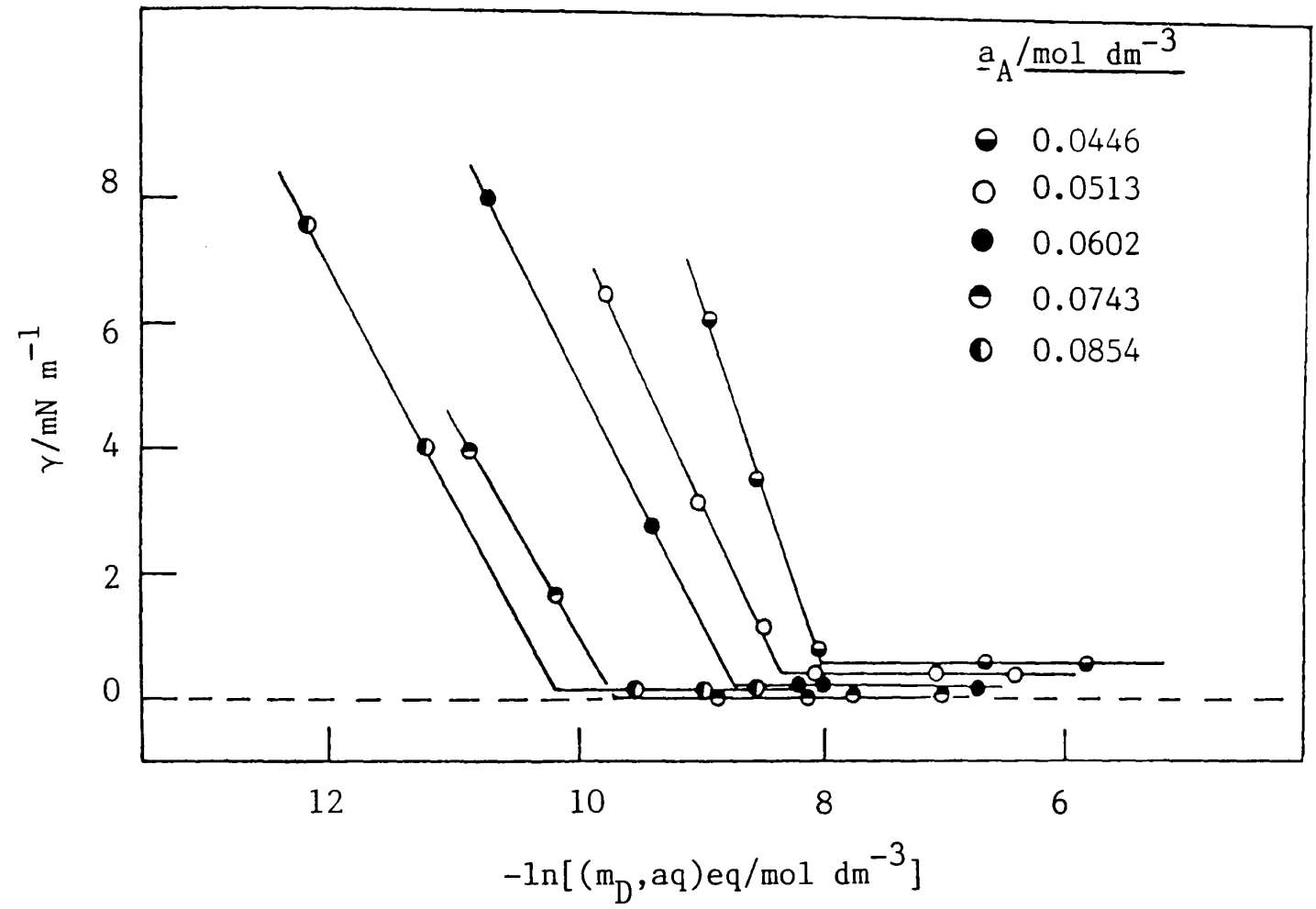

Figure 9.8b Variation of c.m.c. with octanol activity in the same system as in figure 9.8a.

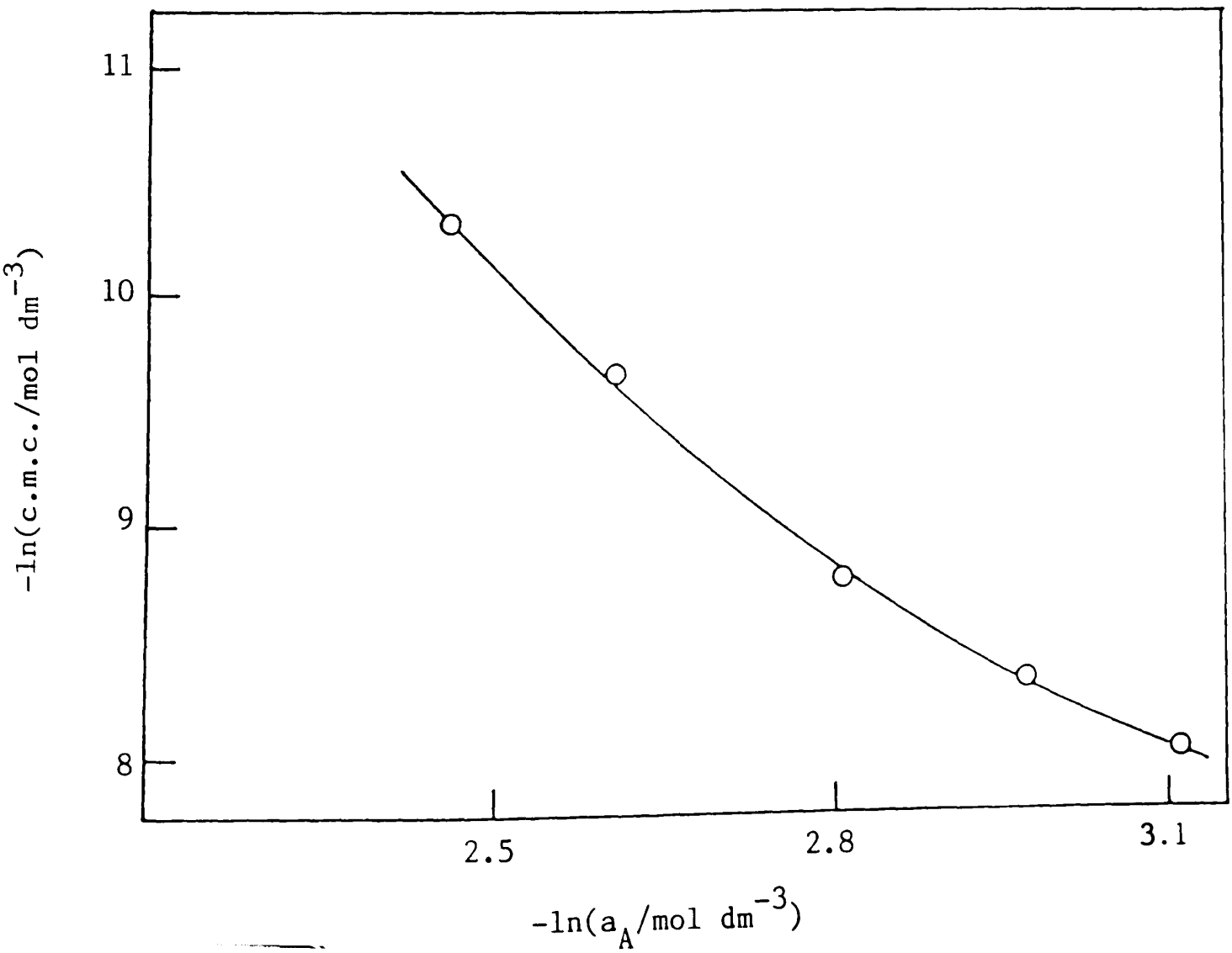

In systems containing AOT, when conditions are such that aggregation occurs in the oil phase, it has been found (§ 3.4.1) that the aqueous phase surfactant concentration remains constant as further AOT is added to the system. In the system containing SDS however, when phase inversion has occurred and SDS is largely in the cyclohexane phase, the equilibrium aqueous phase SDS concentration increases with overall surfactant concentration. The significance of this has not been investigated, but the affect appears to be associated with the presence of fairly high alkanol concentrations. In a system containing AOT and dodecanol the increase in aqueous phase concentration referred to above was not found (§ 8.2.1), but the phase inversion occurred at lower alkanol concentration. Similar effects to those observed here with SDS do however occur with AOT if alkanol concentrations are high enough.

The variation of the c.m.c. (expressed as the equilibrium aqueous phase concentration) with a_A (mol dm^{-3} in oil) is shown in Figure 9.8b and is represented by

$$\ln (cmc/mol\ dm^{-3}) = -103.48 \exp(1.3067 \ln a_A) - 6.162 \quad (9.3)$$

for a_A between 0.045 and 0.085 mol dm^{-3}. Values of Γ_A/Γ_D and N_A/N_D calculated using equations 8.7 and 8.6 together with Γ_D (from the plots in Figure 9.8a) are shown in Figure 9.9 versus a_A. It is clear that the shape of the (log γ_c, a_A) curve (Figure 9.4b) results from only small differences in composition of interface and aggregates. The ratios vary from about 2 to 6

Figure 9.9 Variation of the ratios N_A/N_D and Γ_A/Γ_D with a_A in the system containing SDS and aq. 0.3 mol dm^{-3} NaCl in contact with octanol in cyclohexane at 30°C

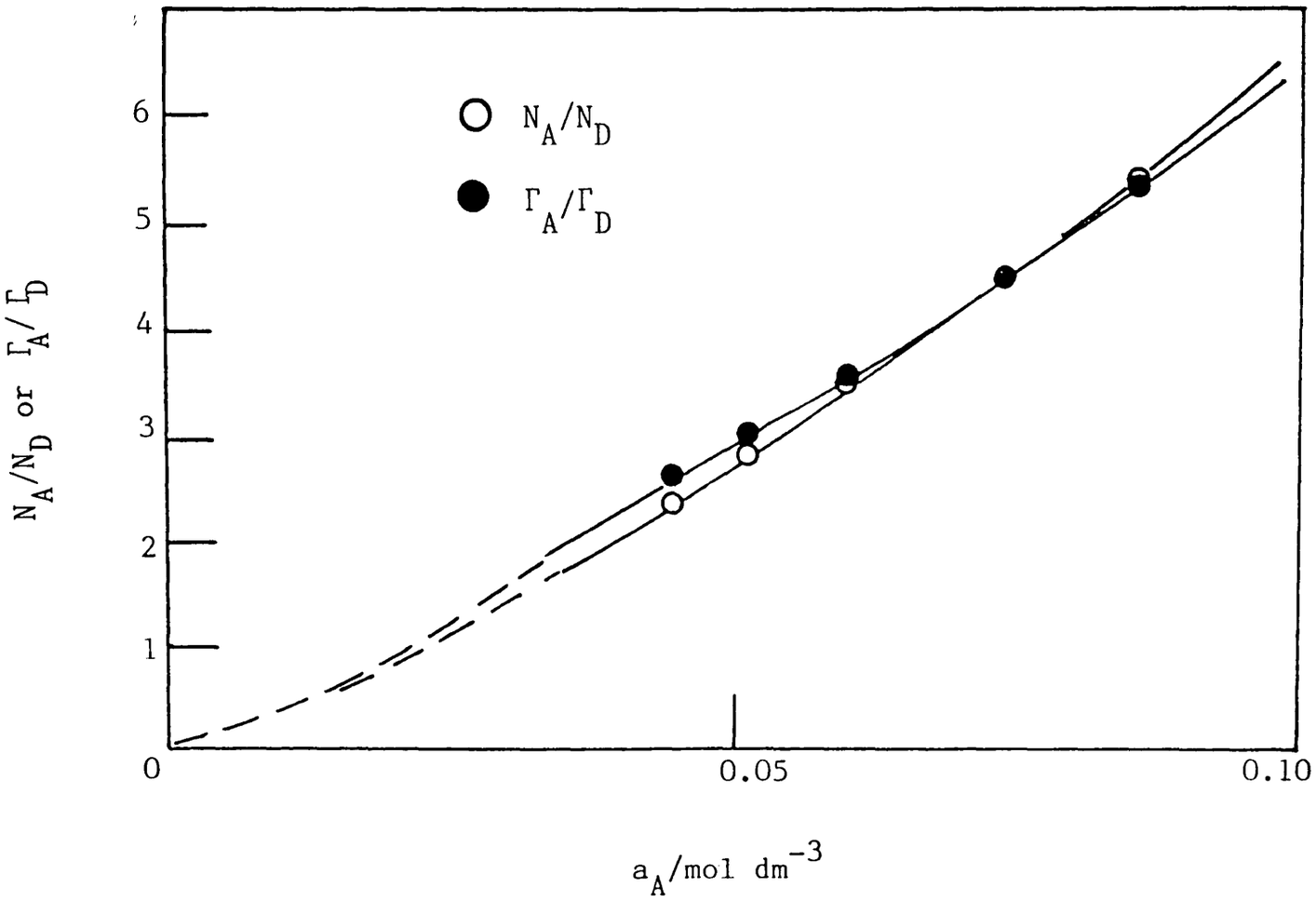

and at minimum γ_c condition, (where $\Gamma_A/\Gamma_D = N_A/N_D$) it is about 4.2 octanol molecules to 1 SDS molecule, as compared to the corresponding ratio, 0.36, in the AOT/heptane/0.017 mol dm^{-3} NaCl system containing dodecanol (§ 8.3.2). Although dodecanol is more effective in lowering γ_c than is octanol (§ 8.2.2) the large difference in the two ratios is undoubtedly a result of differences in the structure of the two surfactants. Aerosol OT is twin-tailed and at m_s = 0.017 mol dm^{-3}, a_c and a_h are close ($a_h \equiv A_s \simeq 0.83$ nm^2, $a_c \simeq 0.72$ nm^2 from Figure 3.13). In the case of SDS, a_h at m_s = 0.3 mol dm^{-3} is expected to be $\simeq 0.44$ nm^2 (Table 9.1) whereas a_c, although unknown, is presumably considerably less and around 0.25 nm^2.[172]

The values obtained for Γ_A/Γ_D can be shown to be reasonable as follows. At minimum γ_c, the area A_s per SDS molecule is approximately 1.15 nm^2 (from data in Figure 9.8a) and $\Gamma_A/\Gamma_D \simeq 4$. As seen, the limiting area of an SDS molecule (in the absence of alkanol) at high salt concentration is approximately 0.44 nm^2 (Table 9.1). Hence the cross-sectional area of an octanol molecule at the interface is calculated to be (1.15 - 0.44)/4 = 0.18 nm^2, which appears to be realistic. The area per octanol molecule, A_A, is equal to 1.15/4 $\simeq$ 0.29 nm^2; Overbeek *et al.*[32] quote a corresponding value for a pentanol molecule (in an otherwise equivalent system) of 0.30 nm^2.

Chapter Ten

CHAPTER 10

SUMMARY AND CONCLUSIONS

The surface and colloidal properties of various oil + water + surfactant systems have been investigated and the data have been analysed both in terms of the effective molecular geometry of the surfactant molecules and by means of thermodynamics. The results obtained may be conveniently summarised as follows:

(1) In systems containing oil, aqueous NaCl and AOT, very low interfacial tensions, γ, can be attained. For fixed temperature (T) and salt concentration (m_s), γ falls as the AOT concentration increases and levels off at a value of γ_c at a concentration (c.m.c.) corresponding to the onset of surfactant aggregation in either the aqueous or oil phase, depending on conditions. It appears possible to achieve very low tensions ($\simeq 10^{-3}$ mN m^{-1}) by simple monolayer adsorption. In the case of nonionic surfactants the c.m.c. condition corresponds to a high concentration in the oil phase and a low concentration in the aqueous phase.

(2) By varying m_s, T, alkane chain length, N, or concentration of cosurfactant, m_A, γ_c can be made to pass through a minimum value. At low m_s, AOT resides in the aqueous phase both below and above the c.m.c. At higher m_s surfactant transfers to the oil phase and leaves the aqueous phase close to the c.m.c.,

but devoid of micelles. At intermediate values of m_s a third, surfactant-rich phase is formed. Surfactant transfer and phase inversion of the coarse emulsions formed by agitation of the systems are observed around conditions corresponding to minimum γ_c. For systems containing NaCl, AOT resides in the oil at low T and in the aqueous phase at higher T. Surfactant resides in the alkane for low N and in the water for larger chain lengths. Transfer of AOT from the aqueous to the oil phase occurs as the concentration of added alkanol (cosurfactant) is increased.

(3) When surfactant passes into an alkane phase it is accompanied by water. The water has been shown to be in the form of reasonably monodisperse droplets, coated with close-packed monolayers of surfactant. Thus, under certain conditions, the equilibrium oil phases are dilute water-in-oil microemulsions. It appears (from P.C.S.) that the area per AOT molecule at the droplet surface is $\simeq 0.50$ nm^2, whereas at a plane surface (at high m_s, with heptane as the oil) it is 0.72 nm^2. The droplets have hydrodynamic radii in the range 2-20 nm and so the surfaces are highly curved, and the difference in areas is thought to be due to the 'wedge' shape of the AOT molecule. Under conditions where the surfactant is in the water phase above the c.m.c., the associated surfactant is presumably in the form of aggregates swollen by the solubilisation of alkane i.e. an oil-in-water microemulsion exists. The curvature of the surface containing surfactant is opposite in aqueous and oil phases. The size of aggregates increases as the condition for minimum γ_c is approached.

(4) The way in which surfactant aggregates in oil-water systems change as phase inversion is approached has been discussed in terms of surfactant molecular geometry. It is believed that the minimum γ_c occurs when, for the surfactant in the monolayer, the effective cross-sectional area, a_c, of the hydrophobic chain becomes equal to that, a_h, of the hydrophobic headgroup. Addition of salt reduces a_h due to screening of lateral electrical repulsion between headgroups. Increasing T probably results in a decrease in a_c as the surfactant chains become more flexible and elongate. Penetration of alkane into the chain region of surfactant monolayers is greater the smaller N so that the presence of small alkanes induces w/o microemulsion formation. In systems containing cosurfactants, minimum γ_c is believed to occur when mean a_h and mean a_c are equal. The effect of cosurfactant (having the property $a_c > a_h$) is to increase the mean a_c for the mixed film relative to mean a_h for the film.

Studies of interfacial tension have yielded values for the area per surfactant molecule, A_s, in a saturated monolayer as a function of m_s and N. It is argued that at low m_s, $A_s = a_h$. As m_s is increased, A_s falls to a limiting value A_s^{ℓ} which is equal to a_c. The value of a_c falls as N increases. Under conditions where $a_h \simeq a_c$, the surfactant resides mainly in a third phase which one might loosely regard as an infinitely large surfactant aggregate, in which monolayers exhibit almost zero net curvature. Preliminary results indicate that aromatic oils like toluene penetrate surfactant chains to a greater extent than do n-alkanes.

Future work into the behaviour of mixed oils (i.e. aliphatic and aromatic) should highlight the reasons for the differing degrees of penetration.

(5) A thermodynamic treatment of the occurrence of minima in γ_c with respect to salt concentration, temperature and cosurfactant concentration has been developed. The variation in γ_c with m_s is in part a consequence of the way in which the c.m.c. and the surfactant activity coefficients change with salt concentration. The minimum γ_c is seen to result when the effective degree of dissociation of surfactant in the micelle (α_m) and at the oil-water interface (α_p) are equal and close to zero. This may occur when the curvature of the micelle surface is negligible. At the temperature corresponding to a minimum tension the entropy change on transferring a mole of surfactant (and other associated species) from solution to the plane oil-water interface is equal to the entropy of formation of micelles containing a mole of surfactant. A thermodynamic treatment of the effect of cosurfactant demonstrates that minimum γ_c results when the molar ratio of surfactant to cosurfactant is equal at the plane oil-water interface and in mixed agregates, as expected from the simple geometrical picture.

(6) In oil + water systems containing the single chain surfactant SDS, salt alone cannot yield a minimum in γ_c, nor is γ_c very low. Addition of cosurfactant (octanol) to systems

containing SDS above its c.m.c. can however result in very low values of γ_c and also a minimum as m_A is varied. The effects are discussed in terms of the effective molecular geometry of surfactant and cosurfactant and the composition of interfacial monolayers.

Appendices

APPENDIX I

SALT EFFECTS

Surface tensions vs AOT concentration at 25°C

(a) $m_s = 0$

$\ln(m_D/M)$	γ/mN m^{-1}	$\ln(m_D/M)$	γ/mN m^{-1}
-15.3	70	-14.6	68.1
-13.9	65.4	-13	61.5
-12.3	58.2	-11.7	55.5
-11.1	53.2	-10.7	51.7
-10	48	-9.45	45.8
-8.83	42.5	-8.4	40.3
-7.71	36.5	-7.48	35.1
-7.15	33.3	-6.9	32.3
-6.69	31.1	-6.53	30.3
-6.26	28.8	-6.15	28.2
-6.1	28.1	-5.4	28
-4.8	28	-4.5	28

(b) 0.0256M

-13	55.7	-11.8	52
-10.7	45.5	-9.91	41.6
-9.09	37.4	-8.76	35.3
-8.5	34.2	-8.4	33.5
-8.22	32.5	-7.93	30.7
-7.71	29.5	-7.3	27.4
-7.01	25.9		

$\ln(m_D/M)$	γ/mN m^{-1}	$\ln(m_D/M)$	γ/mN m^{-1}
-6.6	25.4	-6.45	25.4
-6.25	25.4	-6.14	25.4

(c) 0.0308M

-9.54	39.8	-9.05	36.8
-8.54	34.1	-8.06	31.1

(d) 0.0376M

-10.1	41.4	-9.45	38.2
-8.82	34.7	-8.17	30.9

(e) 0.0427M

-10.3	42.4	-9.62	38.8
-8.95	35	-8.31	31.2

(f) 0.0513M

-10	38.8	-9.79	37.6
-9.6	36.5	-9.32	35
-9.13	34	-8.98	33.1
-8.65	31.3	-8.45	30.2
-8.24	29.2	-8.06	28.1
-7.85	27		

$\ln(m_D/M)$	γ/mN m^{-1}	$\ln(m_D/M)$	γ/mN m^{-1}

(g) 0.060M

-10.2	40.5	-9.6	37.3
-9.07	34.2	-8.52	30.9

(h) 0.0684M

-10.3	40.4	-9.75	37.5
-9.17	34.3	-8.64	31.1

(i) 0.0855M

-10.4	40.4	-9.91	37.5
-9.37	34.3	-8.83	31.2

(j) 0.1026M

-15.3	61	-13	51.7
-11.9	46.3	-10.7	40.2
-10	36.7	-9.6	34.6
-9.32	32.8	-9.09	31.5
-8.91	30.6	-8.76	30
-8.62	29	-8.5	28.3
-8.4	27.8	-8.22	26.7
-8.1	26	-7.98	25.4
-7.7	25.3	-6.8	25.4

(k) 0.1367M

-11.3	43	-10.4	38.2
-9.71	34.2	-8.8	28.7

AOT air-solution, 25°C

$\ln(m_{Na}/M)$	$\ln(cmc/M)$	$\ln(m_{Na}/M)$	$\ln(cmc/M)$
-3.63	-6.84	-3.26	-7.19
-3.14	-7.28	-2.96	-7.45
-2.81	-7.58	-2.67	-7.62
-2.45	-7.83	-2.27	-8.04

m_s/M	$A_s/\mathring{A}^2$ molecule^{-1}	m_s/M	$A_s/\mathring{A}^2$ molecule^{-1}
0	140	0.0257	78.5
0.0257	79.6	0.0308	73
0.0376	75.6	0.0428	74.3
0.0513	76.4	0.0599	71.6
0.0684	73.9	0.0856	72.5
0.103	75.3	0.137	72.4

Heptane-solution tensions vs [AOT] at 25°C

(a) m_s = 0.00427M

$\ln(m_D/M)$	γ/mN m^{-1}	$\ln(m_D/M)$	γ/mN m^{-1}
-9.88	22	-9.15	18
-8.61	15	-8.06	12.1
-7.61	9.45	-7.18	6.9
-6.71	4.2		

(b) 0.00855M

-9.92	19	-9.3	15.8
-8.63	12.4	-8.08	9.9
-7.72	8.1	-6.93	4

$\ln(m_D/M)$	γ/mN m^{-1}	$\ln(m_D/M)$	γ/mN m^{-1}

(c) 0.0171M

-10.4	19.8	-9.7	16.6
-9.21	14	-8.76	11.6
-8.12	8.2	-7.8	6.6
-7.39	4.5		

(d) 0.0256M

-11	20.9	-10.7	19.2
-10	15.5	-9.91	15
-9.5	12.7	-9.09	10.6
-8.76	8.8	-8.5	7.4
-8.4	6.9	-8.22	5.9
-8	4.8	-7.93	4.4
-7.65	2.7	-7.3	1
-6.85	0.0562	-5.51	0.0561

(e) 0.0513M

-12.3	25.2	-12	23.5
-11.6	21.5	-11.4	20.2
-11	18.1	-10.9	17.8
-10.4	15	-10	12.6
-9.83	11.8	-9.6	10.2
-9.32	8.9	-9.09	7.5
-8.86	6.2	-8.62	5.1
-8.4	3.6	-8.17	2.4
-8.05	1.72	-8.03	1.51
-7.6	0.00067	-7.15	0.00075
-7	0.0007	-6.55	0.0006
-6.2	0.00058	-5.89	0.0007
-5.65	0.00081		

$-\ln(m_D/M)$	γ/mN m^{-1}	$-\ln(m_D/M)$	γ/mN m^{-1}
(f) 0.0513M			
4.34	0.00076	4.81	0.0008
5.07	0.0005	5.55	0.00068
6.1	0.00041	6.1	0.00053
6.79	0.00071	7.52	0.00089
7.59	0.00073	7.6	0.00067
7.66	0.0008	7.68	0.001
7.71	0.00073		
7.71	0.00067	7.73	0.0011
7.78	0.041	7.79	0.0086
7.8	0.125	7.83	0.25
7.85	0.41	7.87	0.53
7.89	0.75	7.96	1.16
8.03	1.51	8.05	1.72
8.17	2.4	8.4	3.6

$\ln(m_D/M)$	γ/mN m^{-1}	$\ln(m_D/M)$	γ/mN m^{-1}
(g) 0.077M			
-11.7	20.9	-10.6	14.7
-10.3	12.8	-9.55	8.9
-9	5.8	-8.42	2.55

(h) 0.1026M

-13	25.2	-11.9	19.5
-11.1	15.7	-10.7	13.2
-10.3	11.2	-10	9.2
-9.6	6.85	-9.32	5.15
-9.09	4	-8.91	3.02
-8.62	1.43	-8.41	0.132
-7.71	0.128		

AOT/heptane/NaCl/25°C

$\ln(m_{Na}/M)$	ln(cmc/M)	$\ln(m_{Na}/M)$	ln(cmc/M)
-3.64	-7.18	-3.36	-7.41
-2.96	-7.76	-2.45	-8.2
-1.99	-8.59		

AOT/heptane/no salt/25°C

$\ln(m_D/M)$	γ/mN m^{-1}	$\ln(m_D/M)$	γ/mN m^{-1}

(a) Sigma

-10	28.8	-9.45	24.5
-8.83	20.5	-8.4	16.2
-7.71	11.6	-7.15	7.77
-6.7	4.44	-6.53	3.25
-5.8	2.49	-4.83	2.57

(b) Purified Fluka

-11	36.2	-10.3	31
-9.22	23	-8.5	17.8
-7.42	9.78	-7.3	8.78
-6.7	4.23	-6.09	2.57
-5.54	2.49	-5.19	2.48

(c) Unpurified Fluka

-11.1	26.5	-10.7	25.2
-9.24	17.1	-8.47	13.6
-7.48	7.8	-6.9	4.5
-6.53	1.97	-6.3	2.18
-5.4	2.52		

Effect of m_s on γ_c for AOT/heptane/25°C

m_s/M	$\gamma_c/mN\ m^{-1}$	m_s/M	$\gamma_c/mN\ m^{-1}$

(a) Nonequilibrated (clear aqueous)

0.015	0.19	0.0257	0.0622
0.0318	0.0282	0.0349	0.0314
0.0371	0.0115	0.0394	0.0108
0.0424	0.00467	0.045	0.00149
0.045	0.00165	0.0476	0.00034
0.0477	0.00027	0.0504	0.001
0.0513	0.00098	0.053	0.0045
0.0583	0.009	0.0601	0.0157
0.0636	0.02	0.0684	0.0254
0.077	0.0482	0.103	0.136
0.103	0.123		

(b) Nonequilibrated (turbid aqueous)

0.0416	0.0055	0.0454	0.00133
0.0491	0.00019	0.0506	0.00089
0.0544	0.007		

m_s/M	$\gamma_c/mN\ m^{-1}$	m_s/M	$\gamma_c/mN\ m^{-1}$

(c) Equilibrated

0.0171	0.253	0.0318	0.039
0.0342	0.02	0.0371	0.0178
0.0424	0.0031	0.0477	0.00032
0.0504	0.00087	0.0513	0.001
0.053	0.0051	0.0583	0.0136
0.0636	0.0187	0.0685	0.0292
0.0856	0.0751	0.103	0.124
0.12	0.168	0.12	0.166

(d) Surface laser light scattering technique

0.02	0.252	0.03	0.0538
0.04	0.0122	0.05	0.00191
0.06	0.0151	0.07	0.0355
0.08	0.0743	0.09	0.115

Tensions vs DHBS concentration at 25°C

$\ln(m_D/M)$	$\gamma/mN\ m^{-1}$	$\ln(m_D/M)$	$\gamma/mN\ m^{-1}$

(a) $m_s = 0$ (air)

-9.31	51.7	-8.98	49.6
-8.62	47.3	-7.92	42.7
-7.7	41	-7.46	39.4
-7.24	37.7	-7.01	36.3
-6.67	34.2	-6.54	33
-6.32	31.5		

$\ln(m_D/M)$	γ/mN m^{-1}	$\ln(m_D/M)$	γ/mN m^{-1}

(b) 0.0513M (air)

-13.2	60	-11.6	56.4
-10.9	53.7	-9.54	47.7
-9.13	45.2	-8.85	43.8
-8.62	42	-7.52	34.5
-7.23	33.2	-7.01	31.7
-6.83	30.9	-6.67	30
-6.54	29.4	-6.42	28.9
-6.32	28.8	-6.2	28.8

(c) 0.0684M (air)

-10	48.2	-9.76	46.8
-9.31	44	-8.62	40.1
-8.16	37.4	-7.7	34.8
-7.23	32	-6.83	29.6

(d) 0.0513M (heptane)

-13.2	37.5	-11.6	30.1
-10.9	25.5	-10.2	21.4
-9.54	17.8	-9.13	15.1
-8.84	13.4	-8.62	12.2
-7.92	7.7	-7.52	5.15
-7.23	3.55	-7.01	2.1
-6.83	0.12	-6.54	0.116
-6.32	0.111		

(e) 0.0684M (heptane)

-10	17	-9.76	15.7
-9.31	13.2	-8.91	11.3
-8.62	9.4	-8.16	6.85
-7.7	3.8	-7.32	1.8

DHBS/NaCl/25°C/(a) heptane

m_s/M	γ_c/mN m^{-1}	m_s/M	γ_c/mN m^{-1}
0.005	0.118	0.0075	0.0465
0.01	0.032	0.0125	0.0213
0.015	0.0102	0.0175	0.00923
0.02	0.0092	0.025	0.03
0.03	0.042	0.035	0.054
0.04	0.069	0.05	0.113
0.0513	0.113	0.06	0.132
0.0609	0.137	0.0684	0.157
0.0717	0.171	0.0723	0.183
0.08	0.196	0.084	0.217
0.0856	0.213	0.101	0.267
0.103	0.265	0.117	0.328
0.12	0.346	0.12	0.344
0.141	0.423	0.15	0.451

(b) dodecane

0.01	0.364	0.02	0.152
0.045	0.031	0.0526	0.0265
0.0566	0.026	0.0621	0.0231
0.0674	0.0253	0.0728	0.0274
0.0849	0.0368	0.0978	0.0491
0.118	0.0832		

m_s/M	R	m_s/M	R
0.025	60	0.03	55
0.035	45	0.04	43
0.05	37	0.06	36
0.08	29	0.1	26
0.12	23	0.15	21
0.2	18.3		

DHBS/heptane/25°C

R	r_H/nm	R	r_H/nm
10	2.72	20	4.42
23	4.33	30	5.36
36	5.96	43	7.57
50	7.99	55	8.65
57.3	9.07	60	9.96

γ_c, m_s data for $C_{12}E_5$/nonane/31°C

m_s/M	γ_c/mN m^{-1}	m_s/M	γ_c/mN m^{-1}
(a) nonequilibrated			
0	0.133	0.0856	0.0823
0.171	0.0507	0.342	0.0167
0.513	0.00569	0.684	0.0153
0.856	0.0205	1.03	0.0658
1.35	0.111	1.37	0.134
1.71	0.266		
(b) equilibrated			
0.1	0.0543	0.4	0.00299
0.5	0.00461	0.7	0.0148
1	0.0304	1.3	0.094
1.5	0.19		

APPENDIX II

TEMPERATURE EFFECTS

Effect of T on γ_c for AOT/heptane systems

(a) m_s = 0.0342M

T/°C	$-\gamma_c$/mN m^{-1}	T/°C	$-\gamma_c$/mN m^{-1}
8.2	0.0272	8.5	0.0216
8.6	0.0205	9.45	0.0177
10.2	0.0118	11.8	0.0078
12.3	0.0047	13.9	0.0015
13.9	0.0013	14.1	0.0014
14.6	0.001	14.6	0.001
15.9	0.00145	16	0.0011
16.3	0.0034	16.9	0.0025
17.5	0.0056	18	0.0054
19.1	0.0085	20	0.0089
22.1	0.0197	23.5	0.0254

(b) 0.0513M

8	0.0804	10.4	0.0584
12.4	0.0531	13	0.0456
13.5	0.0445	14.4	0.0385
14.9	0.0402	15	0.033
16.2	0.0248	17	0.0237
19.2	0.0122	19.4	0.0143
19.5	0.0117	21.5	0.00555

T/°C	γ_c/mN m^{-1}	T/°C	γ_c/mN m^{-1}
22.8	0.0024	23	0.0027
23.7	0.00185	23.8	0.0026
24.5	0.00115	25.3	0.0009
27	0.0009	27.7	0.0008
29.8	0.0044	30.7	0.0073
30.9	0.0068	32	0.0178
35.3	0.0444		

(c) 0.0855M

25	0.0751	27	0.0582
30	0.0423	31.3	0.0276
33.1	0.0192	34.9	0.0135
35.2	0.0132	37.2	0.0075
37.3	0.0074	39	0.0054
39.2	0.0051	40.7	0.0037
41	0.0041	42.6	0.0028
42.7	0.0029	44.4	0.0021
45.1	0.0013	47	0.0007
49.4	0.0028	50.2	0.0044
51	0.0066	52.3	0.011
53.5	0.016	54.5	0.0222
55.8	0.0268	57	0.0314
59.5	0.0396		

T/°C	γ_c/mN m^{-1}	T/°C	γ_c/mN m^{-1}

(d) 0.1026M

25	0.126	26.6	0.122
27.9	0.1	29.2	0.0943
30.6	0.0893	34.2	0.0596
37.1	0.0387	41.7	0.0217
43.5	0.0163	45.5	0.0106
47.1	0.0048	52.8	0.0043
55	0.0103	59.5	0.0295

γ_c vs T for m_s = 0.0855M and various [AOT] in octane

(a) wt.% = 1.174

25	0.52	28.7	0.44
31.3	0.41	34.1	0.36
38.5	0.37	41.1	0.37
44	0.37	47.1	0.37

(b) 2.251

25.4	0.036	27.4	0.025
29.6	0.015	31.4	0.0091
33.3	0.0036	35.4	0.0016
37.5	0.0075	38.7	0.0057
40.3	0.0027	42.5	0.01
45.2	0.019	47.7	0.034

(c) 3.241

25	0.036	27	0.026
29	0.017	31	0.011
33	0.0047	35	0.0017
36.8	0.0011	39	0.00067
40.6	0.0045	42.6	0.01
44.8	0.018	47.6	0.028

T/°C	γ_c/mN m^{-1}	T/°C	γ_c/mN m^{-1}

(d) 4.154

24.9	0.04	26.9	0.03
28.8	0.022	31	0.013
33	0.0066	35	0.0024
36.7	0.00065	37.2	0.0004
39.5	0.0017	42	0.011
44.3	0.017	47.1	0.03

(e) 5.000

24.9	0.039	27.1	0.031
29	0.02	31.1	0.011
33	0.005	35.2	0.0021
36.8	0.00037	39.1	0.0015
41.5	0.01	44.2	0.024
47.1	0.041		

Salt scans AOT/heptane/(a) 10°C

m_s/M	γ_c/mN m^{-1}	m_s/M	γ_c/mN m^{-1}
0	4.83	0.0068	0.67
0.0125	0.141	0.0162	0.036
0.0212	0.0098	0.0255	0.00071
0.03	0.00355	0.0346	0.01
0.04	0.026	0.055	0.073

(b) 40°C

0	1.84	0.0171	1.3
0.0345	0.921	0.0513	0.624
0.0684	0.176	0.0769	0.0039
0.0855	0.0081	0.094	0.0301
0.111	0.0393	0.137	0.104

T/°C	-ln(cmc/M)	T/°C	-ln(cmc/M)
25	8.2	35	8.12
50	7.88	59.5	7.64

APPENDIX III

EFFECTS OF OIL TYPE

γ_c, N data for AOT/NaCl/25°C

(a) m_s = 0.0513M

N	γ_c/mN m^{-1}	N	γ_c/mN m^{-1}
5	0.0441	6	0.0161
7	0.0004	8	0.00536
9	0.0283	10	0.0559
11	0.0822	12	0.111
13	0.148	14	0.187
15	0.305		

(b) 0.0684M

5	0.0914	6	0.0574
7	0.0251	8	0.00484
9	0.00038	10	0.0107
11	0.0312	12	0.0606
13	0.0794	14	0.184
15	0.29		

(c) 0.0855M

6	0.107	7	0.0709
8	0.036	9	0.0119
10	0.0017	10.5	0.00103
11	0.00586	12	0.0239
13	0.047	14	0.0835
15	0.316		

(d) 0.1026M

6	0.164	7	0.113
8	0.0716	9	0.0405
10	0.0186	11	0.0262
12	0.0236	13	0.0289
14	0.0913	15	0.308

(e) 0.1196M

6	0.215	7	0.151
8	0.1	9	0.0692
10	0.0497	11	0.0355
12	0.0656	13	0.0971
14	0.122	15	0.272

γ_c, m_s data for AOT/25°, various alkanes

m_s/M	$\gamma_c/mN\ m^{-1}$	m_s/M	$\gamma_c/mN\ m^{-1}$

(a) N = 9

0.0265	0.101	0.0433	0.0405
0.0517	0.0258	0.0687	0.00039
0.0858	0.0106	0.103	0.0376
0.12	0.065		

(b) 11

0.0265	0.196	0.0433	0.0932
0.0517	0.0763	0.0687	0.029
0.0858	0.00517	0.103	0.0244
0.12	0.0346		

(c) 14

0.0265	0.285	0.0433	0.187
0.0517	0.187	0.0858	0.0835
0.103	0.0913	0.12	0.122

AOT/tetradecane/25°C

$\ln(m_{Na}/M)$	ln(cmc/M)	$\ln(m_{Na}/M)$	ln(cmc/M)
-3.35	-7.08	-2.96	-7.4
-2.45	-7.83	-1.99	-8.21

Dodecane-aq.solution interfacial tensions AOT/25°C

$-\ln(m_D/M)$	γ/mN m^{-1}	$-\ln(m_D/M)$	γ/mN m^{-1}

(a) m_s = 0.00855M

8.5	14.9	9	17.4
9.5	20.8	10	23.4
10.5	26.3	11	28.9

(b) 0.0171M

8.5	12.4	9	15.2
9.5	17.7	10	20.3
10.5	23	11	26.1

(c) 0.0513M

9	9.8	9.5	12.7
9.99	15.7	10.5	18.9
11	21.8	11.4	24
11.9	27.2		

(d) 0.0769M

9.5	10.7	10	14.2
10.5	17.1	11	20.3
11.5	23.6	12	26.9

(e) 0.1026M

$-\ln(m_D/M)$	γ/mN m^{-1}	$-\ln(m_D/M)$	γ/mN m^{-1}
9.7	10.3	10	11.8
10.3	14	10.7	16.4
11	18.3	11.4	21.2
11.7	23.5	12.1	25.6
12.5	28.9		

(f) 0.1367M

9.99	11	10.3	12.9
10.7	15.1	11.1	18.1
11.5	20	11.8	22.8
12.1	24.4		

γ, $\ln m_D$ data AOT/m_s = 0.1026M/25°, various alkanes

$\ln(m_D/M)$	γ/mN m^{-1}	$\ln(m_D/M)$	γ/mN m^{-1}
(a) N = 9			
-12.5	25.6	-11.9	21.5
-11.5	19.3	-11.1	16.8
-10.6	14.1	-9.83	14.5
(b) 11			
-12.5	27.2	-11.9	22.9
-11.5	20.5	-11.1	18
-10.6	15		
(c) 14			
-12.5	29.9	-11.9	25.4
-11.5	22.9	-11.1	20.2
-10.6	16.9		
(d) 16			
-12.5	31.6	-11.9	27
-11.5	24.4	-11.1	21.7
	18.4	-9.9	13.5

$\underline{AOT/m_s = 0.0684M/25°C}$

N	-ln(cmc/M)	N	-ln(cmc/M)
6	8.09	7	8.02
9	7.9	10	7.81
12	7.74	14	7.66

$\underline{\gamma_c, m_s \text{ data AOT/25°C mixed oil phases}}$

m_s/M	$\gamma_c/mN\ m^{-1}$	m_s/M	$\gamma_c/mN\ m^{-1}$
(a) toluene			
0	1.9	0.0048	1.26
0.009	0.52	0.0135	0.131
0.0201	0.16	0.029	0.32
0.048	0.56	0.059	0.64
0.1	0.97	0.115	1
(b) 0.736 m.f. heptane in toluene			
0.0075	1.01	0.015	0.425
0.017	0.193	0.0255	0.0936
0.0305	0.0251	0.039	0.0398
0.0535	0.193	0.115	0.373
(c) 0.480 m.f. heptane in toluene			
0.006	1.14	0.015	0.349
0.019	0.063	0.0225	0.0102
0.0255	0.0326	0.0305	0.0769
0.0395	0.181	0.0535	0.316
0.115	0.83		

Tensions vs [AOT] for m_s = 0.1026M, 25°C

$-\ln(m_D/M)$	γ/mN m^{-1}	$-\ln(m_D/M)$	γ/mN m^{-1}
(a) toluene			
8.95	2.5	9.57	4.8
10.2	8	10.9	11
11.4	13.4	12.1	16.4
12.8	18.7		
(b) cyclohexane			
9.55	5.2	10.1	7.8
10.7	11.2	11.2	13.6
11.8	16.7		

APPENDIX IV

COSURFACTANT EFFECTS (AOT)

AOT/m_s = 0.0171M, various mol. fraction activities dodecanol in heptane, 30°C

(a) $a_A = 0$

$-\ln(m_D/M)$	γ/mN m^{-1}	$-\ln(m_D/M)$	γ/mN m^{-1}
7.5	4.36	7.89	6.65
8.27	8.74	8.63	10.7
8.91	12.3	9.19	13.6
9.76	17.1	10.2	19.4

(b) 3.66×10^{-3}

6.65	0.245	6.89	0.255
6.92	0.246	7.03	0.507
7.18	1.29	7.25	1.67
7.34	2.1	7.49	2.85
7.5	3.08	7.66	3.99
7.87	5.01	7.89	5.46
8.27	7.51	8.63	9.41
8.91	10.8	9.19	12
9.76	14.9	10.2	17.1

(c) 5.15×10^{-3}

7.5	2.86	7.89	4.93
8.27	6.93	8.63	8.73
8.91	10.1	9.19	11
9.76	14.2	10.2	16.4

$-\ln(m_D/M)$	γ/mN m^{-1}	$-\ln(m_D/M)$	γ/mN m^{-1}
(d) 6.13×10^{-3}			
6.75	0.02	6.89	0.0105
6.99	0.0129	7.11	0.42
7.21	0.97	7.32	1.64
7.42	2.27	7.5	2.58
7.73	3.84	7.89	4.66
8.01	5.15	8.27	6.64
8.63	8.45	8.63	8.45
8.91	9.94	9.19	10.8
9.76	13.7	10.2	15.7
(e) 6.95×10^{-3}			
7.5	2.34	7.89	4.44
8.27	6.26	8.63	7.98
8.91	9.36	9.19	10.5
9.76	13.3	10.2	15.5
(f) 8.07×10^{-3}			
6.7	0.00127	6.89	0.00102
7.01	0.00159	7.11	0.112
7.23	0.653	7.42	1.65
7.5	2.02	7.53	2.02
7.68	2.93	7.83	3.44
7.89	4.24	8.07	5
8.27	6.02	8.43	6.7
8.63	7.69	8.88	8.9
8.91	9.15	9.19	10.1
9.4	11.4	9.76	12.8
9.94	13.2	10.2	14.6
10.4	15.2	11.1	17.6
11.8	19.6		

$-\ln(m_D/M)$	γ/mN m^{-1}	$-\ln(m_D/M)$	γ/mN m^{-1}

(g) 8.79×10^{-3}

7.5	1.77	7.89	3.94
8.27	5.91	8.63	7.47
8.91	8.71	9.19	9.77
9.76	12.6	10.2	14.4

(h) 9.51×10^{-3}

7.5	1.64	7.89	3.78
8.27	5.75	8.63	7.27
8.91	8.45	9.19	9.55
9.76	12.2	10.2	14.2

(i) 10.12×10^{-3}

6.75	0.182	6.88	0.193
6.89	0.186	7.05	0.298
7.29	0.683	7.5	1.45
7.55	1.47	7.74	2.66
7.89	3.57	8.01	4.21
8.23	4.78	8.27	5.45
8.39	5.46	8.63	7.03
8.66	6.47	8.91	8.25
9.19	9.34	9.76	11.8
9.76	12.8	10.2	13.8

AOT/heptane/30°C, activity of dodecanol

(a) $m_s = 0$

a_A/M	γ_c/mN m^{-1}	a_A/M	γ_c/mN m^{-1}
0	2.46	0.069	1.99
0.071	1.82	0.081	1.26
0.092	1.58	0.106	1.82
0.13	2.14		

(b) 0.0171M

0	0.561	0.003	0.565
0.007	0.551	0.01	0.558
0.023	0.238	0.033	0.0639
0.038	0.0207	0.041	0.0114
0.045	0.00441	0.05	0.0016
0.0522	0.00805	0.054	0.0164
0.057	0.0412	0.058	0.0988
0.062	0.18	0.066	0.258

(c) 0.0427M

0	0.0316	0.006	0.0106
0.016	0.00692	0.023	0.0186
0.034	0.0549		

(d) 0.0684M

0	0.0151	0.0062	0.0269
0.016	0.0525	0.0237	0.0977
0.035	0.19		

(e) 0.1026M

0	0.102	0.0075	0.148
0.024	0.355	0.039	0.575
0.054	0.933	0.063	1.62

γ_c, mol. fraction activity, AOT/dodecanol in heptane

$10^3 a_A$	γ_c/mN m^{-1}	$10^3 a_A$	γ_c/mN m^{-1}
1.58	0.518	2.84	0.255
3.58	0.24	5.14	0.0605
5.33	0.0629	6.01	0.0208
6.13	0.0105	6.52	0.00932
6.95	0.00445	7.21	0.00413
7.46	0.00096	8.02	0.00152
8.07	0.00102	8.44	0.00818
8.75	0.016	9.16	0.0406
9.5	0.1	9.51	0.0793
10.1	0.186	10.1	0.182
10.4	15.2	10.8	0.26

γ_c, mol. fraction x_A data AOT/m_s = 0.0171M/heptane/30°C

(a) Pentanol

x_A	γ_c/mN m^{-1}	x_A	γ_c/mN m^{-1}
0.00914	1.22	0.0167	1.55
0.0263	1.76	0.0387	1.94

(b) Hexanol

0.0013	0.568	0.00876	0.584
0.011	0.576	0.024	0.58
0.0355	0.586		

(c) Octanol

0.0059	0.498	0.0095	0.426
0.012	0.316	0.0155	0.234
0.0195	0.0525	0.0215	0.0105
0.0235	0.0178	0.028	0.0501

x_{A-}	γ_c/mN m^{-1}	x_{A-}	γ_c/mN m^{-1}

(d) Nonanol

0.0058	0.359	0.0101	0.167
0.0133	0.1	0.015	0.0215
0.0168	0.00378	0.0194	0.0123
0.0237	0.151	0.0297	0.341
0.0357	0.451		

(e) Decanol

0.00457	0.27	0.00923	0.0738
0.0112	0.00191	0.0141	0.00254
0.0169	0.0109	0.0192	0.0396
0.0211	0.117	0.0235	0.207
0.0283	0.396		

(f) Dodecanol

0	0.577	0.00158	0.518
0.00389	0.24	0.00627	0.0629
0.00734	0.0208	0.0082	0.00932
0.00948	0.00413	0.00998	0.00962
0.0117	0.00152	0.0121	0.00818
0.0129	0.016	0.014	0.0406
0.015	0.1	0.017	0.182
0.0195	0.26		

(g) Tetradecanol

x_{A-}	γ_c/mN m^{-1}	x_{A-}	γ_c/mN m^{-1}
0.00366	0.409	0.00629	0.0468
0.00764	0.0324	0.0083	0.0108
0.009	0.0027	0.0104	0.0036
0.0114	0.013	0.0132	0.0198
0.0162	0.081	0.0199	0.252
0.0275	0.351		

(h) Hexadecanol

0.00251	0.261	0.00544	0.0468
0.007	0.0126	0.0091	0.0012
0.0107	0.0036	0.0137	0.0114
0.0152	0.0251	0.0173	0.0864
0.0213	0.121	0.028	0.378

AOT/m_s = 0.0171M/dodecanol in heptane/30°C

a_{A-}	-ln(cmc/M)	a_{A-}	-ln(cmc/M)
0.00366	6.92	0.00514	6.96
0.00613	6.99	0.00695	7.03
0.00807	7.09	0.00879	7.11
0.00951	7.18	0.0101	7.27

Numerical analysis for predicted c.m.c. variation with a_A.

Equation 8.12 may be written

$$-\ln cmc = \frac{\gamma_c}{RT\Gamma_D} + \int \frac{\Gamma_A}{\Gamma_D} .d\ln a_A - \int \gamma_c \frac{d(1/RT\Gamma_D)}{d\ln a_A} . d\ln a_A \qquad (A.1)$$

(1) (2) (3)

By combination of equations 8.8 and 8.10, term (1) becomes

$$\frac{\gamma_c}{RT\Gamma_D} = \left[10^{-(1.94\times10^6 a_A^{2.767}+0.3128)} + 10^{-(225.73\ln a_A+24.967(\ln a_A)^2+510.8)}\right] \times (0.02796\ln a_A + 0.3481) \qquad (A.2)$$

Term (2) may be written (using equation 8.9)

$$\int \frac{\Gamma_A}{\Gamma_D} . d\ln a_A = 142a_A^{1.286} + B \qquad (A.3)$$

Term (3) becomes

$$\int \gamma_c . \frac{d(1/RT\Gamma_D)}{d\ln a_A} .d\ln a_A = 0.02796 \int \gamma_c .d\ln a_A \qquad (A.4)$$

The numerical integration of equation A.4 is difficult. Instead, being a definite integral, it is equal to the area under the curve of γ_c versus $\ln a_A$. It has been shown that the magnitude of this term (for various values of a_A) is negligible compared with those from equations A.2 and A.3.

Thus equation A.1 simply becomes

$$-\ln cmc = 142a_A^{1.286} + (0.02796\ln a_A + 0.3481)\left[10^{-(1.94\times10^6 a_A^{2.767}+0.318)} + 10^{-(225.73\ln a_A+24.967(\ln a_A)^2+510.8)}\right] + B$$

To give the minimum in the sum of squared residuals B was found as 6.811.

APPENDIX V

SYSTEMS CONTAINING SDS

Tension vs [SDS], heptane-0.1M NaCl interface, 20°C

$\ln(m_D/M)$	γ/mN m^{-1}	$\ln(m_D/M)$	γ/mN m^{-1}
-7.62	13.7	-7.31	11
-7.17	9.52	-6.98	7.76
-6.86	6.71	-6.72	5.51
-6.55	4.91	-6.11	4.86
-5.53	4.86	-4.6	4.89

γ, $\ln m_D$ data at heptane-solution interface, 30°C

(a) m_s = 0.01M

$-\ln(m_D/M)$	γ/mN m^{-1}	$-\ln(m_D/M)$	γ/mN m^{-1}
4.6	6.5	5.49	6.55
5.6	7.66	5.89	10.8
6.14	13.9	6.45	16.9

(b) 0.05M

4.6	5.4	5.55	5.4
6.09	5.45	6.4	6.1
6.76	9.34	7	11.5
7.2	13.3		

(c) 0.10M

$-\ln(m_D/M)$	γ/mN m^{-1}	$-\ln(m_D/M)$	γ/mN m^{-1}
4.6	4.92	6	4.9
6.71	4.9	6.83	5.07
7.07	7.49	7.32	9.7
7.61	12.7		

(d) 0.20M

4.71	4.4	6.2	4.41
7.19	4.45	7.33	4.84
7.63	7.45	7.96	10.7
8.3	14.1		

SDS-heptane-NaCl-30°C

$-\ln(m_{Na}/M)$	$-\ln(cmc/M)$	$-\ln(m_{Na}/M)$	$-\ln(cmc/M)$
1.6	4.72	2.3	5.18
2.94	5.64	4.25	6.53

m_s/M	γ_c/mN m^{-1}	m_s/M	γ_c/mN m^{-1}
0.00815	7.23	0.0101	6.55
0.0171	6.13	0.0463	5.45
0.0498	5.5	0.0706	5.14
0.1	4.9	0.101	4.88
0.15	4.42	0.2	4.4
0.213	4.18		

Tensions vs wt.% pentanol in cyclohexane, 30°C

wt.%	γ_c/mN m^{-1}	wt.%	γ_c/mN m^{-1}
0	2.24	5.5	1.09
10.1	0.152	12	0.0282
14	0.00226	17.4	0.0195
21	0.0348	25	0.0398
30	0.144		

γ_c, activity octanol in cyclohexane, m_s = 0.3M (a) nonequilibrated

a_A/M	γ_c/mN m^{-1}	a_A/M	γ_c/mN m^{-1}
0.034	1.32	0.06	0.794
0.075	0.251	0.079	0.0741
0.085	0.012	0.0915	0.0501
0.097	0.101	0.116	0.251
0.14	0.316	0.158	0.468

(b) Equilibrated

0	3.16	0.03	1.26
0.045	0.631	0.05	0.417
0.06	0.0794	0.076	0.017
0.079	0.0251	0.085	0.0692
0.103	0.251		

γ_c, activity dodecanol in heptane, m_s = 0.1M at 30°C

a_A/M	γ_c/mN m^{-1}	a_A/M	γ_c/mN m^{-1}
0	5.01	0.012	2.88
0.024	1.51	0.036	0.933
0.055	0.457	0.059	0.38
0.061	0.305	0.0718	0.0676
0.0772	0.0199	0.081	0.0398
0.096	0.144	0.12	0.316
	0.501		

SDS/octanol/m_s = 0.3M/cyclohexane/30°C

$\ln(a_A/M)$	$\ln(cmc/M)$	$\ln(a_A/M)$	$\ln(cmc/M)$
-3.11	-7.95	-2.97	-8.3
-2.81	-8.75	-2.61	-9.65
-2.46	-10.3		

$\ln(a_A/M)$	N_A/N_D	$\ln(a_A/M)$	N_A/N_D
-3.11	2.32	-2.97	2.79
-2.81	3.44	-2.61	4.49
-2.46	5.43		

Absorbance vs [octanol] in cyclohexane at 30°C

m_A/M	A'	m_A/M	A'
0.00242	0.006	0.00484	0.01
0.00726	0.0103	0.00968	0.015
0.0121	0.0166	0.0145	0.0254
0.0169	0.027	0.0194	0.0318
0.029	0.042	0.0484	0.0655
0.0726	0.081	0.0968	0.097
0.145	0.114	0.194	0.126
0.242	0.136	0.29	0.144
0.339	0.146	0.387	0.153
0.436	0.155	0.484	0.153

Activity coefficients for octanol in cyclohexane, 30°C

m_A/M	f_A	m_A/M	f_A
0.029	0.851	0.0484	0.796
0.0726	0.656	0.0968	0.589
0.145	0.464	0.194	0.383
0.242	0.331	0.29	0.292
0.339	0.253	0.387	0.232
0.436	0.209	0.484	0.186

Curve Fitting

Curve fitting i.e. numerical analysis of experimental data, has been used extensively in the present work. This has been possible using the 'Curve Fitter' programme† written by Dr. J. Mead, to whom I am most grateful. I also thank him for his help with some of the analyses. The programme allows the fitting of either functions supplied by the operator (with up to one non-linear variable) or a standard polynomial to data entered from either the keyboard or disc.

---

† A copy exists in the Chemistry Department, University of Hull.

References

REFERENCES

1 J.W. McBain and C.S. Salmon, *J. Am. Chem. Soc.*, **43**, 426 (1920).

2 F.W. Fowkes, in *Solvent Properties of Surfactant Solutions*, ed. K. Shinoda (Dekker, New York, 1967), chap. 3.

3 T.P. Hoar and J.H. Schulman, *Nature*, **152**, 102 (1943).

4 M. Rosoff, *Prog. Surf. Membr. Sci.*, 12, 405 (1978).

5 L.M. Prince, in *Emulsions and Emulsion Technology Part I*, ed. K.J. Lissant (Dekker, New York, 1975), chap. 3.

6 M.K. Sharma and D.O. Shah, in *Macro and Microemulsions*, ed. D.O. Shah (Wiley, New York, 1985), chap. 1.

7 *Microemulsions*, ed. I.D. Robb (Plenum Press, New York, 1982).

8 E. Ruckenstein, *Soc. Pet. Eng. J.*, 21, 593 (1981).

9 *Micellisation, Solubilisation and Microemulsions*, ed. K.L. Mittal (Plenum Press, New York, 1977).

10 *Solution Behaviour of Surfactants*, ed. K.L. Mittal and E.J. Fendler (Plenum Press, New York, 1982).

11 *Surfactants in Solution*, ed. K.L. Mittal and B. Lindman (Plenum Press, New York, 1984).

12 *Surfactants*, ed. Th. F. Tadros (Adademic Press, London, 1984).

13 P.D. Fleming and J.E. Vinatieri, *J. Colloid Interface Sci.*, **81**, 319 (1981).

14 E.I. Franses, J.E. Puig, Y. Talmon, W.G. Miller, L.E. Scriven and H.T. Davis, *J. Phys. Chem.*, 84, 1547 (1980).

15 D.J. Mitchell and B.W. Ninham, *J. Chem. Soc., Faraday Trans. 2*, **77**, 601 (1981).

[16] J.Th.G. Overbeek, *Faraday Discuss. Chem. Soc.*, 65, 7 (1978).

[17] H. Kunieda and K. Shinoda, *J. Dispersion Sci. Technol.*, 3, 233 (1982).

[18] K. Shinoda and H. Kunieda, *J. Colloid Interface Sci.*, 42, 381 (1973).

[19] H. Kunieda and K. Shinoda, *Bull. Chem. Soc. Jpn.*, 55, 1777 (1982).

[20] B. Widom, *J. Chem. Phys.*, 62, 1332 (1975).

[21] J.C. Lang, P.K. Lim and B. Widom, *J. Phys. Chem.*, 80, 1719 (1976).

[22] A. Pouchelon, J. Meunier, D. Langevin, D. Chatenay and A.M. Cazabat, *Chem. Phys. Lett.*, 76, 277 (1980).

[23] S. Ross and R.E. Patterson, *J. Chem. Eng. Data*, 24, 111 (1979).

[24] P.D. Fleming and J.E. Vinatieri, *J. Chem. Eng. Data*, 26, 172 (1981).

[25] W.H. Wade, J.C. Morgan, R.S. Schechter, J.K. Jacobson and J.L. Salager, *Soc. Pet. Eng. J.*, 12, 242 (1978).

[26] P.D. Fleming, J.E. Vinatieri and G.R. Glinsmann, *J. Phys. Chem.*, 84, 1526 (1980).

[27] S. Fisk and B. Widom, *J. Chem. Phys.*, 50, 3219 (1969).

[28] A.C. Hall, *Colloids Surf.*, 1, 209 (1980).

[29] J.E. Puig, E.I. Franses and W.G. Miller, *J. Colloid Interface Sci.*, 89, 441 (1982).

[30] J.E. Puig, M.T. Mares, W.G. Miller and E.I. Franses, *Colloids Surf.*, 16, 139 (1985).

[31] F. Billoudet and M. Dupeyrat, *J. Chim. Phys.*, 78, 635 (1981).

[32] J.Th.G. Overbeek, P.L. de Bruyn and F. Verhoechx, in *Surfactants*, ed. Th.F. Tadros (Academic Press, London, 1984), chap. 5.

[33] K.S. Chan and D.O. Shah, *J. Dispersion Sci. Technol.*, **1**, 55 (1980).

[34] A.M. Cazabat, D. Langevin, J. Meunier and A. Pouchelon, *Adv. Colloid Interface Sci.*, **16**, 175 (1982).

[35] J. Meunier and D. Langevin, *J. Phys. Lett.*, **43**, 185 (1982).

[36] S. Mukherjee, C.A. Miller and T. Fort, *J. Colloid Interface Sci.*, **91**, 223 (1983).

[37] E.A. Guggenheim, *Thermodynamics*, (North Holland, Amsterdam, 5th edn., 1967).

[38] R. Aveyard and D.A. Haydon, *An Introduction to the Principles of Surface Chemistry*, (Cambridge University Press, 1973), chap. 2.

[39] K. Tajima, *Bull. Chem. Soc. Jpn.*, 43, 3063 (1970).

[40] K. Tajima, H. Murata and T. Tsutsui, *J. Colloid Interface Sci.*, 85, 534 (1982).

[41] K. Tajima, M. Muramatsu and T. Sasaki, *Bull. Chem. Soc. Jpn.*, **43**, 1991 (1970).

[42] E. Matijevic and B.A. Pethica, *Trans. Faraday Soc.*, 54, 1382 (1958).

[43] K. Tajima, *Bull. Chem. Soc. Jpn.*, **44**, 1767 (1971).

[44] L. Wilhelmy, *Ann. Phys.*, **119**, 177 (1863).

[45] A. Dognon and M. Abribat, *Compt. Rend. Acad. Sci. (Paris)*, **208**, 1881 (1939).

[46] L. Du Noüy, *J. Gen. Physl.* 1, 521 (1919).

[47] W.D. Harkins and H.F. Jordan, *J. Am. Chem. Soc.*, 52, 1751 (1930).

[48] B.B. Freud and H.Z. Freud, *J. Am. Chem. Soc.*, 52, 1772 (1930).

[49] H.H. Zuidema and G.W. Waters, *Ind. Eng. Chem.*, 13, 312 (1941).

[50] A.W. Adamson, *Physical Chemistry of Surfaces* (Wiley, New York, 1976), chap. 1.

[51] Y. Rotenberg, S. Schürch, J.F. Boyce and A.W. Neumann, in *Surfactants in Solution*, ed. K.L. Mittal and B. Lindman (Plenum Press, New York, 1984), p.2113.

[52] D. Chatenay, D. Langevin, J. Meunier, D. Bourbon, P. Lalanne and A.M. Bellocq, *J. Dispersion Sci. Technol.*, 3, 245 (1982).

[53] B. Vonnegut, *Rev. Sci. Instr.*, 13, 6 (1942).

[54] A. Couper, R. Newton and C. Nunn, *Colloid Polymer Sci.*, 261, 371 (1983).

[55] H.M. Princen, I.Y.Z. Zia and S.G. Mason, *J. Colloid Interface Sci.*, 23, 99 (1967).

[56] J.C. Slattery and J.D. Chen, *J. Colloid Interface Sci.*, 64, 373 (1978).

[57] C.D. Manning and L.E. Scriven, *Rev. Sci. Instr.*, 48, 1699 (1977).

[58] D.J. Donahue and F.E. Bartell, *J. Am. Chem. Soc.*, 56, 480 (1952).

[59] J.M. Andreas, E.A. Hauser and W.B. Tucker, *J. Phys. Chem.*, 42, 1001 (1938).

[60] K.J. Randle, *Chem. Ind.*, 74 (1980).

[61] P.N. Pusey, D.E. Koppel, D.W. Schaefer, R.D. Camrerini-Otero and S.H. Koenig, *Biochem. J.*, 13, 953 (1974).

[62] M. Corti and V. Degiorgio, *Chem. Phys. Lett.*, 49, 141 (1977).

63 R.A. Day, B.H. Robinson, J.H. Clarke and J.V. Doherty, *J. Chem. Soc., Faraday Trans. 1*, **74**, 132 (1978).

64 M. Zulauf and H.F. Eicke, *J. Phys. Chem.*, **83**, 480 (1979).

65 A.M. Cazabat, D. Langevin and A. Pouchelon, *J. Colloid Interface Sci.*, **73**, 1 (1980).

66 *Malvern Instruments Correlator Manual* (1983).

67 D.E. Koppel, *J. Chem. Phys.*, **57**, 4814 (1972).

68 V.W. Reid, G.F. Longman and E. Heinerth, *Tenside*, 4, 292 (1967).

69 J.H. Jones, *J. Assoc. Agric. Chem.*, **28**, 398 (1945).

70 R.A. Greff, E.A. Setzkorn and W.D. Leslie, *J. Am. Oil Chem. Soc.*, **42**, 180 (1965).

71 B.Z. Wurzschmitt, *Anal. Chem.*, **130**, 105 (1950).

72 K. Fischer, *Angew. Chem.*, **48**, 394 (1935).

73 D.M. Smith, W.M.D. Bryant and J. Mitchell, *J. Am. Chem. Soc.*, **61**, 2407 (1939).

74 *C.R.C. Handbook of Chemistry and Physics* (C.R.C. Press, Florida, 65th edn., 1985).

75 *Operating instructions for Abbé 60 refractometer* (Bellingham and Stanley Ltd.).

76 *International Critical Tables* (McGraw-Hill, London, 1928), **4**, 447.

77 J. Timmermans, *Physico-chemical constants of pure organic compounds* (Elsevier, New York, 1950).

78 R. Aveyard and D.A. Haydon, *Trans. Faraday Soc.*, **61**, 2255 (1965).

79 R. Aveyard and S.M. Saleem, *J. Chem. Soc., Faraday Trans. 1*, **72**, 1609 (1976).

80 C.A. Martin and L.J. Magid, *J. Phys. Chem.*, **85**, 3938 (1981).

[81] J.M. Corkill, J.F. Goodman and T. Walker, *Trans. Faraday Soc.*, **61**, 589 (1965).

[82] E.F. Williams, N.T. Woodberry and J.K. Dixon, *J. Colloid Sci.*, **12**, 452 (1957).

[83] K. Shinoda and K. Ito, *J. Phys. Chem.*, 65, 1499 (1961).

[84] D. Vollhardt and G. Czichocki, *Colloids Surf.*, 11, 209 (1984).

[85] E.G. Cockbain, *Trans. Faraday Soc.*, 50, 874 (1954).

[86] B.R. Vijayendran and T.P. Bursh, *J. Colloid Interface Sci.*, **68**, 383 (1979).

[87] A. Kitahara, T. Kobayashi and T. Tachibana, *J. Phys. Chem.*, **66**, 363 (1962).

[88] E.I. Franses and T.J. Hart, *J. Colloid Interface Sci.*, **94**, 1 (1983).

[89] P. Delord and F.C. Larché, *J. Colloid Interface Sci.*, 98, 277 (1984).

[90] H. Schott, *J. Pharm. Sci.*, 69, 852 (1980).

[91] C. Tanford, *The Hydrophobic Effect and Formation of Micelles and Biological Membranes* (Wiley, New York, 2nd edn., 1980).

[92] P.A. Winsor, *Trans. Faraday Soc.*, **44**, 376 (1948).

[93] K. Shinoda and H.J. Saito, *J. Colloid Interface Sci.*, 26, 70 (1969).

[94] K. Shinoda and H. Kunieda, in *Microemulsions, Theory and Practice* ed. L.M. Prince (Academic Press, New York, 1977).

[95] H. Saito and K. Shinoda, *J. Colloid Interface Sci.*, 32, 647 (1970).

[96] E.I. Franses, Y. Talmon, L.E. Scriven, H.T. Davis and W.G. Miller, *J. Colloid Interface Sci.*, 86, 449 (1982).

[97] A. Pouchelon, J. Meunier, D. Langevin and A.M. Cazabat, *J. Phys. Lett.*, **41**, 239 (1980).

[98] A. Pouchelon, D. Chatenay, J. Meunier and D. Langevin, *J. Colloid Interface Sci.*, **82**, 418 (1981).

[99] H. Kunieda and K. Shinoda, *J. Colloid Interface Sci.*, **75**, 601 (1980).

[100] M.P. Lascaux, O. Dusart, R. Granet and S. Piekarski, *J. Chim. Phys.*, **80**, 615 (1983).

[101] R. Aveyard and R.W. Mitchell, *Trans. Faraday Soc.*, **65**, 2645 (1969).

[102] J.L. Salager, I.L. Maldonado, M.M. Perez and F. Silva, *J. Dispersion Sci. Technol.*, **3**, 279 (1982).

[103] L.E. Scriven, in *Micellisation, Solubilisation and Microemulsions*, ed. K.L. Mittal (Plenum Press, New York, 1977).

[104] R. Aveyard, B.P. Binks and J. Mead, paper in preparation.

[105] W.C. Tosch, S.C. Jones and A.W. Adamson, *J. Colloid Interface Sci.*, **31**, 297 (1969).

[106] J.D. Nicholson and J.H. Clarke, in *Surfactants in Solution*, ed. K.L. Mittal (Plenum Press, New York, 1984).

[107] B.H. Robinson, C. Toprakcioglu, J.C. Dore and P. Chieux, *J. Chem. Soc., Faraday Trans. 1*, **80**, 13 (1984).

[108] C. Tanford, *Physical Chemistry of Macromolecules* (Wiley, New York, 1961).

[109] A.M. Cazabat and D. Langevin, *J. Chem. Phys.*, **74**, 3148 (1981).

[110] J.H. Schulman and D.P. Riley, *J. Colloid Sci.*, **3**, 383 (1948).

[111] P.D.I. Fletcher, B.H. Robinson, F. Bermejo-Barrera, D. Oakenfull, J.C. Dore and D.C. Steytler, in *Microemulsions*, ed. I.D. Robb (Plenum Press, New York, 1982).

[112] N.J. Bridge and P.D.I. Fletcher, *J. Chem. Soc., Faraday Trans. 1*, **79**,2161 (1983).

[113] P.D.I. Fletcher, A.M. Howe, N.M. Perrins, B.H. Robinson, C. Toprakcioglu and J.C. Dore, in *Surfactants in Solution*, ed. K.L. Mittal and B. Lindman (Plenum Press, New York, 1984).

[114] J.W. Mehl, J.L. Oncley and R. Simha, *Science*, **92**, 132 (1940).

[115] M. Muthukumar and K.F. Freed, *J. Chem. Phys.*, **76**, 6195 (1982).

[116] P.C. Hiemenz, *Principles of Colloid and Surface Chemistry*, (Dekker, New York, 1977).

[117] P.D.I. Fletcher, M.F. Galal and B.H. Robinson, *J. Chem. Soc., Faraday Trans. 1*, **80**, 3307 (1984).

[118] A. de Geyer and J. Tabony, *Chem. Phys. Lett.*, **113**, 83 (1985).

[119] P.D.I. Fletcher, *J. Chem. Soc., Faraday Trans. 1*, submitted for publication.

[120] A. Graciaa, J. Lachaise, P. Chabrat, L. Letamendia, J. Rouch, C. Vaucamps, M. Bourrel and C. Chambu, *J. Phys. Lett.*, **38**, 253 (1977).

[121] R. Huan, C.A. Miller and T. Fort, *J. Colloid Interface Sci.*, **68**, 221 (1979).

[122] D. Langevin, J. Meunier and A.M. Cazabat, *La Recherche*, **16**, 720 (1985).

[123] P.A. Winsor, *Solvent Properties of Amphiphilic Compounds*, (Butterworths, London, 1954).

[124] S. Friberg, I. Lapczynska and G. Gillberg, *J. Colloid Interface Sci.*, **56**, 19 (1976).

[125] D.G. Oakenfull, *J. Chem. Soc., Faraday Trans. 1*, **76**, 1875 (1980).

[126] E. Ruckenstein, *Chem. Phys. Lett.*, **118**, 435 (1985).

[127] C.A. Miller, *J. Dispersion Sci. Technol.*, **6**, 159 (1985).

[128] J. Israelachvili, in *Surfactants in Solution*, ed. K.L. Mittal and P. Bothorel (Plenum Press, New York, 1986).

[129] D. Guest and D. Langevin, *J. Colloid Interface Sci.*, 112, 208 (1986).

[130] M.J. Grimson and F. Honary, *Phys. Lett.*, 102, 241 (1984).

[131] H. Kunieda and S. Friberg, *Bull. Chem. Soc. Jpn.*, 54, 1010 (1981).

[132] R. Aveyard and T.A. Lawless, *J. Chem. Soc., Faraday Trans 1*, in press.

[133] R. Aveyard, B.P. Binks, T.A. Lawless and J. Mead, *J. Chem. Soc., Faraday Trans. 1*, 81, 2155 (1985).

[134] M. Manabe, M. Koda and K. Shirahasma, *Bull. Chem. Soc. Jpn.*, 48, 3553 (1975).

[135] M.J. Schick, *J. Colloid Sci.*, 17, 801 (1962).

[136] E.H. Crook, D.B. Fordyce and G.F. Trebbi, *J. Phys. Chem.*, 67, 1987 (1963).

[137] R. Aveyard, B.P. Binks and J. Mead, *J. Chem. Soc., Faraday Trans 1*, 81, 2169 (1985).

[138] E. Ruckenstein, *J. Dispersion Sci. Technol.*, 2, 1 (1981).

[139] E. Ruckenstein and J.A. Beunen, *J. Colloid Interface Sci.*, 98, 55 (1984).

[140] R. Defay, I. Prigogine, A. Bellemans and D.H. Everett, *Surface Tension and Adsorption*, (Longmans, London, 1966).

[141] R.A. Robinson and R.H. Stokes, *Electrolyte Solutions*, (Butterworths, Sevenoaks, 1959).

[142] D.G. Hall, in *Aggregation Processes in Solution*, ed. E. Wyn-Jones and J. Gormally (Elsevier, Amsterdam, 1983).

[143] F. Long and W. McDevit, *Chem. Rev.*, 51, 119 (1952).

[144] F.L. Wilcox and E.E. Schrier, *J. Phys. Chem.*, 75, 3757 (1971).

[145] N. Nishikido and R. Matuura, *Bull. Chem. Soc. Jpn.*, 50, 1690 (1977).

[146] P. Mukerjee, *J. Phys. Chem.*, 69, 4038 (1965).

[147] M.J. Rosen, A.W. Cohen, M. Dahanayake and X. Hua, *J. Phys. Chem.*, 86, 541 (1982).

[148] R. Aveyard, S.M. Saleem and R. Heselden, *J. Chem. Soc., Faraday Trans 1*, 73, 84 (1977).

[149] R. Aveyard, *Can. J. Chem.*, 60, 1317 (1982).

[150] W.D. Bancroft, *J. Phys. Chem.*, 17, 501 (1913).

[151] R. Aveyard, B.P. Binks, S. Clark and J. Mead, *J. Chem. Soc., Faraday Trans. 1*, 82, 125 (1986).

[152] K. Shinoda, M. Hanrin, H. Kunieda and H. Saito, *Colloids Surf.*, 2, 301 (1981).

[153] Th.F. Tadros and B. Vincent, in *Encyclopaedia of Emulsion Technology Vol. 1*, ed. P. Becher 1983 (Dekker, New York) p.129.

[154] S.J. Chen, D.F. Evans, B.W. Ninham, D.J. Mitchell, F.D. Blum and S. Pickup, *J. Phys. Chem.*, 90, 842 (1986).

[155] F.D. Blum, S. Pickup, B.W. Ninham, S.J. Chen and D.F. Evans, *J. Phys. Chem.*, 89, 711 (1985).

[156] R. Aveyard, B.P. Binks and J. Mead, *J. Chem. Soc., Faraday Trans.*, 82, 1755, (1986).

[157] M. Fromon, this laboratory (1985).

[158] M. Kahlweit and R. Strey, *Angew. Chem.*, 24, 654 (1985).

[159] D.W.R. Gruen, *Biochim. Biophys. Acta.*, 595, 161 (1980).

[160] M. Kahlweit, E. Lessner and R. Strey, *J. Phys. Chem.*, 87, 5032 (1983).

[161] A. Leo, C. Hansch and D. Elkins, *Chem. Rev.*, 71, 525 (1971).

[162] R.L. Venable, K.L. Elders and J. Fang, *J. Colloid Interface Sci.*, **109**, 330 (1986).

[163] J. Biais, M. Barthe, M. Bourrel, B. Clin and P. Lalanne, *J. Colloid Interface Sci.*, **109**, 576 (1986).

[164] R. Aveyard, B.J. Briscoe and J. Chapman, *Trans. Faraday Soc.*, **69**, 1772 (1973).

[165] R. Vochten and G. Petre, *J. Colloid Interface Sci.*, **42**, 320 (1973).

[166] R. Aveyard and B.P. Binks, *J. Chem. Soc., Faraday Trans. 1*, submitted for publication.

[167] R.J. Williams, J.N. Phillips and K.J. Mysels, *Trans. Faraday Soc.*, **51**, 728 (1955).

[168] I. Prigogine and R. Defay, in *Chemical Thermodynamics*, (Longmans, London, 1954), p.414.

[169] R. Mecke, *Discuss. Faraday Soc.*, 9, 161 (1950).

[170] B.D. Anderson, J.H. Rytting and T. Higuchi, *Int. J. Pharm.*, **1**, 15 (1978).

[171] M.J. Rosen and D.S. Murphy, *J. Colloid Interface Sci.*, **110**, 224 (1986).

[172] R. Aveyard and B.J. Briscoe, *J. Chem. Soc., Faraday Trans. 1*, **68**, 478 (1972).